11-12-2018

Experimental Evaluation of Surfactant-based Nanofluids on Wettability Alteration and Oil Recovery

Mohammad Foad Haeri
Louisiana State University and Agricultural and Mechanical College, foadhaeri@gmail.com

EXPERIMENTAL EVALUATION OF SURFACTANT-BASED NANOFLUIDS ON WETTABILITY ALTERATION AND OIL RECOVERY

A Dissertation

Submitted to the Graduate Faculty of the
Louisiana State University and
Agricultural and Mechanical College
in partial fulfillment of the
requirements for the degree of
Doctor of Philosophy

in

The Craft & Hawkins Department of Petroleum Engineering

by
Mohammad Foad Haeri
B.Sc., Petroleum University of Technology, 2002
M.Sc., University of Louisiana at Lafayette, 2007
December 2018

This dissertation is dedicated

to my *Father*

who suffered grievously, so I could bloom

and

to my *Mother*

who loved me unconditionally, so I could rise

ACKNOWLEDGMENT

I would like to express my sincere gratitude to my advisor Dr. Dandina N. Rao for his relentless motivation, constructive trust, and insightful guidance to be a true research scientist. Without his invaluable support, encouragement, and patience, this dissertation would not have been possible.

I am also thankful to Dr. Seung Kam and Dr. Mehdi Zeidouni for their kind acceptance to serve as the members on the examination committee and Dr. Amitava D. Roy for serving as a committee member and providing support through the Center for Advance Microstructures and Devices.

I would like to thank the EOR team in Sasol company at Lake Charles for providing insight and supplying surfactants particularly throughout the initial stages of this research and Computer Modeling Group (CMG) Ltd. for providing the simulation software license.

I would also like to express my appreciation to Nicholas Dinecola from LSU Advance Manufacturing and Machining Facility, Joe M. Bell and Nick S. Lombardo from LSU ChemE Shop, and Fenelon Nunes from Department of Petroleum Engineering for their supportive cooperation during this research.

Finally, I would like to thank all the faculty members and my colleagues especially Bikash D. Saikia, Paulina Mwangi, Mohammed Al-Ryami, Sandeep Gupta, and Shayan Sombolestani for their valuable support throughout the course of this research.

TABLE OF CONTENTS

LIST OF TABLES

LIST OF FIGURES

NOMENCLATURE

e_o	oil Corey exponent
e_w	water Corey exponent
f_w	water fractional flow
h	film thickness
K_{rw}	relative permeability to water
K_{ro}	relative permeability to oil
k_{rw}	relative permeability to water at S_{or}
k_{ro}	relative permeability to oil at S_{iw}
N_c	capillary number
S_w	water saturation
S_{iw}	irreducible water saturation
S_{or}	residual oil saturation
S	normalized saturation
θ	contact angle between fluid-fluid interface and solid surface
μ	viscosity of the displacing phase
μ_w	water viscosity
μ_o	oil viscosity
v	velocity of the displacing phase
Π_h	disjoining pressure of a wetting film
σ	interfacial tension between fluid phases
σ_s	surface free energy

σ_f surface tension of the fluid

σ_{sf} interfacial tension between fluid and solid

ABSTRACT

Economic concerns about chemical flooding could be taken as opportunities to develop new cost-effective technologies that lead to high recoveries. Application of surfactants to lower oil-water interfacial tension has never been an economically attractive EOR method due to the high amount of adsorption. However, the use of inexpensive surfactants in low concentrations or combination of diluted surfactants with other low-cost chemicals to change the wettability of the system could play a major role in reducing the residual oil saturation and consequently improving oil recovery. This experimental study aims at investigating the potential of nanoparticles to improve the ability of surfactants for enhancing oil recovery in carbonate rocks through wettability alteration using contact angle measurements and coreflood experiments at different experimental conditions.

Dual-Drop Dual-Crystal (DDDC) technique was used to measure the dynamic water advancing contact angles along with the interfacial tension at both ambient and reservoir conditions. A range of surfactants with different chemical structures was tested to select a candidate with the weakest and strongest ability for wettability alteration. The optimum concentration of nanoparticles was determined to combine with the surfactant. The improvements in the wettability alteration behavior of surfactant-based nanofluids were determined through contact angle measurements and supported by coreflood experiments through oil recovery and simulated relative permeability curves.

The optimum concentration of nanoparticles (0.4% wt.) helped to change the wettability of a limestone rock from strongly oil-wet (water advancing contact angle of 167°) to weakly oil-wet (146°) at ambient conditions. The combination of nanoparticles with the least effective surfactant resulted in an incremental recovery of about 37% and improved the wettability alteration capability to reach an intermediate-wet condition (116°) and stayed in the intermediate-wet zone (121°) even

after lowering the concentration of surfactant. The combination of nanoparticles with the most effective surfactant reached an incremental recovery of about 45% compared to using only surfactant. At reservoir conditions, the surfactant-based nanofluid changed the wettability behavior from strongly oil-wet (156°) to intermediate-wet (108°) and led to an incremental recovery of about 30%. The contact angle measurements agreed well with the oil recovery and oil-water relative permeabilities simulated from the coreflood experiments. A preliminary cost analysis showed that combining nanoparticles with diluted surfactants could result in an extra $4.39 profit per barrel of oil.

By measuring precise and reproducible advancing contact angles at both ambient and reservoir conditions and conducting coreflood experiments at different experimental conditions and through investigating the simulated relative permeability curves, this study clearly reveals a potential for nanoparticles to improve the performance of surfactants to change the wettability of carbonate rocks toward less-oil wet or intermediate-wet, which could lead to a significant reduction in the residual oil saturation and enhancement in the oil recovery. Introducing nanoparticles to diluted surfactant solutions affords an opportunity to change the wettability of carbonate rocks toward enhancing oil recovery, thus provides an economically appealing chemical flooding technique.

1. INTRODUCTION

1.1. Background

When oil and gas industry is at a low point with slow activities, lay-offs and uncertainties about the future, great opportunities are provided for technical innovations to develop systems that will make the oil and gas production more affordable and benefit the industry to face any possible depressions in the future. As traditional oil and gas sources are anticipated to continue dominating the energy market, the global demand for energy is expected to increase in the upcoming decades (EIA, 2018). However, while most of the major producing fields in the world are facing the last stages of production, the rate of discovering new fields has dropped in last few decades (BP Stats, 2018). Therefore, the importance of enhanced oil recovery methods to reach about two thirds of the nation's known resources that cannot be recovered by the conventional methods is undeniable (DOE, 2015). While 8.4% of the total US daily oil production belongs to EOR methods, chemical flooding accounts only for 1.5% of the total number of active US EOR projects (OGJ, 2014). The number of successful chemical projects worldwide is now 27, out of which 24 projects are on polymer in sandstone reservoirs and 3 on surfactant with only 1 in carbonate reservoirs (OGJ, 2016). Despite the resulting high recovery, most of the chemical flooding methods are too expensive to be economical. This poses a great opportunity for developing new cost-effective chemical flooding technologies that lead to high oil recoveries.

Over the past few decades, nanotechnology has revolutionized many industries including the oil and gas industry. The application of nanotechnology in different areas of oil and gas industry, such as exploration, drilling, and recently enhancing oil recovery has revealed its potential to initiate groundbreaking changes. The fact that nano-scale particles are much smaller than typical pore spaces that are at minimum 5 to 50 microns, promotes a preference for

nanotechnology over other methods to influence the interfacial properties in the porous media and consequently improve oil recovery.

1.2. Research objectives

This work is an experimental research to study the influence of nanoparticles on the interfacial characteristics of the carbonate rocks and their behavior in combination with surfactants at different experimental conditions. The specific objectives of this research are listed as follows:

1. To evaluate the effect of a wide variety of surfactants on the interfacial properties of carbonate rocks, which leads to selecting candidates for mobilizing trapped oil through wettability alteration quantified by contact angle measurements at both ambient and reservoir conditions and coreflood experiments at different experimental conditions.
2. To investigate the influence of nanoparticles and their concentration on the interfacial properties of carbonate rocks, which leads to finding the optimum concentration for wettability alteration. And to study the behavior of nanoparticles in combination with surfactants through contact angle and interfacial tension measurements at both ambient and reservoir conditions.
3. To study the effect of nanoparticles, with and without surfactants, on the oil recovery and flow characteristics of a carbonate system through wettability alteration using coreflood experiments and relative permeability curves generated by simulating the coreflood results at different experimental conditions.

1.3. Dissertation organization

This dissertation consists of five main sections. First an introduction to this work is provided, which includes the background, research objectives, and organization of the dissertation. Then, a thorough literature review on the wettability, methods to measure the wettability, and techniques to investigate wettability alteration behavior in sandstone and carbonate reservoirs is presented. This section also reviews the role of surfactants in wettability alteration and the influence that nanoparticles can have on improving the oil recovery through changing the wettability behavior of the system. Next section covers the methodology of this research, which includes the coreflood procedure to screen a wide range of surfactants to select the candidates for enhancing oil recovery through wettability alteration. Also, the experimental procedure for contact angle measurements to study the wettability alteration of nanoparticles and their combination with surfactants is explained. Moreover, the coreflood experiments and simulation procedures to investigate the effects on the oil recovery and relative permeability curves are covered. Next section presents the results and discussion of the contact angle measurements and coreflood experiments to evaluate how ability of surfactants as wettability modifiers can be improved by adding nanoparticles through contact angle measurements at both ambient and reservoir conditions and coreflood experiments at different experimental conditions. A preliminary economic analysis is also provided to roughly estimate how profitable would be to use surfactant-based nanofluid in the field. The last part of this section discusses the microscopic investigation of using surfactant-based nanofluid. And the final section concludes the research by listing the findings and providing recommendations for future work.

2. LITERATURE REVIEW

2.1. Wettability

Wettability is defined as the tendency of a solid to be in contact with a fluid in comparison with another fluid due to the imbalance of surface and interfacial forces. It is important to understand the wettability because it plays a significant role in controlling the location, flow, and distribution of fluids in a reservoir (Anderson, 1986). A reservoir rock can have a structural affinity for either oil or water and can be water-wet, oil-wet, or intermediate-wet. The original wettability of a formation shapes the profile of initial water saturation, which affects the productivity during the primary and secondary recovery (Anderson, 1987). Altering wettability can reduce the capillary forces within the pores of a reservoir rock, which leads to the reduction of residual oil saturation and consequently raising the ultimate production during the process of enhanced oil recovery.

The contact angle measurement is the most common approach to determine the wettability of surfaces (Morrow, 1990). At an interface between a fluid and a solid, contact angle is described as the angle between the surface of the fluid and the contact surface. According to Young's equation (Eq. 1.1), contact angle is related to the surface and interfacial tensions at the contact area of the solid and fluid (Figure 2.1).

$$\sigma_s = \sigma_{sf} + \sigma_f \cdot \cos\theta \quad \text{..... (1.1)}$$

, where σ_s is surface free energy, σ_{sf} is interfacial tension between fluid and solid, σ_f is surface tension of the fluid, and θ is the contact angle.

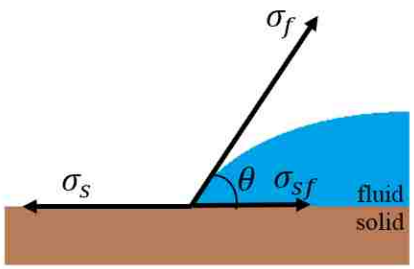

Figure 2.1. Schematic diagram of contact angle and surface/interfacial tensions.

2.2. Contact angle measurements

The contact angle in a reservoir is defined for the oil-water interface against the rock surface and therefore the wettability of the reservoir is evaluated by the water advancing contact angle, which corresponds to the displacement of oil by water. The reservoir is considered to be water-wet when the contact angle ranges between 0° to 60° and oil-wet when it is between 120° to 180°. The contact angles of 60° to 120° represent the intermediate wettability.

A variety of techniques used in industry regarding the contact angle method includes: Sessile drop, modified form of sessile drop, Wilhelmy plate, and Dual-Drop-Dual-Crystal (DDDC). The first three techniques in general have some limitations regarding the wettability characterization through contact angle measurements. For instance, they are not sensitive to roughness and heterogeneity of the reservoir rocks. Also, the contact angle measurements resulted from these techniques are not accurate and reproducible. However, the DDDC technique addressed the concern about the surface roughness (Vijapurapu & Rao, 2003) and was proved to be able to generate precise, consistent, and reproducible contact angle measurements for several reservoir cases (Rao & Girard, 1996).

In DDDC technique, dynamic contact angles are measured using two oil droplets that are placed on two polished crystals made from the reservoir rock. The crystals and droplets are aged

in a cell filled with reservoir or synthetic brine. Then the lower crystal is flipped and the oil droplets on both crystals are merged. At the stage of measuring the contact angle, the lower crystal is gradually shifted while the three-phase-contact-line (TPCL) is monitored. Once TPCL moved, the angle made by the droplet at the point of movement on the lower crystal in the water phase is measured as the dynamic water advancing angle (Figure 2.2).

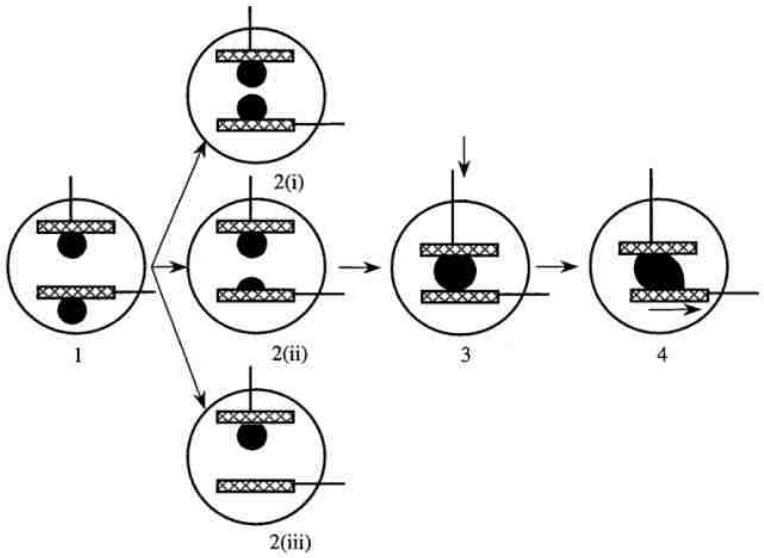

Figure 2.2. Schematic depiction of DDDC technique and the steps to measure dynamic water advancing contact angle (Rao, 2002).

The concept of advancing and receding contact angles and how they relate to reservoir conditions are further studied by Rao (2002). The water receding angle mostly represents the native wettability of the reservoir when oil migrated and displaced the water. In the case of waterflooding, however, oil is expelled from the reservoir by water, which suggests that the water advancing contact angle is the correct indicator for wettability characterization of the system.

2.3. Wettability alteration

2.3.1. Sandstone reservoirs

Changing wettability from mixed-wet or water-wet toward more water-wet conditions in naturally water-wet formations, such as sandstones, have been studied several times in last decades. The areas of studies include but not limited to the following concepts:

2.3.1.1. Low-salinity injection

Morrow et al. (1998) studied the dependency of wettability and laboratory waterflood recoveries on brine compositions and oil/brine/rock interactions and their sensitivity to temperature and crude oil compositions. They found that contact angle measurements at smooth quartz surfaces provide a useful guide for wettability alteration through adsorption but not spontaneous imbibition of brine. They also discovered that oil displacement by condensed water from steam injection can change the wettability by a combined effect of temperature and brine composition. The injection of dilute brine, by considering the avoidance of formation damage, was suggested by them as a preferable method to improve oil recovery.

Webb et al. (2004) conducted a log-inject-log test to observe the effect of low salinity waterflooding on oil recovery within the well region of a reservoir rather than in the laboratory. By ensuring about the establishment of a stable saturation after injection of each brine and through conducting an extensive water sampling to confirm the brine salinities, they found that waterflooding with low salinity brine significantly improved the oil recovery through wettability alteration and controlled removal of clay constituents and showed 25-50% reduction in the residual oil saturation.

Zhang et al. (2007) conducted corefloods using high/low salinity brines and high/low viscosity crude and mineral oil. They showed that the tertiary recovery from the cores with mixed-wettability by injection of low salinity brine produced about 7-14% of OOIP, which was significantly higher than that of high salinity brine. This increase in the oil recovery was observed to be convoyed by a slight change in the pH of the effluent brine and a sharp increase in the pressure drop across the cores. Also, a slight recovery and small pressure response to low salinity waterflood were reported when switching to mineral oil due to an adsorbed oil film remained on the rock surface.

Agbalaka et al. (2009) performed coreflood studies to determine the benefits of low salinity waterflood and the role of wettability in enhancing oil recovery. They examined the low salinity floods in tertiary and secondary recovery process and found that decreasing the brine salinity and increasing the brine temperature gave consistent increase in oil production due to the reduction of residual oil saturation and wettability alteration toward more water-wet especially in the case of secondary recovery process.

The microscopic mechanism of the low salinity effect was clarified by Berg et al. (2010) through providing a direct visualization of the detachment of crude oil from clay minerals. By changing the brine from high salinity to low salinity, they could observe the release of crude oil from a substrate covered with clay particles inside a flow cell. For very low salinity, they found up to 80% of crude oil release along with the decomposition of clay minerals and migration of fines referred to a formation damage. The use of high salinity brine, however, led to the release of oil and lower amount of clay swelling named as controlled formation damage.

Alotaibi et al. (2010) studied the oil/water/rock interactions at different salinity levels (synthetic formation brines, aquifer, and seawater) by determining wettability through contact

angle and zeta potential techniques at high pressure/high temperature conditions for sandstone reservoirs. By observing a direct relationship between the zeta potential and ionic strength, they found that the surface charges of clay and sandstone particles are highly affected by salinity of the injection water.

A systematic study combining Amott/USBM methods with corefloods to determine the key mechanisms of oil recovery by low-salinity injection was performed by Shakershiran and Skauge (2012). Although the clay content in Berea cores favors oil recovery in low salinity waterflooding, the oil-wet characteristics of the Bentheimer cores were reported to be a more important factor for improving oil recovery.

Nasralla et al. (2013) investigated the causes of wettability alteration by low-salinity water by studying the effect of changing ionic strength on the electro kinetic charges and conducting corefloods to correlate that with oil recovery improvement. They discovered that low-salinity water made the surface charges at rock/brine and oil/brine interfaces strongly negative which resulted an increase in the repulsive forces at the rock/oil interface and led to wettability alteration and oil recovery improvement confirmed by coreflood experiments.

Shabib-Asl et al. (2015) also studied the mechanism by conducting an exclusive study on 31 sandstone core slices saturated with formation water and aged in crude oil at 80 ℃ and ambient pressure. They used a low-salinity water, consisting of 30 samples of different compositions with concentrations ranging from 500 to 6500 ppm. Their results showed a significant change in wettability with low-salinity water composition of potassium and sodium monovalent ions as compared to the divalent cations of magnesium and calcium.

2.3.1.2. Mixed-wettability state

The unusually efficient displacement of oil by water and the very low residual oil saturation in the East Texas reservoir made Salathiel (1973) to investigate the mechanism through some systematic laboratory examinations. A mixed-wettability state was defined when neither strongly water-wet nor strongly oil-wet porous rocks can be flooded by water to unusually low oil saturations. In this state the small pores and grains are water-wet and large pores are oil-wet, which provides paths for oil to flow even at very low saturations.

Melrose (1982) studied the nature of the mixed-wettability state in the reservoirs by performing a physio-chemical analysis of the attractive and repulsive forces existing in the thin aqueous wetting films. It was shown that there existed a lower limit to the pore size, in which thin wetting films would occur and that limiting size depended on the brine salinity. It was also shown that the effect of the pore size on wettability of the system was related to the pore size distribution and the initial water saturation of the rock.

Wood et al. (1991) discovered a strong dependency of residual oil saturation on pore volume injected in the mixed-wettability reservoirs. They conducted laboratory examinations to minimize uncertainty in predicting effective residual oil saturation by considering the effects of relative permeability, gravity forces, and imbibition capillary pressure. They also presented a mechanistic simulation approach to scale up the laboratory results that account for all the active forces.

Tong et al. (2003) studied the effect of oil compositions on wettability alteration through establishment of mixed-wettability in sandstones. They showed that a close reproducibility of sequential spontaneous imbibition measurements provides a measure of stability for induced mixed-wettability states. Further indication of reproducible wetting states for two different crude

oils were also provided by geometric mean viscosity of oil and water through scaling of recovery of mineral oils.

Kumar et al. (2008) developed a technique using radio frequency plasma treatment in water vapor to modify the surface energy of clastic and carbonate rocks and micro-tomographic observations of the pore-scale fluid distributions. By establishing a mixed-wet state, they provided insight into the role of rock microstructure and surface energy variability in determining recovery, which led to another complimentary approach to observe the multiphase-fluid occupancy in pores by combining the detailed knowledge of the 3D pore structure and information on the surface chemistry of pore walls (Kumar et al., 2012).

A combination of low-salinity brine and surfactant flood was tested on mixed-wet sandstone cores by Alagic and Skauge (2010) to find the possible underlying mechanism leading to 90% recovery. They found the mechanism to be the destabilization of oil layers caused by change in brine salinity and simultaneous mobilization of the residual oil at low interfacial tension.

Kathel & Mohanty (2013) evaluated several surfactants at reservoir temperature and salinity by measuring contact angles on clay-rich sandstones and conducting spontaneous imbibition on reservoir rocks to identify chemicals to add to the injection water to induce imbibition into a mixed-wet tight fractured sandstone reservoir. They showed that the use of 0.1 wt.% surfactant solution can change the wettability from oil-wet towards less oil-wet condition on mineral plates and 68% incremental recovery can be obtained through spontaneous imbibition on 10 mD oil-wet/mixed-wet sandstone reservoir cores.

Arsalan and Nguyen (2016) performed a systematic approach to characterize the mixed-wet characterizations of sandstone and carbonate rocks by establishing a relation between the volume fraction of the mixed-wet reservoir and rocks and surface energy of the mixture. They

found that Lifshitz-van der Waals component of the rock mixture did not change with wettability alteration of the system. But acid-based components showed a significant decrease with increasing oil wetness.

2.3.1.3. Spontaneous imbibition

Spontaneous imbibition is a process in which a non-wetting fluid is displaced by a wetting fluid in a porous media under the effect of capillary driving forces. A useful characterization of wettability can be provided by measuring the rate of spontaneous imbibition. Morrow (1994) proposed a new method to quantify wettability by correlating with capillary driving forces through saturation vs. time curves, which were used to obtain pseudo imbibition capillary pressure curves. He defined a wettability index based on relative areas under these curves as the relative pseudo work of imbibition. The method was used for different oil/brine/rock system to link the wettability indices with waterflood recoveries.

Another method was developed by Li and Horne (2001) to characterize the process of spontaneous water imbibition into gas-saturated rocks to calculate the water relative permeability and capillary pressure curves from the imbibition data. They discovered a linear relationship between the imbibition rate and reciprocal of gas recovery and experimentally confirmed it at different initial water saturation rate and found almost no effect of initial water saturation on residual gas saturation by spontaneous water imbibition.

Babadagli (2003) analyzed the mechanisms and performed up-scaling exercises for oil recovery by the spontaneous imbibition of surfactant solutions from naturally fractured reservoirs. He observed that the imbibition recovery by surfactant solution was strictly controlled by the surfactant concentration for some of the rock samples such as chalks. He also correlated the

ultimate recoveries to the Inverse Bond Number using twenty-five cases covering four types of rock, oil and surfactant samples.

Hatiboglu and Babadagli (2006) investigated optimum matrix oil recovery strategies in naturally fractured reservoirs by comparing two cases: the primary counter-count spontaneous imbibition followed by the diffusion of a miscible phase and primary diffusion of miscible fluid without pre-flush of matrix by the spontaneous imbibition. They found the recovery with capillary imbibition followed by diffusion the optimal way in water-wet cases. For limestone and aged sandstone samples starting the recovery by diffusion led to a higher recovery rate and higher ultimate recovery.

Kerunwa et al. (2016) developed an analytical model to characterize the scale the counter-current spontaneous water imbibition for different oil/water/rock systems and found a linear correlation between the oil recovery and the square root of imbibition time. They confirmed the model with experimental work on sandstone reservoir cores to observe that the spontaneous imbibition in oil saturated rocks with different permeabilities and interfacial tension values can be predicted by the model. The experimental data were also scaled up for different injection fluid to design proper improved recovery methods.

2.3.1.4. Chemical flooding

Chemical agents are used to increase the oil recovery by altering the wettability of the reservoir toward less oil-wet. The economics of the chemical flooding processes is always a factor to question the applicability of the method. Froning and Leach (1967) conducted a small-scaled field test at a single well for measuring chemical requirements to provide a more reliable evaluation of the applicability and economics of the process. They showed that for a sulfide agent in a sandstone

reservoir and a carbonate-phosphate agent in a limestone reservoir, the potential chemical costs are less than one dollar per barrel of additional oil.

Smith (1978) examined the efficiency of pre-flushing in ion-exchanging situations by studying the replacement of divalent cations by less offensive monovalent cations in sandstone reservoirs. The proposed one-dimensional model could make idealized estimations of reservoir pre-flush efficiency using the experimental information on CEC, shape of exchange isotherm, and composition of resident and pre-flush brines.

Wu et al. (1996) used a reservoir simulator and combined the results with an economic model to study the design and optimization of a low-cost chemical flooding in a sandstone reservoir. They found the best results for the case, where low concentrations of both surfactant and polymer were simultaneously injected. Their sensitivity analysis showed that the most important economic variables in designing the optimum chemical floods were oil price, discount rate, operating cost, and chemical prices.

Kumar et al. (2008) studied the mechanisms of wettability alteration by crude oil components and surfactants on silicon and mica substrates using atomic force microscopy process. They investigated surfactant imbibition into the parallel plates filled with crude oil and found that wettability is controlled by the adsorption of asphaltenes. They also suggested that the anionic surfactants can remove the adsorbed components from the mineral surfaces and change the wettability toward more water-wet faster than cationic.

A field-scale polymer flooding process was studied by Xiaoqin et al. (2013) on a low permeability thin sandstone layers with narrowly-developed channel sands and poor continuity of sand bodies. By strictly selecting the objectives, carefully dividing the layer groups of

development, shortening the well spacing, and strengthening the injecting of polymer into the separated-layers, they were able to enhance the recovery of polymer flooding by more than 10%.

2.3.2. Carbonate reservoirs

The oil-wet nature of formations (such as carbonates) creates the opportunity to investigate a variety of concepts with regards to changing the wettability toward intermediate-wet and water-wet conditions. These concepts include but not limited to the following:

2.3.2.1. Rock-fluid interactions

Cuiec (1984) performed a study to evaluate the wettability of 20 non-water wet reservoirs from Europe, North Africa and Middle East and understand the rock/crude-oil interactions responsible for the existence of such reservoirs. Besides finding a correlation between the wettability and asphaltene content for most of the reservoirs, it was discovered that the products from crude oils with a boiling point below 350 °C are most likely not involved in solid/crude-oil interactions. It was also realized that the intermediate fractions of crude oils have great influence on the wettability, amount of which varied with fractions and rock type. It was reported that no correlation existed between wettability and the amount of resin, aromatic hydrocarbon, and nitrogen in the crude oil.

Based on an investigation on the intermolecular surface forces, Hirasaki (1991) provided a wettability description through morphological aspects of the pore space with contact angle as a boundary condition for the fluid distribution. His approach originated with Derjaguin-Landau-Verwey-Overbeekk's (DLVO) theory of colloidal stability, which is based on electrostatic and van der Waals interactions. Using this approach, he examined the values of the contact angles when the wetting film collapses, while taking capillary pressure and the curvature of the pore walls into

account. His work helped to understand how fundamental surface forces affect the magnitude of advancing and receding contact angles to describe the wettability of the petroleum reservoirs.

Vijapurapu & Rao (2003) examined the effect of rock mineralogy and surface roughness on wettability in rock/brine/hydrocarbon systems for calcite and dolomite. They compared the advancing and receding contact angles averaged over surface area of solid substrates from Wilhelmy-plate and DDDC techniques and characterized the surfaces using an optical profilometer and Scanning Electron Microscopy. They found that DDDC technique showed significant effects of mineralogy and roughness on dynamic contact angles while Wilhelmy plate technique exhibited insensitivity. They also showed that dolomite and calcite surfaces almost retained a strongly oil-wet nature within the range of roughness inspected.

Strand et al. (2006) studied the chemical mechanism behind the wettability alteration process through investigating the water film between the rock and the oil phase by measuring the Zeta potentials of the oil-water and oil-rock interfaces for carbonates. They showed that the sulfate presence in the seawater as the injection fluid could change the wettability of the chalk from oil-wet to water-wet at high temperatures. They also found that higher temperatures increased the imbibition rate and recovery rate due to a stronger adsorption of Ca^{2+} and SO_4^{2-} onto the chalk surface. They discussed the wettability alteration mechanism based on the results from the chromatographic adsorption and the imbibition studies and, using the zeta potential measurements, confirmed that the relative concentration of Ca^{2+} and SO_4^{2-} dictated the charge properties of the chalk surface to play a significant role in the wettability alteration.

2.3.2.2. Fractured reservoirs

Civan et al. (1999) developed a mathematical model to study the wettability alteration effects of matrix-to-fracture flow on oil displacement by water imbibition in naturally fractured reservoirs. They coupled the two-phase flow in the fracture network and porous matrix through an oil-water exchange function that incorporates the rate of oil transfer from dead-end pores to pore networks and eventually fractures. They found that the rate constants and matrix wettability play important roles in obtaining an accurate description of the oil recovery during waterflooding in naturally fractured reservoirs.

Hirasaki and Zhang (2004) evaluated sodium carbonate and anionic surfactant solutions for enhancing oil recovery by spontaneous imbibition from oil-wet fractured carbonate formations. They developed a process to overcome the retention of oil by working on the wettability and capillarity using surfactants. They found that the positively charged calcite could be made negatively charged through the presence of Na_2CO_3/$NahCO_3$ in the brine. By using an alkaline surfactant solution to reduce IFT at alter wettability towards more water-wet conditions, they also discovered that oil displacement could occur by both buoyancy and capillarity, if the contact angle is less than 90°.

Ayirala et al. (2006) explored the benefit of surfactants in altering the wettability of oil-wet fractured formations, which occurs through surfactant diffusion form the fracture into the matrix that enables imbibition of even more surfactant into the matrix. They believed that the sequential process of initial diffusion followed by imbibition would lead to a significant enhancement in the oil recovery. To examine that, they developed a new experimental procedure using the DDDC technique to simulate the matrix-fracture interactions in fractured reservoirs by measuring highly reproducible dynamic contact angles ad IFT values. They found that the higher

concentrations of nonionic surfactants (500-3500 ppm) and all the concentrations of anionic surfactants (50-3500 ppm) were effective in changing the wettability of the strongly oil-wet dolomite surface to less oil-wet or intermediate wet. They also quantitatively better explained the rock-fluids interactions using the dimensionless Bond number that includes contact angle term.

By identifying the underlying mechanisms, Gupta & Mohanty (2008) studied the effect of salinity, surfactant concentration, electrolyte concentration, and temperature on the wettability alteration of oil-wet fractured carbonate reservoirs through measuring the contact angles, interfacial tensions, and phase behavior. They found that the extent of maximum wettability alteration decreases as the reservoir salinity increases, but the surfactant concentration needed for that extent decreases. They also found that wettability of carbonates can be changed by divalent ions at high temperature and sulfate and calcium ions play a more important role than magnesium ions in altering wettability.

Delshad et al. (2009) performed a scaled-up study using a chemical compositional reservoir simulator with the capability to model oil recovery from mixed-wet carbonate rocks in both static imbibition and dynamic fractures block experiments by altering wettability. Their simulator captured the key recovery elements of capillary and neutral imbibition, wettability alteration, buoyancy, oil mobilization, and viscous pressure gradient in imbibition experiments. By generating dimensionless scaling groups for each experimental condition, they found that a collaboration of wettability alteration, ultra-low IFT, and emulsification under small viscous pressure gradient, provides a profitable opportunity in fractured carbonate reservoirs. Based on their scaled-up simulations, the static and dynamic imbibition experiments were dominated by buoyancy and viscous force respectively.

2.3.2.3. Wettability alteration using surfactants

Austad et al. (1998) conducted spontaneous imbibition experiments using cationic surfactants on low-permeable oil-wet and water-wet chalk cores at ambient and reservoir conditions. Using an oil-wet chalk, they produced about 13% and 65% of the oil from the core with a very low imbibition rate in 90 days before and after applying surfactant solution respectively, which was related to the wettability alteration toward water-wet conditions. They also performed imbibition experiments for a stack of actual low-permeable water-wet chalk cores using crude oil and cationic surfactant mixed in brine, which resulted in producing a negligible extra oil after applying surfactant as a tertiary flood condition following a waterflood. By running centrifuge experiments, they confirmed that extra oil production by gravity forces under tertiary flood conditions was more difficult for a water-wet system than for a mixed-wet system.

Similarly, Standnes et al. (2002) used nonionic and cationic surfactants to improve spontaneous imbibition of water into the oil-wet carbonate cores with different levels of heterogeneity at room temperature. They were able to produce more oil using the nonionic surfactant, being 40-50% and 65% for the short and long cores respectively. They observed no systematic influence of cores heterogeneity on oil recovery. They also found that wettability alteration using nonionic surfactant was very small and fluid flow was mainly governed by gravity force. However, the cationic surfactant changed the wettability toward more water-wet conditions combining the capillary and gravity forces for driving the fluid.

Seethepalli et al. (2004) further investigated the interaction of 10 different dilute alkaline anionic surfactant solutions with crude oil on carbonate mineral surfaces by conducting experiments on wettability, phase behavior, interfacial tension, and adsorption in the presence of crude oil and synthetic reservoir brine. They identified anionic surfactants as more affecting agents

to alter the wettability of the calcite surface to intermediate/water-wet conditions compared to cationic surfactants. They showed that all different carbonate surfaces (lithographic, limestone, marble, dolomite, and calcite) have similar behavior in terms of wettability alteration with an anionic surfactant. They also found that the adsorption of sulfonate surfactants can be significantly reduced by adding Na_2CO_3 to the brine.

Rao et al. (2006) studied the potential of enhancing oil recovery using low-cost surfactants to alter wettability characterized by contact angles and oil-water relative permeabilities at ambient and reservoir conditions. They used different combinations of rock-fluids systems with Berea sandstone/Yates dolomite, Yates stock tank/live crude oil, and Yates synthetic brine to evaluate the effect of nonionic and anionic surfactants on wettability alteration. The DDDC technique was adopted to measure the contact angles and was combined with oil-water relative permeabilities computed by history matching the oil recovery and pressure drop data from the coreflood experiments. They suggested that the shifts in the relative permeability ratio curves would indicate the ability of both surfactants to develop mixed-wettability in the sandstone cores. They also found that for Yates live oil/dolomite system, the nonionic surfactant altered the wettability from weakly water-wet to a mixed-wet condition, while anionic surfactant changed the wettability to strongly oil-wet system. They reported that both surfactants resulted in a wettability alteration from strongly oil-wet to weakly oil-wet for Yates dolomite/Yates stock tank oil/Yates brine system.

Sharma and Mohanty (2011) investigated carbonate reservoirs at high-temperature high-salinity conditions to change the wettability using three types of diluted surfactant solutions. They conducted initial contact angle measurements and spontaneous imbibition to screen the surfactants before coreflooding with and without surfactant as the secondary recovery method. They observed that some of dual-surfactants (mixture of two different type) proved to be effective for wettability

alteration and led to a recovery of 70 to 80% of OOIP during the spontaneous imbibition. They also found that secondary flooding using the effective surfactants increased the recovery from 29% for waterflood to 40% for surfactant flood.

To address the non-uniformity of wettability alteration in a complex reservoir rock and its dependence on time, Kalaei et al. (2013) developed a time-dependent wettability alteration model to correlate the contact angle to the surfactant concentration through an empirical correlation based on experimental data. They achieved a good quantitative agreement between the simulation outcomes and experimental data from the literature. Based on the simulation of the surfactant solution imbibition in laboratory scale cores using the proposed model, they discovered the dynamic behavior of the wettability alteration, which plays an important role in history matching and prediction of oil recovery from oil-wet reservoirs.

Nguyen et al. (2014) studied different types of surfactants including: non-ionic, cationic, anionic, and amphoteric, for spontaneous imbibition into oil-wet Eagle Ford shale outcrop cores and Bakken shale reservoir cores. They investigated the mechanisms of wettability alteration under the effect of salinity, surfactant concentration, electrolyte concentration, and temperature. They found the wettability alteration from oil-wet to water-wet a more significant factor than a low interfacial tension in enhancing oil recovery rate from fractured oil-wet reservoirs, especially for nonionic and amphoteric surfactants. They reported an incremental oil recovery of about 24% for 0.1% cationic surfactant and 57% for 0.1% nonionic surfactant.

Neog and Schechter (2016) analyzed the potential of surfactants in changing wettability and improving the oil recovery through spontaneous imbibition in ultra-tight oil-rich Wolfcamp shale reservoir. By measuring contact angles and IFT at reservoir temperature and conducting

spontaneous imbibition using 3D computed tomography methods, they showed that the Wolfcamp shale is intermediate-wet and surfactants have the potential to alter the wettability toward water-wet condition. They found the highest oil recoveries corresponding to the surfactants that changed the wettability significantly but lowered the IFT slightly due to the strong capillary driven forces. They found the traditional nonionic surfactants to be more cost-effective options compared to the novel proprietary surfactant blends for stimulating and EOR applications in Wolfcamp shale.

2.4. Surfactant flooding

The number of chemical projects in the US has been drastically declining in the last three decades from 206 projects in 1986 (OGJ, 2006) to only 3 projects in 2014 (OGJ, 2014). The expense of utilizing surfactant for EOR was so high that no project was reported in 2006 (Figure 2.3). The number of successful chemical projects worldwide is now 27, out of which 24 projects are on polymer in sandstone reservoirs and 3 on surfactant with only 1 in carbonate reservoirs (OGJ, 2016). Most of the investments in the chemical flooding had always been directed toward studies that focused on polymers as mobility control agents and their combination with alkaline and surfactants to simultaneously provide a stable reduction in the interfacial tension and ultimately improve the oil recovery.

Bauer and Klemmensen (1982) developed a water-soluble acrylic polymer as a cost-effective, mobility control agent for enhancing oil recovery. The polymer was designed to be stable to mechanical shear, non-plugging in porous media, demonstrable tertiary oil recovery, stable in the presence of salt and chemicals, and retention of viscosity after extended exposure to high temperatures. They performed corefloods using both polymer-augmented waterfloods and caustic-polymer waterfloods and found the similar enhanced oil recovery with no indication of core plugging compared to the commercial partially hydrolyzed polyacrylamides.

Li et al. (2000) applied the method of orthogonal-test-design by measuring phase behavior and transient interfacial tension of the oil/aqueous phase to screen the alkaline/surfactant/polymer flooding systems. Using cheap and naturally mixed materials, the optimal cases they obtained increased the oil recovery by 26.8% of original oil in place.

Nedjhioui et al. (2005) examined the influence of combining two anionic surfactants with polymer solutions containing Xanthan gum and NaOH as an alkali on properties of the mixed systems. They applied the optimum ASP to an Algerian crude oil and showed the significant effects of synergetic action of two surfactants on the interfacial tension and conductivity of the crude-oil/water system.

Mandal and Ojha (2008) also obtained an optimal ASP formulation using sodium dodecyl sulfate and sodium dodecylbenzene as anionic surfactants mixed with NaOH and polyacrylamide. They studied the variation of conductivity and surface tension and their corresponding effect on the polymer viscosity to find that 0.7 wt.% alkali with 2000 ppm polymer and 0.1 wt.% and 0.075 wt.% surfactant concentrations resulted in a significant influence on the mobility and interfacial tension to improve the oil recovery.

However, recently surfactants themselves slowly started to find their own place among EOR chemical projects and gradually dominate polymer treatments. As shown in Figure 2.3, the number of chemical flooding projects that used surfactants increased from 1 project in 2008 to 3 projects in 2014.

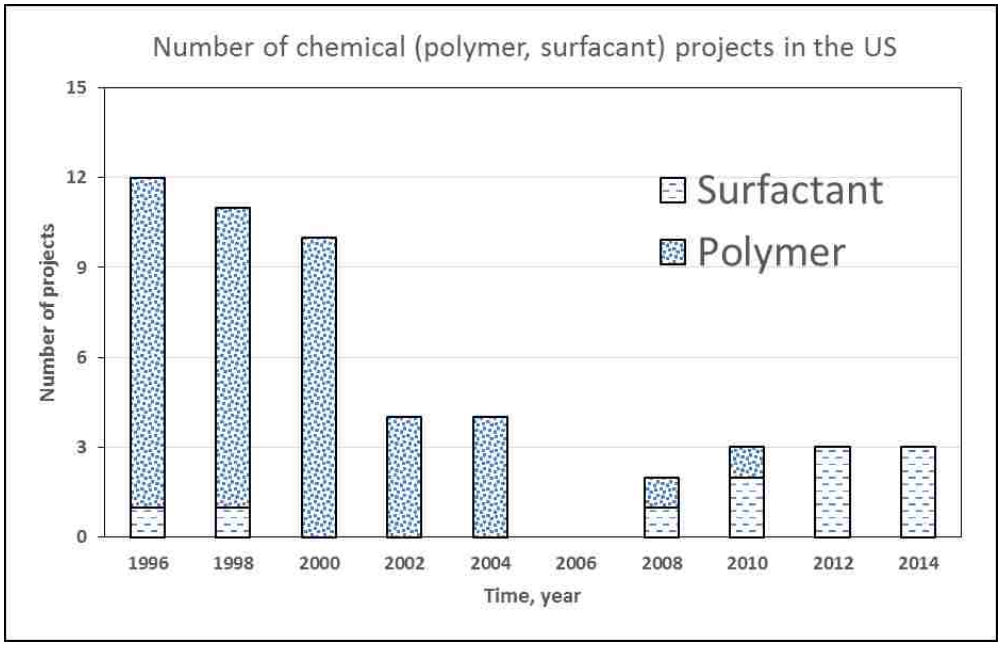

Figure 2.3. Total number of chemical, polymer, and surfactant projects in the US (OGJ, 2006 & 2014).

The two basic characteristics of surfactants that make them useful in the EOR projects are the ability to both lower the oil-water interfacial tension and change the reservoir rock wettability behavior. The degree to which a surfactant is effective in EOR applications can be well understood by using capillary number, which is the ratio of viscous to capillary forces (Eq. 2.1):

$$N_c = {}^{v\mu}/_{(\sigma \cos\theta)} \quad \text{..... (2.1)}$$

, where N_c is the capillary number, v and μ are the velocity and viscosity of the displacing phase respectively, σ is the interfacial tension between fluid phases, and θ is the contact angle between fluid-fluid interface and solid surface.

Surfactants are capable of increasing the capillary number by lowering the oil-water interfacial tension and changing the contact angle. In order to significantly reduce residual oil saturation and improve oil recovery, four to six orders of magnitude increase in the capillary

number is required (Klins, 1984). To apply several orders of magnitude reduction in oil-water interfacial tension, a huge amount of surfactant is required due to their tendency to adsorb on the rock surface. This has made surfactant flooding an uneconomical EOR method in most of the conventional attempts that relied mainly on reducing oil-water interfacial tension. On the other hand, by changing the contact angle toward 90° to make the capillary number infinitely large, surfactants can play a major role in economically improving the oil recovery by altering the wettability of oil-wet reservoirs toward intermediate and mixed wettability conditions. The tendency of oil industry to invest more on surfactants flooding in recent years is believed to be due to the focus of researches on the wettability alteration ability of the surfactants.

Rao (2002) presented a newly developed DDDC technique to generate reproducible and highly accurate measurements of water-advancing and water-receding contact angles at elevated reservoir pressures and temperatures. This technique was designed to consider the dynamic behavior of the oil-water-rock three-phase boundary in water-wet, intermediate-well, and oil-wet solid-fluid systems. One of the main applications of the technique was mentioned to be providing detailed understanding of the effect of different surfactants used in the oil field operations on reservoir wettability alteration. He also compared DDDC to various conventional contact angle measurements techniques along with case studies and showed that it overcomes some of the limitations such as inability to account for the effect of the adhesion interaction at the solid-liquid-liquid interface (Rao, 2003).

Vijapurapu and Rao (2003) examined the effect of rock minerology and surface roughness on wettability in rock-brine-hydrocarbon systems by measuring the contact angles. They used Wilhelmy-plate technique to obtain dynamic contact angles averaged over the surface area of the solid substrate and compared to DDDC technique used for both smooth and rough solid surfaces

of different minerology. They characterized the surfaces using Optical Profilometer and Scanning Electron Microscope methods and found that DDDC technique demonstrated the effects of minerology and roughness on dynamic contact angles and hysteresis while Wilhelmy-plate technique showed insensitivity. Their work was followed by other studies to examine the wettability alteration potential of diluted low-cost surfactants (Rao et al., 2006) and their beneficial effects in oil-wet fractured reservoirs (Ayirala et al., 2006).

Later, Xu et al. (2008) used live and stock-tank crude oils at reservoir conditions of 82 ºF and 700 psi to measure interfacial tension (IFT) and dynamic contact angles in the presence of different surfactants. They found that nonionic surfactant altered the water-wet behavior of the live oil system to intermediate-wet and had no effect on the strongly oil-wet behavior of stock-tank oil system. On the other hand, anionic surfactant changed the strong oil-wet behavior of the stock-tank oil to less oil-wet and weakly water-wet behavior of the live oil to strongly oil-wet indicating the possibility of that surfactant to develop continuous oil-wet paths for potential mixed wettability state.

Chen and Mohanty (2014) developed strategies to improve oil recovery at high temperatures in highly fractured carbonate reservoirs that contain high salinity and high hardness formation brines using surfactants. They showed that the nonionic surfactant was stable at high salinity and high temperature with great influence on the wettability alteration and imbibition oil recovery. They also formulated anionic surfactants to recover oil mainly by gravity drainage since there was no wettability alteration effect in the hard brine.

2.5. Nanotechnology

Since 1959, when the concept of micro machines was first presented by the Nobel Prize winner Richard Feynman, miniaturization has been a major trend in the modern science (Choi, 1998) and an inspiration for the new field of nanotechnology. When the utilization and development of nanomaterials became practical in early 60's, nanotechnology started to be applied in different industries, such as medicine, electronics, aviation, and energy sectors (Kaasa, 2013).

Nanotechnology, in general, is defined as fabrication, manipulation, and application of objects in the size range of 1 to 100 nm (Edwards, 2006). The nanoscale proportion of the objects is the key point that creates unique properties especially in the upstream domain of oil and gas industry (Kapusta et al., 2011). In exploration, nano sensors help to collect more precise information about the reservoir and enhance the imaging resolution. In drilling, nanomaterials can be used to make or coat the equipment and platforms to improve resistance against corrosion, wear, and shock and also to enhance thermal conductivity. They have also been widely employed to increase cement strength (Kong and Ohadi, 2010).

Over the past decade, nanotechnology has also revealed its potentials to initiate groundbreaking changes in enhanced oil recovery methods. The fact that nanoscale particles are much smaller than typical pore spaces that are at minimum 5 to 50 microns promotes a preference for nanotechnology over other methods to influence the interfacial properties in the porous media and consequently enhance oil recovery.

2.6. Nanoparticles

Nanoparticles, which typically have sizes in the range of 1 to 100 nm are much smaller than typical rock pore channels with sizes in microns (Li et al., 2013). Therefore, nanoparticles can penetrate

through the reservoir easily. Since the thermal, rheological, and stress-strain properties of nanoparticles strongly depend on their size and shape (Miranda et al., 2012), the amount of nanoparticles to apply in oil wells and consequently the cost of it becomes significantly low (Ayatollahi, 2012).

Nanoparticles can be manufactured in the desired shape, size, structure, and functionalities, both mechanically and synthetically (Kaasa, 2013). Das et al. (2007) described a nanoparticle as a combination of two main parts: a core that could be ceramic, metallic, or polymeric and a thin shell, which may be ionic, molecular, polymeric, ceramic, or metallic. Typically, a ceramic or metallic core and a molecular shell is the type of nanoparticles encountered in the researches. The properties of a nanoparticle depend mainly on its core. The solubility or dispersion of the nanoparticle is determined by the chemical nature of the shell. The molecular shell consists of three distinct regions to protect the core: a tail group, an active head group, and a hydrocarbon chain, as seen in Figure 2.4.

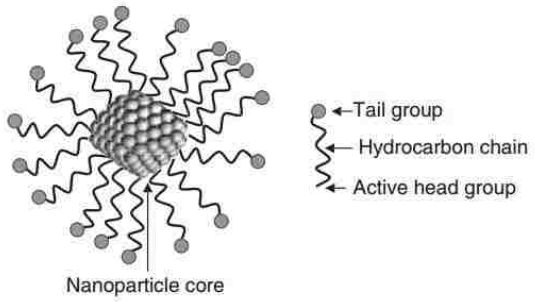

Figure 2.4. Schematic of a nanoparticle consisting of core and shell. The shell has three distinct regions of head, chain, and tail (Das et al., 2007).

A nanoparticle with a size on the order of nanometer has a core that contains several thousands of atoms of a certain material. The molecular shell has chemical affinity with the nanoparticle core through the active head group atoms. For instance, in an oxide nanoparticle, the

metal at the core surface can link with an alkoxide (–OR, where R is alkyl). This set of links covers the whole surface of the core and is called protective monolayer. The hydrocarbon chain could be long or just absent depending on the application of the nanoparticle. As the protective monolayer assembly becomes organized (as in the case of long chains) the ions and molecules of the medium fluid cannot access the core leading to a higher chemical stability of the nanoparticle.

2.7. Nanofluids

Nanofluids are prepared by adding nanoparticles to a dispersing medium fluid or solvent, such as water, oil, propanol, ethanol etc. Nanoparticle disperse in the medium fluid or solvent by interacting through its tail group. Nanoparticles typically behave like surfactants molecules but stronger, especially if absorbed on a fluid-fluid interface (Binks, 2002). Based on the type of the tail group, nanoparticles may be divided into three groups (Hendraningrat et al., 2013; Onyekonwu et al., 2010): hydrophilic nanoparticles that dissolve in polar solvents (e.g. water, brine), hydrophobic nanoparticles that dissolve in non-polar solvents, (e.g. toluene, ethanol, and propanol), and neutral-wet nanoparticles that possess both hydrophobic and hydrophilic parts. For example, in the case of a hydrophilic nanoparticle, the tail group could be –COOH or $–NH_2$, which after ionization may become $–COO^-$ or NH_3^+ to give a net negative or positive charge to each chain connected to the core. Since a nanoparticle can possess both negative and positive charges, the net effect defines the charge of the system. Moreover, the shell protecting the core does not necessarily have to be in a molecular form. In many cases, the shell itself is an inherent part of the core. For example, the surface of silica nanoparticles is often a layer of hydroxyl group that helps the nanoparticles to be easily suspended in water.

Silica is a common name for inorganic water-soluble non-toxic odorless ceramic materials that are composed of silicon dioxide (SiO_2) and can be found or produced in a wide range of

structures from amorphous to crystalline forms, such as quartz (Kaasa, 2013). Silica is the most abundant mineral in the earth crust and is characterized by a very low bulk density (0.04 g/cc-0.1 g/cc) and high specific surface area (200-300 m^2/g). Miranda et al. (2012) listed the advantages of silica nanoparticles as an EOR agent. They have great suspension stability since surface forces easily counterbalance the force of gravity. Also, the size and shape of silica nanoparticles can be tailored during the manufacturing. The chemical properties can also be controlled by changing surface coating chemicals. Finally, silica nanoparticles are very environmentally friendly compared to chemical agents because they are mainly composed of SiO_2, which is the main component of sandstones.

2.7.1. Nanofluids and wettability alteration

In recent years, attentions have been drawn to the influence of nanofluids on the wetting behavior of the reservoir rocks. Wettability alteration by nanoparticles is mainly due to their adsorption on the surface of the rock and forming a layer on it. Hydrophilic nanoparticles can turn an oil-wet rock into water-wet or an already water-wet rock strongly water-wet, while hydrophobic nanoparticles can change a water-wet rock to oil-wet or an already oil-wet rock to strongly oil-wet.

Carpenter (2015) reviewed different wettability alteration methods with nanomaterial applications. After assessing the fundamentals of wettability alteration, the use of nanomaterials for wettability alteration was discussed and it was reported that silica and polysilicon resulted in higher efficiency in terms of incremental oil recovery in waterflooding.

Jiang et al. (2017) investigated the influence of silica nanoparticles on wettability and IFT through contact angle measurements. They showed that the contact angles on quartz plates had

relatively large uncertainty while those on calcite plates showed a clear trend. They found that the smaller the nanoparticle size and the larger the nanofluid concentration, the lower the contact angle. Moreover, they did not observe any effect of silica on IFT. They reported an increase of 8.7% in oil recovery through coreflood experiments using silica nanoparticles due to wettability alteration.

Onyekonwu et al. (2010) studied the ability of three different polysilicon nanoparticles to enhance oil recovery through wettability alteration. They conducted corefloods using two types of oil, one brine, and three types of polysilicon nanofluids on water-wet reservoir rocks from Niger Delta. The nanofluid types included hydrophilic, hydrophobic, and neutral-wet. Their results indicated that hydrophobic and neutral-wet nanofluids enhanced the oil recovery. They recognized the mechanism as the change in wettability and reduction in IFT, which could be achieved by improving the quality of ethanol as the dispersing agent and therefore recommended the dispersion of hydrophobic and neutral-wet nanoparticles in ethanol for enhancing oil recovery in water-wet formations. Hydrophilic nanoparticles were also suggested to be used for oil-wet formations due to their poor EOR performance with water-wet rocks.

Miranda et al. (2012) performed molecular dynamic calculations to investigate the wettability alteration potential of the neutral silica nanoparticles functionalized with different groups (OH, sulfonic acid, PEG, and EG) dispersed in NaCl or $CaCl_2$ for enhanced oil recovery applications at high salinity and temperature conditions and found PEG as a promising group to make the nanoparticles effective toward changing contact angle and enhancing oil recovery.

Ju et al. (2002) studied the permeability change to improve the water injection rate in the porous media through wettability alteration caused by the adsorption of nano-structured polysilicon on the surface of sandstone rocks. They conducted corefloods using nanoparticles

mixed with organic solvents and developed a mathematical model to numerically simulate water injection enhanced by polysilicon nanoparticles through changing wettability for several oil fields. They showed that well treatments with solvent slugs of suspended polysilicon nanoparticles improved the effective permeability of water-phase and also increased the average injection rate by 5 times.

Roustaei et al. (2012) also investigated the impact of hydrophobic and neutral-wet polysilicon nanoparticles dispersed in ethanol on IFT and contact angles for sandstone rocks. Their results showed a wettability alteration toward less water-wet condition and a significant reduction in oil-water interfacial tension from 26.3 mN/m to 1.75 mN/m and 2.55 mN/m for hydrophobic and neutral-wet nanofluids respectively. They also reported increase in oil recoveries by 32.2% and 28.57% using 4 gr/liter concentrations of hydrophobic and neutral-wet nanofluids respectively. The difference in the oil recoveries was described to be influenced by the fact that neutral-wet nanofluids had more contribution in altering the wettability while hydrophobic nanofluids had higher impact on IFT reduction.

Similarly, Shahrabadi et al. (2012) used hydrophobic polysilicon nanoparticles dispersed in organic solvent and applied three different injection scenarios: after waterflood as tertiary recovery method, sequence of water and nanofluids followed by a waterflood, and injection of nanofluid as the secondary recovery method. They reported that the application of hydrophobic nanoparticles on sandstone rocks with concentrations of zero to 4 g/liter, lowered the interfacial tension by a factor of ten and changed the contact angle from 123° to 99° representing a less water-wet conditions. They concluded that injection of nanofluid as a tertiary recovery method enhanced the oil production more significantly than other approaches. A pressure-drop indicating severe permeability impairment was also reported after injecting 3 pore volumes of nanofluids.

The use of silica nanoparticles as an additive to distilled water to improve the oil recovery through wettability alteration during waterflooding before implementation of other EOR treatments was also suggested by Maghzi et al. (2012). They reported an 8.7% increase in ultimate recovery using 0.1 wt.% nanofluid compared to waterflooding. This incremental recovery was improved to 26% by increasing the concentration of nanoparticles from 0.1 wt.% to 3 wt.%. The hydrophilic property of silica nanoparticles, strong hydrogen bonding between silica and water, and consequently an increase in surface free energy were listed as factors responsible for wettability alteration from oil-wet to water-wet in a glass micro-model.

Hendraningrat et al. (2013) investigated the potential of nanofluids for EOR in low to high-permeability sandstone rocks through studying IFT and wettability alteration. They conducted coreflood experiments using water-wet Berea sandstone cores with permeabilities in the range of 9 mD to 400 mD and nanofluids containing hydrophilic silicon dioxide dispersed in reservoir synthetic brine with concentrations of 0.01, 0.05, and 0.1wt.%. They observed that by increasing nanofluid concentration, IFT reduced from 19.2 mN/m to 10.9 mN/m for oil/brine and 7.9 mN/m for oil/nanofluid with the concentrations of 0.01 wt.% and 0.05 wt.% respectively. They also found that nanofluids reduced the contact angles from 54° at initial condition to 22° at 0.1 wt.% nanofluid concentration, changing the wettability toward more water-wet condition. They suggested that the higher the nanofluid concentration the more the impairment of the porosity and permeability in the core plugs, indicating that no additional recovery is guaranteed.

Mohammadi et al. (2014) studied the effect of different concentrations of Gamma-Al_2O_3 nanoparticles dispersed in distilled water (0.1 wt.% to 1 wt.%) on carbonate rocks and found that adsorption of nanoparticles on the calcite surface altered the wettability from oil-wet (about 120°) to water-wet (about 40°) at the optimal concentration of 0.5 wt.%. By conducting nanofluid

corefloods in a tertiary mode, they also observed an 11.25% increase in oil recovery using the optimal nanofluid concentration. They confirmed the adsorption of nanoparticles by analyzing SEM images of calcite slice surfaces before and after aging in nanofluid solutions.

Joonaki and Ghanaatian (2014) performed a similar investigation on sandstone rocks using selected types of nanoparticles, including aluminum oxide, iron oxide, and silicon oxide treated by silane all dispersed in propanol and used different flooding scenarios at ambient conditions. They reported that silicon dioxide as the best agent changed the contact angle from 134° to 82° representing a shift toward intermediate-wet state, while reducing the interfacial tension from 38.5 mN/m to 1.45 mN/m. The most significant contribution to wettability alteration was made by the optimal nanofluid concentration of 1.5 g/L. They also reached a high oil recovery of 95.3% through the injection of nanofluid made by SiO_2 as the tertiary recovery method compared to Al_2O_3 and Fe_2O_3 with 92.5% and 88.6% respectively.

Li et al. (2015) compared the effects of both hydrophilic silica nano-structure particles and colloidal nanoparticles dispersed in 3% NaCl on wettability alteration and oil recovery in Berea sandstone. They observed a difference in the quality of dispersion between two types of nanofluids and studied the wettability using Amott test by spontaneous imbibition and drainage. They found that nanofluids can change oil-wet cores to intermediate-wet cores and increase oil recovery even with very low concentrations. They suggested that wettability alteration and IFT reduction might be the EOR mechanisms for colloidal nanoparticles, while wettability alteration and increase in pressure drop might be the significant reason behind EOR for nano-structure particles.

Abhishek et al. (2015) used silane coated silica nanoparticles dispersed in distilled water, formation water, and 3% KCl brine with the concentrations of 1, 2, 3, and 4 g/L to study the wettability alteration potential of nanofluids with carbonate reservoir rocks. They found 2 g/L to

be the optimal concentration of silica in water-based medium to alter the wettability toward more water-wet state. Their investigation on particle size showed that the extent of agglomeration of nanoparticles was influenced by salinity of the dispersing medium and concentration of the nanofluids.

The effect of SiO_2 nanoparticles on interfacial tension and wettability alteration of carbonate rocks was also analyzed by Roustaei and Bagherzadeh (2015) through static contact angle measurements and corefloods to determine the optimum concentration and ultimate recovery respectively. They found that 4 g/L of nanofluid could significantly alter the wettability of the rock from strongly oil-wet to strongly water-wet condition. The potential of nanofluid to enhance the oil recovery was also demonstrated through two sets of waterflooding scheme. Injecting one pore volume of nanofluid as the tertiary recovery method led to an incremental oil recovery of about 9-12% and then waterflooding after aging the cores in the nanofluid for 24 hours resulted in another 16-17% of incremental oil recovery.

Tola et al. (2017) studied the wettability alteration of sandstone with Zinc oxide nanoparticles. They dispersed 500 ppm to 5000 ppm of ZnO in water solution of sodium dodecyl sulfate as an anionic surfactant. They measured the contact angles of sessile drops on the surface of glass plate and Berea sandstone. They found that the ZnO nanofluid has a potential to shift wettability to more water-wet condition on the surfaces of oil film and sandstone saturated by light crude oil.

2.7.2. Wettability alteration using surfactant-based nanofluids

Surfactants, whose properties can crucially benefit nanotechnologies (Eastoe and Tabor, 2014) have been recently used as dispersing fluid for nanoparticles to find the influence on increasing

the surfactant adsorption and reducing the interfacial tension leading to a significant increase in the efficiency of oil displacement flowrate. The utilization of nanoparticles in the presence of a wetting agent, such as surfactant at concentrations much below the critical micelle concentration is a technique that has been generally applied for treating wellbores and oil and gas reservoirs to enhance the wettability of solid surfaces for wellbore damage removal or flowback of treatment fluids (Holcomb et al., 2012).

Traditionally, surface activity of surfactants can be increased by adding polymer, poly electrolytes and ions/counter-ions to lower the interfacial tension and change the wettability by forming multilayers. The application of nanoparticles dispersed in surfactants as wettability modifies to enhance oil recovery especially in carbonate systems is still in its infancy.

Suleimanov et al. (2011) used an aqueous solution of anionic surfactants with addition of light non-ferrous metal nanoparticles to enhance oil recovery. They showed how dispersed nanoparticles in an aqueous phase can modify the interfacial properties of the liquid/liquid systems if their surface is modified by an ionic surfactant. They found that surfactant adsorption increased by 14.5-18.5 times and surface tension on an oil boundary reduced 70-90% at the presence of nanoparticles. The production rate of oil displaced by the nanofluid was reported to be increased about 1.5 to 4.7-fold compared to surfactant and water respectively.

Le et al. (2011) investigated the effects of SiO_2 nanoparticles and their combination with surfactants on the capacity of reducing the crude-oil/brine IFT and altering reservoir rock surface wetting behaviors. They synthesized SiO_2 nanoparticles, combined them with anionic surfactant solutions, and evaluated the oil displacement efficiencies by measuring contact angles in high temperature. They found that synergistic blends of SiO_2/surfactant exhibited an IFT reduction as high as four times the value recorded for oil/brine interface, resulting in a very high speed of oil

displacement. They also reported that the blend displaced the oil as well as the original surfactant solution with the same total concentration. They suggested that technique to be a new direction for developing effective EOR compositions leading to a more economical and environmentally safer application of surfactants.

Karimi et al. (2012) studied the effect of nanofluids composed of ZrO_2 nanoparticles and mixtures of nonionic surfactants on the wettability alteration of carbonate reservoir rocks. Contact angle measurements showed that designed nanofluids could significantly change the wettability of the rock from strongly oil-wet (about 150°) to strongly water-wet (about 35°) conditions. The adsorption of nanoparticles and formation of nano-textured surfaces were reported as the reasons behind the wettability alteration based on the observation from the SEM images and X-ray diffraction data. They also found that a significant amount of oil can be quickly recovered through free imbibition of the nanofluids into the cores.

Giraldo et al. (2013) also studied the wettability alteration of sandstone cores by nanofluids prepared by dispersing alumina nanoparticles in anionic surfactants. They showed that the effectiveness of the anionic surfactant as a wettability modifier could be improved by adding alumina nanoparticles. The change in contact angles of water/air/rock systems after treatment with nanofluids (from the range of 104° to140° to practically 0°) indicated that the rock wettability was altered from an induced oil-wet to a strongly water-wet condition. In addition, core displacement test results showed a significant reduction in the residual oil saturation and a shift to the right of the oil relative permeability curve and the crossover point. They reported that the oil recovery efficiency of waterflooding in oil-wet rocks can be enhanced by dispersing relatively low concentrations of alumina nanoparticles (100 ppm) in the injected water through altering the wettability of the reservoir rock to a strongly water-wet state.

Roustaei (2014) compared the oil recovery from oil-wet carbonate reservoir cores using cationic surfactants to that of synergic blend of SiO_2 nanoparticles and surfactants at room temperature. He also evaluated the change in wettability and IFT through contact-angle and pendent-drop method. His results showed that adding nanoparticles to surfactant solutions changed the wettability toward more water-wet conditions, shifting from about 85° for 1% surfactant solution to about 56° for combined 3 g/L solution of surfactant and nanoparticles. He also observed an increase in IFT from about 3 mN/m for 1% surfactant solution to about 9 mN/m for 4 g/L concentration of nanofluid. He believed an increase in IFT resulted in an increase in capillary pressure to provide a stronger imbibition of water into small pores after wettability alteration to water-wet condition. The results from imbibition experiments revealed a 46% recovery using surfactant followed by an additional 10% recovery using the nanofluid.

Al-Anssari et al. (2017) investigated the wettability alteration of carbonate rocks using nanoparticles-anionic surfactant flooding at reservoir conditions. They used a high-temperature-pressure vessel to apply nano-modification of oil-wet calcite sample at subsurface conditions (20 MPa and 70 °C). They also used various concentrations of nanoparticles, surfactant, and salinities to perform contact angle measurements (tilting-plate technique) on calcite substrates and spontaneous imbibition test on limestone cores to both natural and modified oil-wet samples to consider the effect of both heterogeneity and rock complexity on surface wettability. They suggested that formulations of sodium dodecylsulfate-silica nanoparticles can change the wettability from oil-wet to strongly water-wet at reservoir conditions. Their spontaneous imbibition results confirmed the role of nano-suspension to render the oil-wet pores to intermediate and water-wet.

Suresh et al. (2018) studied the reduction of surfactant adsorption in porous media using silica nanoparticles. They found colloidal nanoparticles to be adsorbing at a lower rate than surfactant in porous media due to their charge density and high surface area. They concluded that the negative charges of silica nanoparticles adsorbed onto the same active sites in the reservoir as anionic surfactant molecules used in EOR applications. They conducted experiments on sand pack to show that a pre-treatment with silica nanoparticles at 80 °C reduced surfactant adsorption by a factor of three, when using artificial seawater as the injection fluid.

Mashat et al. (2018) investigated about a nanoparticle-based approach for stabilizing the low-cost petroleum sulfonate surfactants in high salinity and temperature water to enable their utility in EOR applications in typical carbonate reservoirs. They demonstrated the ability of nano-surfactants to mobilize oil through colloidal nature that would give them advantages over conventional micellar surfactants by allowing them to migrate deeper in the reservoir due to size exclusion and chromatographic effects.

2.7.3. Mechanism of wettability alteration using surfactant-based nanofluids

Nanoparticles are significantly recognized by their high ratio of surface area to volume. The smaller size and higher concentrations of nanoparticles result in a higher amount of free energy in the medium fluid. The adsorption of these active and energetic materials on a solid surface can significantly alter the surface energy and wettability of the system. Moreover, their high tendency to form nano-textured surfaces in combination with surfactants and their great ability to increase the surface activity of the surfactant molecules lead to more adsorption and consequently affect the wettability in a more pronounced manner.

The spreading and adhesion behavior of the nanoparticles dispersed in surfactants on solid surfaces have technological applications in soil remediation, oily soil removal, lubrication, and enhanced oil recovery (Wasan and Nikolov, 2003). The conventional theories for spreading behavior of a simple liquid on a solid surface suggest a decrease in the spreading velocity resulted from an increase in the liquid viscosity. However, studies have shown that an increase in nanofluid viscosity corresponding to an increase in the nanofluid volume fraction or concentration, would unexpectedly improve the spreading velocity of the nanofluid. (Sefiane et al., 2008; Wasan et al., 2011). Therefore, the spreading behavior of nanofluids on solid surfaces seems to follow its own specific mechanism.

The spreading of nanofluid over a drop of oil on a solid surface is promoted by forming ordered structures or symmetric films (layers) in the confined space of oil/solid/nanofluid contact region (wetting wedge). This arrangement causes the nanoparticles in the bulk fluid with higher entropy to push the nanoparticles in the confined region forward, resulting in an extra pressure (Figure 2.5). The pressure difference that helps to separate the two surfaces (solid and oil) confining the nanofluid is named the structural disjoining pressure gradient (Wasan et al., 2011) and is recognized as the main mechanism of dynamic spreading of nanofluids. The following equation (Eq. 2.1) relates the disjoining pressure to the interfacial force, based on the de Gennes theory (Wasan and Nikolov, 2003).

$$\sigma_s = \Pi_h h + \int \Pi_h \, dh \quad \text{.......} \quad (2.1)$$

, where σ_s is the surface free energy, h is the film thickness, and Π_h is the disjoining pressure of a wetting film.

A single particle applies an extremely weak force, but all the little particles together could create a force up to 50,000 Pa at the vertex of the wetting wedge (McElfresh et al., 2012). The

energy behind this driving force is provided by Brownian motion and electrostatic repulsion between the particles. Therefore, the particle size and accordingly particle charge density affect the strength of this force. The smaller the particle size, the higher the charge density, and the larger electrostatic repulsion between particles, which leads to a better displacement of oil drop to regain equilibrium at the confined wedge. The magnitude of disjoining pressure is also affected by temperature, salinity of the carrier fluid, and the characteristics of the rock surface.

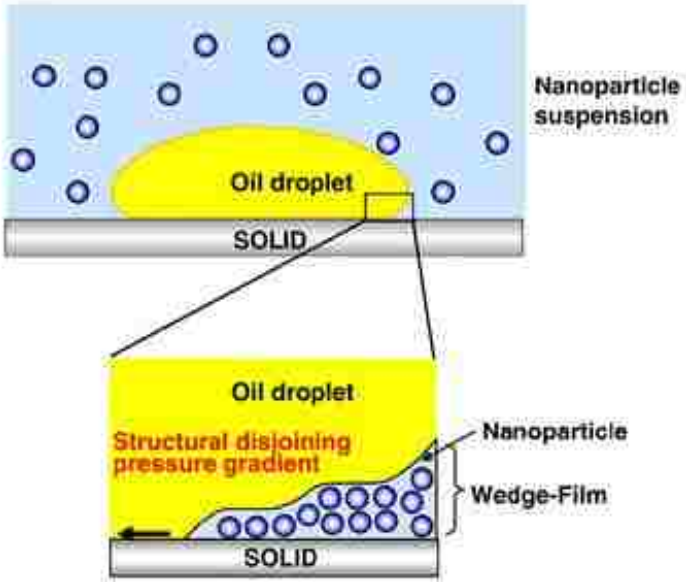

Figure 2.5. Structure of nanoparticles in the oil/solid/nanofluid contact region under the disjoining pressure gradient at the wedge vertex (Wasan et al., 2011).

The surfactant-based nanofluids, however, are composed of complex nano-structures that are required to be analyzed by looking into the physio-chemical behavior of both nanoparticles and surfactant molecules and their interfacial interactions.

The interfacial properties of the surfactant-based nanofluids are the result of three interrelated phenomena (Ravera et al., 2006) as follow:

1- Attachment of particles at the oil/nanofluid interface.

2- Adsorption of surfactants at the oil/nanofluid interface.

3- Adsorption of surfactants on the particles surface.

In the absence of surfactant molecules, nanoparticles influence the properties of the oil/nanofluid interface only based on their level of hydrophilicity. Therefore, in the case of hydrophilic silica nanoparticles, the oil/nanofluid interfacial tension might not significantly be reduced compared to oil/brine, since most of the nanoparticles are wetted inside the dispersion. However, adsorption of surfactant molecules with the positive hydrophilic heads and negative hydrophobic tails on the negative surface of nanoparticles increase the level of hydrophobicity of the nanoparticles, which provides a driving force for attaching at the oil/nanofluid interface. This comes with the price of reducing the amount of surfactant in the solution. Therefore, the interfacial tension between oil and surfactant-based nanofluid is the result of two opposite effects: (1) depletion of surfactant solution leading to an increase of interfacial tension and (2) attachment of nanoparticles at the interfacial layers resulting in a decrease of interfacial tension. The interfacial tension of the surfactant-based nanofluids is determined by a mixed layer composed of nanoparticles and surfactants at the oil/nanofluid interface.

The wettability alteration mechanism of surfactant-based nanofluid at the rock surface is then based on a combined effect of two phenomena: (1) interfacial properties of the nanofluid and (2) arrangement of nanoparticles through disjoining pressure gradient. Chengara et al. (2004) theoretically examined the role of structural disjoining pressure exerted by nanoparticles on the spreading of surfactant-based nanofluids on a solid surface. They claimed that the disjoining pressure is directly correlated with the spreading that occurs due to imbalance of interfacial forces at the oil/rock/fluid contact surface. These forces cause the oil phase to be displaced and the

aqueous phase to enter a highly confined wedge area, where forces are focused at the tip as a thin film of surfactant. Using the aqueous pressure of the bulk liquid, the nanofluid is then able to spread along the surface as a monolayer of particles. Therefore, dispersions of nanoparticles can self-assemble as the wedge widens, which causes both the disjoining pressure and "surfactancy" of the aqueous phase to increase and work through removing the oil together.

Their study was later extended by McElfresh et al. (2012) to present research laboratory and actual field data for improving fluid recoveries and injection rates using nanofluid treatments composed of stable particles and/or micellar colloids. They showed that, by adjusting the surface charge density of the colloid, stable fluids could be employed to more effectively remove or displace hydrocarbons from reservoir surfaces.

The behavior of solutions containing nanoparticles and non-ionic surfactants in an oil-water interface was also studied through a series of molecular dynamics simulations by Ranatunga et al. (2011). They found that lower concentrations of surfactants show a better cooperative behavior with nanoparticles in lowering the oil-water interfacial tension.

Maestro et al. (2011) also performed an experimental study on the structural conformation of the interfacial nanocomposite systems made by combining silica nanoparticles with cationic surfactants and established that adding surfactants altered the intrinsic hydrophilic-lipophilic balance (HLB) of the particles, which consequently changed the particles affinity for the fluids in the interfacial environment.

2.8. Summary

The tendency of oil industry to invest more on surfactants flooding in the last decade is believed to be indebted to the focus of researches on the wettability altering ability of the surfactants,

especially in carbonate reservoirs. On the other hand, nanotechnology as a new cost-effective chemical flooding method has recently been attracting attention of many researchers and oil industry. The structural disjoining pressure gradient promoted by the Brownian motion and electrostatic repulsion between particles is believed to be the main driving force for spreading the nanoparticles in the confined space or wetting wedge of a drop on a solid surface. The effectiveness of surfactants as wettability modifiers has shown to be improved with nanoparticles through a combination of interfacial mechanisms that are yet to be investigated completely.

What differentiates this research from other studies is the application of dual-drop-dual-crystal technique as the most accurate and reproducible technique to measure true dynamic water advancing contact angles of solutions prepared by nanoparticles and their combination with surfactants. These measurements are then compared to the relative permeability curves generated by the simulation of coreflood experiments results at different experimental conditions to investigate the true contribution of nanoparticles in enhancing oil recovery through wettability alteration. Therefore, this research will evaluate the potential of nanoparticles, with and without surfactants, to enhance oil recovery in carbonate rocks through wettability alteration using contact angle measurements and relative permeability curves resulted from coreflood experiments. A potential that could lead to a significant reduction in the residual oil saturation of the carbonate reservoirs and make the surfactant-based nanofluid technology an economically appealing enhanced oil recovery technique.

3. METHODOLOGY

The first part of this research is devoted to conducting coreflood experiments to screen a range of different surfactants with varying chemical structures to select the best candidates based on their ability to enhance oil recovery through changing the wettability of the system. After ensuring that the coreflood results agreed well with the contact angle measurements, the selected surfactant solution is used for combining with nanoparticles. The optimal concentration of nanoparticles to combine with the surfactant candidate is determined through contact angle and IFT measurements at ambient conditions. The surfactant-based nanofluids are also used for contact angle measurements at reservoir conditions. Then, coreflood experiments are conducted for surfactant-based nanofluids to see whether the overall recovery and relative permeability curves agree with the contact angle measurements. The details of the experimental approach are discussed in the following sections.

3.1. Corefloods to screen the surfactants

This research started based on a three-year project with Sasol North America, a chemical company that manufactures and provides a variety of surfactants with different chemical structures. The Sasol's project aimed at investigating the wettability alteration potential of surfactants and their influence on oil recovery through contact angle measurements at ambient and reservoir conditions and coreflood experiments at different experimental conditions for carbonate rocks. Two groups of anionic surfactants, namely ALFOTERRA and SOLOTERRA (classified based on the level of hydrophobicity) were studied. The chemical structures of the surfactants are depicted in Figure 3.1. The contact angle measurements related to the Sasol's project were conducted by another member of the research group (Gupta, 2016). The coreflood part of the Sasol project, however, was the basis of this research.

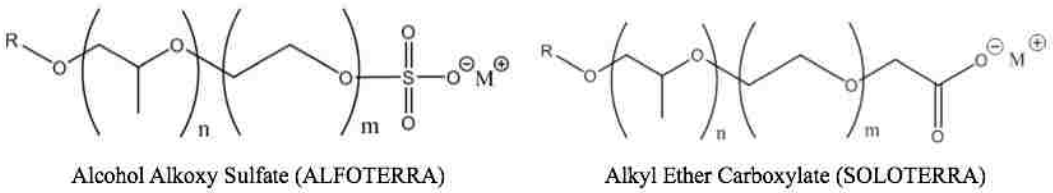

Figure 3.1. Chemical structure of the surfactants tested in the coreflood experiments for screening (Gupta, 2016).

3.1.1. Emulsion stability tests

To determine the optimum surfactant concentration to use in the coreflood experiments, emulsion stability tests were conducted for both surfactants. The presence of a stable emulsion phase inside the core may lead to blocking the pore space and creating issues. Figures 3.2 to 3.5 show the status of 16 samples that were examined for two weeks. The name and concentration of the surfactants, and the emulsion height alteration are indicated under each sample. Every sample cell contains 15 cc of Yates oil and 15 cc of a surfactant. All samples were shaken vigorously every day. The changes in color, emulsion height, and emulsion configuration were monitored for two weeks. At the end, a noticeable change in the surfactant color was observed from ALFOTERRA to SOLOTERRA. Also, different emulsion configurations were noticed when using SOLOTERRA at 500 ppm compared to other samples. Moreover, the emulsion height alteration was low for all samples of ALFOTERRA S23-7S 90M and was high when using 4000 ppm of all the surfactants.

Figure 3.2. Emulsion stability test for ALFOTERRA S23-7S 90M.

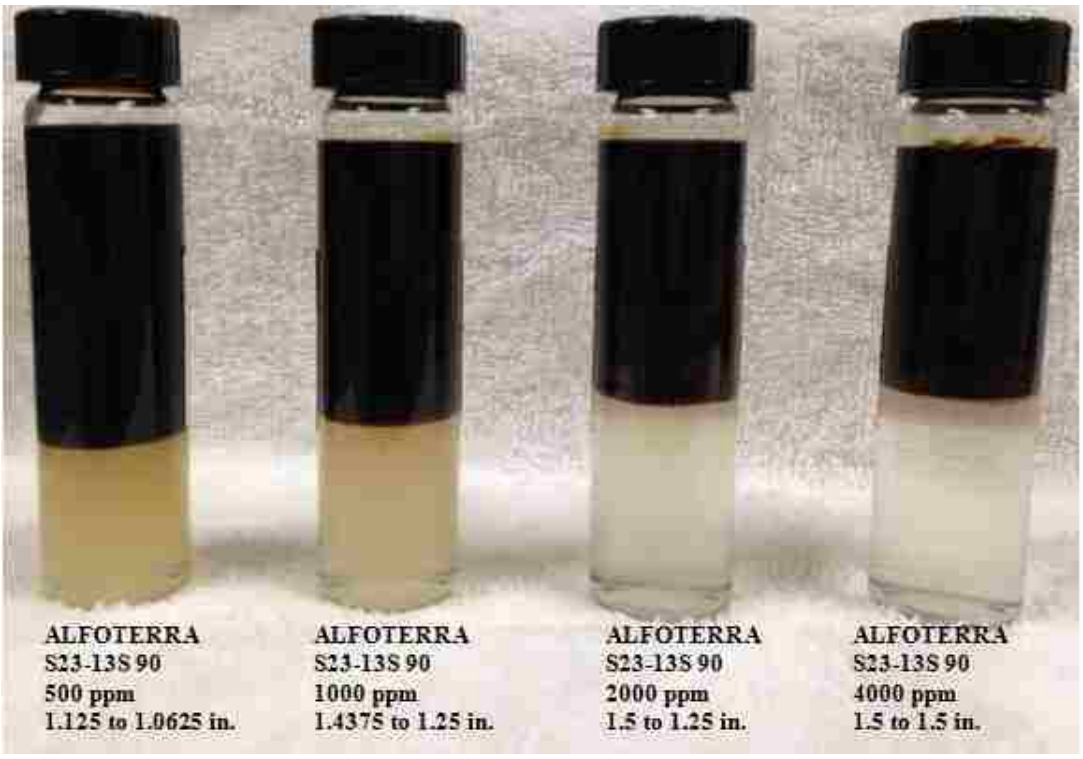

Figure 3.3. Emulsion stability test for ALFOTERRA S23-13S 90M.

Figure 3.4. Emulsion stability test for SOLOTERRA 960.

Figure 3.5. Emulsion stability test for SOLOTERRA 961.

ALFOTERRA S23-7S 90M generated the least amount of emulsion stability. Finally, after monitoring different parameters, 2000 ppm was selected as the optimal concentration for all the surfactants in the coreflood experiments.

3.1.2. Coreflood parameters

Flow tests in cores or coreflood is a set of flow experiments that are conducted to determine the rock permeability and flow behavior during waterflooding, chemical flooding, or gas flooding, and examine their effects on overall oil recovery in laboratory scale. A variety of parameters play a role in a coreflood and need to be adjusted for the system. The parameters adjusted for the coreflood of this research include, pressure and temperature of the system, the appropriate injection rate, rock type, core size, oil type, type and concentration of the brine, type and concentration of the surfactants, and more importantly the aging time for the system.

The proper aging time for the system using Yates oil and limestone cores was determined through a series of waterflood experiments conducted using different aging periods. As shown in Figure 3.6, the overall trend of oil recovery versus the number of pore volume injected for the final two waterflood experiments (with aging time of 8 and 16 days) are almost similar, leading to an ultimate recovery of about 44%. Since the recovery did not change, even after elongating the aging period, 8 days seemed to be the proper aging time for the system. If the aging time is not long enough, oil does not have enough time to interact with the rock and absorb on the pore surfaces, which results in a high ultimate recovery (1, 2, and 4 days for this system). When oil is given enough time to interact with the rock, the final recovery is lowered. The extents of interaction at 8 and 16 days are similar, causing their respective final recoveries to be about the same.

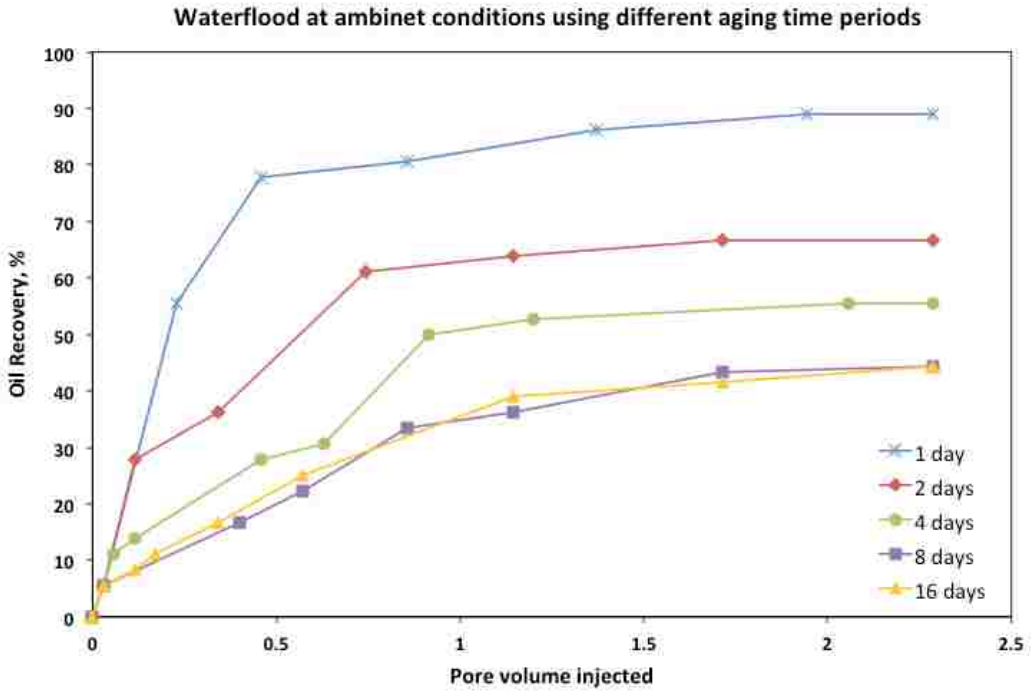

Figure 3.6. Waterflood experiments at 500 psi and 72 ˚F for the system of limestone, Yates oil, and synthetic Yates brine to determine the proper aging time.

3.1.3. Coreflood apparatus and materials

The typical properties recorded during a coreflood experiment are the pressure drop of the flow across the core, number of pore volume of injecting fluid, and the volume of produced fluid all versus time. The collected data are then implemented into a coreflood simulator to estimate oil-water relative permeabilities by history matching the recovery and pressure drop results. Figure 3.7 demonstrates a schematic diagram of the coreflood apparatus. A description of the actual setup is shown in Figure 3.8.

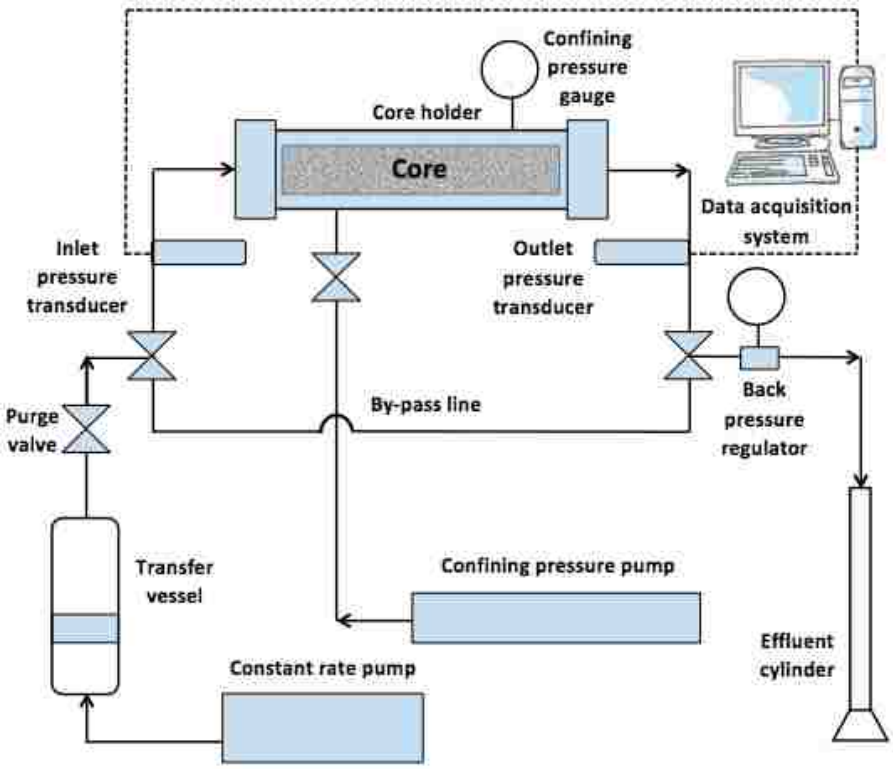

Figure 3.7. Schematic diagram of the coreflood experimental setup.

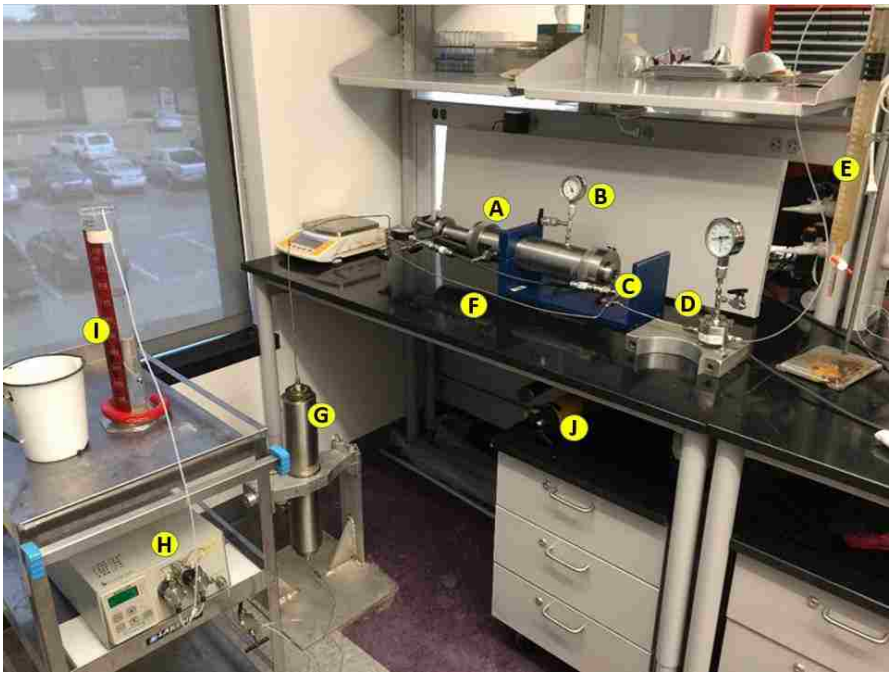

Figure 3.8. Coreflood experimental setup, A: Core holder, B: Confining pressure gauge, C: Pressure transducer, D: Back-pressure regulator, E: Effluent burette, F: By-pass line, G: Transfer vessel, H: Constant-rate pump, I: Pump reservoir, J: Confining pressure pump.

The core holder made by Phoenix Instruments is designed for cores with length of 12 in. and diameter of 2 in. and can maintain high pressures (maximum 5,000 psi) and high temperatures (maximum 210 °F). In case of conducting corefloods at reservoir conditions, high pressure is applied across the core using a backpressure regulator made by Equilibar (maximum 5,000 psi) at the outlet. In order to raise the temperature of the core, heating tape and insulating blanket are used to cover around the core holder. A thermometer made by Hanna Instruments is connected to the core holder to show the approximate temperature of the core. The confining pressure representing the reservoir overburden pressure is exerted using a manual hydraulic oil pump and managed through the confining pressure gauge on the core holder. Two pressure transducers made by Omega (maximum 2500 psi) are used at the inlet and outlet of the core holder to record the pressure data by communicating through the data acquisition system made by Omegabus, which is connected to a computer to monitor the live variation of differential pressure across the core. The amount of production from the core is determined by collecting and measuring the produced fluids at the effluent burette. The injecting fluids such as brine, oil, surfactant, or nanofluid are stored in and injected from the transfer vessel (CoreLab, 500 cc capacity), which is connected to the core holder. The other end of the vessel is linked to a constant-rate pump Series 1500 from LabAlliance.

Silurian dolomite and Indiana limestone outcrop cores to be used in corefloods were purchased from Kocurek Industries. The dead crude oil sample is from Yates reservoir (700 psi and 82 ˚F) with density of 0.874 g/cc. Brine was synthetically prepared in the lab based on the Yates reservoir brine composition at the initial stages of the research. Further in the research, sodium chloride (with density of 1.011 g/cc) replaced the reservoir brine to serve certain applicability purposes. Surfactants were provided by Sasol, the chemical company, as part of the project mentioned previously. The silica nanoparticles dispersed in water (with density of 1.029

g/cc) were purchased from US Research Nanomaterials, Inc. The viscosity of oil and brine were measured using Cannon-Fenske viscometer at both low and high temperatures (72 ˚F and 150 ˚F). Table 3.1 lists the viscosity and density values of Yates crude oil and brine (2 wt.% NaCl) at both conditions.

Table 3.1. Viscosity and density of Yates oil and brine (2% NaCl) at 72 ˚F and 150 ˚F.

	Viscosity (cp)		Density (g/cc)	
	72 ˚F	150 ˚F	72 ˚F	150 ˚F
Yates crude oil	12.52	3.64	0.874	0.852
Brine (2% NaCl)	1.02	0.45	1.011	0.995

3.1.4. Coreflood procedure

To prepare for a coreflood, the core holder parts, tubing lines, Viton sleeve inside the core holder, fittings, valves, transfer vessel, and the effluent burette are cleaned using toluene, acetone and deionized water to remove any contamination. A fresh core is cleaned with air and given a marked number and then is covered with heat shrink Teflon wrap using a heat gun. Then the wrapped core is placed inside the core holder to measure the pore volume.

To prepare the brine solution for the coreflood, 20 grams of NaCl is solved in 1000 cc of DI water to make a 20,000-ppm (2 wt.%) solution. This brine is also used as the base phase to prepare the surfactant and nanofluid solutions. Before loading the transfer vessel with the fluids, the vessel is tested for any leakages to avoid spills, contaminations, or discrepancies in the data during the experiment. By assembling the core holder and tubing lines, the setup is ready to measure the core pore volume.

The pore volume of the core is measured using oil when the core is inside the core holder. First, the core is vacuumed while being under confining pressure of 2000 psi. After ensuring that

the core is holding the vacuum, oil is introduced to the core at a high rate (10 cc/min), while a backpressure of 500 psi is applied at the outlet. Once the core is fully saturated with oil, the injected volume indicates the pore volume of the core.

To measure the absolute permeability of the core, oil is injected at different rates to collect the stabilized pressure drop data for each rate to implement into Darcy's equation. To establish the initial condition of the core, brine is injected at 2 cc/min for 2 PV to replace the oil and followed by oil injection to replace the brine. All the collected fluids are measured to determine the irreducible water saturation and residual oil saturation. The core at initial condition is then aged for 8 days before starting the secondary recovery.

The secondary recovery can be waterflood, surfactant flood, or nanofluid flood. For all the floods, the injection rate is 2 cc/min. Then, the effective permeability is estimated by injecting the fluid at different rates to collect the stabilized pressure drop data for each rate to implement into Darcy's equation. All the produced fluids are collected to determine the recovery and residual oil saturation. Utilize

The absolute/effective permeabilities and water/oil saturation values are used to determine the experimental relative permeability end points, which are utilized in the simulator. The oil recovery and pressure drop variation with time are also collected for history matching in the simulator.

3.1.6. Corefloods performed

A list of all the coreflood experiments conducted in this research to screen the surfactants can be seen in Table 3.2. After attempting with different rock types, brine solutions, surfactant types and concentrations, and aging times, 6 surfactant floods were selected to be investigated more in depth.

Table 3.2. List of all the coreflood experiments conducted to screen the surfactants.

Number	Rock Type	Oil Type	Brine Type	Flood Type	Surfactant Concentration (ppm)	Comment
1	Dolomite	Decane	NaCl (2% w.)	Waterflood	0	
2	Dolomite	Decane	NaCl (2% w.)	TDA-6	1000	
3	Dolomite	Decane	NaCl (2% w.)	TDA-6	3000	
4	Dolomite	Yates Crude Oil	Synthetic Yates	ALFOTERRA S23-7S90M	500	
5	Limestone	Yates Crude Oil	Synthetic Yates	ALFOTERRA S23-7S90M	500	switch to limestone
6	Limestone	Yates Crude Oil	Synthetic Yates	ALFOTERRA S23-13S90M	500	
7	Limestone	Yates Crude Oil	Synthetic Yates	SOLOTERRA 960	500	
8	Limestone	Yates Crude Oil	Synthetic Yates	ALFOTERRA S23-13S90M	2000	2 months aged
9	Limestone	Yates Crude Oil	Synthetic Yates	ALFOTERRA G16-20S	2000	4 days aged
10	Limestone	Yates Crude Oil	Synthetic Yates	ALFOTERRA S23-13S90M	2000	4 days aged
11	Limestone	Yates Crude Oil	Synthetic Yates	ALFOTERRA G16-20S	2000	aging fixed at 8 days
12	Limestone	Yates Crude Oil	Synthetic Yates	ALFOTERRA S23-13S90M	2000	
13	Limestone	Yates Crude Oil	Synthetic Yates	ALFOTERRA S23-11S90M	2000	
14	Limestone	Yates Crude Oil	Synthetic Yates	ALFOTERRA S23-9S90M	2000	
15	Limestone	Yates Crude Oil	Synthetic Yates	ALFOTERRA S23-7S90M	2000	
16	Limestone	Decane	Synthetic Yates	Waterflood	0	
17	Limestone	Yates Crude Oil	Synthetic Yates	Waterflood	0	
18	Limestone	Yates Crude Oil	Synthetic Yates	SOLOTERRA 938	2000	
19	Limestone	Yates Crude Oil	Synthetic Yates	SOLOTERRA 939	2000	
20	Limestone	Yates Crude Oil	Synthetic Yates	SOLOTERRA 960	2000	
21	Limestone	Yates Crude Oil	Synthetic Yates	SOLOTERRA 961	2000	
22	Limestone	Yates Crude Oil	Synthetic Yates	SOLOTERRA 970	2000	
23	Limestone	Yates Crude Oil	NaCl (2% w.)	Waterflood	0	new setup-2x12 core
24	Limestone	Yates Crude Oil	NaCl (2% w.)	ALFOTERRA S23-13S90M	2000	water-wet behavior
25	Limestone	Yates Crude Oil	NaCl (2% w.)	ALFOTERRA S23-11S90M	2000	water-wet behavior
26	Limestone	Yates Crude Oil	NaCl (2% w.)	Waterflood	0	first saturated w oil
27	Limestone	Yates Crude Oil	NaCl (2% w.)	ALFOTERRA S23-11S90M	2000	failed due to leakage
28	Limestone	Yates Crude Oil	NaCl (2% w.)	ALFOTERRA S23-11S90M	2000	repeated-too tight
29	Limestone	Yates Crude Oil	NaCl (2% w.)	ALFOTERRA S23-11S90M	2000	
30	Limestone	Yates Crude Oil	NaCl (2% w.)	ALFOTERRA S23-9S90M	2000	
31	Limestone	Yates Crude Oil	NaCl (2% w.)	ALFOTERRA S23-13S90M	2000	repeated-more oilwet
32	Limestone	Yates Crude Oil	NaCl (2% w.)	ALFOTERRA S23-13S90M	2000	
33	Limestone	Yates Crude Oil	NaCl (2% w.)	ALFOTERRA S23-7S90M	2000	
34	Limestone	Yates Crude Oil	NaCl (2% w.)	SOLOTERRA 939	2000	HPHT-700 psi 150 F
35	Limestone	Yates Crude Oil	NaCl (2% w.)	SOLOTERRA 938	2000	HPHT-700 psi 150 F

For corefloods at 500 psi and 72 ˚F, 4 ALFOTERRA surfactants were selected including: S23-7S 90M, S23-9S 90M, S23-11S 90M, S23-13S 90M. A system of Indiana limestone cores (12 in. by 2 in.), Yates crude oil, and 2 wt.% NaCl was kept fixed for all the corefloods. Each surfactant flood was initially started with a waterflood as the secondary recovery method. Therefore, the surfactant floods were treated as the tertiary recovery method. The waterflood experiments were conducted using 2 wt.% NaCl, which was also used as the base phase to make the surfactant solutions at 2000 ppm concentration. For each coreflood, a fresh limestone core was used and initially saturated with oil. For all the experiments, 500 psi and 2000 psi were used as the backpressure and confining pressure respectively.

For corefloods at reservoir conditions, 2 SOLOTERRA surfactants were selected, including SOLOTERRA 938 and SOLOTERRA 939 and tested at high temperature (150 ºF) and high pressure (700 psi). Each coreflood was started with a waterflood using 2 wt.% NaCl and followed by a surfactant flood with a concentration of 2000 ppm. Each core was initially saturated with oil and 2000 psi was used as the confining pressure.

The relative permeability curves generated by the simulator can indicate the oil-water flow characteristics and wettability alteration potential of each surfactant. These potentials, resulted from the coreflood experiments, were compared to their respective contact angle measurements conducted by the other member of the research group (Gupta, 2016). After ensuring that the coreflood results agreed well with the contact angle measurements, two surfactant candidates were selected for contact angle measurements using nanofluids.

3.2. Contact angle measurements using nanofluids

The surfactant candidates selected from the coreflood experiments results were used to prepare the dispersing solutions for the nanoparticles. The goal was to investigate whether nanoparticles could enhance the performance of a surfactant that had shown no significant effect in terms of wettability alteration.

Contact angles are the indicators of wettability behavior of the system. To study how nanofluids change the wettability of the system, initially the interfacial tension and contact angles were evaluated for different concentrations of nanofluid solutions prepared by nanoparticles and brine at ambient conditions. This procedure led to find the optimal concentration of nanoparticles for altering the wettability. Then the surfactant candidate was combined with the optimal concentration of nanoparticles. The interfacial tension and contact angle measurements were studied to see whether the new surfactant-based nanofluid is capable of changing the wettability of the system in a more profound manner. Finally, the possibility of reducing the surfactant concentration while observing a similar wettability alteration effect was studied. Therefore, the contact angle measurements elucidated whether there is a potential for nanoparticles to enhance the performance of surfactants in changing the wettability of the carbonate system. Moreover, they revealed if nanoparticles would compensate for surfactants in changing the wettability of the carbonate systems toward less oil-wet.

3.2.1. Contact angle measuring apparatus

The experimental setup for measuring the dynamic advancing contact angle is based on the DDDC technique discussed earlier in the literature review section. The measurements are made using Indiana limestone rock tiles (0.4 in. × 0.5 in. × 0.2 in.), Yates crude oil droplets, and different concentrations of nanofluid solutions prepared by nanoparticles mixed in brine (2 wt.% NaCl) or

surfactant solutions (100 ppm). The rock crystals are cut to the size, smoothened by three different polishing papers of variant grit size (120, 240, and 1200), cleaned in the Soxhlet system using an organic solvent made by 83% Methyl Alcohol and 17% Chloroform for 24 hours, boiled in deionized water for 2 hours, and finally dried for 24 hours in oven at 80 ºF.

Figure 3.9 shows the experimental setup for contact angle measurements at ambient conditions. The setup consists of a cell with top and side crystal holders, which move vertically and horizontally respectively. The cell is equipped with a needle at the bottom to inject the oil.

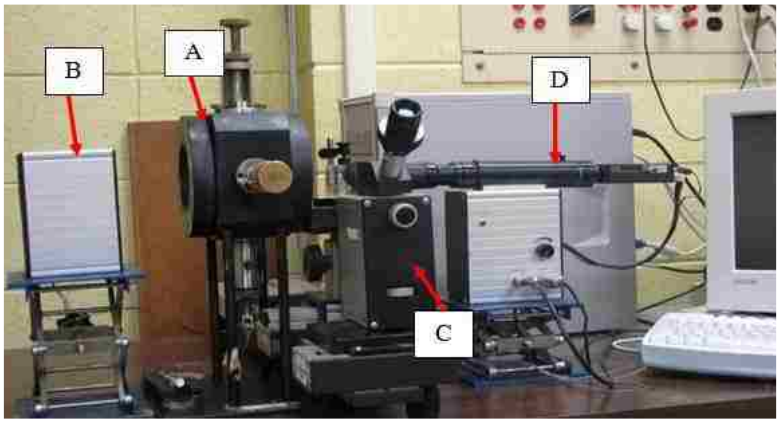

Figure 3.9. IFT and contact angle measurements setup for ambient conditions, A: Optical cell, B: Light source, C: Goniometer, D: Camera (Zheng, 2012).

The light source helps the camera to capture visuals that are displayed on the computer monitor. Other than the goniometer, the Drop Shape Analysis software on the computer could also be used to measure the IFT and contact angles using the visuals. The contact angle measurements setup for high-pressure high-temperature conditions (Figure 3.10) has similar features except that the cell is more robust to hold pressures up to 20,000 psi and temperatures up to 400 ºF. The oven and ducts help to raise the temperature of the cell for reservoir conditions.

Figure 3.10. IFT and contact angle measurements setup for HPHT conditions, A: Optical cell, B: Digital camera, C: Oven (Xu, 2005).

3.2.2. Contact angle measurement procedure

Initially, the optical cell is filled with the experimental fluid (i.e. brine, surfactant, or nanofluid), while rock crystals are hooked up at the tip of the crystal holders. Then the oil droplets are placed underneath of rock crystals using the needle from the bottom. The crystals and the oil droplets are aged inside the cell for 24 hours. Then the bottom crystal is flipped and the droplets are merged before aging for another 24 hours.

The contact angle measuring procedure begins when the side holder is shifted periodically. Every time the side holder is shifted, the sheared oil droplet is given 30 minutes to stabilize and this continues until a change in three-phase contact-line or TPCL is observed. As seen in Figure 3.11, TPCL is normalized by dividing the distance from the lower left corner of the droplet to the edge of tile (L) by the initial distance of the right corner of the droplet to the edge of the tile (R_i). A change in TPCL is recognized when L/R_i or normalized TPCL is reduced,

(i.e. $L < L_i$). This truly satisfies the meaning of dynamic water advancing angle, as water is actually advancing to the area that was pre-occupied by oil. Therefore, the dynamic water advancing angle is measured at the lower left corner of the droplet as shown in Figure 3.11. The wettability alteration behavior of a system is assigned based on the definition of contact angle ranges listed in Table 3.3.

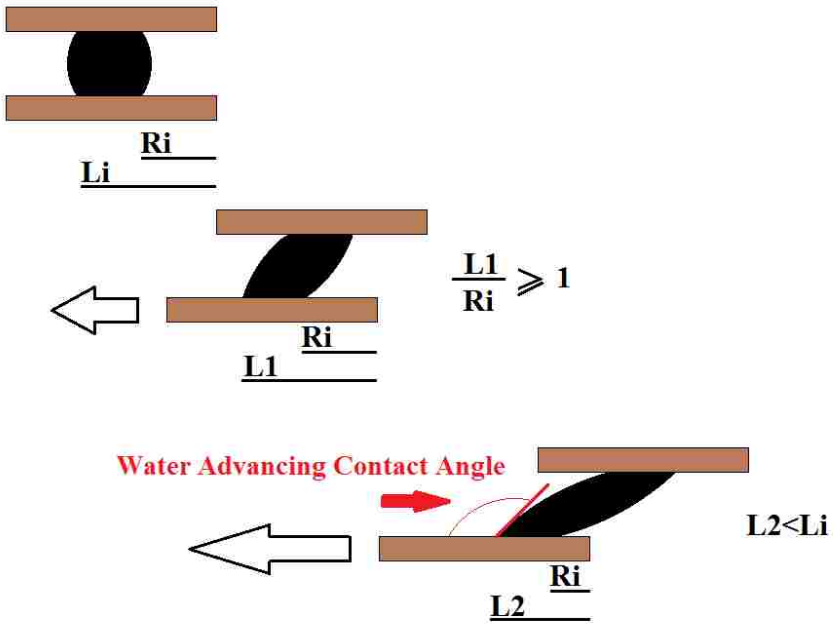

Figure 3.11. TPCL movement in DDDC technique.

Table 3.3. Wettability alteration behavior and contact angle ranges

Contact angle (degrees)	<20	20-40	40-60	60-120	120-140	140-160	>160
Wettability alteration behavior	Strongly Water-wet	Water-wet	Weakly Water-wet	Intermediate wet	Weakly Oil-wet	Oil-wet	Strongly Oil-wet

The IFT and contact angle measurements at ambient conditions are performed in two parts. First, the optimal nanofluid concentration is determined and then the effect of combining surfactants with nanoparticles is investigated. The latter is also performed at reservoir conditions.

The contact angle measurements at each stage are repeated two times to confirm the reproducibility of the results of DDDC technique.

3.2.3. Finding optimal concentration of nanoparticles

Five samples of nanofluids classified by concentration were used for IFT and contact angle measurements at ambient conditions. The first sample was brine with no nanoparticles to establish the initial wettability condition of the system. Using brine as the dispersant fluid, other samples were prepared at 0.1 wt.%, 0.2 wt.%, 0.4 wt.%, and 0.8 wt.% nanoparticle concentrations. Based on the IFT and contact angle measurements, the optimal concentration of nanofluid was determined to combine with surfactants. The most and least effective surfactant candidates for contact angle measurements at ambient conditions were from the family of ALFOTERRA, which are designed to perform better at temperatures below 60 ºC. For reservoir conditions, a surfactant candidate from the group of SOLOTERRA was selected, which are designed for high temperatures (above 60 ºC).

3.2.4. Combining surfactants with nanoparticles

The next step was to add the optimal concentration of nanoparticles to the selected surfactants to prepare surfactant-based nanofluids. For this part of the study, five cases were investigated. The first case was brine with no nanoparticles as the base case. The second case was the surfactant solution with no nanoparticles. For this case, the most and least effective surfactants in terms of wettability alteration were used based on screening results. The third case to compare was the optimal nanofluid concentration with only nanoparticles in brine. The fourth sample was prepared by mixing the optimal nanofluid concentration and the surfactant candidate. In the final sample, the concentration of surfactant was lowered to see how wettability alteration potential of

surfactant-based nanofluid changes. Table 3.4 contains detailed information about all the contact angle measurements performed in this research.

Table 3.4. List of the contact angle measurements using nanofluids.

No.	Experimental Conditions	Solution Type	Composition
1	Ambient	Brine	2 wt% NaCl
2	Ambient	Brine-based Nanofluid	0.1 wt% Nanopartciles
3	Ambient	Brine-based Nanofluid	0.2 wt% Nanopartciles
4	Ambient	Brine-based Nanofluid	0.4 wt% Nanopartciles
5	Ambient	Brine-based Nanofluid	0.8 wt% Nanopartciles
6	Ambient	Surfactant	ALFOTERRA S23-13S 90 (100 ppm)
7	Ambient	Surfactant-based Nanofluid	0.4 wt% Nanopartciles + ALFOTERRA S23-13S 90 (100 ppm)
8	Ambient	Surfactant-based Nanofluid	0.4 wt% Nanopartciles + ALFOTERRA S23-13S 90 (50 ppm)
9	Ambient	Surfactant	ALFOTERRA S23-9S 90 (100 ppm)
10	Ambient	Surfactant-based Nanofluid	0.4 wt% Nanopartciles + ALFOTERRA S23-9S 90 (100 ppm)
11	Ambient	Surfactant-based Nanofluid	0.4 wt% Nanopartciles + ALFOTERRA S23-9S 90 (50 ppm)
12	Reservoir*	Brine	2 wt% NaCl
13	Reservoir*	Surfactant	SOLOTERRA 938 (100 ppm)
14	Reservoir*	Brine-based Nanofluid	0.4 wt% Nanopartciles
15	Reservoir*	Surfactant-based Nanofluid	0.4 wt% Nanopartciles + SOLOTERRA 938 (100 ppm)
16	Reservoir*	Surfactant-based Nanofluid	0.4 wt% Nanopartciles + SOLOTERRA 938 (50 ppm)

Least effective surfactant

Most effective surfactant

* Reservoir Conditions: 700 psi & 150 °F

3.3. Coreflood experiments using nanofluids

To study the influence of nanoparticles and their combinations with surfactants on overall oil recovery and relative permeability curves, a range of different coreflood experiments were planned. This would also allow to confirm the wettability alteration behavior that surfactant-based nanofluids showed through contact angle measurements.

For corefloods at 500 psi and 72 ˚F, the same ALFOTERRA surfactant candidate from the contact angle measurements (the least effective in terms of wettability alteration) at ambient conditions was used to combine with nanoparticles. Additionally, a set of corefloods using the combination of nanoparticles with the most effective surfactant from the family of ALFOTERRA (discovered by the screening) was also conducted at 500 psi and 72 ˚F to determine the extent of nanoparticles impact on surfactants.

At both experimental conditions, the concentration of surfactants was kept at 2000 ppm. A system of Indiana limestone cores (12 in. by 2 in.), Yates crude oil, and 2 wt.% NaCl was used for all the corefloods. Each chemical solution was injected as a secondary recovery method. The brine solution (2 wt.% NaCl) was used as the base phase to make the surfactant and nanofluid solutions. For each coreflood, a fresh limestone core was used and initially saturated with oil. For all the experiments, 500 psi and 2000 psi were used as the backpressure and confining pressure respectively. For corefloods at reservoir conditions, the same SOLOTERRA surfactant candidate from the contact angle measurements at reservoir conditions was used. The experiments were conducted at 700 psi and 150 ºF and 2000 psi was used as the confining pressure.

Similar to the contact angle measurement procedure, the concentration of surfactant was lowered in the last coreflood (at both experimental conditions) to see how the wettability alteration potential of the surfactant-based nanofluids changes. The wettability alteration potential of each flood was revealed through the relative permeability curves that were generated by the simulator. Finally, the coreflood results were compared to their respective contact angle measurements. Table 3.5 includes detailed information about all the coreflood experiments conducted using nanofluids including the ones with the least effective surfactant at 500 psi and 72 ˚F (numbers 3, 4, and 5),

the ones with the most effective surfactant at 500 psi and 72 ˚F (numbers 6,7, and 8), and the ones with the least effective surfactant at reservoir conditions (numbers 10, 12, and 13).

Table 3.5. List of the coreflood experiments using nanofluids at both experimental conditions.

No.	Experimental Conditions	Rock Type	Oil Type	Flood Solution	Fluid Composition
1	500 psi & 72 ˚F	Limestone	Yates Crude Oil	Brine	2 wt.% NaCl
2	500 psi & 72 ˚F	Limestone	Yates Crude Oil	Brine-based nanofluid	0.4 wt.% Nanopartciles
3	500 psi & 72 ˚F	Limestone	Yates Crude Oil	Surfactant	ALFOTERRA S23-13S 90 (2000 ppm)
4	500 psi & 72 ˚F	Limestone	Yates Crude Oil	Surfactant-based nanofluid	0.4 wt.% Nanopartciles + ALFOTERRA S23-13S 90 (2000 ppm)
5	500 psi & 72 ˚F	Limestone	Yates Crude Oil	Surfactant-based nanofluid	0.4 wt.% Nanopartciles + ALFOTERRA S23-13S 90 (1000 ppm)
6	500 psi & 72 ˚F	Limestone	Yates Crude Oil	Surfactant	ALFOTERRA S23-9S 90 (2000 ppm)
7	500 psi & 72 ˚F	Limestone	Yates Crude Oil	Surfactant-based nanofluid	0.4 wt.% Nanopartciles + ALFOTERRA S23-9S 90 (2000 ppm)
8	500 psi & 72 ˚F	Limestone	Yates Crude Oil	Surfactant-based nanofluid	0.4 wt.% Nanopartciles + ALFOTERRA S23-9S 90 (1000 ppm)
9	700 psi & 150 ˚F	Limestone	Yates Crude Oil	Brine	2 wt.% NaCl
10	700 psi & 150 ˚F	Limestone	Yates Crude Oil	Surfactant	SOLOTERRA 938 (2000 ppm)
11	700 psi & 150 ˚F	Limestone	Yates Crude Oil	Brine-based nanofluid	0.4 wt.% Nanopartciles
12	700 psi & 150 ˚F	Limestone	Yates Crude Oil	Surfactant-based nanofluid	0.4 wt.% Nanopartciles + SOLOTERRA 938 (2000 ppm)
13	700 psi & 150 ˚F	Limestone	Yates Crude Oil	Surfactant-based nanofluid	0.4 wt.% Nanopartciles + SOLOTERRA 938 (1000 ppm)

Least effective surfactant

Most effective surfactant

3.4. Coreflood simulation

The main purpose of coreflood simulation is to use optimized history matching of oil recovery and pressure drop data to determine relative permeability curves and fractional flow trends and consequently develop a surfactant-based wettability alteration technology for oil field implementation.

The simulation is based on a semi-analytical relative permeability model developed by Okazawa (1983) and the theory of fractional flow to estimate the recovery and pressure drop at a given time during the displacement process. The pressure drop is calculated by deriving the saturation profile in the core and consequently calculating the total mobility along the core. The capillary pressure effect is neglected in this model. The model estimates relative permeabilities by minimizing the sum-of-squares of the weighted deviations of the experimental pressure and production histories from the calculated values. The equations (Eq. 3.1, 3.2, and 3.3) used by the simulator to generate relative permeabilities curves are as follow:

$$K_{rw} = S^{e_w}.k_{rw} \quad \text{..... (3.1)}$$

$$K_{ro} = (1-S)^{e_o}.k_{ro} \quad \text{..... (3.2)}$$

$$S = (S_w - S_{iw})/(1 - S_{or} - S_{iw}) \quad \text{..... (3.3)}$$

S_w water saturation
S_{iw} irreducible water saturation
S_{or} residual oil saturation
S normalized saturation
K_{rw} relative permeability to water
K_{ro} relative permeability to oil
k_{rw} relative permeability to water at S_{or}
k_{ro} relative permeability to oil at S_{iw}
e_w, e_o Corey exponents

CMG STARS was used in this project as the simulator. First a 28×1×1 grids cartesian model representing the core (12 in. length and 2 in. diameter) was built in the Builder. Then, general properties of the core such as porosity, absolute permeability, reference pressure, and temperature were specified under Array Properties. Two components were defined for the model including water and oil and their densities and viscosities were entered under Phase Properties. Next, the Rock-Fluid properties of the model were completed using the General Table and by entering the end-points according to the experimental endpoints resulted from the coreflood and the Corey exponents. The Corey exponents could be set as a default value of 1.5 until adjusted later during optimization using CMOST. By applying the end-points, CMG creates a default relative permeability table which could be optimized later using CMOST. The final step of building the model would be defining one injection well and one production well in the first and last grid of the model. The maximum surface water rate was set as the injection well constraint according to the experimental injection rate. Also, minimum bottom-hole pressure was set as the production well constraint based on the experimental back-pressure of the core. Table 3.6 lists the parameters used in the model.

Table 3.6. Parameters used in the simulation model.

Model parameters	
Number of grids	28
Length	12 in.
Thickness	2 in.
Pressure	500 & 700 psi
Temperature	75 & 150 °F
Water Viscosity	1 cp
Oil Viscosity	12.8 cp
Waetr Density	1.011 g/cc
Oil Density	0.874 g/cc
Porosity	14-18 %
Permeability	15-60 md
Injection rate	2 cc/min

The final step was to save and run the model using STARS. Then, the plots of cumulative oil and well bottom-hole pressure were created using the Results Graph. To start the history matching process, the experimental oil recovery and pressure drop data were added to the plots using Filed History.

The history match process was done using the CMOST software (part of CMG package) for optimization and sensitivity analysis. In the CMOST, a new project was initiated by setting the Builder datafile as the base dataset. Then, a new study was created by initiating a name, base dataset, and type of study (history matching). In the new study, the most important step is the parametrization, in which certain parameters could be selected to be adjusted during the history match process. There are a few ways to select the parameters, one of which is to use the Builder option that links CMOST to the Builder section of the STAR. In the CMOST Definition windows that pops up, the parameter can be defined under Builder Key Words/Rel Perm Tables/Rock Type/Set 1/Show data. Once the endpoints table is appeared, parameters to be adjusted (relative permeability endpoints and Corey exponents) should be added and renamed to be recognized later in the CMOST. After saving and closing and going back to the CMOST page, parameters can be imported by clicking on Import. On the same page, the lower and upper limit of each parameter can be set under Data Range Settings. The Number of Discrete Levels improves the accuracy of the match with the price of running time. Then, under Objective Function/Basic Simulation Results, two items can be inserted. First one is renamed to Cum_Oil and the second one to BHP, respectively representing the cumulative oil and well bottom-hole pressure plots created previously. The Origin Names can be selected according to the name of the injection and production wells specified in the Builder. The Property would be selected as the cumulative oil and well bottom-hole pressure respectively. Under History Match Quality, two items can be

inserted namely, Cum_Oil_Error and Cum_BHP_Error, which represent the cumulative oil and well bottom-hole pressure errors during the history matching process. For each item, an Original Time Series Term must be inserted in the bottom window, which links the Origin Name (injection and production wells) and Property (cumulative oil and well bottom-hole pressure) to the specified error items. Under Control Centre/Engine Settings, Global Objective Function Name must be specified as GlobalHmError, which describes the total error of the history match considering both cumulative oil and well bottom-hole pressure plots. Under the Simulation Settings, the Local Scheduler (the computer that is being used to simulate) must be set to Active. Under Pre-Simulation Commands, the option Run CMG Builder Silently must be inserted to run the Builder in the background and update the relative permeability table according to each run. Finally, by clicking on the Control Centre and pressing the Play button, the CMOST engine can be started. While running, CMOST creates simulation datasets and run them with the CMG STAR simulator. After CMOST is completed, a wide variety of results are created and listed under Results and Analyses. For example, under Time Series/Observers, history match plots can be observed and under objective Functions/Cross Plot, the trends of cumulative oil and well bottom-hole pressure data points can be seen. However, the most useful feature for the purpose of this study was the Experiments Table under Control Centre, where the characteristics of each history match run including the defined errors were listed. By sorting the table based on the GlobalHmError, the most precise history match with the minimum global error can be found. By selecting the row with the minimum error and linking to its specific dataset in the Builder, the relative permeability table of the best history match can be achieved.

4. RESULTS AND DISCUSSION

The results are categorized into five sections. First, the results of coreflood experiments to screen the surfactants are presented. These results are compared to the contact angle measurements that were performed by the other member of the research group. Then, the surfactant candidates for combining with nanoparticles are selected. In the second section, the contact angle measurements for nanofluids are displayed for both ambient and reservoir conditions. These results will show how nanoparticles are effective in altering the wettability through changing the contact angles. Next section is to show how overall recovery and relative permeability curves are influenced by nanoparticles through the results of coreflood experiments for both experimental conditions. Next, a preliminary economic analysis is provided to see how the use of surfactant-based nanofluid as a chemical flooding agent could be economically appealing. And finally, the results of microscopic investigation are discussed.

4.1. Corefloods to screen the surfactants

The results of this section are described in 6 separate parts for 6 surfactant corefloods including 4 ALFOTERRA surfactant floods at 500 psi and 72 ˚F and 2 SOLOTERRA surfactant floods at reservoir conditions (700 psi and 150 ˚F). Each part starts with a table representing the specific parameters for the coreflood including the name of the core, rock type, porosity, absolute permeability, pore volume of the core, the type of oil/brine/surfactant used in the coreflood, the injection rate, and finally the waterflood recovery achieved before injecting the surfactant.

The surfactant floods of this part of the research were conducted as a tertiary recovery method, following a waterflood as a secondary method and produced a very little amount of oil. Therefore, the oil recovery and pressure drop data could only be collected for the waterfloods. And

for that reason, the history match process of simulation was only applied on the oil recovery and pressure drop data from the waterfloods. Therefore, the simulated relative permeability curves only represent the influence of waterflood. The effects of surfactant floods are shown by the experimental endpoints. The history match of waterfloods are optimized using the CMOST software by adjusting the parameters including k_{rw} (water relative permeability endpoint) and k_{ro} (oil relative permeability endpoint) and their corresponding saturation values S_{or} (residual oil saturation) and S_{iw} (irreducible water saturation), and Corey exponents. The final history match plots include experimental and simulation trends for both oil recovery and pressure drop for each waterflood conducted before a surfactant flood.

Once the simulated oil recovery and pressure drop data from the model are reasonably matched with the experimental results, the simulated relative permeability curves for the waterfloods can be generated. Each relative permeability plot shown here includes the water and oil relative permeability curves for a waterflood in addition to the experimental endpoints for a surfactant flood.

The experimental endpoints are compared to their respective simulated values in tables adjacent to the relative permeability curves. Note that the simulated values are only available for the waterfloods, since no simulations were performed on the surfactant floods.

In the following parts, the final results from each coreflood are evaluated separately and the observations with regards to the contact angle measurements are discussed.

4.1.1. ALFOTERRA S23-7S 90

The first surfactant from the family of ALFOETERRA is applied on an Indiana limestone core with the porosity of about 15% and absolute permeability of about 19 md describing a rather tight core at 500 psi and 72 ˚F (Table 4.1). The waterflood recovery of about 21% shows a relative oil-wet behavior of the core before injecting the surfactant. The simulated oil recovery and pressure drop data are reasonably matched with the experimental values (Figure 4.1). The gradual increase of oil recovery after the water breakthrough corresponds to the oil produced from the small pores and reveals the oil-wet behavior of the core. The subsequent waterflood relative permeability curves (Figure 4.2) also describe the initial conditions with an oil-wet behavior based on the Craig's rules of thumb (e.g. the cross-over point of the curves is below the saturation of 0.5 and water relative permeability endpoint is higher than oil relative permeability endpoint). The position of the experimental endpoints resulting from the surfactant flood (injected as tertiary recovery method) estimates a very small shift to the right in the surfactant flood relative permeability curves (shown by the potential surfactant flood curves) compared to that of waterflood. This minor shift to the right represents a very small wettability alteration in the system toward less oil-wet caused by the surfactant leading to a lower amount of residual oil saturation and consequently higher amount of oil production. The residual oil saturation is changing from 0.66 for waterflood to 0.63 for the surfactant flood as seen in Table 4.2. The comparison of endpoints listed in Table 4.2 shows how close the experimental data are to the simulated values in the waterflood relative permeability curves. Note that the surfactant flood is not simulated here. Hypothetically

Table 4.1. Initial coreflood parameters using ALFOTERRA S23-7S at 500 psi and 72 ˚F.

Core name:	Indiana Limestone-13 (12X2)	
Porosity:	15.24	%
Abs. Perm:	18.94	md
Pore Volume	117	cc
Oil	Yates crude oil	
Brine (NaCl)	2%	wt
Surfactant (ALF S23-7S)	2000	ppm
Injection rate	2	cc/min
Waterflood Recovery	20.62	%

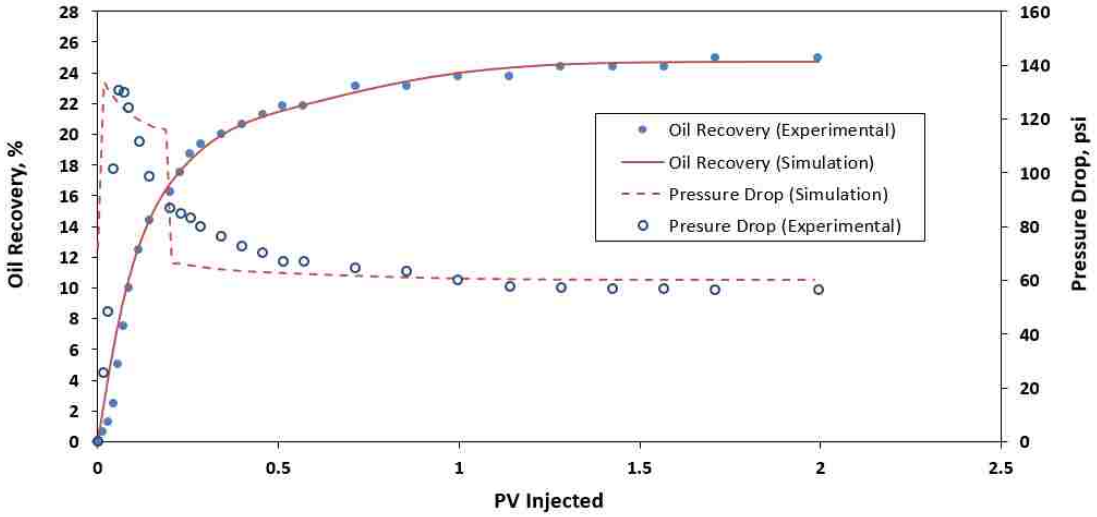

Figure 4.1. History match of oil recovery and pressure drop for waterflood at 500 psi and 72 ˚F before injecting ALFOTERRA S23-7S 90.

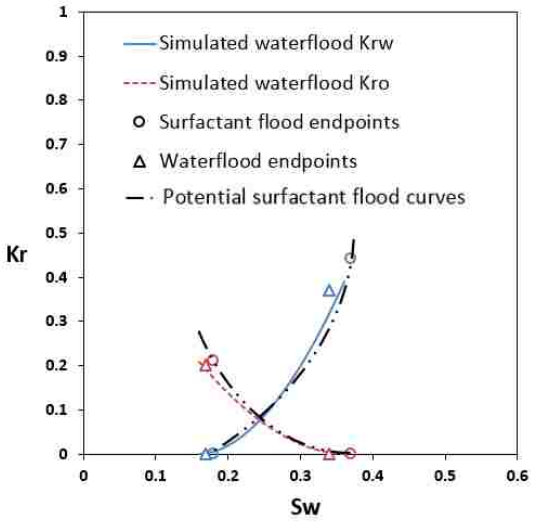

Table 4.2. Experimental and simulation endpoints for ALFOTERRA S23-7S 90 at 500 psi and 72 ˚F.

		Waterflood	ALF 7S
Experimental	Siw	0.17	0.18
	Sor	0.66	0.63
	krw	0.37	0.44
	kro	0.2	0.21
Simulation	Siw	0.16	N/A
	Sor	0.645	
	Krw	0.389	
	Kro	0.21	

Figure 4.2. Simulated relative permeability curves for waterflood at 500 psi and 72 ˚F before injecting ALFOTERRA S23-7S 90.

4.1.2. ALFOTERRA S23-9S 90

The second ALFOTERRA is applied on an Indiana limestone core with the porosity of about 16% and absolute permeability of 13.5 md describing a relatively tight core at ambient conditions (Table 4.3). The waterflood recovery of about 29% shows a relative oil-wet behavior of the core before injecting the surfactant. The simulated oil recovery and pressure drop data are reasonably matched with the experimental values (Figure 4.3). The waterflood relative permeability curves (Figure 4.4) also describe the initial conditions with an oil-wet behavior due to the position of the cross-over point that is below 0.5 and also higher water relative permeability endpoint compared to the oil relative permeability endpoint. The position of the experimental endpoints resulting from the surfactant flood (injected as tertiary recovery method) predicts a clear shift to the right for the surfactant flood relative permeability curves (shown by the potential surfactant flood curves) compared to that of waterflood. This shift to the right represents a wettability alteration in the system toward less oil-wet caused by the surfactant leading to a lower amount of residual oil saturation and consequently higher amount of oil production. The residual oil saturation is changing from 0.57 for the waterflood to 0.52 for the surfactant flood as seen in Table 4.4. This table also shows how near the experimental data are to the simulated values in the waterflood relative permeability curves. Note that the surfactant flood is not simulated here.

Table 4.3. Initial coreflood parameters using ALFOTERRA S23-9S at 500 psi and 72 ˚F.

Core name:	Indiana Limestone-06 (12X2)	
Porosity:	15.95	%
Abs. Perm:	13.50	md
Pore Volume	98.5	cc
Oil	Yates crude oil	
Brine (NaCl)	2%	wt
Surfactant (ALF S23-9S)	2000	ppm
Injection rate	2	cc/min
Waterflood Recovery	28.93	%

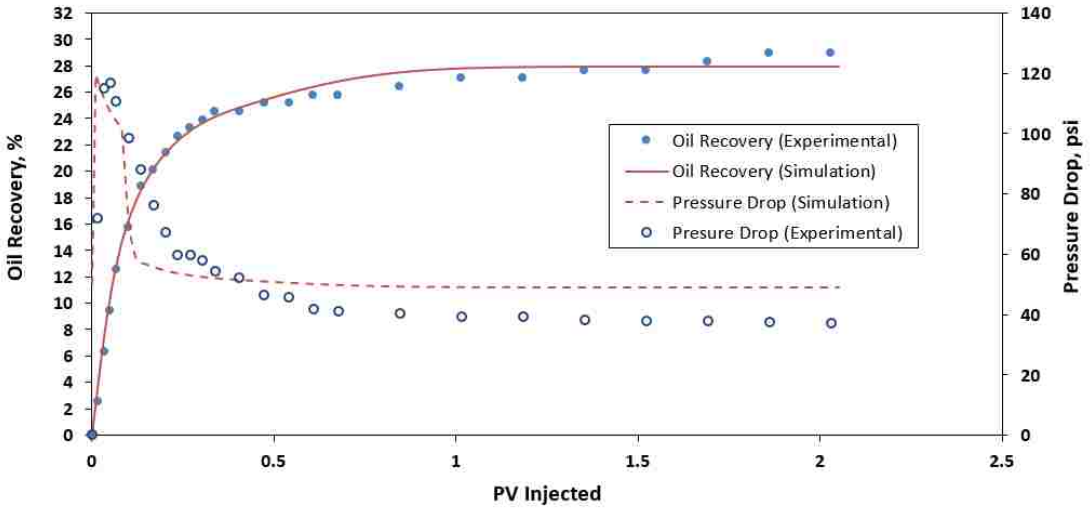

Figure 4.3. History match of oil recovery and pressure drop for waterflood at 500 psi and 72 ˚F before injecting ALFOTERRA S23-9S 90.

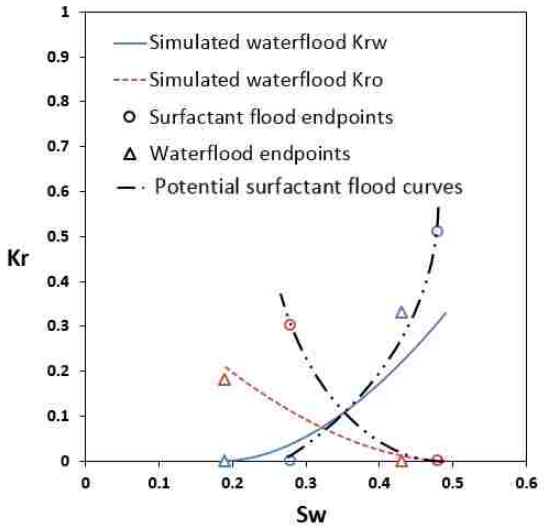

Table 4.4. Experimental and simulation endpoints for ALFOTERRA S23-9S 90 at 500 psi and 72 ˚F.

		Waterflood	ALF 9S
Experimental	Siw	0.19	0.28
	Sor	0.57	0.52
	krw	0.33	0.51
	kro	0.18	0.30
Simulationl	Siw	0.19	N/A
	Sor	0.518	
	Krw	0.33	
	Kro	0.206	

Figure 4.4. Simulated relative permeability curves for waterflood at 500 psi and 72 ˚F before injecting ALFOTERRA S23-9S 90.

4.1.3. ALFOTERRA S23-11S 90

The third ALFOTERRA is applied on an Indiana limestone core with the porosity of about 15.5% and absolute permeability of about 15 md depicting a rather tight core at 500 psi and 72 ˚F (Table 4.5). The waterflood recovery of about 28% shows a relative oil-wet behavior of the core before injecting the surfactant. The simulated oil recovery and pressure drop data match well with the experimental values (Figure 4.5). The waterflood relative permeability curves (Figure 4.6) also describe the initial conditions with an oil-wet behavior due to the position of cross-over point that is below 0.5 and also higher water relative permeability endpoint compared to the oil relative permeability endpoint. The position of the experimental endpoints resulting from the surfactant flood (injected as tertiary recovery method) seems to suggest a small shift to the right in the surfactant flood relative permeability curves (shown by the potential surfactant flood curves) compared to that of waterflood. This shift to the right represents a wettability alteration in the system toward less oil-wet caused by the surfactant leading to a lower amount of residual oil saturation and consequently higher amount of oil production. The residual oil saturation is changing from 0.57 for the waterflood to 0.55 for the surfactant flood as seen in Table 4.6. This table also shows how close the experimental data are to the simulated values in the waterflood relative permeability curves. Note that the surfactant flood is not simulated here.

Table 4.5. Initial coreflood parameters using ALFOTERRA S23-11S at 500 psi and 72 ˚F

Core name:	Indiana Limestone-09 (12X2)	
Porosity:	15.55	%
Abs. Perm:	15.39	md
Pore Volume	96	cc
Oil	Yates crude oil	
Brine (NaCl)	2%	wt
Surfactant (ALF S23-11S)	2000	ppm
Injection rate	2	cc/min
Waterflood Recovery	27.6	%

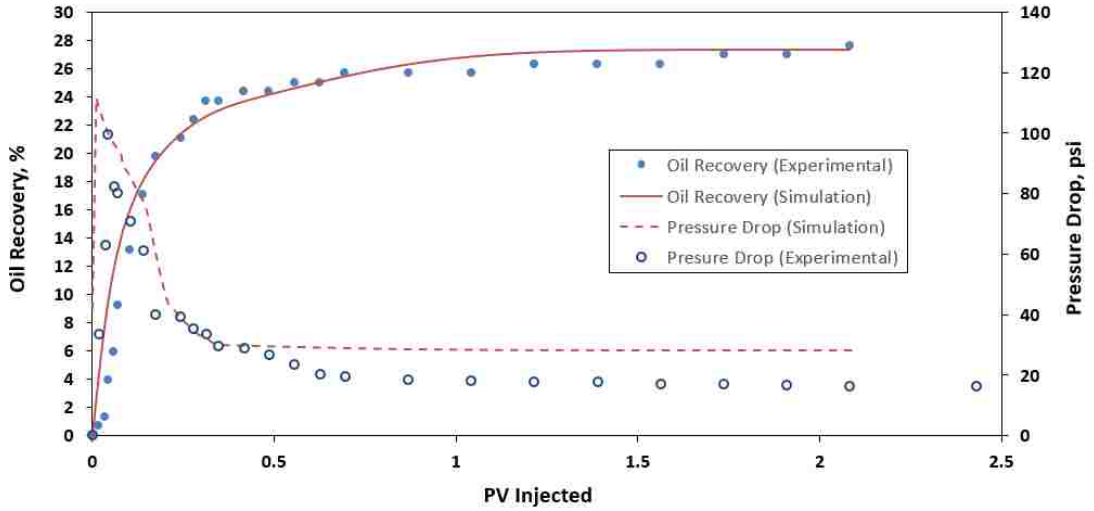

Figure 4.5. History match of oil recovery and pressure drop for waterflood at 500 psi and 72 ˚F before injecting ALFOTERRA S23-11S 90.

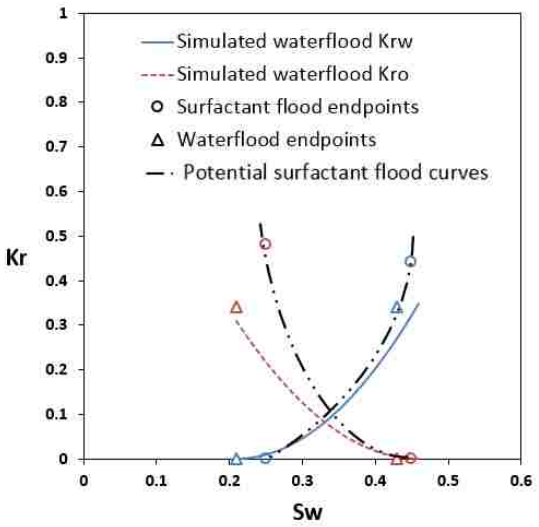

Table 4.6. Experimental and simulation endpoints for ALFOTEARRA S23-11S 90 at 500 psi and 72 ˚F

		Waterflood	ALF 11S
Experimental	Siw	0.21	0.25
	Sor	0.57	0.55
	krw	0.34	0.44
	kro	0.34	0.48
Simulation	Siw	0.21	N/A
	Sor	0.54	
	Krw	0.347	
	Kro	0.316	

Figure 4.6. Simulated relative permeability curves for waterflood at 500 psi and 72 ˚F before injecting ALFOTERRA S23-11S 90.

4.1.4. ALFOTERRA S23-13S 90

The last surfactant from the ALFOTERRA group is applied on an Indiana limestone core with the porosity of about 18% and absolute permeability of about 23.5 md depicting a rather tight core at 500 psi and 72 ˚F (Table 4.7). The waterflood recovery of about 20.5% shows a relative oil-wet behavior of the core before injecting the surfactant. The simulated oil recovery and pressure drop data match well with the experimental values (Figure 4.7). The waterflood relative permeability curves also describe an oil-wet initial condition due to the position of cross-over point that is below 0.5 and also higher water relative permeability endpoint compared to the oil relative permeability endpoint (Figure 4.8). The position of the experimental endpoints resulting from the surfactant flood (injected as tertiary recovery method) describes almost no shift to the right in the surfactant flood relative permeability curves (shown by the potential surfactant flood curves) compared to that of waterflood. This phenomenon suggests that no wettability alteration effect is caused by this surfactant. Therefore, this surfactant does not help to reduce the residual oil saturation and consequently does not improve the oil production. The residual oil saturation is not changing from waterflood to the surfactant flood and stays at 0.66 as seen in Table 4.8. This table also shows how close the experimental data are to the simulated values in the waterflood relative permeability curves. Note that the surfactant flood is not simulated here.

Table 4.7. Initial coreflood parameters using ALFOTERRA S23-13S at 500 psi and 72 ˚F.

Core name:	Indiana Limestone-10 (12X2)	
Porosity:	18.14	%
Abs. Perm:	23.59	md
Pore Volume	112	cc
Oil	Yates crude oil	
Brine (NaCl)	2%	wt
Surfactant (ALF S23-13S)	2000	ppm
Injection rate	2	cc/min
Waterflood Recovery	20.43	%

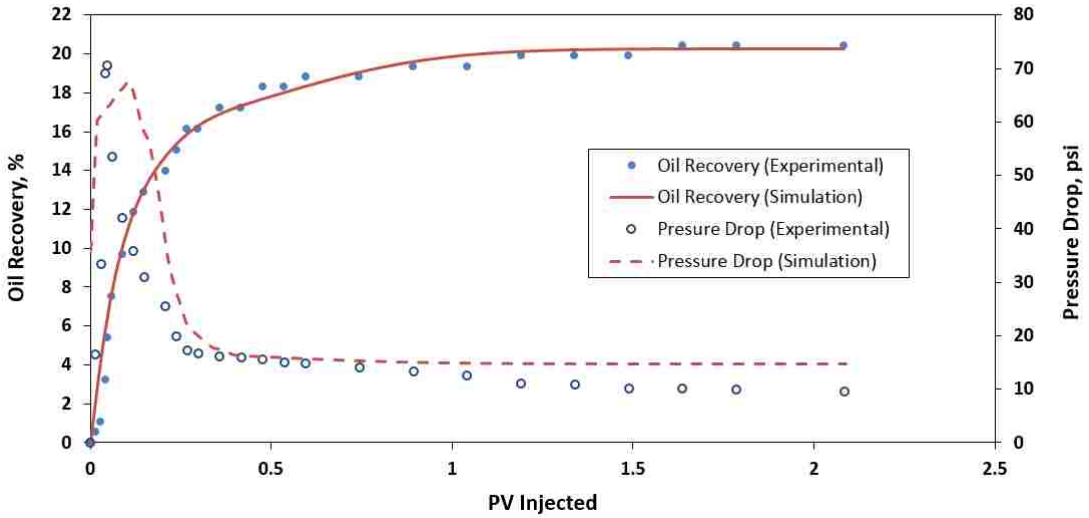

Figure 4.7. History-match of oil recovery and pressure drop for waterflood at 500 psi and 72 ˚F before injecting ALFOTERRA S23-13S 90.

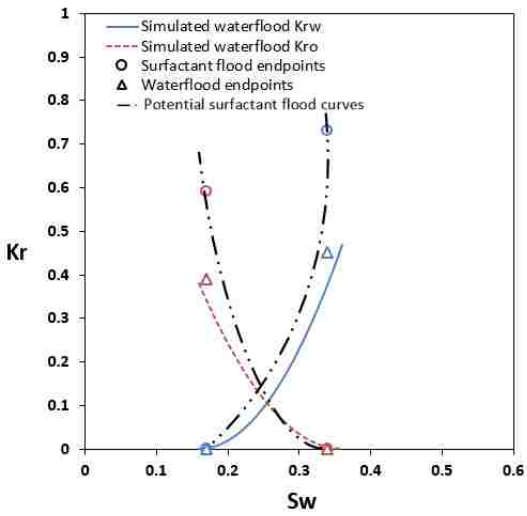

Table 4.8. Experimental and simulation endpoints for ALFOTERRA S23-13S 90 at 500 psi and 72 ˚F.

		Waterflood	ALF 13S
Experimental	Siw	0.170	0.15
	Sor	0.660	0.66
	krw	0.450	0.73
	kro	0.390	0.59
Simulation	Siw	0.160	N/A
	Sor	0.644	
	Krw	0.466	
	Kro	0.381	

Figure 4.8. Simulated relative permeability curves for waterflood at 500 psi and 72 ˚F before injecting ALFOTERRA S23-13S 90.

4.1.5. SOLOTERRA 939

The first SOLOTERRA is applied on an Indiana limestone core with the porosity of about 16% and absolute permeability of about 16.5 md (Table 4.9) describing a rather tight core at high pressure and high temperature or reservoir conditions (700 psi, 150 ºF). The waterflood recovery of about 20 % shows a relative oil-wet behavior of the core before injecting the surfactant. The simulated oil recovery and pressure drop data match reasonably well with the experimental values (Figure 4.9). The waterflood relative permeability curves also describe the initial conditions with an oil-wet behavior due to the position of cross-over point that is below 0.5 and also higher water relative permeability endpoint compared to the oil relative permeability endpoint (Figure 4.10). The position of the experimental endpoints resulting from the surfactant flood (injected as tertiary recovery method) seems to suggest a very little shift to the right in the surfactant flood relative permeability curves (shown by the potential surfactant flood curves) compared to that of waterflood. Although this shift is very small, it represents a wettability alteration in the system toward less oil-wet caused by the surfactant leading to a lower amount of residual oil saturation and consequently higher amount of oil production. The residual oil saturation is changing from 0.62 for waterflood to 0.61 for the surfactant flood as seen in Table 4.10. This table also shows how near the experimental data are to the simulated values in the waterflood relative permeability curves. Note that the surfactant flood is not simulated here.

Table 4.9. Initial coreflood parameters using SOLOTERRA 939 at reservoir conditions (700 psi, 150 ºF).

Core name:	Indiana Limestone-11 (12X2)	
Porosity:	16.19	%
Abs. Perm:	16.47	md
Pore Volume	100	cc
Oil	Yates crude oil	
Brine (NaCl)	2%	wt
Surfactant (SOL 939)	2000	ppm
Injection rate	2	cc/min
Waterflood Recovery	19.6	%

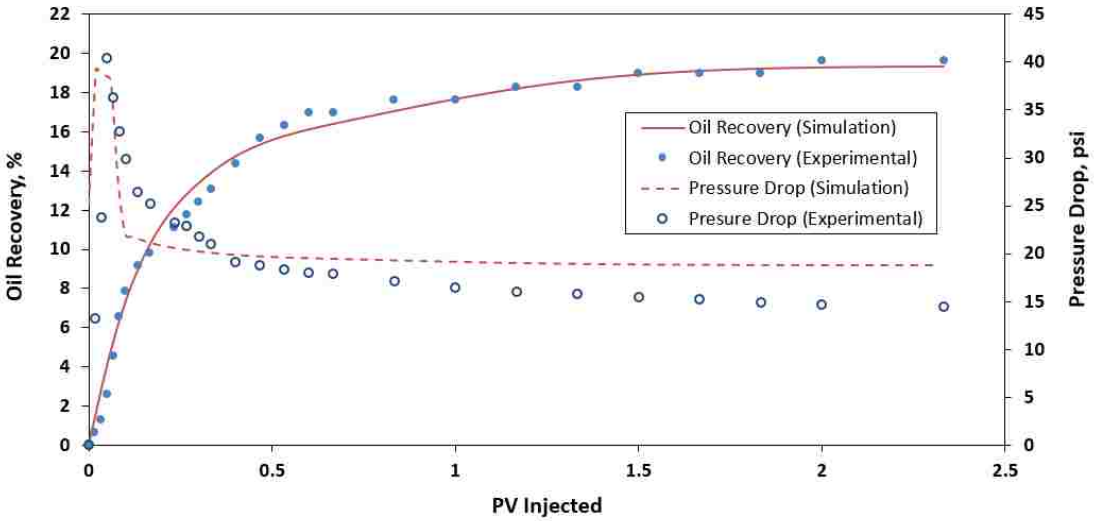

Figure 4.9. History match of oil recovery and pressure drop for waterflood at reservoir conditions (700 psi, 150 ºF) before injecting SOLOTERRA 939.

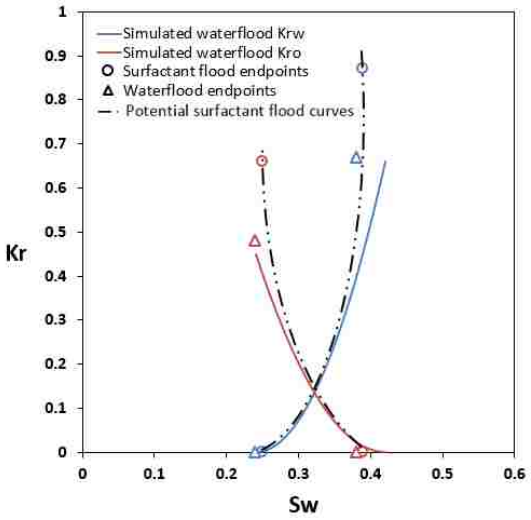

Table 4.10. Experimental and simulation endpoints for SOLOTERRA 939 at reservoir conditions (700 psi, 150 ºF).

		Waterflood	SOL 939
Experimental	Siw	0.24	0.25
	Sor	0.62	0.61
	krw	0.67	0.87
	kro	0.48	0.66
Simulation	Siw	0.24	N/A
	Sor	0.588	
	Krw	0.66	
	Kro	0.457	

Figure 4.10. Simulated relative permeability curves for waterflood at reservoir conditions (700 psi, 150 ºF) before injecting SOLOTERRA 939.

4.1.6. SOLOTERRA 938

The second SOLOTERRA is applied on an Indiana limestone core with the porosity of about 16% and absolute permeability of about 15 md (Table 4.11) describing a rather tight core at high pressure and high temperature or reservoir conditions (700 psi, 150 ºF). The waterflood recovery of 17.5% shows a relative oil-wet behavior of the core before injecting the surfactant. The simulated oil recovery and pressure drop data match reasonably well with the experimental values (Figure 4.11). The waterflood relative permeability curves also describe the initial conditions with an oil-wet behavior due to the position of cross-over point that is below 0.5 and also higher water relative permeability endpoint compared to the oil relative permeability endpoint (Figure 4.12). The position of the experimental endpoints resulting from the surfactant flood (injected as tertiary recovery method) seems to suggest almost no shift to the right in the surfactant flood relative permeability curves (shown by the potential surfactant flood curves) compared to that of waterflood. This phenomenon suggests that no wettability alteration toward less oil-wet is caused by this surfactant. The residual oil saturation is changing from 0.65 in case of waterflood to 0.64 for the surfactant flood as seen in Table 4.12. This table also shows how close the experimental data are to the simulated values in the waterflood relative permeability curves. Note that the surfactant flood is not simulated here.

Table 4.11. Initial coreflood parameters using SOLOTERRA 938 at reservoir conditions (700 psi, 150 ºF).

Core name:	Indiana Limestone-12 (12X2)	
Porosity:	16.35	%
Abs. Perm:	14.86	md
Pore Volume	101	cc
Oil	Yates crude oil	
Brine (NaCl)	2%	wt
Surfactant (SOL 938)	2000	ppm
Injection rate	2	cc/min
Waterflood Recovery	17.5	%

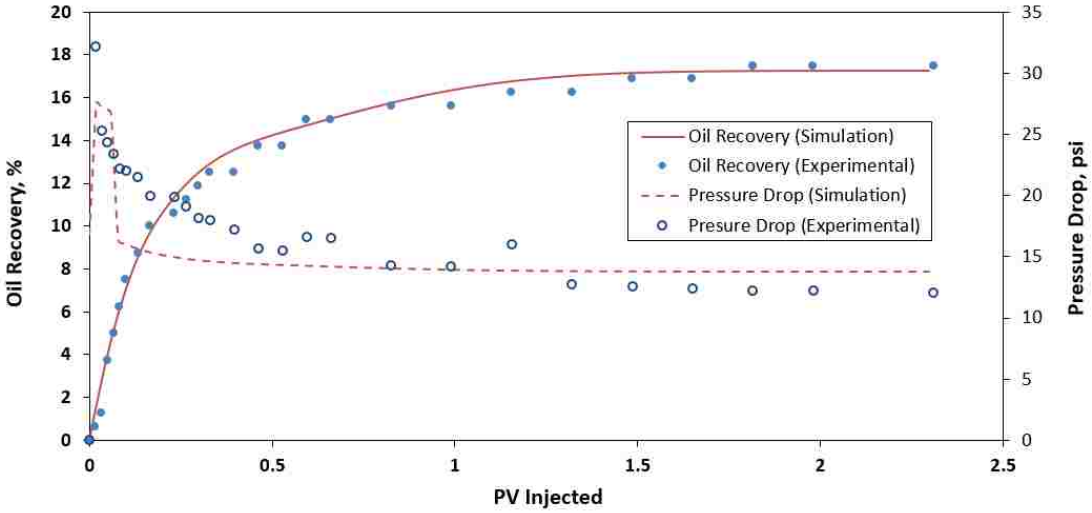

Figure 4.11. History match of oil recovery and pressure drop for waterflood at reservoir conditions (700 psi, 150 ºF) before injecting SOLOTERRA 938.

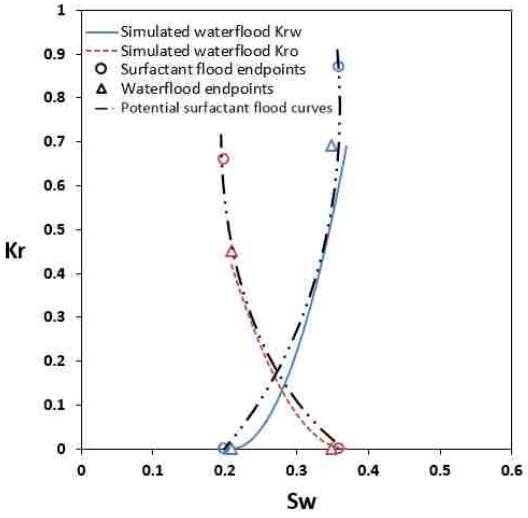

Table 4.12. Experimental and simulation endpoints for SOLOTERRA 938 at reservoir conditions (700 psi, 150 ºF).

		Waterflood	SOL 938
Experimental	Siw	0.210	0.2
	Sor	0.650	0.64
	krw	0.690	0.87
	kro	0.450	0.66
Simulation	Siw	0.210	N/A
	Sor	0.630	
	Krw	0.690	
	Kro	0.420	

Figure 4.12. Simulated relative permeability curves for waterflood at reservoir conditions (700 psi, 150 ºF) before injecting SOLOTERRA 938.

4.1.7. Summary

The coreflood results are compared to the contact angle measurements that were performed by the other member of the research group (Gupta, 2016), before selecting the surfactant candidates for nanofluid experiments. Table 4.13 summarizes the characterizations of each coreflood including the porosity and absolute permeability of the core, waterflood recovery, surfactant type injected after the waterflood, experimental conditions, and finally ranking of the surfactants based on their performance in altering the wettability revealed through the corefloods and relative permeability curves. Based the scoring mechanism, a surfactant with the largest shift-to-right in relative permeability curves is given the highest score of 4 and a surfactant with no shift-to-right is given the lowest score of 0. Therefore, the performances of other surfactants are scored accordingly.

Table 4.13. Summary of the coreflood results for screening the surfactants.

Core (#)	Porosity (%)	Absolute Permeability (mD)	Waterflood Recovery (%)	Surfactant Type (2000 ppm)	Experimental Conditions	Wettability Alteration Behavior Shift-to-Right Score (0 to 4)	Contact Angle Measurements (degrees)*
1	15.24	18.94	20.62	ALFOTERRA S23-7S	500 psi & 72° F	3	145° to 137°
2	15.95	13.50	28.93	ALFOTERRA S23-9S	500 psi & 72° F	4	152° to 90°
3	15.55	15.39	27.60	ALFOTERRA S23-11S	500 psi & 72° F	2	166° to 152°
4	18.14	23.59	20.43	ALFOTERRA S23-13S	500 psi & 72° F	0	155°
5	16.19	16.47	19.60	SOLOTERRA 939	700 psi & 150° F	1	170° to 135°
6	16.35	14.86	17.50	SOLOTERRA 938	700 psi & 150° F	1	170° to 155°

* Contact angle measurements conducted by Gupta (2016)

The results from the coreflood experiments suggest that ALFOTERRA S23-9S 90 is the strongest surfactant in terms of wettability alteration because it generated the largest shift-to-right in the relative permeability curves. This agrees well with the contact angle measurements that displayed a change of angle from 152° to 90°, meaning a great wettability alteration from strongly oil-wet to intermediate-wet. On the other hand, ALFOTERRA S23-13S 90 is the weakest surfactant in terms of wettability alteration because it generated no shift-to-right in the relative

permeability curves. This also agrees well with the contact angle measurements that displayed no change of angle for this surfactant (155°), which means it was not able to change the wettability and the system stayed in the strongly oil-wet zone even after applying the surfactant.

Based on this final evaluation, ALFOTERRA S23-13S 90 was selected as the least effective and ALFOTERRA S23-9S 90 as the most effective candidate in changing the wettability toward less oil-wet for contact angle measurements using nanofluids to see how adding nanoparticles impact their performance for wettability alteration at ambient conditions. On the other hand, SOLOTERRA 938 showed a poor performance in changing wettability at reservoir conditions. There was almost no shift-to-right observed in the relative permeability curves (score of 1) and the ability to change the contact angle was not significant, as it lowered the angle from 170° to 155° compared to SOLOTERRA 939 that lowered the angle from 170° to 135°. Therefore, SOLOTERRA 938 was selected as the least effective candidate with poor performance in changing wettability to prepare surfactant-based nanofluids for contact angle measurements at reservoir conditions.

4.2. Contact angle measurements using nanofluids

The results of this section are presented in three parts. First, the optimal concentration of nanofluids made by nanoparticles dispersed in brine is determined through IFT and contact angle measurements at ambient conditions to find the best scenario for wettability alteration. Then, the most effective concentration of nanoparticles is added to the surfactant candidates for both ambient and reservoir conditions. In the second part, the potential of prepared surfactant-based nanofluid for changing wettability is studied through IFT and contact angle measurements at ambient conditions. Finally, similar measurements are performed at reservoir conditions for the respective surfactant-based nanofluids. For each experiment in all three parts, actual images taken during the

DDDC method to measure the contact angles are provided along with the plots of advancing contact angle and TPCL movement vs. time. At the end of each part, the overall summary of the measurements is described using a bar chart and listed in a table.

4.2.1. Finding optimal concentration of nanoparticles

To measure the advancing contact angle at initial condition, brine (2 wt.% NaCl) was used with no nanoparticles. Figure 4.13 shows the actual images of the droplet at each stage starting with the static contact angle of 145° and ending with the dynamic advancing contact angle of 167°, which represents the strongly oil-wet behavior of the system.

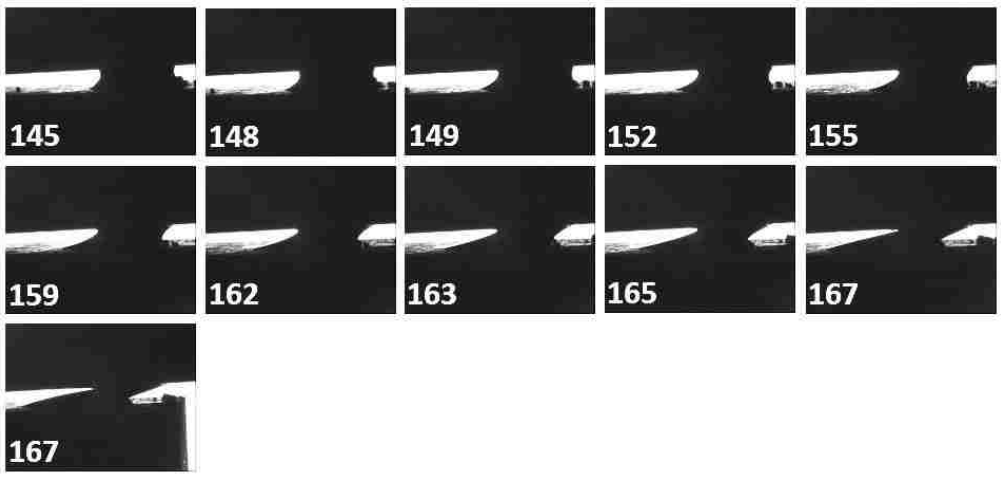

Figure 4.13. Actual images of DDDC method and the corresponding contact angles using Yates oil, limestone, and brine at ambient conditions.

The variation of the contact angles and TPCL movement with time during the DDDC method along with the repeats of the measurements are described in Figure 4.14 with the highest angle of 167° as the true water advancing contact angle, where the normalized TPCL drops. To ensure the accuracy and reproducibility of the measurements, each experiment is repeated by moving the rock back to its original position and mingling the droplets again. The repeats of the

measurements are also depicted in Figure 4.14 and show a similar trend of measured angles ending at about 167°.

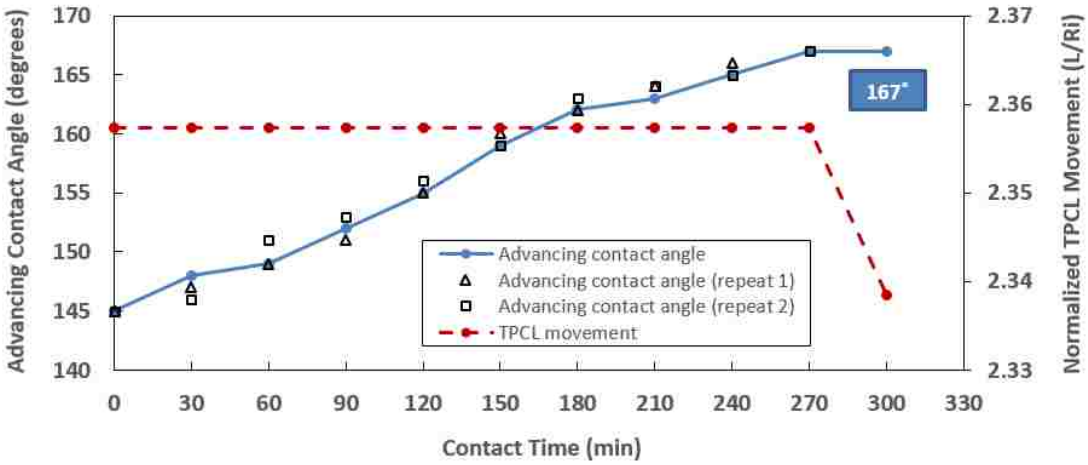

Figure 4.14. Contact angles variation and TPCL movement using Yates oil, limestone, and brine at ambient conditions.

To study the effect of nanoparticles on the advancing contact angle, 0.1 wt.% of nanoparticles was dispersed in brine and the solution was used to fill the DDDC cell. Figure 4.15 describes the actual images of the drop at each stage starting with the static contact angle of 135° and ending with the dynamic advancing contact angle of 165°. This shows that 0.1 wt.% brine-based nanofluid is not strong enough to change the wettability of the system as it stays in the strongly oil-wet zone. The variation of contact angles and TPCL movement with time during the DDDC method along with the repeats of the measurements are described in Figure 4.16, with the highest angle of 165° as the true advancing contact angle, where the normalized TPCL drops.

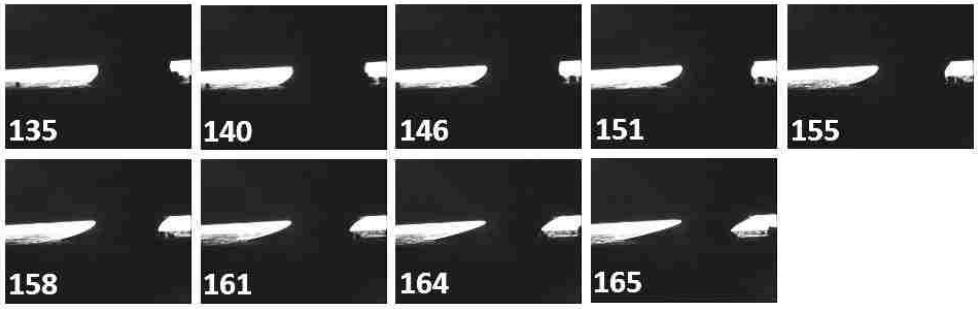

Figure 4.15. Actual images of DDDC method and the corresponding contact angles using Yates oil, limestone, and 0.1 wt.% brine-based nanofluid at ambient conditions.

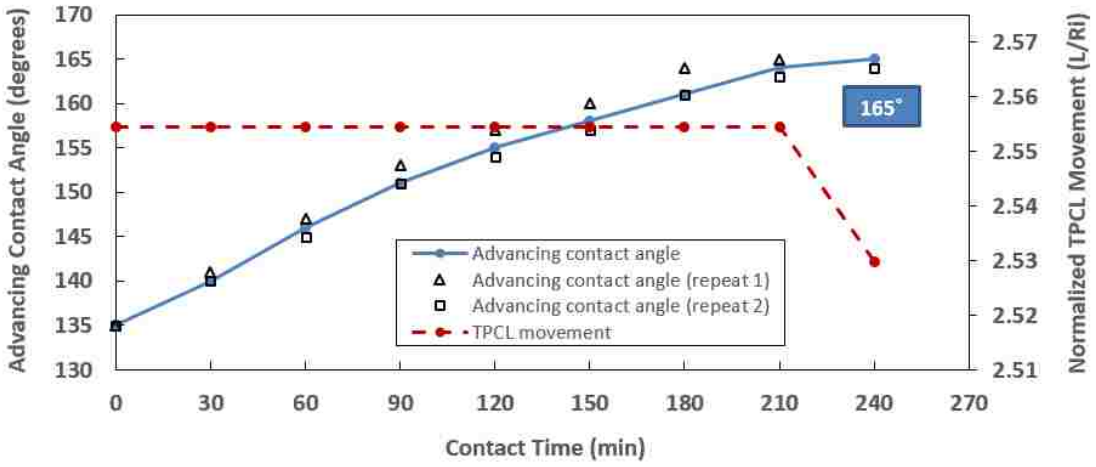

Figure 4.16. Contact angles variation and TPCL movement using Yates oil, limestone, and 0.1 wt.% brine-based nanofluid at ambient conditions.

The next experiment is using 0.2 wt.% nanoparticles in brine and the actual images of the droplet during the DDDC method is shown in Figure 4.17, in which the contact angles start from 131° and end at 156° as the advancing contact angle for the system. Therefore, the advancing contact angle in this case is lower than last case (165°), meaning that higher nanofluid concentration is effective toward altering the wettability from strongly oil-wet toward oil-wet. The variation of angles and TPCL movement with time and the repeats of the measurements are shown in Figure 4.18.

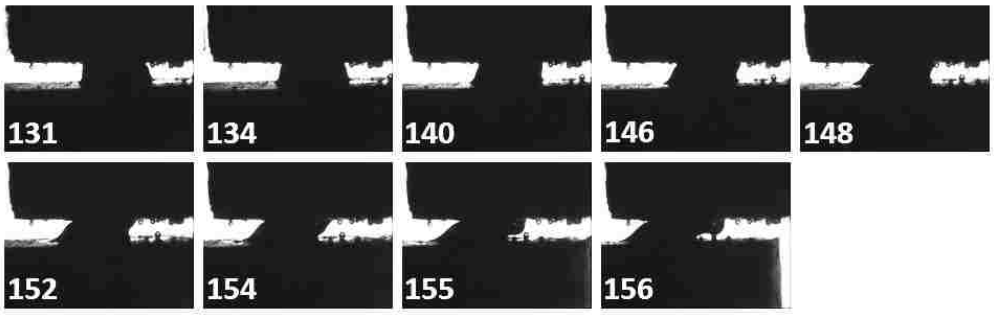

Figure 4.17. Actual images of DDDC method and the corresponding contact angles using Yates oil, limestone, and 0.2 wt.% brine-based nanofluid at ambient conditions.

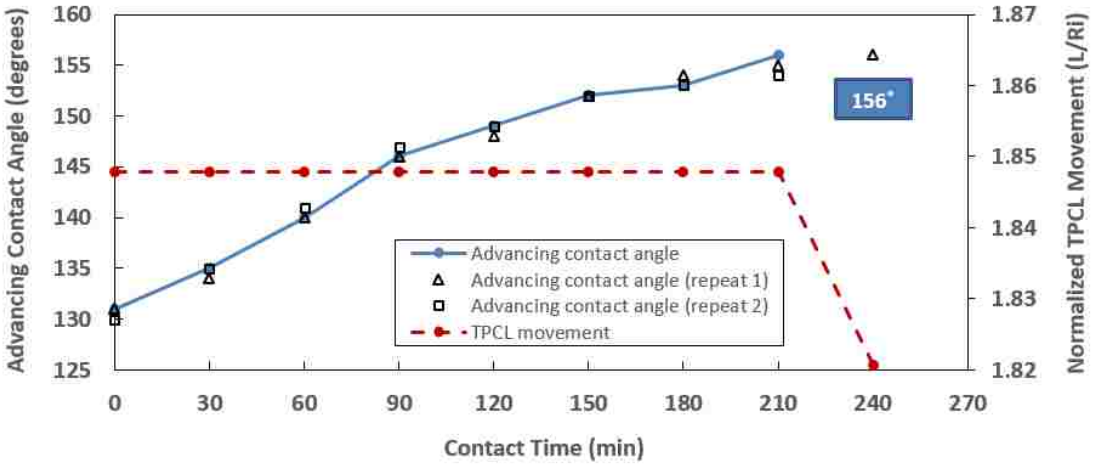

Figure 4.18. Contact angles variation and TPCL movement using Yates oil, limestone, and 0.2 wt.% brine-based nanofluid at ambient conditions.

The lowest advancing contact angle among different cases is achieved by 0.4 wt.% brine-based nanofluid at 146° (Figure 4.19) that shows a wettability alteration toward weakly oil-wet zone. The variation of contact angles and TPCL movement described in Figure 4.20 also show that the highest angle or the advancing contact angle is reached within a shorter time (150 minutes) compared to other cases (240 and 300 minutes). Therefore, a direct influence of higher nanofluid concentration on lowering the adhesion of oil to the rock for this system is observed.

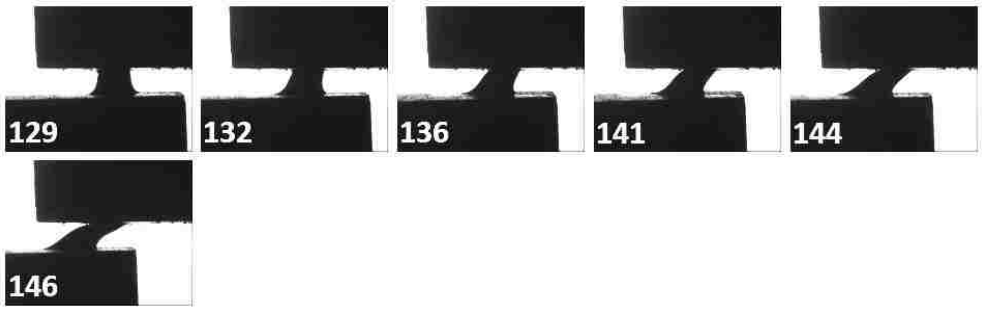

Figure 4.19. Actual images of DDDC method and the corresponding contact angles using Yates oil, limestone, and 0.4 wt.% brine-based nanofluid at ambient conditions.

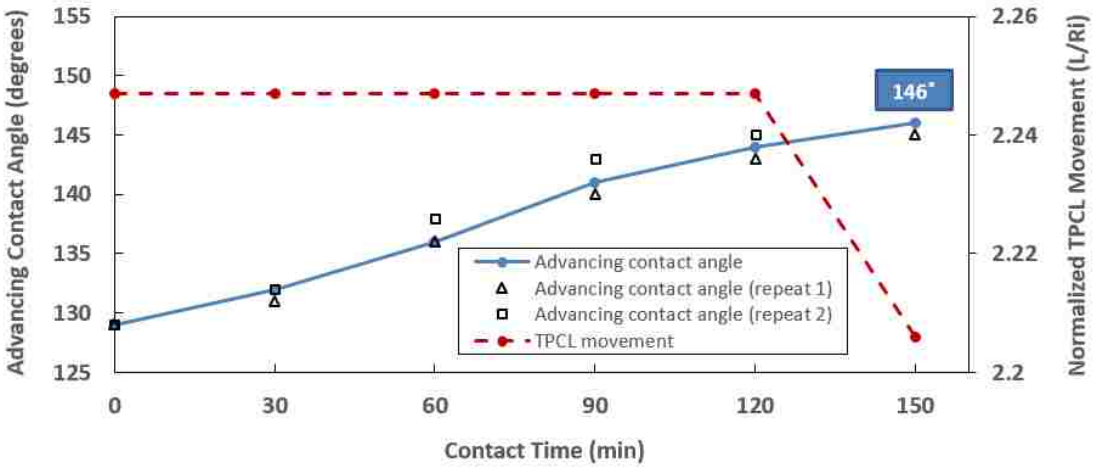

Figure 4.20. Contact angles variation and TPCL movement using Yates oil, limestone, and 0.4 wt.% brine-based nanofluid at ambient conditions.

The highest concentration of nanofluid used in the experiments was 0.8 wt.%, which resulted in an advancing contact angle of 143° as shown in Figure 4.21. The variation of contact angles and TPCL movement in Figure 4.22 depicts that the highest angle was reached within 180 minutes. Since doubling the nanofluid concentration in this case did not significantly contribute in lowering the advancing contact angle or shortening the time, as in previous cases, the nanofluid concentration of 0.4 wt.% was selected as the optimum concentration in lowering the advancing contact angle and changing the wettability toward less oil-wet state.

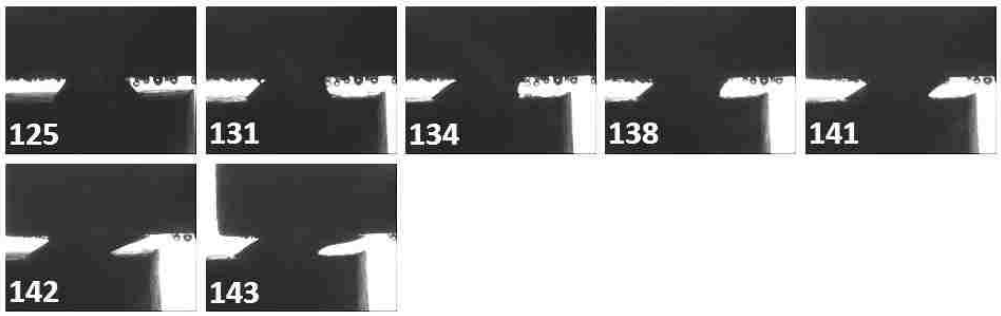

Figure 4.21. Actual images of DDDC method and the corresponding contact angles using Yates oil, limestone, and 0.8 wt.% brine-based nanofluid at ambient conditions.

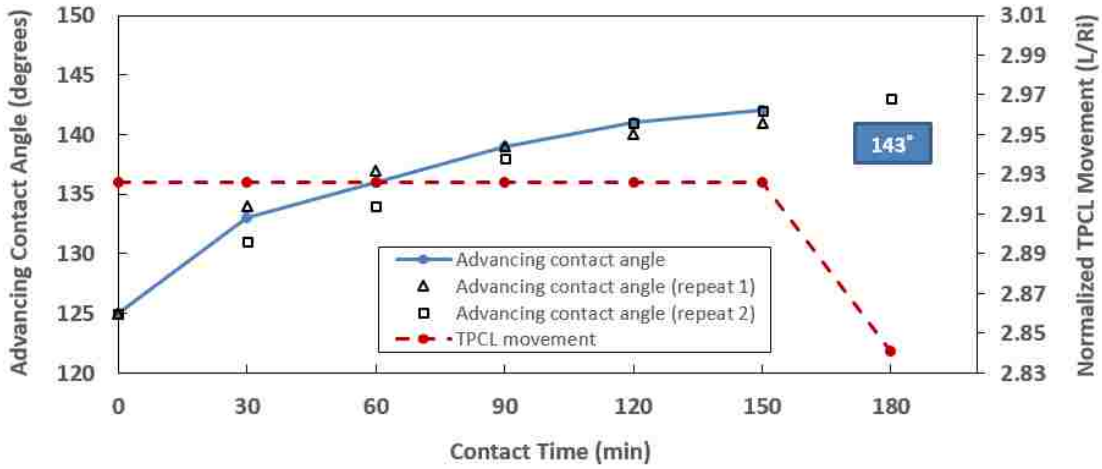

Figure 4.22. Contact angles variation and TPCL movement using Yates oil, limestone, and 0.8 wt.% brine-based nanofluid at ambient conditions.

Before measuring the contact angles for each case, the interfacial tension (IFT) of the oil and the nanofluid was measured in the cell and estimated using the Drop Shape Analysis software. Figure 4.23 describes a bar chart representing the dynamic advancing contact angles of brine-based nanofluids with different concentrations along with their respective IFT values.

The initial condition when brine contains no nanoparticles results in an IFT value of 23.2 mN/m. This value immediately is reduced to 13.1 mN/m by adding 0.1 wt.% nanoparticles to the brine, which shows the influence of nanoparticles in raising the surface activity of the system and lowering the IFT. The IFT reduction continues with a lower slope by doubling the concentration

of nanoparticles to reach 9.8 mN/m and 7.2 mN/m for the concentrations of 0.2 wt.% and 0.4 wt.% respectively. The slope of IFT reduction is lowered again toward the higher concentration of nanofluid. This results in an IFT value of 6.5 mN/m for 0.8 wt.% nanofluid, which is fairly close to the previous case. Since doubling the concentration of nanofluid to 0.8 wt.% does not significantly contribute in lowering the IFT as well as the advancing contact angle, 0.4 wt.% brine-based nanofluid seems to be the right optimum concentration in terms of wettability alteration.

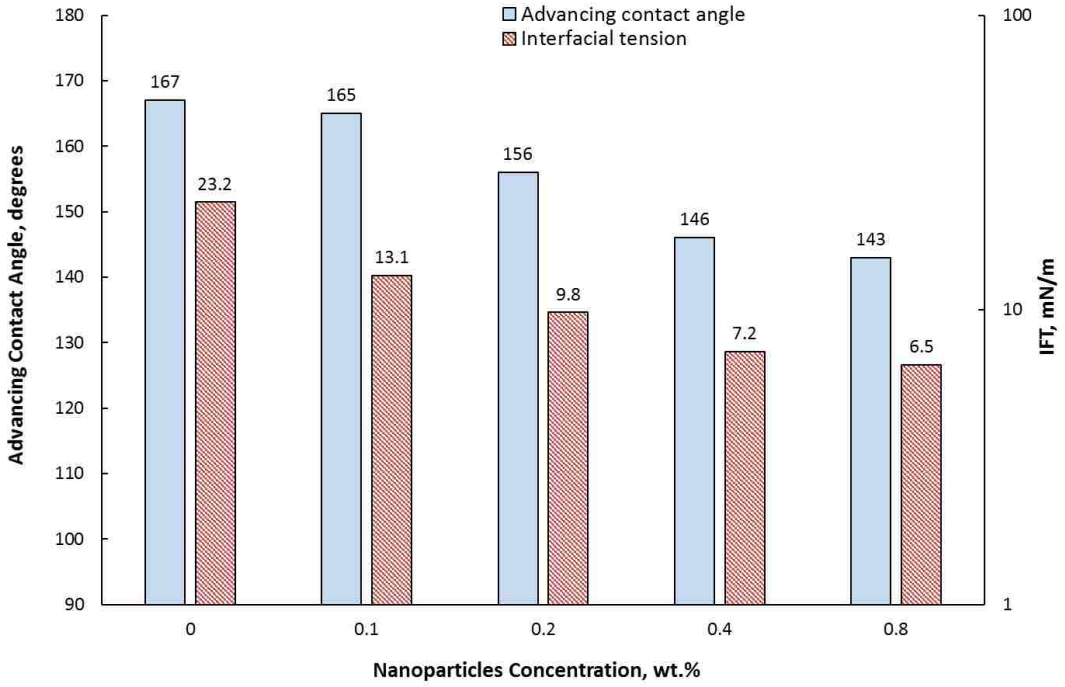

Figure 4.23. Comparison of IFT and contact angle values for different concentrations of brine-based nanofluids at ambient conditions.

4.2.2. Contact angle measurements using nanofluids at ambient conditions

To study the potential effect of nanoparticles on the wettability alteration performance of surfactants at ambient conditions, ALFOTERRA S23-13S 90 and ALFOTERRA S23-9S 90 were selected as the least and most effective surfactants based on the screening results. It was observed

in the contact angle measurements (Gupta, 2016) and confirmed with the coreflood results that ALFOTERRA S23-13S 90 had no effect (contact angle of 155°) and ALFOTERRA S23-9S 90 had the strongest effect (contact angle of 90°) in terms of altering the wettability of the system at ambient conditions. Therefore, the same type of surfactants and concentrations (100 ppm) were used to prepare the surfactant-based nanofluids of this study for contact angle measurements at ambient conditions.

To see how ALFOTERRA S23-13S 90, by itself, performs in terms of wettability alteration, a DDDC experiment was conducted using only surfactant at 100 ppm. Figure 4.24 describes the actual images of the droplet at each stage starting with the static contact angle of 139° and ending with the dynamic advancing contact angle of 162°. This means that the surfactant has not been effective in terms of wettability alteration as the advancing contact angle is still in the strongly oil-wet zone. Figure 4.25 shows the variation of contact angles and TPCL movement with time.

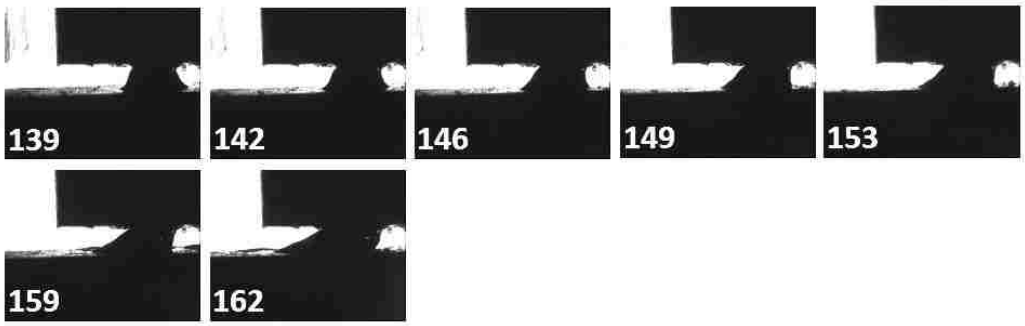

Figure 4.24. Actual images of DDDC method and the corresponding contact angles using Yates oil, limestone, and surfactant (ALF 13S, 100 ppm) at ambient conditions.

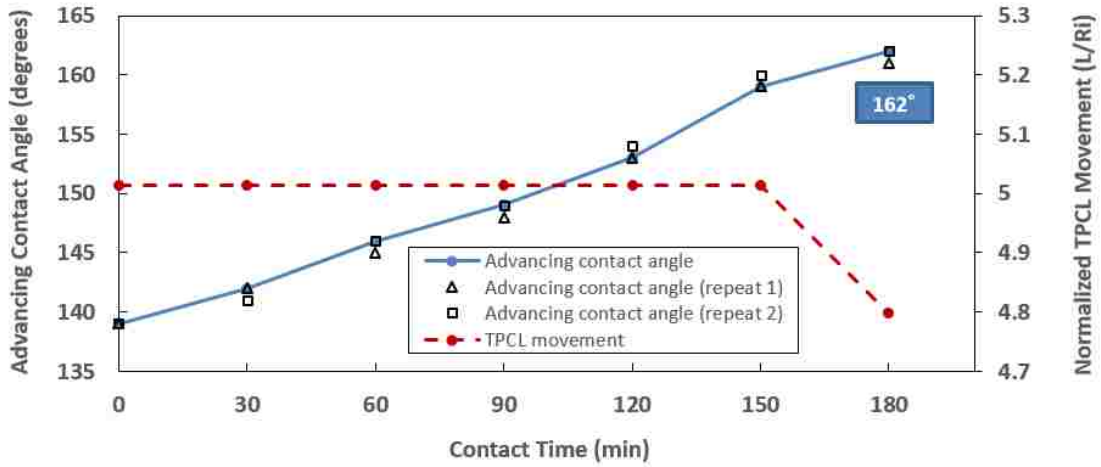

Figure 4.25. Contact angles variation and TPCL movement using Yates oil, limestone, and surfactant (ALF 13S, 100 ppm) at ambient conditions.

The next experiment was conducted by mixing the optimal nanofluid concentration (0.4 wt.%) and ALFOTERRA S23-13S 90 (100 ppm) to see if nanoparticles can enhance the performance of the surfactant to alter the wettability of the system. Figure 4.26 describes the great effect of nanoparticles in lowering the advancing contact angle from 162° (in the case of only surfactant) to 116° for the combination of nanoparticles and surfactant. This shift from the strongly oil-wet zone to intermediate-wet in 210 minutes (Figure 4.27) shows the great potential of surfactant-based nanofluid for altering the wettability of the limestone-Yates oil system at ambient conditions.

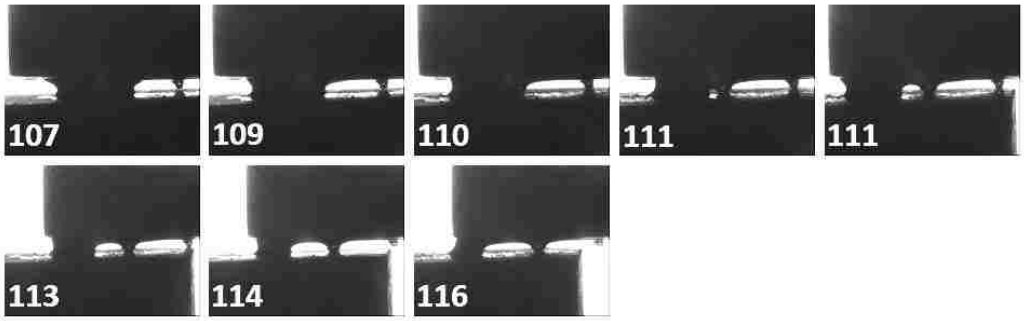

Figure 4.26. Actual images of DDDC method and the corresponding contact angles using Yates oil, limestone, and surfactant-based nanofluid (0.4 wt.% NP+ALF 13S, 100 ppm) at ambient conditions.

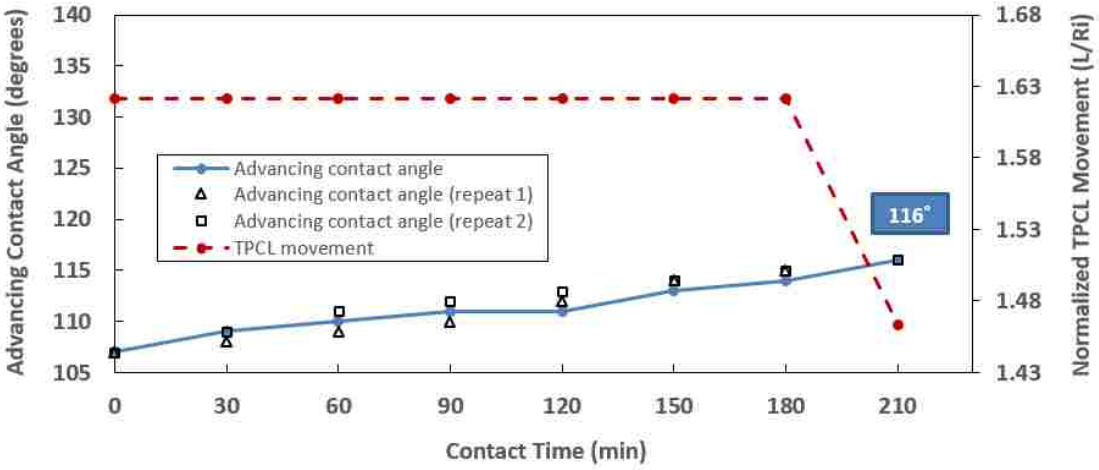

Figure 4.27. Contact angles variation and TPCL movement using Yates oil, limestone, and surfactant-based nanofluid (0.4 wt.% NP+ALF 13S, 100 ppm) at ambient conditions.

The next step is to study the contribution level of nanoparticles in changing the wettability. This helps to understand whether there is a potential to lower the concentration of surfactant and still observe the similar wettability alteration behavior to make surfactant-based nanofluid an economically appealing chemical agent. Figure 4.28 depicts how a combination of 0.4 wt.% nanoparticles with 50 ppm of ALFOTERRA S23-13S 90 plays an effective role. This surfactant-based nanofluid lowers the advancing contact angle from 162° (in the case of just surfactant) to 121° within 150 minutes (Figure 4.29). This represents a shift from strongly oil-wet to near intermediate-wet condition, when the surfactant concentration is lowered 50%.

Figure 4.28. Actual images of DDDC method and the corresponding contact angles using Yates oil, limestone, and surfactant-based nanofluid (0.4 wt.% NP+ALF 13S, 50 ppm) at ambient conditions.

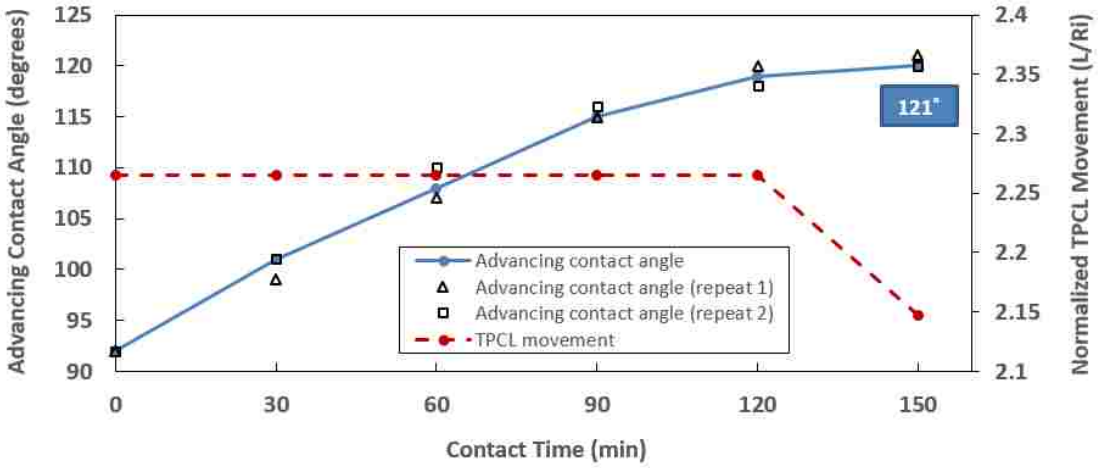

Figure 4.29. Contact angles variation and TPCL movement using Yates oil, limestone, and surfactant-based nanofluid (0.4 wt.% NP+ALF 13S, 50 ppm) at ambient conditions.

Therefore, a similar trend of wettability alteration (from strongly oil-wet to intermediate-wet conditions) is observed even after lowering the concentration of surfactant. This shows that silica nanoparticles have a potential to compensate for this specific surfactant in changing the wettability of the system toward less oil-wet at ambient conditions. The bar chart in Figure 4.30 describes the dynamic advancing contact angles of surfactant-based nanofluids (prepared by the least effective surfactant) along with their respective IFT values. First, the brine at initial condition is compared to ALFOTERRA S23-13S 90 (100 ppm). Adding surfactant significantly reduces the IFT from 23.2 mN/m to 0.02 mN/m. However, 0.4 wt.% nanoparticles seem to be able to boost up the IFT of solution two orders of magnitude (from 0.02 mN/m to 1.2 mN/m), when combined with 100 ppm of surfactant. The IFT value increases slightly when the concentration of surfactant is lowered to 50 ppm but stays fairly close to the previous case. This confirms the fact that a nearly consistent wettability alteration and IFT reduction behavior can be achieved even after lowering the concentration of surfactant.

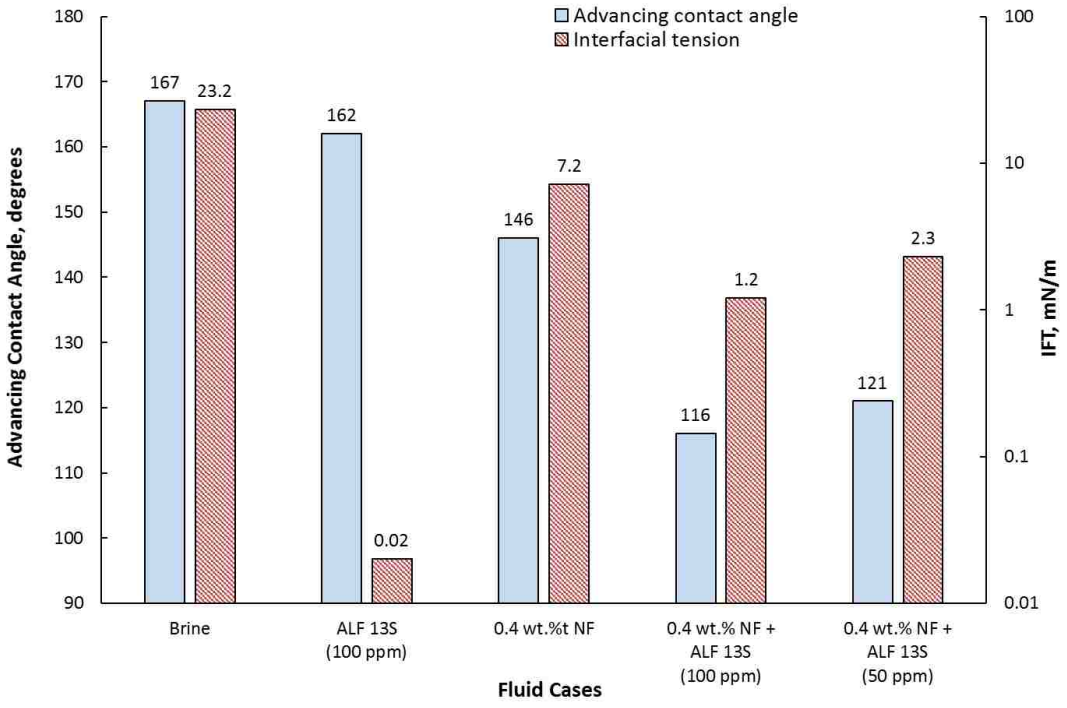

Figure 4.30. Comparison of IFT and contact angle values for surfactant-based nanofluids made by the least effective surfactant at ambient conditions.

A similar evaluation was conducted using the most effective surfactant (ALFOTERRA S23-9S 90) at ambient conditions to see how nanoparticles influence the performance of a strong surfactant in terms of wettability alteration. To see how ALFOTERRA S23-9S 90, by itself, performs in terms of wettability alteration, a DDDC experiment was conducted using only surfactant at 100 ppm. Figure 4.31 describes the actual images of the droplet at each stage starting with the static contact angle of 111° and ending with the dynamic advancing contact angle of 117°. This means that the surfactant has been very effective in terms of wettability alteration as the advancing contact angle is in the intermediate-wet zone. Figure 4.32 shows the variation of contact angles and TPCL movement with time.

Figure 4.31. Actual images of DDDC method and the corresponding contact angles using Yates oil, limestone, and surfactant (ALF 9S, 100 ppm) at ambient conditions.

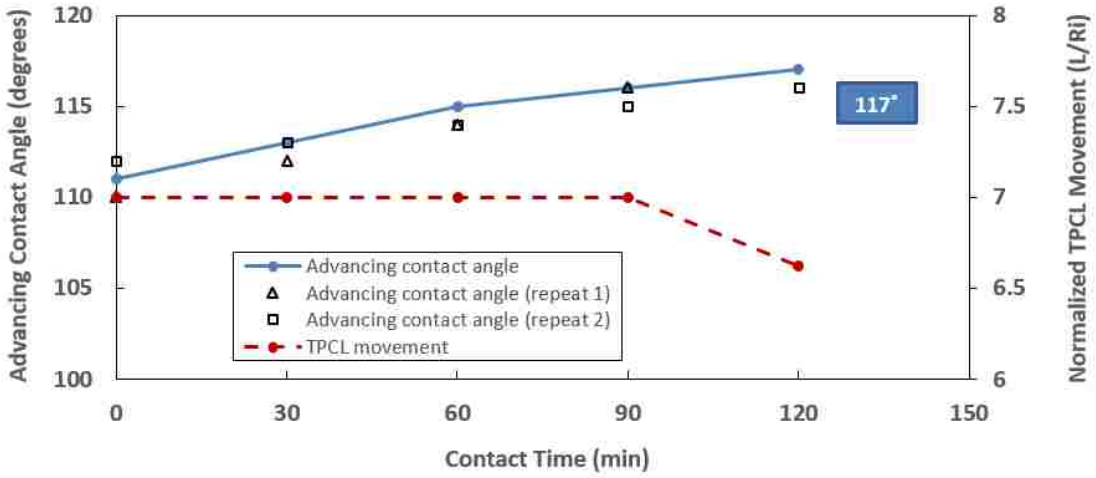

Figure 4.32. Contact angles variation and TPCL movement using Yates oil, limestone, and surfactant (ALF 9S, 100 ppm) at ambient conditions.

The next experiment was conducted by mixing the optimal nanofluid concentration (0.4 wt.%) and ALFOTERRA S23-9S 90 (100 ppm) to see if nanoparticles can improve the performance of the surfactant which was already effective in altering wettability of the system. Figure 4.33 describes the influence of nanoparticles in lowering the advancing contact angle from 117° (in the case of only surfactant) to 98° for the combination of nanoparticles and surfactant. This shift from the weakly intermediate-wet to strongly intermediate-wet zone only in 90 minutes (Figure 4.34) shows the great potential of surfactant-based nanofluid for altering the wettability of the limestone-Yates oil system at ambient conditions.

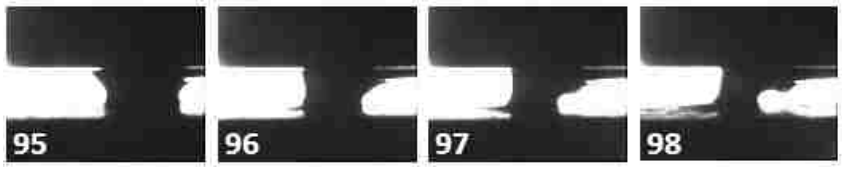

Figure 4.33. Actual images of DDDC method and the corresponding contact angles using Yates oil, limestone, and surfactant-based nanofluid (0.4 wt.% NP+ALF 9S, 100 ppm) at ambient conditions.

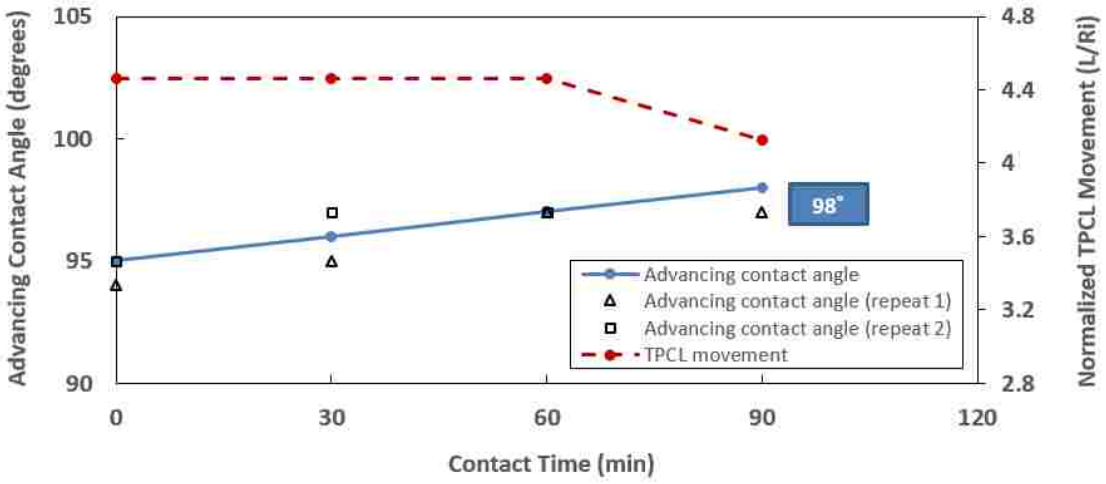

Figure 4.34. Contact angles variation and TPCL movement using Yates oil, limestone, and surfactant-based nanofluid (0.4 wt.% NP+ALF 9S, 100 ppm) at ambient conditions.

The next step is to study the contribution level of nanoparticles in changing the wettability. This helps to understand whether there is a potential to lower the concentration of surfactant and still observe the similar wettability alteration behavior to make surfactant-based nanofluid an economically appealing chemical agent. Figure 4.35 depicts how a combination of 0.4 wt.% nanoparticles with 50 ppm of ALFOTERRA S23-9S 90 plays an effective role. This surfactant-based nanofluid lowers the advancing contact angle from 117° (in the case of just surfactant) to 109° within 120 minutes (Figure 4.36). This represents a shift from weakly intermediate-wet toward more intermediate-wet condition, when the surfactant concentration is lowered 50%.

Figure 4.35. Actual images of DDDC method and the corresponding contact angles using Yates oil, limestone, and surfactant-based nanofluid (0.4 wt.% NP+ALF 9S, 50 ppm) at ambient conditions.

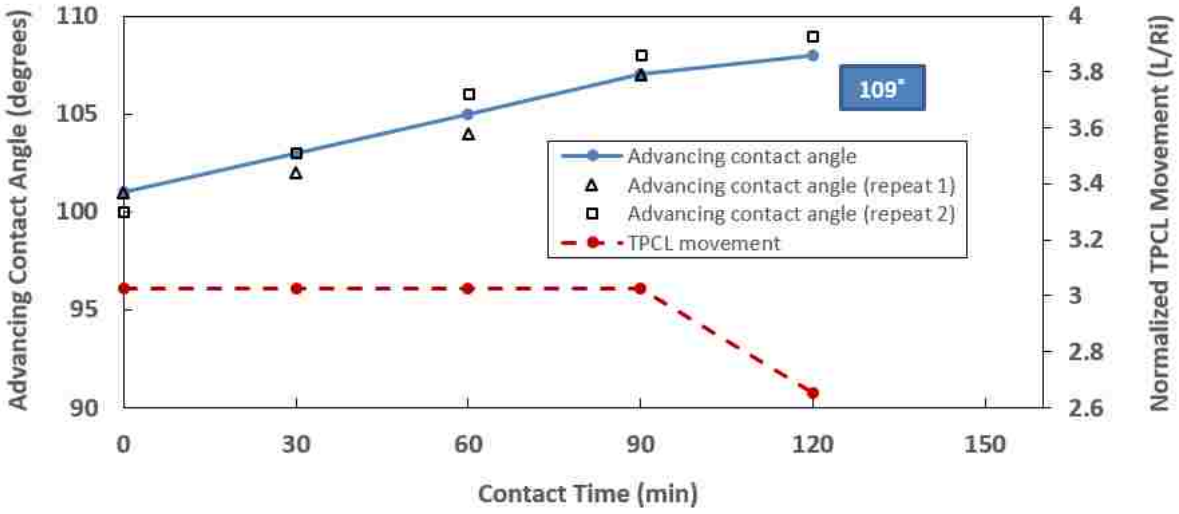

Figure 4.36. Contact angles variation and TPCL movement using Yates oil, limestone, and surfactant-based nanofluid (0.4 wt.% NP+ALF 13S, 50 ppm) at ambient conditions.

Therefore, a similar type of wettability alteration is observed even after lowering the concentration of surfactant. This shows that nanoparticles have a potential to compensate for both type of surfactants (least and most effective) in changing the wettability of the system toward less oil-wet at ambient conditions.

The bar chart in Figure 4.37 describes the dynamic advancing contact angles of surfactant-based nanofluids (prepared by the most effective surfactant) along with their respective IFT values. First, the brine at initial condition is compared to ALFOTERRA S23-9S 90 (100 ppm). Adding surfactant significantly reduces the IFT from 23.2 mN/m to 0.02 mN/m. However, 0.4 wt.%

nanoparticles seem to be able to boost up the IFT of solution one order of magnitude (from 0.02 mN/m to 0.85 mN/m), when combined with 100 ppm of surfactant. The IFT value increases slightly (1.6 mN/m) when the concentration of surfactant is lowered to 50 ppm but stays fairly close to the previous case. This confirms the fact that a nearly consistent wettability alteration and IFT reduction behavior can be achieved even after lowering the concentration of surfactant.

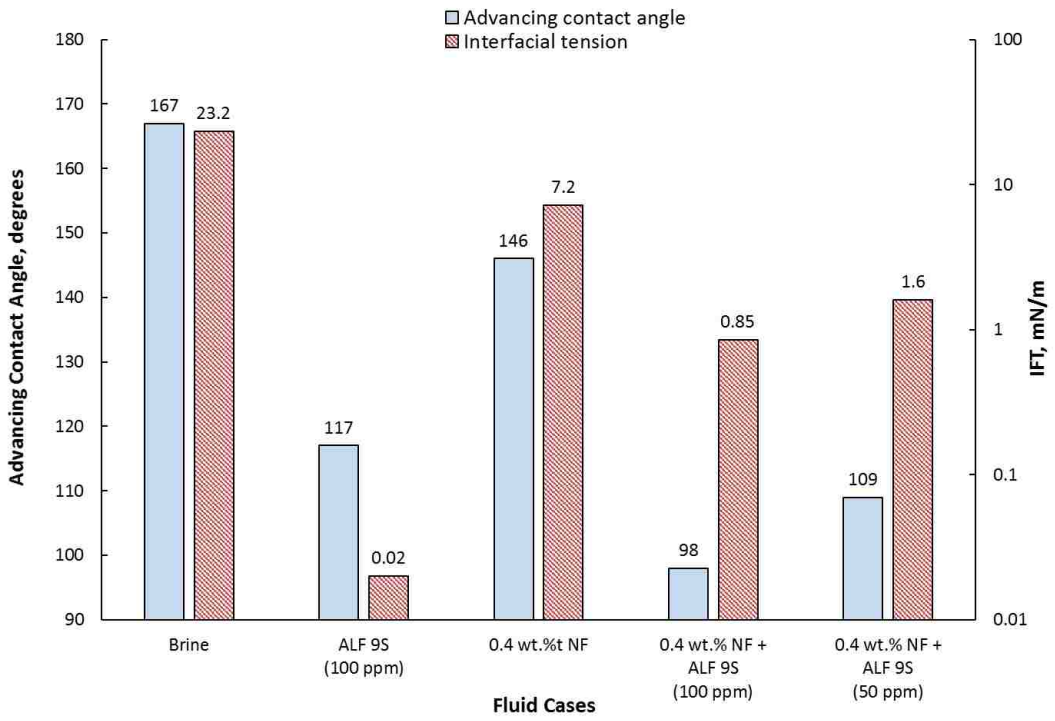

Figure 4.37. Comparison of IFT and contact angle values for surfactant-based nanofluids made by the most effective surfactant at ambient conditions.

4.2.3. Contact angle measurements using nanofluids at reservoir conditions

To measure the initial advancing contact angle at reservoir conditions, brine (2 wt.% NaCl) was used along with no nanoparticles. Figure 4.38 shows the actual images of the droplet at each stage

starting with the static contact angle of 129° and ending with the dynamic advancing contact angle of 156°, which represents the strongly oil-wet behavior of the system.

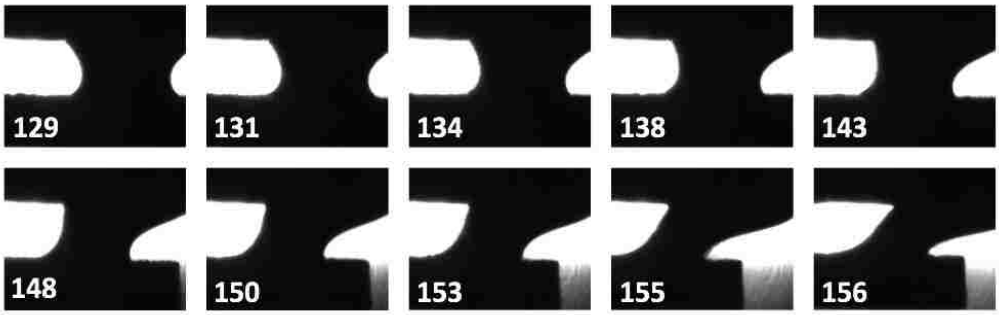

Figure 4.38. Actual images of DDDC method and the corresponding contact angles using Yates oil, limestone, and brine at reservoir conditions (700 psi & 150 ˚F).

The variation of contact angles and TPCL movement with time during the DDDC method along with the repeats of the measurements are described in Figure 4.39 with the highest angle of 156° as the true advancing contact angle when the normalized TPCL movement drops. To ensure the accuracy and reproducibility of the measurements, each experiment is repeated by moving the rock back to its original position and mingling the droplets again. The repeats of the measurements are also depicted in Figure 4.32 and show a similar trend of measured angles ending at about 156°.

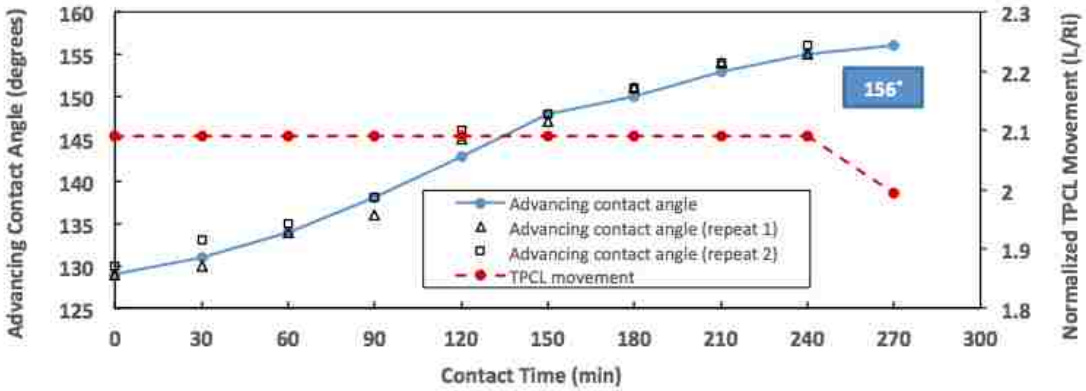

Figure 4.39. Contact angles variation and TPCL movement using Yates oil, limestone, and brine at reservoir conditions (700 psi & 150 ˚F).

To study the potential influence of nanoparticles on the wettability alteration performance of surfactants at reservoir conditions, SOLOTERRA 938 was selected. It was observed on the contact angle measurements (Gupta, 2016) and confirmed with the coreflood results that SOLOTERRA 938 had only a little effect on the wettability of the system at reservoir conditions. Therefore, the same type of surfactant and concentration (100 ppm) were used to prepare the surfactant-based nanofluids for contact angle measurements at reservoir conditions.

To see how SOLOTERRA 938, by itself, performs in terms of wettability alteration, a DDDC experiment was conducted using only surfactant at 100 ppm. Figure 4.40 describes the actual images of the droplet at each stage starting with the static contact angle of 127° and ending with the dynamic advancing contact angle of 150°. This means that surfactant has not significantly been effective in terms of wettability alteration as the advancing contact angle is still in the strongly oil-wet zone. Figure 4.41 shows the variation of contact angles and TPCL movement with time.

The effect of just nanoparticles at reservoir conditions was studied by mixing 0.4 wt.% of nanoparticles in brine. The advancing contact angle shows a shift from 156° (at initial condition with no nanoparticles) to 135° (with nanoparticles), in the weakly oil-wet zone (Figure 4.42). The variation of contact angles and TPCL movement described in Figure 4.43 shows that the highest angle or the advancing contact angle is reached within 150 minutes. Therefore, a direct effect of nanoparticles on lowering the adhesion of oil to the rock for this specific system at reservoir conditions is observed.

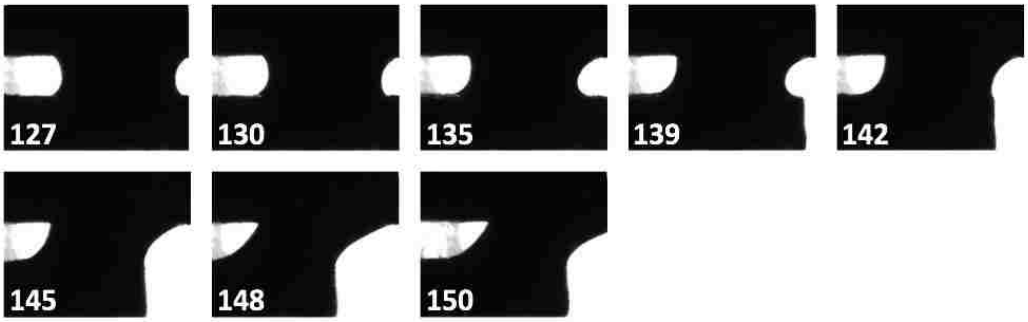

Figure 4.40. Actual images of DDDC method and the corresponding contact angles using Yates oil, limestone, and surfactant (SOLOTERRA 938) at reservoir conditions (700 psi & 150 ˚F).

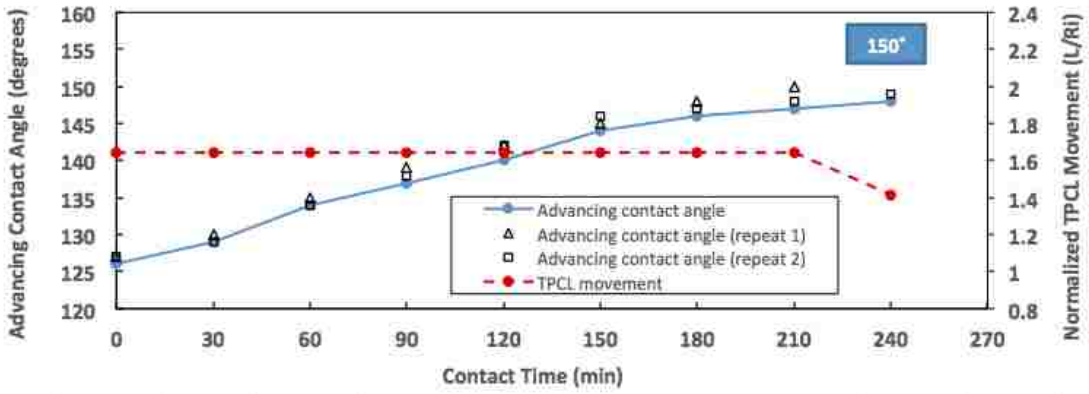

Figure 4.41. Contact angles variation and TPCL movement using Yates oil, limestone, and surfactant (SOLOTERRA 938) at reservoir conditions (700 psi & 150 ˚F).

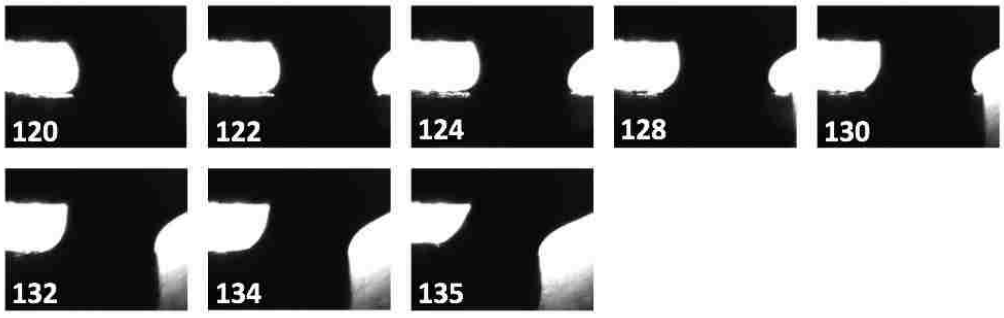

Figure 4.42. Actual images of DDDC method and the corresponding contact angles using Yates oil, limestone, and brine-based nanofluid at reservoir conditions (700 psi & 150 ˚F).

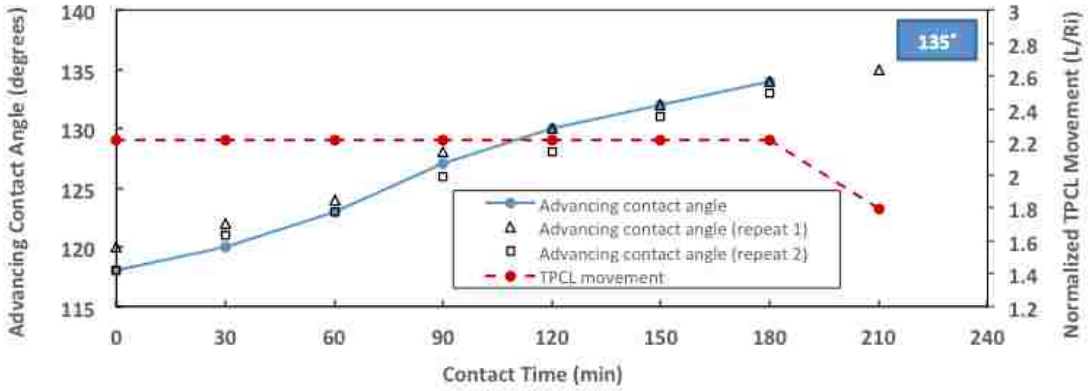

Figure 4.43. Contact angles variation and TPCL movement using Yates oil, limestone, and brine-based nanofluid at reservoir conditions (700 psi & 150 ˚F).

To see whether nanoparticles can enhance the performance of surfactant to alter the wettability of the system at reservoir conditions, SOLOTERRA (100 ppm) was mixed with 0.4 wt.% of nanoparticles. Figure 4.44 describes the significant effect of nanoparticles in lowering the advancing contact angle from 150° (in the case of just surfactant) to 108° for the combination of nanoparticles and surfactant. This shift from the strongly oil-wet to intermediate-wet zone in 150 minutes (Figure 4.45) shows the great potential of surfactant-based nanofluid in altering the wettability of the limestone-Yates oil system at reservoir conditions.

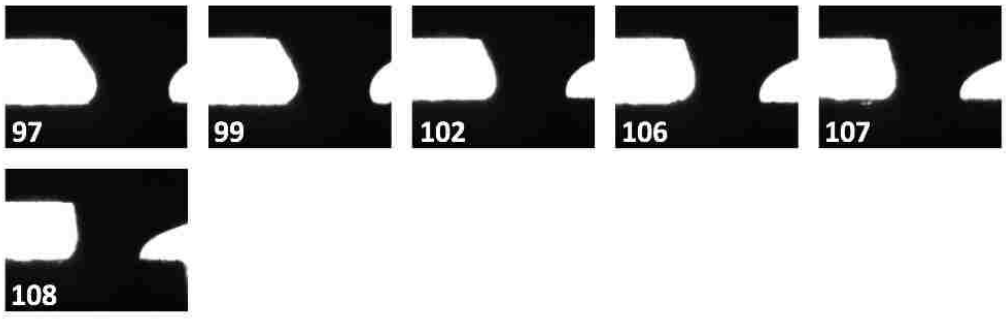

Figure 4.44. Actual images of DDDC method and the corresponding contact angles using Yates oil, limestone, and surfactant-based nanofluid (100 ppm surfactant) at reservoir conditions (700 psi & 150 ˚F).

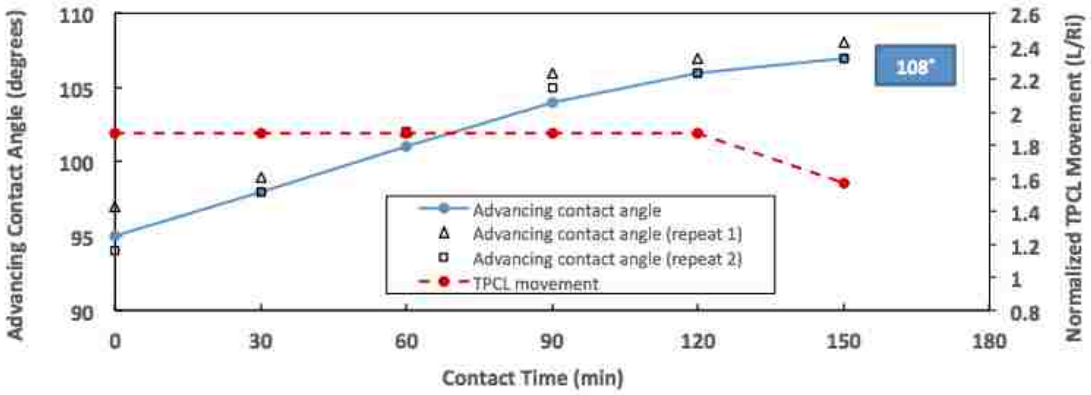

Figure 4.45. Contact angles variation and TPCL movement using Yates oil, limestone, and surfactant-based nanofluid (100 ppm surfactant) at reservoir conditions (700 psi & 150 ˚F).

The next step is to study the contribution level of nanoparticles in changing the wettability. This helps to understand whether there is a potential to lower the concentration of surfactant and still observe the similar wettability alteration behavior to make surfactant-based nanofluid an economically appealing chemical agent. Figure 4.46 depicts how the combination of 0.4 wt.% nanoparticles with 50 ppm of SOLOTERRA 938 plays an effective role by lowering the advancing contact angle from 150° (in the case of just surfactant) to 114° within 180 minutes (Figure 4.47). This represents a shift from strongly oil-wet to intermediate-wet zone, when the surfactant concentration is lowered 50%.

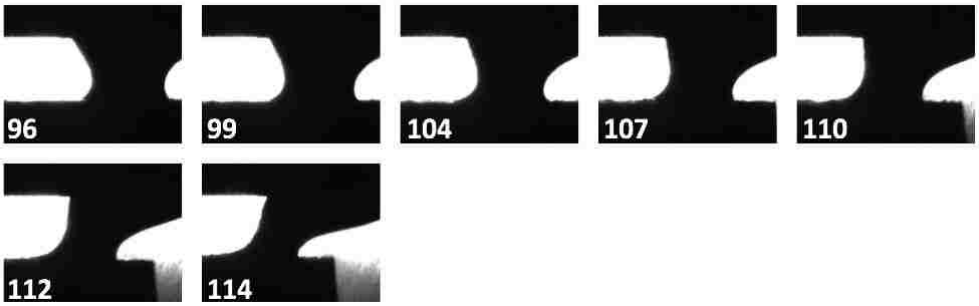

Figure 4.46. Actual images of DDDC method and the corresponding contact angles using Yates oil, limestone, and surfactant-based nanofluid (50 ppm surfactant) at reservoir conditions (700 psi & 150 ˚F).

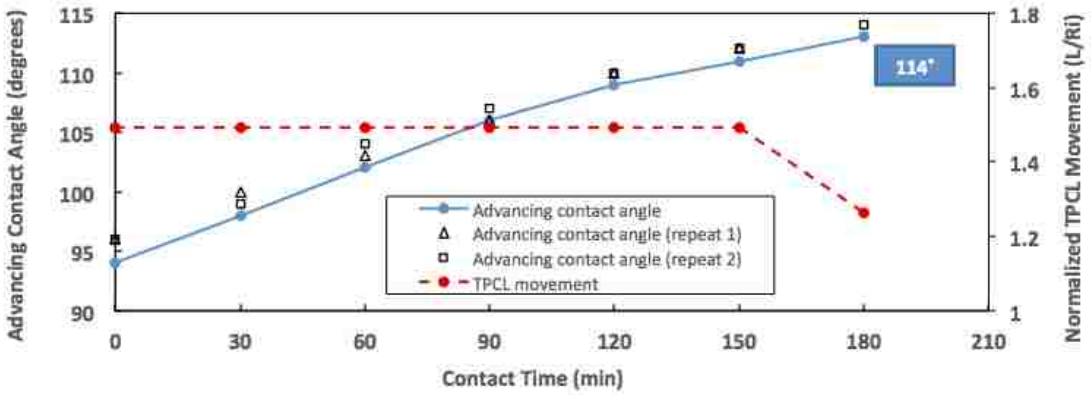

Figure 4.47. Contact angles variation and TPCL movement using Yates oil, limestone, and surfactant-based nanofluid (50 ppm surfactant) at reservoir conditions (700 psi & 150 ˚F).

Therefore, a similar type of wettability alteration is observed even after lowering the concentration of surfactant. This shows that nanoparticles have a potential to compensate for this specific surfactant in changing the wettability of the system toward less oil-wet at reservoir conditions.

The variation of dynamic advancing contact angles of surfactant-based nanofluids with different concentrations along with their respective IFT values at reservoir conditions are displaced in Figure 4.48. First, the brine at initial condition is compared to SOLOTERRA 938 (100 ppm). Adding surfactant significantly reduces the IFT from 20.4 mN/m to 0.02 mN/m. However, 0.4 wt.% nanoparticles seem to be able to boost up the IFT of surfactant solution two orders of magnitude (from 0.02 mN/m to 1.5 mN/m) when combined with 100 ppm of the surfactant. The IFT value increases slightly when the concentration of surfactant is lowered to 50 ppm but stays close to the previous case. This confirms the fact that a rather consistent wettability alteration and IFT reduction behavior can be achieved even after lowering the concentration of surfactant. Therefore, a potential of developing an effective and economically attractive surfactant-based nanofluid agent for wettability alteration at reservoir conditions can be observed.

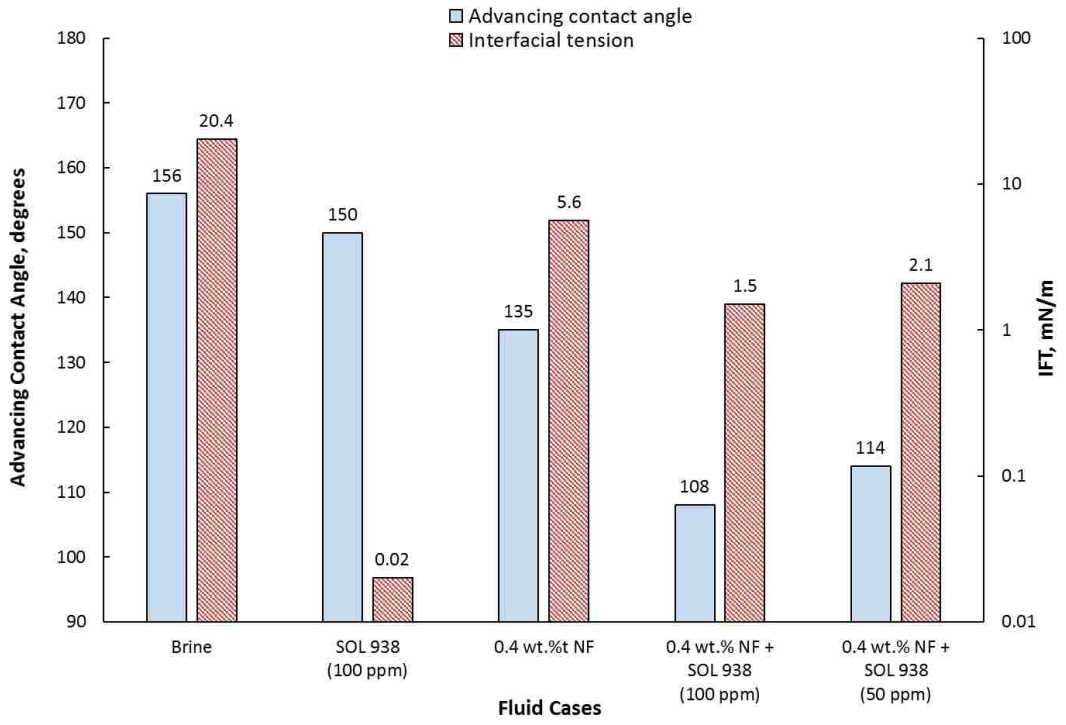

Figure 4.48. Comparison of IFT and contact angle values for different concentrations of surfactant-based nanofluids at reservoir conditions (700 psi & 150 ˚F).

4.2.4. Summary

Table 4.14 summarizes all the contact angle measurements using nanofluids at both ambient and reservoir conditions along with the interfacial tension values and the wettability alteration behavior for each case. These results suggest that nanoparticles mixed in brine can shift the wettability of the system from strongly oil-wet to weakly oil-wet. They can also enhance the performance of a surfactant (the least and most effective) in terms of changing the wettability. Using a combination of nanoparticles and surfactants, the wettability can be moved from strongly oil-wet to intermediate-wet condition (in case of the least effective surfactant), and from weakly intermediate-wet to strongly intermediate-wet condition (in case of the most effective surfactant). These results also indicate that, nanoparticles have a potential to compensate for surfactants (both

the least and most effective), as lowering the surfactant concentration did not significantly seem to affect the wettability alteration behavior. This trend appears to be similar in both ambient and reservoir conditions. The only difference is that, in general, the contact angles at reservoir conditions seem to be lower than that of their respective cases at ambient conditions. For example, brine-based nanofluids caused the wettability to change from strongly oil-wet to weakly oil-wet at both ambient and reservoir conditions. But the change at ambient conditions was from 167° to 146° and at reservoir conditions from 156° to 135°. Similarly, the surfactant-based nanofluids at both ambient and reservoir conditions resulted in a shift from strongly oil-wet to intermediate-wet. But the shift at ambient conditions (for the least effective) was from 162° to 116° and at reservoir conditions from 150° to 108°.

Table 4.14. Summary of the contact angle measurements at both ambient and reservoir conditions (700 psi & 150 ˚F).

No.	Experimental Conditions	Solution Type	Composition	IFT (mN/m)	Advancing Contact Angle (degrees)	Wettability Alteration Behavior
1	Ambient	Brine	2 wt.% NaCl	23.2	167	Strongly oil-wet
2	Ambient	Brine-based Nanofluid	0.1 wt.% Nanopartciles	13.1	165	Strongly oil-wet
3	Ambient	Brine-based Nanofluid	0.2 wt.% Nanopartciles	9.8	156	Oil-wet
4	Ambient	Brine-based Nanofluid	0.4 wt.% Nanopartciles	7.2	146	Weakly oil-wet
5	Ambient	Brine-based Nanofluid	0.8 wt.% Nanopartciles	6.5	143	Weakly oil-wet
6	Ambient	Surfactant	ALFOTERRA S23-13S 90 (100 ppm)	0.02	162	Strongly oil-wet
7	Ambient	Surfactant-based Nanofluid	0.4 wt.% Nanopartciles + ALFOTERRA S23-13S 90 (100 ppm)	1.2	116	Intermediate-wet
8	Ambient	Surfactant-based Nanofluid	0.4 wt.% Nanopartciles + ALFOTERRA S23-13S 90 (50 ppm)	2.3	121	Intermediate-wet
9	Ambient	Surfactant	ALFOTERRA S23-9S 90 (100 ppm)	0.02	117	Intermediate-wet
10	Ambient	Surfactant-based Nanofluid	0.4 wt.% Nanopartciles + ALFOTERRA S23-9S 90 (100 ppm)	0.85	98	Intermediate-wet
11	Ambient	Surfactant-based Nanofluid	0.4 wt.% Nanopartciles + ALFOTERRA S23-13S 90 (50 ppm)	1.6	109	Intermediate-wet
12	Reservoir*	Brine	2 wt.% NaCl	20.4	156	Strongly oil-wet
13	Reservoir*	Surfactant	SOLOTERRA 938 (100 ppm)	0.02	150	Strongly oil-wet
14	Reservoir*	Brine-based Nanofluid	0.4 wt.% Nanopartciles	5.6	135	Weakly oil-wet
15	Reservoir*	Surfactant-based Nanofluid	0.4 wt.% Nanopartciles + SOLOTERRA 938 (100 ppm)	1.5	108	Intermediate-wet
16	Reservoir*	Surfactant-based Nanofluid	0.4 wt.% Nanopartciles + SOLOTERRA 938 (50 ppm)	2.1	114	Intermediate-wet

Least effective surfactant

Most effective surfactant

* Reservoir Conditions: 700 psi & 150 ˚F

4.3. Coreflood experiments using nanofluids

This section is presented in four parts. First, the coreflood results of experiments conducted using surfactant-based nanofluids made by the least effective surfactants are displayed and discussed for both experimental conditions (500 psi & 72 ˚F and 700 psi & 150 ˚F). Secondly, the coreflood results of surfactant-based nanofluids made by the most effective surfactant are evaluated at 500 psi and 72 ˚F. Then, the experimental recovery of all the corefloods at both experimental conditions are studied to see how nanoparticles contribute to the overall oil recovery. Finally, the water fractional flow curves of all the corefloods, which were estimated using the simulated relative permeability curves are investigated to understand the influence of nanoparticles in changing the flow characteristics of the system.

4.3.1. Coreflood results of nanofluids made by the least effective surfactant

This part discusses the coreflood results of surfactant-based nanofluids prepared by the combination of nanoparticles with the least effective surfactants (selected in the screening stage of this research) at both experimental conditions. The parameters related to each coreflood including the name and size of the core, rock type, porosity, absolute permeability and pore volume of the core, the type of oil and the injecting fluid (brine, surfactant, or nanofluid) used in the coreflood, the injection rate, and finally the overall recovery of the flood are initially listed in tables.

All the chemical fluids of this part are injected as a secondary recovery method. The history match of recovery and pressure drop, resulted from the simulation and optimization, are displayed for each experiment. The resulting relative permeability curves along with the experimental endpoints are depicted. The experimental endpoints (k_{rw}: water relative permeability endpoint, k_{ro}: oil relative permeability endpoint) and their corresponding saturation values (S_{or}: residual oil saturation, S_{iw}: irreducible water saturation) are compared to their simulated estimations in tables.

In the following parts, the final results of each coreflood are evaluated individually and the observations regarding their respective contact angle measurements are discussed.

4.3.1.1. Corefloods at 500 psi and 72 ˚F

4.3.1.1.1. Waterflood

The first coreflood at 500 psi and 72 ˚F is the waterflood to set the base case. Since ALFOTERRA S23-13S 90 was selected in the screening stage as the least effective surfactant with no significant effect in terms of wettability alteration and decided to be used for combining with nanoparticles at ambient conditions, its corresponding waterflood results are being presented here again. For this flood, 2 wt.% NaCl was injected at 2 cc/min into a 12 in. by 2 in. Indiana limestone core with the porosity of about 18% and absolute permeability of about 23.5 md depicting a rather tight core (Table 4.15). The oil recovery of about 20.5% shows a relatively oil-wet behavior of the core. The simulated oil recovery and pressure drop data agree well with the experimental values (Figure 4.49). The relative permeability curves also describe the oil-wet behavior of the system. This can be observed by looking at the position of crossover point that is below 0.5 and higher water relative permeability endpoint compared to the oil relative permeability endpoint (Figure 4.50). The experimental endpoints are shown on the plot as well as in Table 4.16 to indicate how accurately the relative permeability curves are simulated. The relatively high value of the residual oil saturation (Sor=0.644) confirms the oil-wet initial condition of the core. This is also supported by the contact angle measurements as the advancing contact angle of 167° indicated the strongly oil-wet behavior of the system at ambient conditions.

Table 4.15. Initial parameters for waterflood using brine (2 wt.% NaCl) at 500 psi and 72 ˚F.

Core name:	Indiana Limestone-10 (12X2)	
Porosity:	18.14	%
Abs. Perm:	23.59	md
Pore Volume	112	cc
Oil	Yates crude oil	
Brine (NaCl)	2%	wt
Injection rate	2	cc/min
Oil Recovery	20.43	%

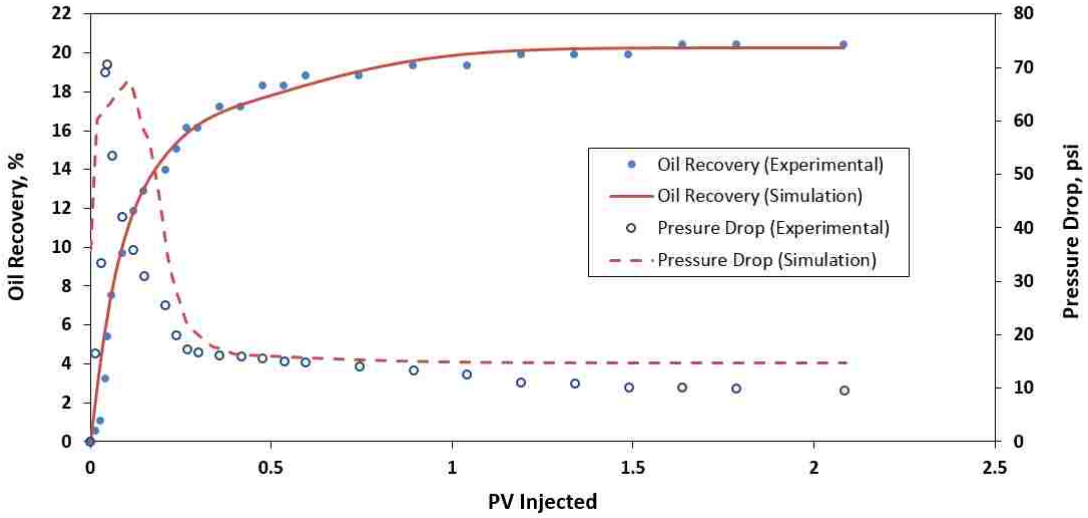

Figure 4.49. History match of oil recovery and pressure drop for waterflood (2 wt.% NaCl) at 500 psi and 72 ˚F.

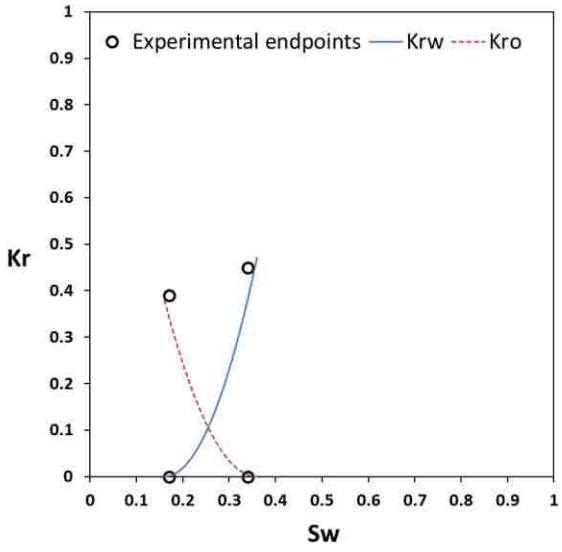

Table 4.16. Experimental and simulation endpoints for waterflood (2 wt.% NaCl) at 500 psi and 72 ˚F.

Relative Permeability Endpoints		
Experimental	Siw	0.170
	Sor	0.660
	krw	0.450
	kro	0.390
Simulation	Siw	0.160
	Sor	0.644
	Krw	0.466
	Kro	0.381

Figure 4.50. Simulated relative permeability curves for waterflood (2 wt.% NaCl) at 500 psi and 72 ˚F.

4.3.1.1.2. Surfactant flood

For this coreflood, ALFOTERRA S23-13S 90 was used. It was previously shown, in the screening stage, that this surfactant had no influence on the wettability alteration. The reason this coreflood is repeated here is that, previously surfactant was injected as a tertiary recovery method following a waterflood. Now, however, surfactant is injected immediately after the initial condition was established and core was aged, thus as a secondary recovery method. The surfactant with concentration of 2000 ppm was injected at 2 cc/min into a 12 in. by 2 in. Indiana limestone core with the porosity of about 16% and absolute permeability of about 26 md depicting a rather tight core (Table 4.17). The oil recovery of about 21% shows a relatively oil-wet behavior of the core, meaning that the surfactant has not significantly been effective toward improving the oil recovery. This was also suggested by the coreflood results from the screening stage, where the surfactant experimental endpoints did not shift to the right of waterflood relative permeability curves. Figure 4.51 depicts that the simulated oil recovery and pressure drop of the surfactant flood agree well with the experimental values. The simulated relative permeability curves also describe the oil-wet behavior of the system, since the crossover point is below 0.5 and water relative permeability endpoint is higher than that of oil (Figure 4.52). No significant shift-to-right is observed in the relative permeability curves compared to that of waterflood (Figure 4.50), indicating the poor performance of this surfactant in changing the wettability. The experimental endpoints are shown on the plot as well as listed in Table 4.18 to indicate how accurately the relative permeability curves are simulated. The relatively high value of the residual oil saturation (S_{or}=0.656) also indicates the oil-wet condition of the core even after the surfactant flood. This is also supported by the contact angle measurements as the advancing contact angle of 162° indicated the strongly oil-wet behavior of the system using this surfactant at ambient conditions.

Table 4.17. Initial parameters for coreflood using surfactant (ALF 13S, 2000 ppm) at 500 psi and 72 ˚F.

Core name:	Indiana Limestone-15 (12X2)	
Porosity:	16.03	%
Abs. Perm:	26.24	md
Pore Volume	99	cc
Oil	Yates crude oil	
Brine (NaCl)	2%	wt
Surfactant	ALF 13S (2000 ppm)	
Injection rate	2	cc/min
Oil Recovery	20.73	%

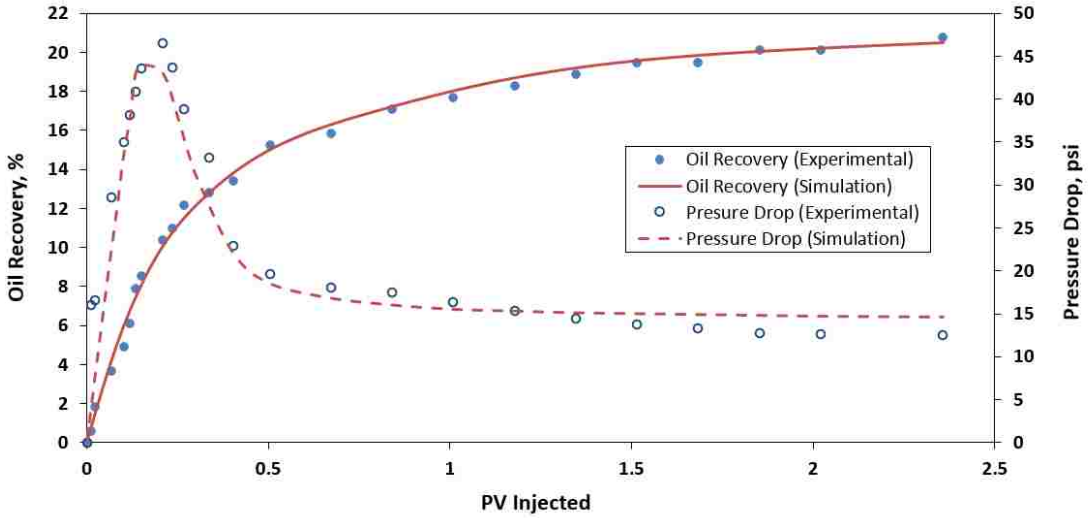

Figure 4.51. History match of oil recovery and pressure drop using surfactant (ALF 13S, 2000 ppm) at 500 psi and 72 ˚F.

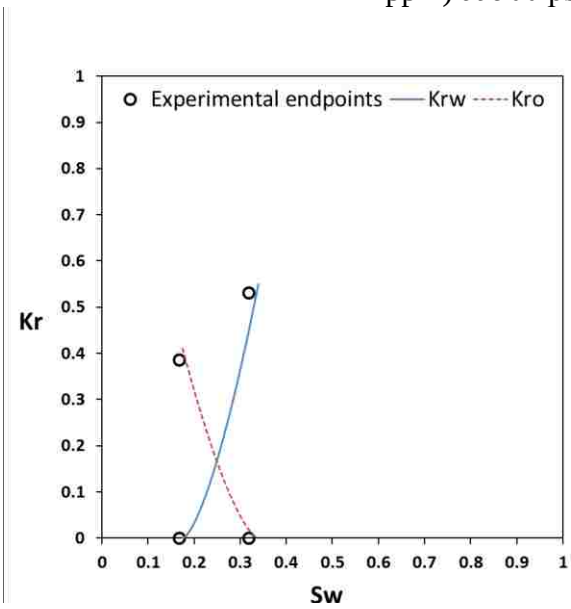

Table 4.18. Experimental and simulation endpoints for coreflood using surfactant (ALF 13S, 2000 ppm) at 500 psi and 72 ˚F.

Relative Permeability Endpoints		
Experimental	Siw	0.168
	Sor	0.682
	krw	0.532
	kro	0.386
Simulation	Siw	0.175
	Sor	0.656
	Krw	0.549
	Kro	0.410

Figure 4.52. Simulated relative permeability curves for coreflood using surfactant (ALF 13S, 2000 ppm) at 500 psi and 72 ˚F.

4.3.1.1.3. Brine-based nanofluid flood

For this coreflood, 0.4 wt.% of nanoparticles were mixed in brine (2% NaCl) to prepare the nanofluid with the optimal concentration, based on the observations from the contact angle measurements. The brine-based nanofluid was injected immediately after the initial condition was established and the core was aged, thus as a secondary recovery method. The injection was at 2 cc/min into a 12 in. by 2 in. Indiana limestone core with the porosity of about 15% and absolute permeability of about 18.5 md depicting a rather tight core (Table 4.19). The coreflood using the brine-based nanofluid resulted in an incremental oil recovery of about 10% compared to the pure waterflood and reached to about 30.5%. This clearly expresses the direct influence of nanoparticles in improving oil recovery. Figure 4.53 describes the great agreement of simulated oil recovery and pressure drop with the experimental values. The simulated relative permeability curves, in Figure 4.54, show a shift-to-right in the crossover point compared to that of waterflood (Figure 4.50), although the water relative permeability endpoint is still higher than that of oil. This means that the nanoparticles were able to change the wettability of the system from strongly oil-wet toward less oil-wet, leading to a reduction in the residual oil saturation (from S_{or}=0.644 for waterflood to S_{or}=0.451), as seen in Table 4.20, and an improvement in the oil recovery. This is also supported by the contact angle measurements as the brine-based nanofluid (0.4 wt.%) resulted in an advancing contact angle of 146° indicating a weakly oil-wet behavior at ambient conditions. The experimental endpoints are shown on the relative permeability plots as well as listed in Table 4.21 to indicate how accurately the relative permeability curves are simulated.

Table 4.19. Initial parameters for coreflood using brine-based nanofluid (0.4 wt.% NP in 2% NaCl) at 500 psi and 72 ˚F.

Core name:	Indiana Limestone-14 (12X2)	
Porosity:	14.73	%
Abs. Perm:	18.59	md
Pore Volume	91	cc
Oil	Yates crude oil	
Brine (NaCl)	2%	wt
Nanofluid (brine-based)	0.4 wt.% NP	
Injection rate	2	cc/min
Oil Recovery	30.51	%

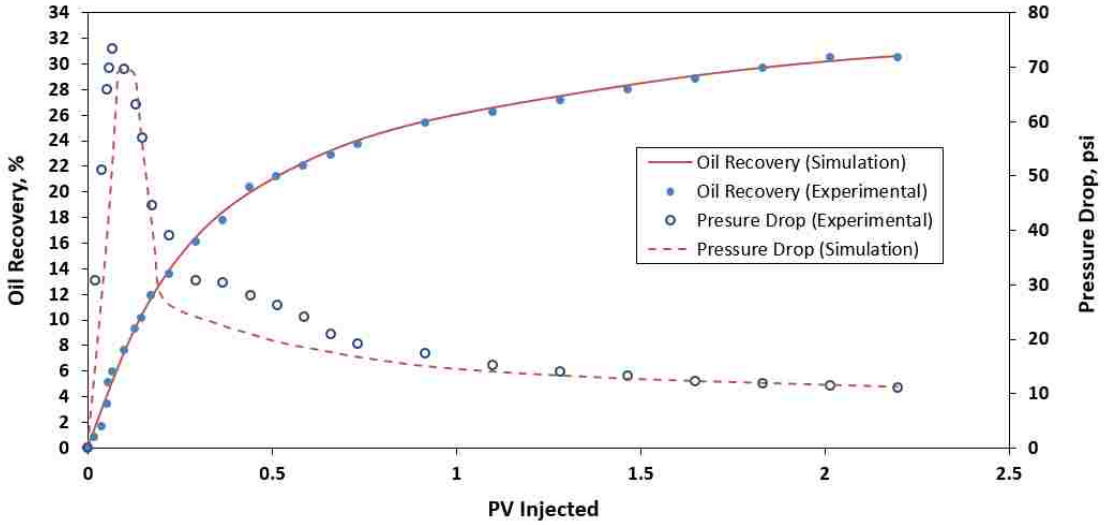

Figure 4.53. History match of oil recovery and pressure drop using brine-based nanofluid (0.4 wt.% NP in 2% NaCl) at 500 psi and 72 ˚F.

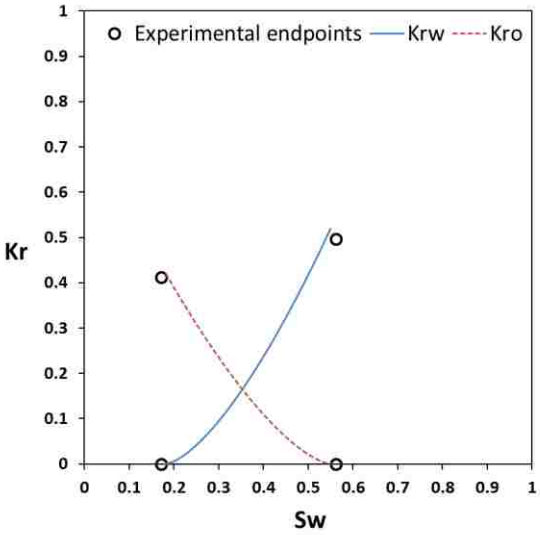

Table 4.20. Experimental and simulation endpoints for coreflood using brine-based nanofluid (0.4 wt.% NP in 2% NaCl) at 500 psi and 72 ˚F.

Relative Permeability Endpoints		
Experimental	Siw	0.172
	Sor	0.438
	krw	0.497
	kro	0.412
Simulation	Siw	0.182
	Sor	0.451
	Krw	0.516
	Kro	0.419

Figure 4.54. Simulated relative permeability curves for coreflood using brine-based nanofluid ((0.4 wt.% NP in 2% NaCl) at 500 psi and 72 ˚F.

4.3.1.1.4. Surfactant-based nanofluid flood

For this flood, ALFOTERRA S23-13S 90 (2000 ppm), as the surfactant that showed no effect in terms of wettability alteration and did not improve the oil recovery, is mixed with nanoparticles (0.4 wt.%). The resultant surfactant-based nanofluid once showed a great potential for changing the wettability from strongly oil-wet to intermediate-wet through the contact angle measurements. Now, the composite fluid is injected as a secondary recovery method. The injection was at 2 cc/min into a 12 in. by 2 in. Indiana limestone core with the porosity of about 16.5% and absolute permeability of about 8.5 md depicting a really tight core (Table 4.21). The coreflood resulted in an incremental oil recovery of more than 30% compared to the surfactant flood and reached to about 57%. Figure 4.55 describes how simulated oil recovery and pressure drop match with the experimental values. The simulated relative permeability curves, in Figure 4.56, show a great shift-to-right in the crossover point compared to that of surfactant flood (Figure 4.52), although the water relative permeability endpoint is still higher than that of oil. This means that the nanoparticles were able to significantly improve the ability of surfactant in changing the wettability of the system from strongly oil-wet toward less oil-wet, leading to a great reduction in the residual oil saturation (from S_{or}=0.656 for surfactant flood to S_{or}=0.314), as seen in Table 4.22, and an improvement in the oil recovery. This is also supported by the contact angle measurements as the surfactant-based nanofluid (100 ppm) resulted in an advancing contact angle of 116° indicating an intermediate-wet behavior at ambient conditions. The experimental endpoints are shown on the relative permeability plots as well as listed in Table 4.23 to indicate how accurately the relative permeability curves are simulated.

Table 4.21. Initial parameters for coreflood using surfactant-based nanofluid (0.4 wt.% NP + ALF 13S, 2000 ppm) at 500 psi and 72 ˚F.

Core name:	Indiana Limestone-16 (12X2)	
Porosity:	16.52	%
Abs. Perm:	8.49	md
Pore Volume	102	cc
Oil	Yates crude oil	
Brine (NaCl)	2%	wt
Nanofluid (surfactant-based)	0.4 wt.% NP + ALF 13S (2000 ppm)	
Injection rate	2	cc/min
Oil Recovery	57.33	%

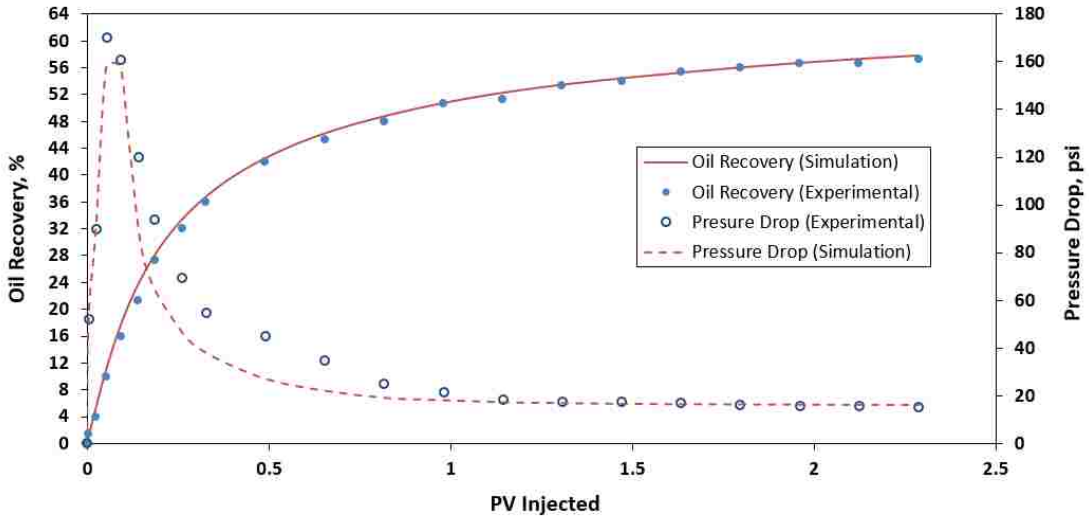

Figure 4.55. History match of oil recovery and pressure drop using surfactant-based nanofluid (0.4 wt.% NP + ALF 13S, 2000 ppm) at 500 psi and 72 ˚F.

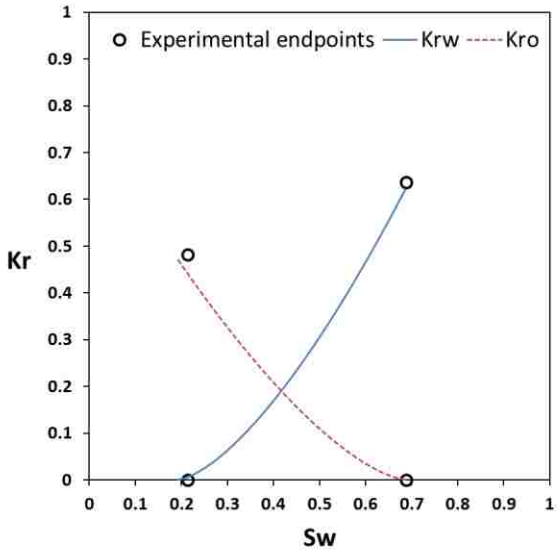

Table 4.22. Experimental and simulation endpoints for coreflood using surfactant-based nanofluid (0.4 wt.% NP + ALF 13S, 2000 ppm) at 500 psi and 72 ˚F.

Relative Permeability Endpoints		
Experimental	Siw	0.214
	Sor	0.312
	krw	0.637
	kro	0.482
Simulation	Siw	0.193
	Sor	0.314
	Krw	0.619
	Kro	0.467

Figure 4.56. Simulated relative permeability curves for coreflood using surfactant-based nanofluid (0.4 wt.% NP + ALF 13S, 2000 ppm) at 500 psi and 72 ˚F.

4.3.1.1.5. Surfactant-based nanofluid flood (lower concentration of surfactant)

For this flood, the concentration of ALFOTERRA S23-13S 90 was reduced to 1000 ppm to see if nanoparticles can compensate for the surfactant in the coreflood as well as they did in the contact angle measurements. The surfactant-based nanofluid is injected immediately after the initial condition was established as a secondary recovery method. The injection was at 2 cc/min into a 12 in. by 2 in. Indiana limestone core with the porosity of about 17% and absolute permeability of about 16 md depicting a rather tight core (Table 4.23). The coreflood resulted in an incremental oil recovery of about 30% compared to the surfactant flood and reached to about 53%. Figure 4.57 describes how simulated oil recovery and pressure drop data match with the experimental values. The simulated relative permeability curves, in Figure 4.58, show a great shift-to-right in the crossover point compared to that of surfactant flood (Figure 4.52), although the shift is not as large as it was in the previous case, where the surfactant concentration was twice higher (Figure 4.56). This means that, even after reducing the concentration of surfactant, the surfactant-based nanofluid was still able to greatly alter the wettability of the system from strongly oil-wet toward less oil-wet, leading to a reduction in the residual oil saturation (from S_{or}=0.656 for surfactant flood to S_{or}=0.339), as seen in Table 4.24, and an improvement in the oil recovery. This is also supported by the contact angle measurements as the surfactant-based nanofluid (50 ppm) resulted in an advancing contact angle of 121°, indicating a nearly intermediate-wet behavior at ambient conditions. The experimental endpoints are shown on the relative permeability plots as well as listed in Table 4.25 to indicate how accurately the relative permeability curves are simulated.

Table 4.23. Initial parameters for coreflood using surfactant-based nanofluid (0.4 wt.% NP + ALF 13S, 1000 ppm) at 500 psi and 72 ˚F.

Core name:	Indiana Limestone-17 (12X2)	
Porosity:	17.17	%
Abs. Perm:	15.81	md
Pore Volume	106	cc
Oil	Yates crude oil	
Brine (NaCl)	2%	wt
Nanofluid (surfactant-based)	0.4 wt.% NP + ALF 13S (1000 ppm)	
Injection rate	2	cc/min
Oil Recovery	52.63	%

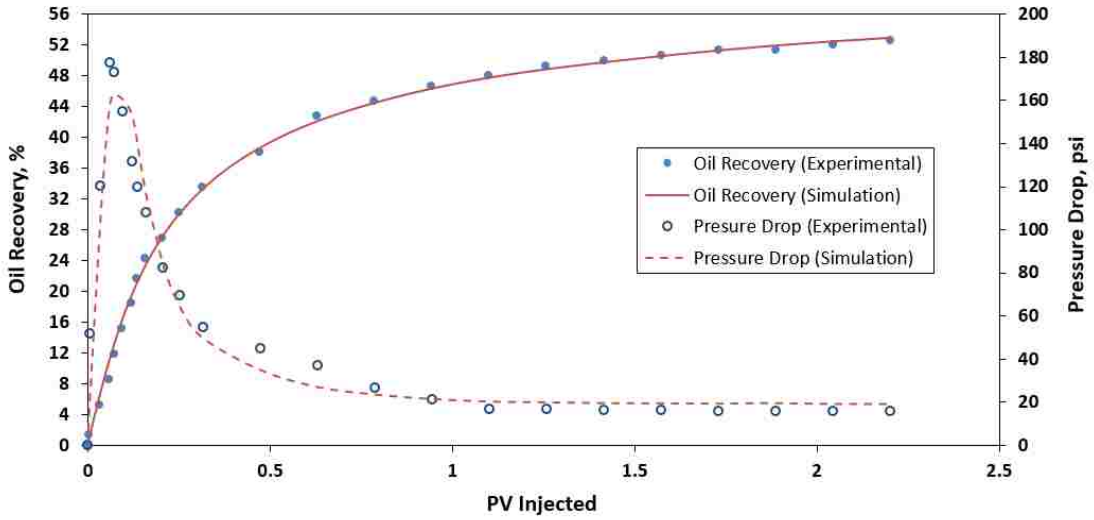

Figure 4.57. History match of oil recovery and pressure drop using surfactant-based nanofluid (0.4 wt.% NP + ALF 13S, 1000 ppm) at 500 psi and 72 ˚F.

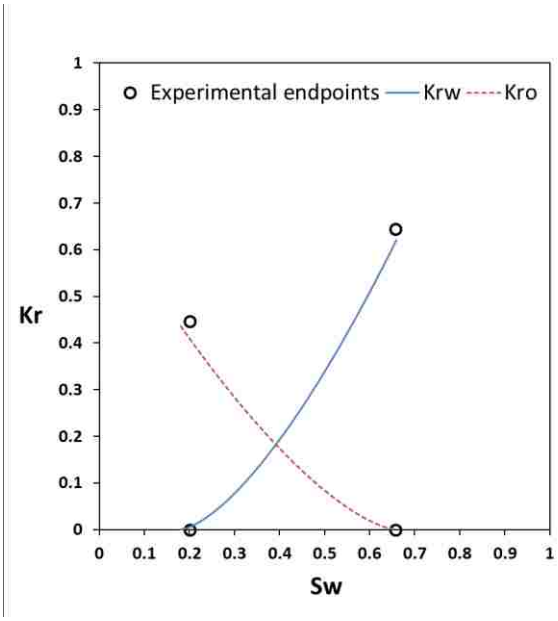

Table 4.24. Experimental and simulation endpoints for coreflood using surfactant-based nanofluid (0.4 wt.% NP + ALF 13S, 1000 ppm) at 500 psi and 72 ˚F.

Relative Permeability Endpoints		
Experimental	Siw	0.201
	Sor	0.342
	krw	0.645
	kro	0.447
Simulation	Siw	0.182
	Sor	0.339
	Krw	0.621
	Kro	0.436

Figure 4.58. Simulated relative permeability curves for coreflood using surfactant-based nanofluid (0.4 wt.% NP + ALF 13S, 1000 ppm) at 500 psi and 72 ˚F.

4.3.1.2. Corefloods at reservoir conditions (700 psi and 150 ºF)

4.3.1.2.1. Waterflood

The first coreflood at reservoir conditions (700 psi and 150 ºF) is the waterflood to set the base case. Since SOLOTERRA 938 was selected in the screening stage as a surfactant with no significant effect in terms of wettability alteration and decided to be used for combining with nanoparticles at reservoir conditions, its respective waterflood results are being presented here again. For this flood, 2 wt.% NaCl was injected at 2 cc/min into a 12 in. by 2 in. Indiana limestone core with the porosity of about 16.5% and absolute permeability of about 15 md depicting a rather tight core (Table 4.25). The oil recovery of about 17.5% shows a relatively oil-wet behavior of the core. The simulated oil recovery and pressure drop data match well with the experimental values (Figure 4.59). The relative permeability curves also describe the oil-wet behavior of the system. This can be observed by looking at the position of the crossover point that is below 0.5 and also higher water relative permeability endpoint compared to the oil relative permeability endpoint (Figure 4.60). The experimental endpoints are shown on the relative permeability plot as well as listed in Table 4.26 to indicate how accurately the relative permeability curves are simulated. The relatively high value of the residual oil saturation (Sor=0.630) confirms the oil-wet initial condition of the core. This is also supported by the contact angle measurements as the advancing contact angle of 156° indicated the strongly oil-wet behavior of the system at reservoir conditions.

Table 4.25. Initial parameters for waterflood using brine (2 wt.% NaCl) at reservoir conditions (700 psi & 150 ˚F).

Core name:	Indiana Limestone-12 (12X2)	
Porosity:	16.35	%
Abs. Perm:	14.87	md
Pore Volume	101	cc
Oil	Yates crude oil	
Brine (NaCl)	2%	wt
Injection rate	2	cc/min
Oil Recovery	17.5	%

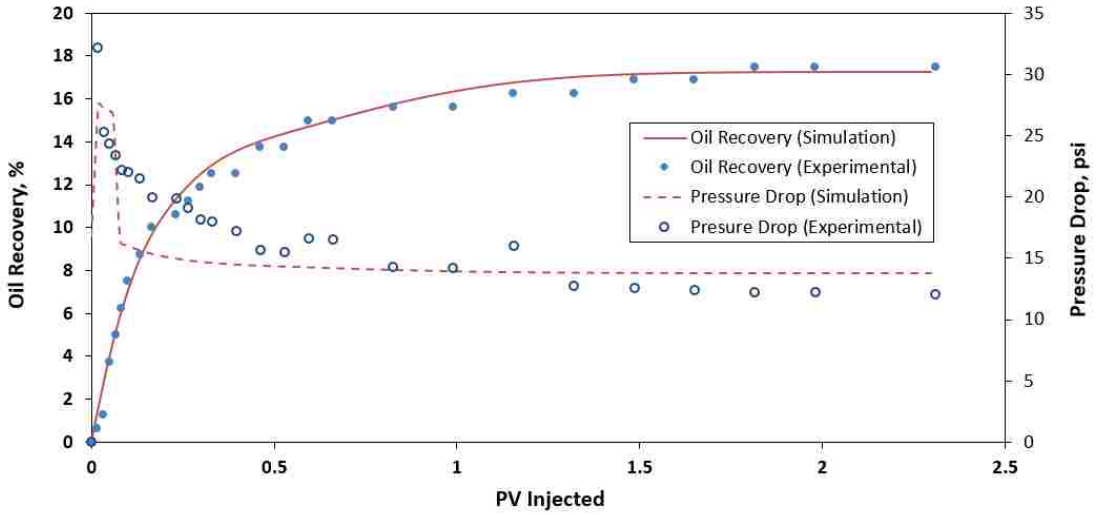

Figure 4.59. History match of oil recovery and pressure drop for waterflood (2 wt.% NaCl) at reservoir conditions.

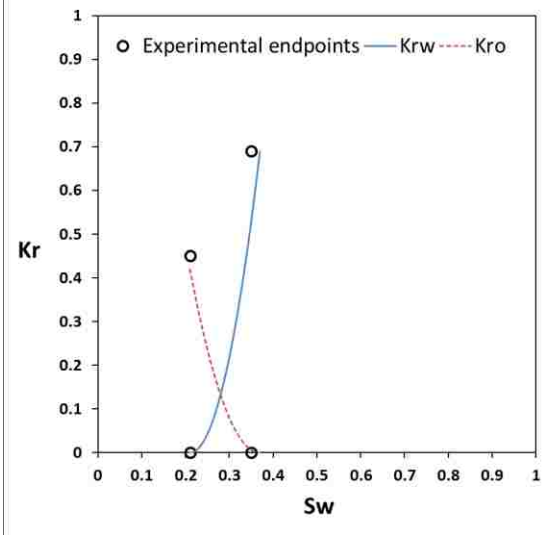

Table 4.26. Experimental and simulation endpoints for waterflood at (2 wt.% NaCl) reservoir conditions (700 psi & 150 ˚F).

Relative Permeability Endpoints		
Experimental	Siw	0.210
	Sor	0.650
	krw	0.690
	kro	0.450
Simulation	Siw	0.210
	Sor	0.630
	Krw	0.690
	Kro	0.420

Figure 4.60. Simulated relative permeability curves for waterflood (2 wt.% NaCl) at reservoir conditions (700 psi & 150 ˚F).

4.3.1.2.2. Surfactant flood

For this coreflood, SOLOTERRA 938 was used. It was previously shown, in the screening stage, that this surfactant had no significant influence on the wettability alteration. The reason this coreflood is repeated here is that, previously surfactant was injected as a tertiary recovery method following a waterflood. Now, however, surfactant is injected immediately after the initial condition was established and the core was aged, thus as a secondary recovery method. The surfactant with concentration of 2000 ppm was injected at 2 cc/min into a 12 in. by 2 in. Indiana limestone core with the porosity of about 16% and the absolute permeability of about 25 md depicting a rather tight core (Table 4.27). The oil recovery of about 21.5% shows a relatively oil-wet behavior of the core, meaning that the surfactant has not significantly been effective toward improving the oil recovery. This was also suggested by the coreflood results from the screening stage, where the surfactant experimental endpoints did not significantly shift to the right of the waterflood relative permeability curves. Figure 4.61 depicts that the simulated oil recovery and pressure drop of the surfactant flood agree well with the experimental values. The simulated relative permeability curves also describe the oil-wet behavior of the system, since the crossover point is below 0.5 and water relative permeability endpoint is higher than that of oil (Figure 4.62). No significant shift-to-right is observed in the relative permeability curves compared to that of waterflood (Figure 4.60), indicating the poor performance of this surfactant in changing the wettability. The experimental endpoints are shown on the plot as well as listed in Table 4.28 to indicate how accurately the relative permeability curves are simulated. The relatively high value of the residual oil saturation (S_{or}=0.639) also expresses the oil-wet condition of the core even after the surfactant flood. This is also supported by the contact angle measurements as the advancing contact angle of 150° indicated the strongly oil-wet behavior of the system using this surfactant at reservoir conditions.

Table 4.27. Initial parameters for coreflood using surfactant (SOL 938, 2000 ppm) at reservoir conditions (700 psi & 150 ˚F).

Core name:	Indiana Limestone-18 (12X2)	
Porosity:	15.71	%
Abs. Perm:	24.92	md
Pore Volume	97	cc
Oil	Yates crude oil	
Brine (NaCl)	2%	wt
Surfactant	SOL 938 (2000 ppm)	
Injection rate	2	cc/min
Oil Recovery	21.52	%

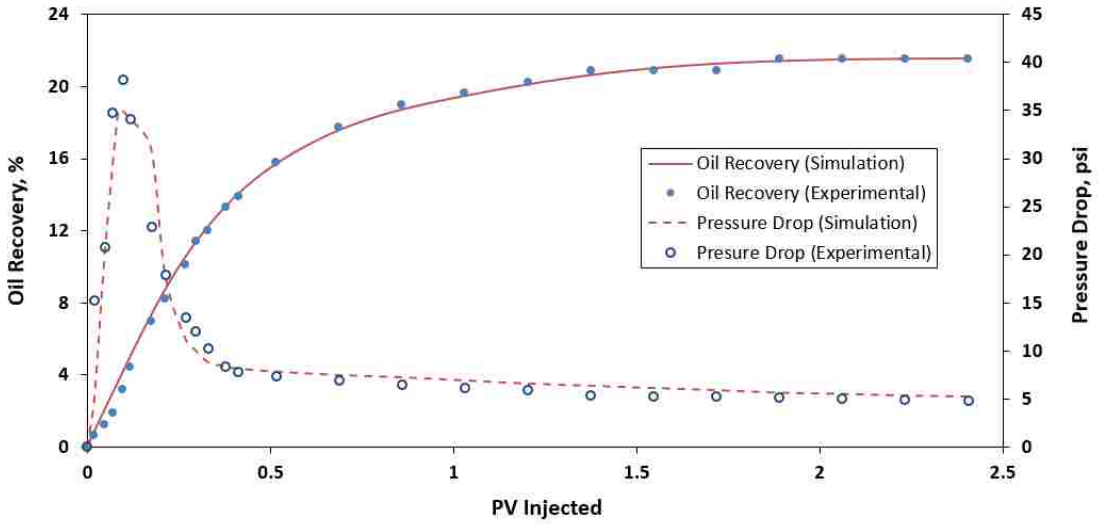

Figure 4.61. History match of oil recovery and pressure drop using surfactant (SOL 938, 2000 ppm) at reservoir conditions (700 psi & 150 ˚F).

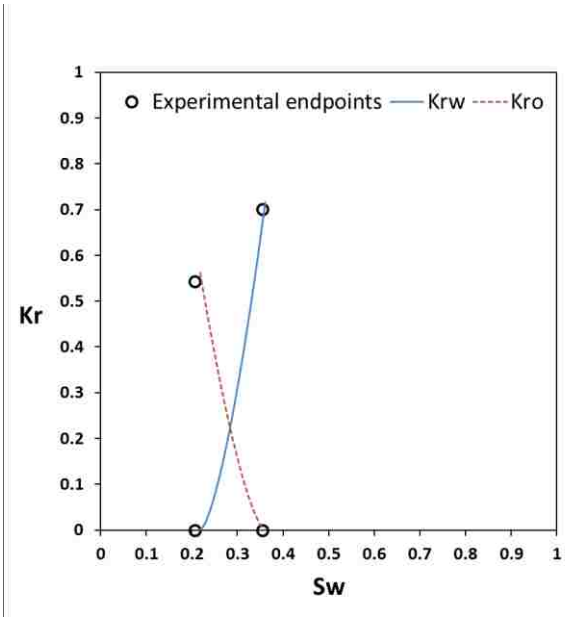

Table 4.28: Experimental and simulation endpoints for coreflood using surfactant (SOL 938, 2000 ppm) at reservoir conditions (700 psi & 150 ˚F).

Relative Permeability Endpoints		
Experimental	Siw	0.207
	Sor	0.645
	krw	0.701
	kro	0.543
Simulation	Siw	0.218
	Sor	0.639
	Krw	0.717
	Kro	0.562

Figure 4.62. Simulated relative permeability curves for coreflood using surfactant (SOL 938, 2000 ppm) at reservoir conditions (700 psi & 150 ˚F).

4.3.1.2.3. Brine-based nanofluid flood

For this coreflood, 0.4 wt.% of nanoparticles were mixed in brine (2 wt.% NaCl) to prepare the nanofluid with the optimal concentration, based on the observations from the contact angle measurements. The brine-based nanofluid was injected immediately after the initial condition was established and the core was aged, thus as a secondary recovery method. The injection was at 2 cc/min into a 12 in. by 2 in. Indiana limestone core with the porosity of 17% and absolute permeability of about 31 md depicting a rather tight core (Table 4.29). The coreflood using the brine-based nanofluid resulted in an incremental oil recovery of more than 10% compared to the pure waterflood and reached to about 29%. This clearly expresses the direct influence of nanoparticles in improving the oil recovery. Figure 4.63 describes the great agreement of simulated oil recovery and pressure drop with the experimental values. The simulated relative permeability curves, in Figure 4.64, show a shift-to-right in the crossover point compared to that of waterflood (Figure 4.60), although the water relative permeability endpoint is still higher than that of oil. This means that the nanoparticles were able to change the wettability of the system from strongly oil-wet toward less oil-wet, leading to a reduction in the residual oil saturation (from S_{or}=0.630 for waterflood to S_{or}=0.524), as seen in Table 4.30, and an improvement in the oil recovery. This is also supported by the contact angle measurements as the brine-based nanofluid (0.4 wt.%) resulted in an advancing contact angle of 135° indicating a weakly oil-wet behavior at reservoir conditions. The experimental endpoints are shown on the relative permeability plots as well as listed in Table 4.30 to indicate how accurately the relative permeability curves are simulated.

Table 4.29. Initial parameters for coreflood using brine-based nanofluid (0.4 wt.% NP in 2% NaCl) at resesrvoir conditions (700 psi & 150 ˚F).

Core name:	Indiana Limestone-19 (12X2)	
Porosity:	17.00	%
Abs. Perm:	31.29	md
Pore Volume	105	cc
Oil	Yates crude oil	
Brine (NaCl)	2%	wt
Nanofluid (brine-based)	0.4 wt.% NP	
Injection rate	2	cc/min
Oil Recovery	28.57	%

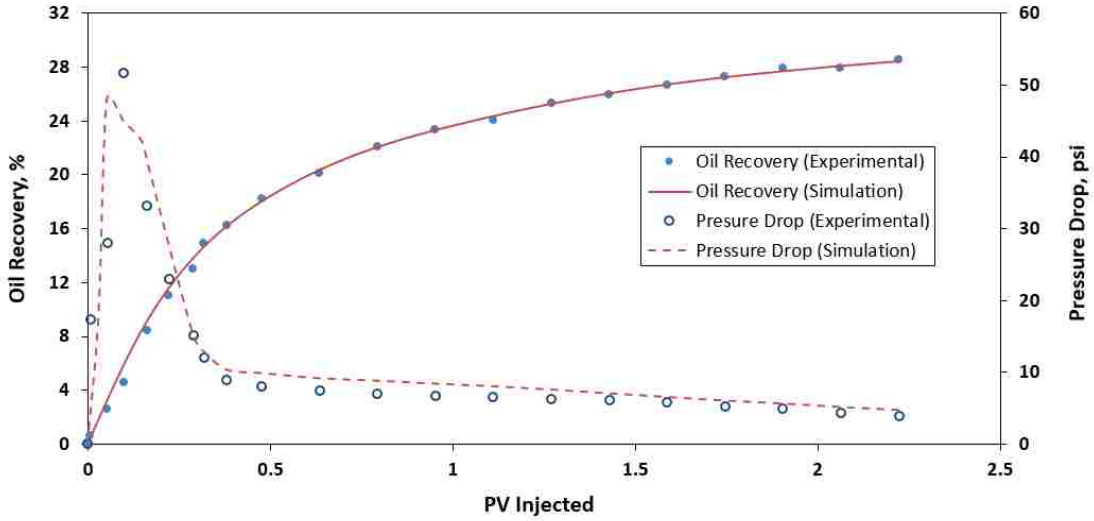

Figure 4.63. History match of oil recovery and pressure drop using brine-based nanofluid (0.4 wt.% NP in 2% NaCl) at reservoir conditions (700 psi & 150 ˚F).

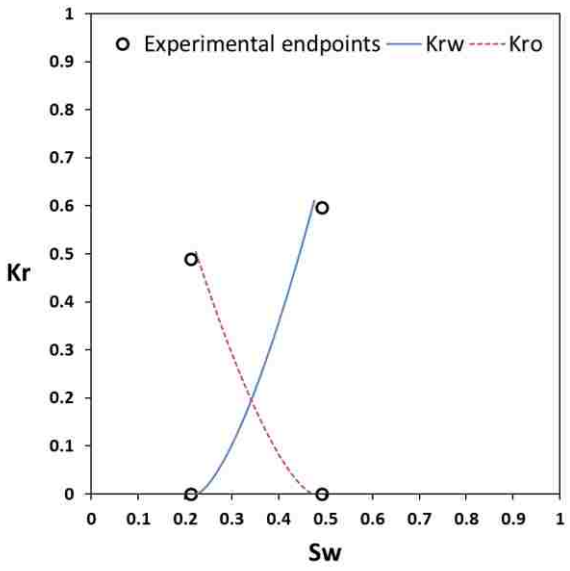

Table 4.30. Experimental and simulation endpoints for coreflood using brine-based nanofluid (0.4 wt.% NP in 2% NaCl) at reservoir conditions (700 psi & 150 ˚F).

Relative Permeability Endpoints		
Experimental	Siw	0.212
	Sor	0.508
	krw	0.597
	kro	0.489
Simulation	Siw	0.223
	Sor	0.524
	Krw	0.611
	Kro	0.505

Figure 4.64. Simulated relative permeability curves for coreflood using brine-based nanofluid ((0.4 wt.% NP in 2% NaCl) at reservoir conditions (700 psi & 150 ˚F).

4.3.1.2.4. Surfactant-based nanofluid flood

For this flood, SOLOTEARRA 938 (2000 ppm), as the surfactant that showed no significant effect in terms of wettability alteration and did not majorly improve the oil recovery, is mixed with nanoparticles (0.4 wt.%). The resultant surfactant-based nanofluid once showed a great potential for changing the wettability from strongly oil-wet to intermediate-wet through the contact angle measurements. Now, the composite fluid is injected as a secondary recovery method. The injection was at 2 cc/min into a 12 in. by 2 in. Indiana limestone core with the porosity of about 15% and absolute permeability of about 50 md (Table 4.31). The coreflood resulted in an incremental oil recovery of more than 30% compared to the surfactant flood and reached to about 52%. Figure 4.65 describes how well the simulated oil recovery and pressure drop data match with the experimental values. The simulated relative permeability curves, in Figure 4.66, show a great shift-to-right in the crossover point compared to that of surfactant flood (Figure 4.62), although the water relative permeability endpoint is still a little higher than that of oil. This means that the nanoparticles were able to significantly improve the ability of surfactant in changing the wettability of the system from strongly oil-wet toward less oil-wet, leading to a great reduction in the residual oil saturation (from S_{or}=0.639 for surfactant flood to S_{or}=0.333), as seen in Table 4.32, and an improvement in the oil recovery. This is also supported by the contact angle measurements as the surfactant-based nanofluid (100 ppm) resulted in an advancing contact angle of 108° indicating an intermediate-wet behavior at reservoir conditions. The experimental endpoints are shown on the relative permeability plots as well as listed in Table 4.32 to indicate how accurately the relative permeability curves are simulated.

Table 4.31. Initial parameters for coreflood using surfactant-based nanofluid (0.4 wt.% NP + SOL 938, 2000 ppm) at reservoir conditions (700 psi & 150 ˚F).

Core name:	Indiana Limestone-20 (12X2)	
Porosity:	15.06	%
Abs. Perm:	49.70	md
Pore Volume	93	cc
Oil	Yates crude oil	
Brine (NaCl)	2%	wt
Nanofluid (surfactant-based)	0.4 wt.% NP + SOL 938 (2000 ppm)	
Injection rate	2	cc/min
Oil Recovery	51.56	%

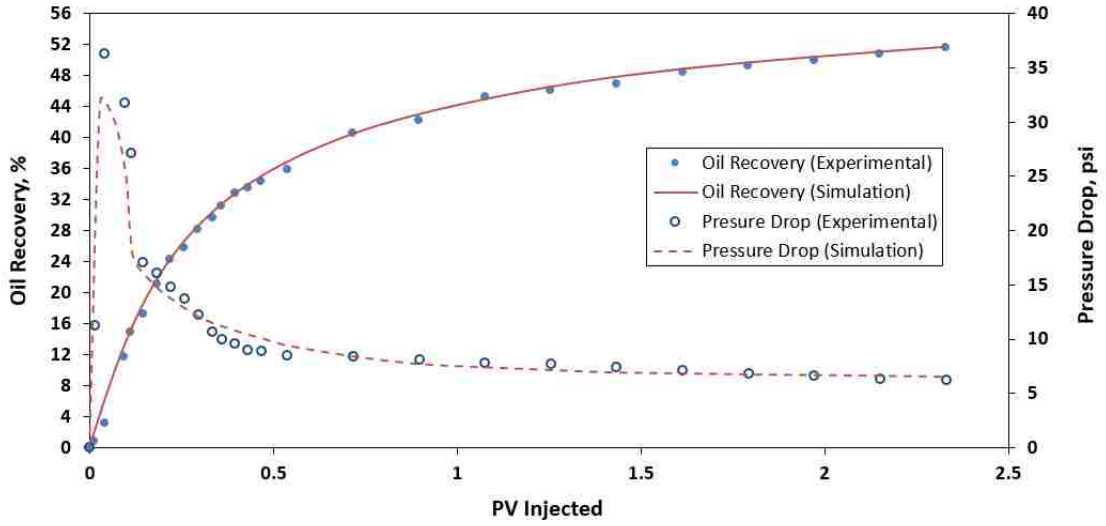

Figure 4.65. History match of oil recovery and pressure drop using surfactant-based nanofluid (0.4 wt.% NP + SOL 938, 2000 ppm) at reservoir conditions (700 psi & 150 ˚F).

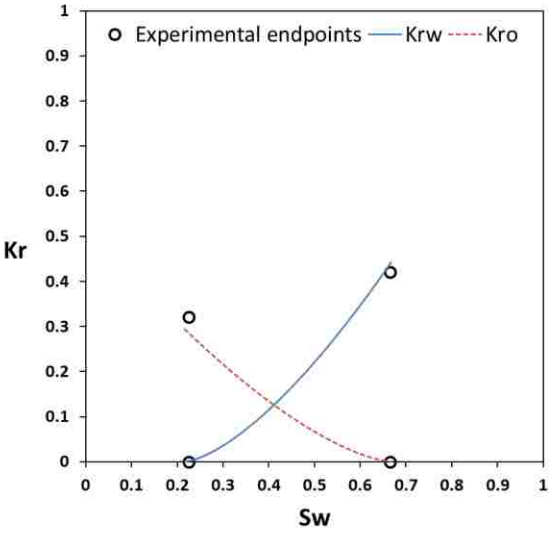

Table 4.32. Experimental and simulation endpoints for coreflood using surfactant-based nanofluid (0.4 wt.% NP + SOL 938, 2000 ppm) at reservoir conditions (700 psi & 150 ˚F).

Relative Permeability Endpoints		
Experimental	Siw	0.225
	Sor	0.335
	krw	0.420
	kro	0.321
Simulation	Siw	0.217
	Sor	0.333
	Krw	0.442
	Kro	0.294

Figure 4.66. Simulated relative permeability curves for coreflood using surfactant-based nanofluid (0.4 wt.% NP + SOL 938, 2000 ppm) at reservoir conditions (700 psi & 150 ˚F).

4.3.1.2.5. Surfactant-based nanofluid flood (lower concentration of surfactant)

For this flood, the concentration of SOLOTERRA 938 was reduced to 1000 ppm to see if nanoparticles can compensate for the surfactant in the coreflood as well as they did in the contact angle measurements. The surfactant-based nanofluid is injected immediately after the initial condition was established as a secondary recovery method. The injection was at 2 cc/min into a 12 in. by 2 in. Indiana limestone core with the porosity of about 17% and absolute permeability of about 63 md (Table 4.33). The coreflood resulted in an incremental oil recovery of more than 20% compared to the surfactant flood and reached to about 45%. Figure 4.67 describes how well the simulated oil recovery and pressure drop match with the experimental values. The simulated relative permeability curves, in Figure 4.68, show a great shift-to-right in the crossover point compared to that of surfactant flood (Figure 4.62), although the shift is not as large as it was in the previous case, where the surfactant concentration was twice higher (Figure 4.66). This means that, even after reducing the concentration of surfactant, the surfactant-based nanofluid was still able to greatly alter the wettability of the system from strongly oil-wet toward less oil-wet, leading to a reduction in the residual oil saturation (from S_{or}=0.639 for surfactant flood to S_{or}=0.368), as seen in Table 4.34, and an improvement in the oil recovery. This is also supported by the contact angle measurements as the surfactant-based nanofluid (50 ppm) resulted in an advancing contact angle of 114° indicating an intermediate-wet behavior at reservoir conditions. The experimental endpoints are shown on the relative permeability plots as well as listed in Table 4.34 to indicate how accurately the relative permeability curves are simulated.

Table 4.33. Initial parameters for coreflood using surfactant-based nanofluid (0.4 wt.% NP + SOL 938, 1000 ppm) at reservoir conditions (700 psi & 150 ˚F).

Core name:	Indiana Limestone-21 (12X2)	
Porosity:	17.17	%
Abs. Perm:	62.77	md
Pore Volume	106	cc
Oil	Yates crude oil	
Brine (NaCl)	2%	wt
Nanofluid (surfactant-based)	0.4 wt.% NP + SOL 938 (1000 ppm)	
Injection rate	2	cc/min
Oil Recovery	45.07	%

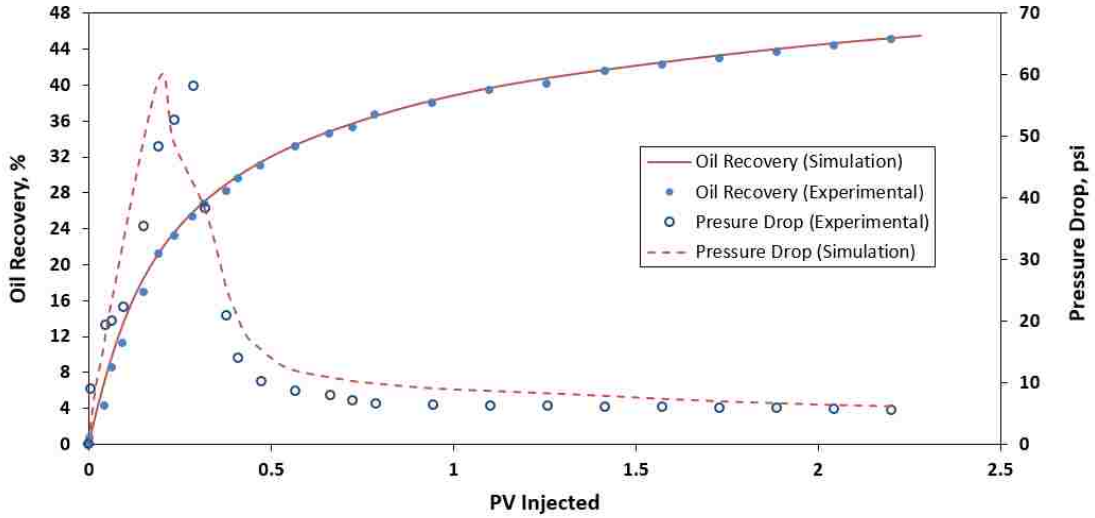

Figure 4.67. History match of oil recovery and pressure drop using surfactant-based nanofluid (0.4 wt.% NP + SOL 938, 1000 ppm) at reservoir conditions (700 psi & 150 ˚F).

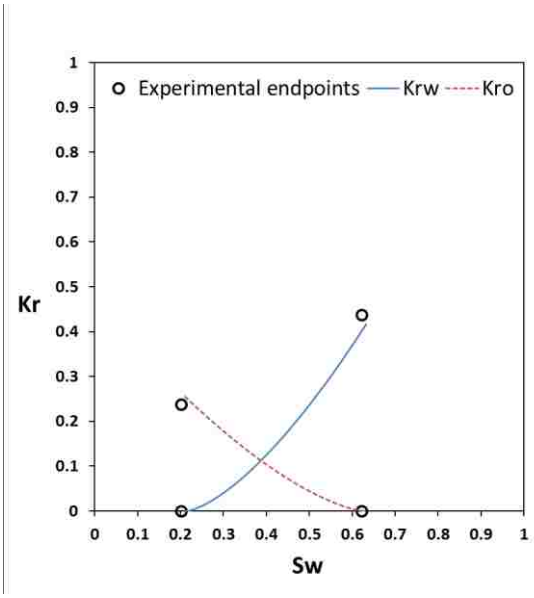

Table 4.34. Experimental and simulation endpoints for coreflood using surfactant-based nanofluid (0.4 wt.% NP + SOL 938, 1000 ppm) at reservoir conditions (700 psi & 150 ˚F).

Relative Permeability Endpoints		
Experimental	Siw	0.201
	Sor	0.378
	krw	0.437
	kro	0.238
Simulation	Siw	0.210
	Sor	0.368
	Krw	0.417
	Kro	0.255

Figure 4.68. Simulated relative permeability curves for coreflood using surfactant-based nanofluid (0.4 wt.% NP + SOL 938, 1000 ppm) at reservoir conditions (700 psi & 150 ˚F).

4.3.2. Corefloods results for nanofluids made by the most effective surfactant

In last section, the potential influence of nanoparticles on enhancing the performance of the least effective surfactants (ALFOETERRA S23-13S 90 at 500 psi and 72 ˚F and SOLOTERRA 938 for reservoir conditions (700 psi and 150 ºF)) was evaluated. The relative permeability curves showed that nanoparticles were able to improve the ability of surfactants in changing the wettability of the system towards less oil-wet at both experimental conditions.

In this section, the impact of nanoparticles on the most effective surfactant is evaluated. To study the influence of nanoparticles on the performance of a surfactant that is already efficient in changing the wettability, ALFOTERRA S23-9S 90 was selected. As seen in section 4.1, this surfactant generated the largest shift to the right in the relative permeability curves along with resulting in a change of angle from 152° to 90°, meaning a wettability alteration from strongly oil-wet to intermediate-wet.

The coreflood procedure of this section was slightly different than that of the rest of the corefloods. A limestone core was initially vacuumed and saturated with oil. After measuring porosity and absolute permeability, the oil was displaced by brine to reach initial water saturation. After aging for 8 days, a secondary recovery was conducted using surfactant flood and the recovery and pressure drop data were collected. Then, 5 pore-volume of brine was injected through the core to remove any surfactant before saturating the core with oil again. Next, the core was flooded with the combination of surfactant and nanoparticles. After cleaning with brine and saturating with oil, the surfactant-based nanofluid with lower concentration of surfactant was injected. The following are the final results of each coreflood in addition to the simulated relative permeability curves.

4.3.2.1. Surfactant flood

For this coreflood, ALFOTERRA S23-9S 90 was used. It was previously shown that this surfactant had a great influence on the wettability alteration. The reason this coreflood is repeated here is that, the surfactant was formerly injected as a tertiary recovery method following a waterflood. Now, however, the surfactant is injected immediately after aging thus as a secondary recovery method at 500 psi and 72 ˚F. The surfactant with concentration of 2000 ppm was injected at 2 cc/min into a 12 in. by 2 in. Indiana limestone core with the porosity of about 16% and absolute permeability of about 18 md, depicting a rather tight core (Table 4.35). The great oil recovery of more than 48% shows that the surfactant has significantly been effective toward improving the oil recovery, compared to 20% waterflood recovery of the system at 500 psi and 72 ˚F. This was also suggested by the coreflood results from the screening stage, where the experimental endpoints of the surfactant flood demonstrated a great shift-to-right in the relative permeability curves. Figure 4.69 describes that the simulated oil recovery and pressure drop of the surfactant flood agree well with the experimental values. The simulated relative permeability curves, in Figure 4.70, also illustrate a great shift to the right in the crossover point compared to that of waterflood at 500 psi and 72 ˚F (Figure 4.50) and higher endpoint of oil relative permeability compared to that of water. This means that the surfactant was able to alter wettability of the system from strongly oil-wet to rather intermediate-wet or at least to less oil-wet, leading to a reduction in residual oil saturation (from S_{or}= 0.644 for waterflood to S_{or}=0.426), as seen in Table 4.36. The experimental endpoints are shown on the relative permeability plots as well as listed in Table 4.36 to indicate how accurately the relative permeability curves are simulated.

Table 4.35. Initial parameters for coreflood using surfactant (ALF 9S, 2000 ppm) at 500 psi and 72 ˚F.

Core name:	Indiana Limestone-X (12X2)	
Porosity:	16.36	%
Abs. Perm:	17.95	md
Pore Volume	101	cc
Oil	Yates crude oil	
Brine (NaCl)	2%	wt
Surfactant	ALF 9S (2000 ppm)	
Injection rate	2	cc/min
Oil Recovery	48.19	%

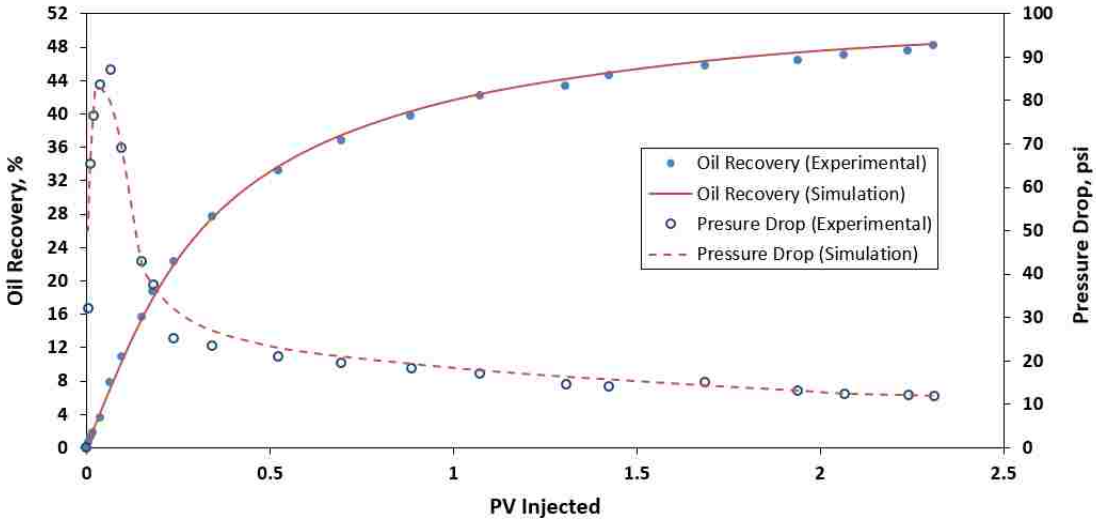

Figure 4.69. History match of oil recovery and pressure drop using surfactant (ALF 9S, 2000 ppm) at 500 psi and 72 ˚F.

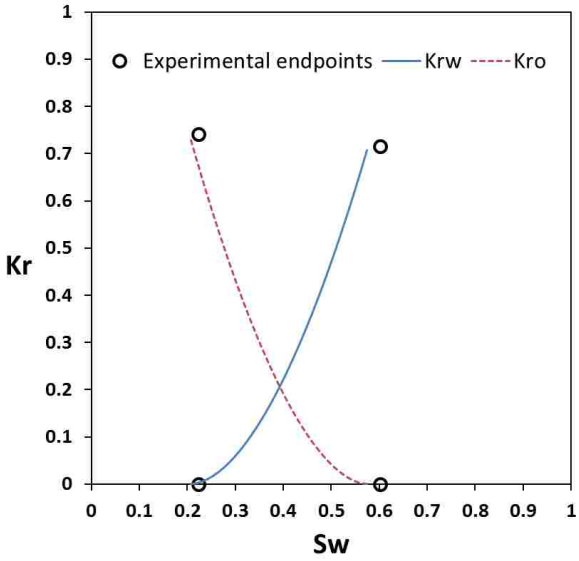

Table 4.36. Experimental and simulation endpoints for coreflood using surfactant (ALF 9S, 2000 ppm) at 500 psi and 72 ˚F.

Relative Permeability Endpoints		
Experimental	Siw	0.224
	Sor	0.398
	krw	0.716
	kro	0.741
Simulation	Siw	0.208
	Sor	0.426
	Krw	0.707
	Kro	0.729

Figure 4.70. Simulated relative permeability curves for coreflood using surfactant (ALF 9S, 2000 ppm) at 500 psi and 72 ˚F.

4.3.2.2. Surfactant-based nanofluid flood

For this coreflood, ALFOTERRA S23-9S 90 (2000 ppm), as the surfactant with strong ability to change the wettability and improve the recovery was mixed with nanoparticles (0.4 wt.%) and injected as a secondary recovery method. The injection was at 2 cc/min into the same core as in the last section with the porosity of about 16% and absolute permeability of about 18 md, depicting a rather tight core (Table 4.37). The coreflood resulted in an excellent oil recovery of about 93% (incremental recovery of about 45% compared to the surfactant flood) showing that the surfactant-based nanofluid has considerably been effective toward improving the oil recovery. Figure 4.71 describes how simulated oil recovery and pressure drop match with the experimental values. The simulated relative permeability curves, in Figure 4.72, also illustrate a great shift to the right in the crossover point compared to that of surfactant flood (Figure 4.70) and higher endpoint of oil relative permeability compared to that of water. This means that the nanoparticles were able to significantly improve the ability of the surfactant in altering the wettability of the system toward less oil-wet (even into the weakly water-wet or intermediate-wet zone with crossover point being to the right of 0.5), resulting in a great reduction in the residual oil saturation (from S_{or}= 0.426 for surfactant flood to S_{or}=0.061), as seen in Table 4.38. The experimental endpoints are shown on the relative permeability plots as well as listed in Table 4.38 to indicate how accurately the relative permeability curves are simulated.

Table 4.37. Initial parameters for coreflood using surfactant-based nanofluid (0.4 wt.% NP+ALF 9S, 2000 ppm) at 500 psi and 72 ˚F.

Core name:	Indiana Limestone-X (12X2)	
Porosity:	16.36	%
Abs. Perm:	17.95	md
Pore Volume	101	cc
Oil	Yates crude oil	
Brine (NaCl)	2%	wt
Nanofluid (surfactant-based)	0.4 wt.% NP + ALF 9S (2000 ppm)	
Injection rate	2	cc/min
Oil Recovery	92.68	%

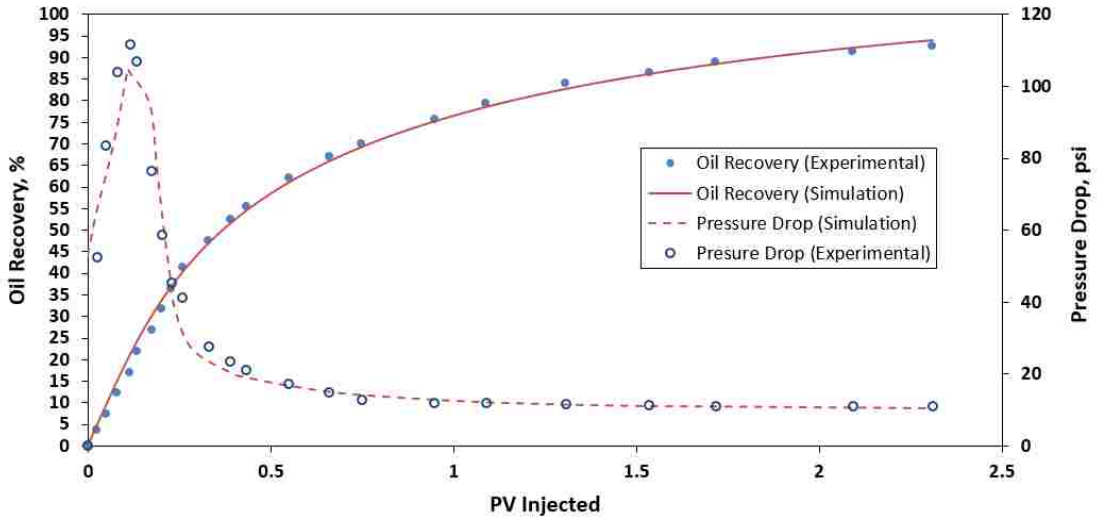

Figure 4.71. History match of oil recovery and pressure drop using surfactant-based nanofluid (0.4 wt.% NP+ALF 9S, 2000 ppm) at 500 psi and 72 ˚F.

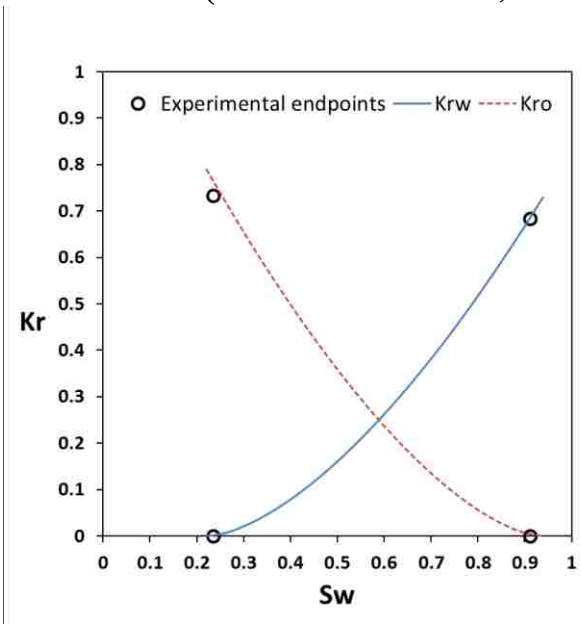

Table 4.38. Experimental and simulation endpoints for coreflood surfactant-based nanofluid (0.4 wt.% NP+ALF 9S, 2000 ppm) at 500 psi and 72 ˚F.

Relative Permeability Endpoints		
Experimental	Siw	0.235
	Sor	0.088
	krw	0.684
	kro	0.733
Simulation	Siw	0.221
	Sor	0.061
	Krw	0.730
	Kro	0.790

Figure 4.72. Simulated relative permeability curves for coreflood using surfactant-based nanofluid (0.4 wt.% NP+ALF 9S, 2000 ppm) at 500 psi and 72 ˚F.

4.3.2.3. Surfactant-based nanofluid flood (lower concentration of surfactant)

For this coreflood, the concentration of ALFOTERRA S23-9S 90 was reduced to 1000 ppm (and combined with 0.4 wt.% nanoparticles) to see whether nanoparticles can compensate for the surfactant in the coreflood. The surfactant-based nanofluid was injected immediately after the initial condition was established as a secondary recovery method. The injection was at 2 cc/min into the same core as in the last section with the porosity of about 16% and absolute permeability of about 18 md, depicting a rather tight core (Table 4.39). The coreflood resulted in a great oil recovery of about 86% (incremental recovery of about 38% compared to the surfactant flood) showing that the surfactant-based nanofluid has still been significantly effective toward improving the oil recovery. Figure 4.73 describes how simulated oil recovery and pressure drop match with the experimental values. The simulated relative permeability curves, in Figure 4.74, also describe a great shift to the right in the crossover point compared to that of surfactant flood (Figure 4.70) and higher endpoint of oil relative permeability compared to that of water. This means that the nanoparticles were still able to significantly improve the ability of the surfactant in altering the wettability of the system toward less oil-wet (still into the weakly water-wet or intermediate-wet zone with crossover point being to the right of 0.5), resulting in a great reduction in the residual oil saturation (from S_{or}= 0.426 for surfactant flood to S_{or}=0.110), as seen in Table 4.40. The experimental endpoints are shown on the relative permeability plots as well as listed in Table 4.40 to indicate how accurately the relative permeability curves are simulated.

Table 4.39. Initial parameters for coreflood using surfactant-based nanofluid (0.4 wt.% NP+ALF 9S, 1000 ppm) at 500 psi and 72 ˚F.

Core name:	Indiana Limestone-X (12X2)	
Porosity:	16.36	%
Abs. Perm:	17.95	md
Pore Volume	101	cc
Oil	Yates crude oil	
Brine (NaCl)	2%	wt
Nanofluid (surfactant-based)	0.4 wt.% NP + ALF 9S (1000 ppm)	
Injection rate	2	cc/min
Oil Recovery	86.25	%

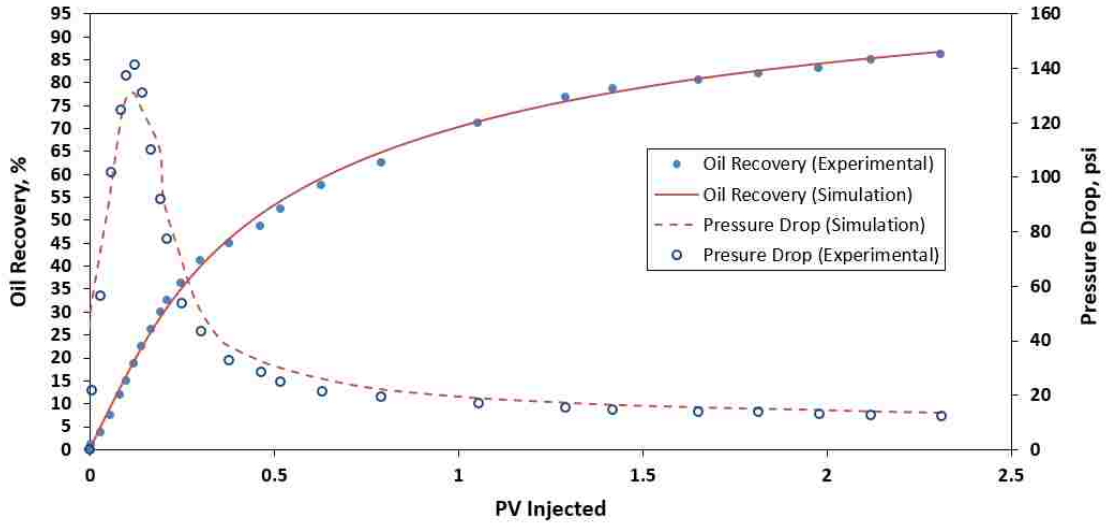

Figure 4.73. History match of oil recovery and pressure drop using surfactant-based nanofluid (0.4 wt.% NP+ALF 9S, 1000 ppm) at 500 psi and 72 ˚F.

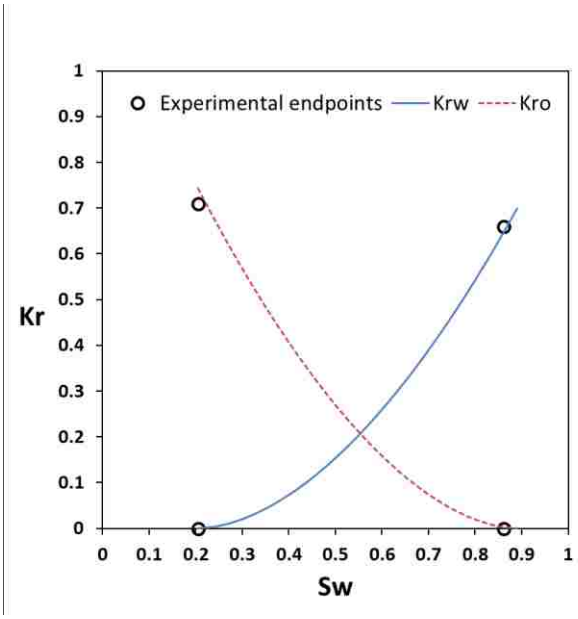

Table 4.40. Experimental and simulation endpoints for coreflood surfactant-based nanofluid (0.4 wt.% NP+ALF 9S, 1000 ppm) at 500 psi and 72 ˚F.

Relative Permeability Endpoints		
Experimental	Siw	0.201
	Sor	0.138
	krw	0.659
	kro	0.709
Simulation	Siw	0.205
	Sor	0.109
	Krw	0.703
	Kro	0.740

Figure 4.74. Simulated relative permeability curves for coreflood using surfactant-based nanofluid (0.4 wt.% NP+ALF 9S, 1000 ppm) at 500 psi and 72 ˚F.

4.3.3. Overall coreflood recovery results

In this section, the overall experimental recovery of all the nanofluid corefloods are evaluated for both experimental conditions. At 500 psi and 72 ˚F, as seen in Figure 4.75, the waterflood helped to produce only about 20% of the original oil in place. This clearly shows the oil-wet nature of the limestone core at the initial condition. Moreover, ALFOTERRA S23-13S 90 at 2000 ppm (as the least effective surfactant at 500 psi and 72 ˚F) was not able to improve the recovery and reached to about 21%. On the other hand, brine-based nanofluid (at optimum concentration of 0.4 wt.%) led to an oil recovery of about 31%. Consequently, after adding nanoparticles to the non-effective surfactant, the recovery boosted up to more than 57%. The participation of nanoparticles in the recovery was so effective that the recovery stayed at around 53%, even after reducing the concentration of surfactant to 1000 pm in the surfactant-based nanofluid.

At reservoir conditions, as seen in Figure 4.76, the waterflood helped to produce only about 17.5% of the original oil in place. This clearly shows the oil-wet nature of the limestone core at the initial conditions. Moreover, SOLOTERRA 938 (as the least effective surfactant at reservoir conditions) at 2000 ppm was not able to significantly improve the recovery and reached to about 22%. On the other hand, brine-based nanofluid (at optimum concentration of 0.4 wt.%) led to an oil recovery of about 29%. Eventually, nanoparticles were added to the non-effective surfactant resulting in a rise in the recovery to about 52%. The participation of nanoparticles in the recovery was so effective that the recovery stayed at around 45%, even after reducing the concentration of surfactant to 1000 pm in the surfactant-based nanofluid.

The impact of nanoparticles combined with the most effective surfactant on the oil recovery is described in Figure 4.77. As seen before, the waterflood and brine-based nanofluid (0.4 wt.%) at 500 psi and 72 ˚F produced 20% and 30% of the oil in place respectively. However,

ALFOTERRA S23-9S 90 at 2000 ppm (as the most effective surfactant at 500 psi and 72 ˚F) resulted in a recovery of about 48%. This improvement in the recovery became even more pronounced after adding nanoparticles to reach a very high recovery of about 93%. The contribution of nanoparticles in the recovery was so effective that the recovery stayed at around 86%, even after reducing the concentration of surfactant to 1000 pm in the surfactant-based nanofluid.

Therefore, nanoparticles not only enhanced the oil recovery for this system, but they could also improve the performance of a non-effective surfactant at both experimental conditions. And this impact is even more pronounced when nanoparticles are combined with an effective surfactant. The economic considerations of using surfactant-based nanofluids are discussed later in this chapter.

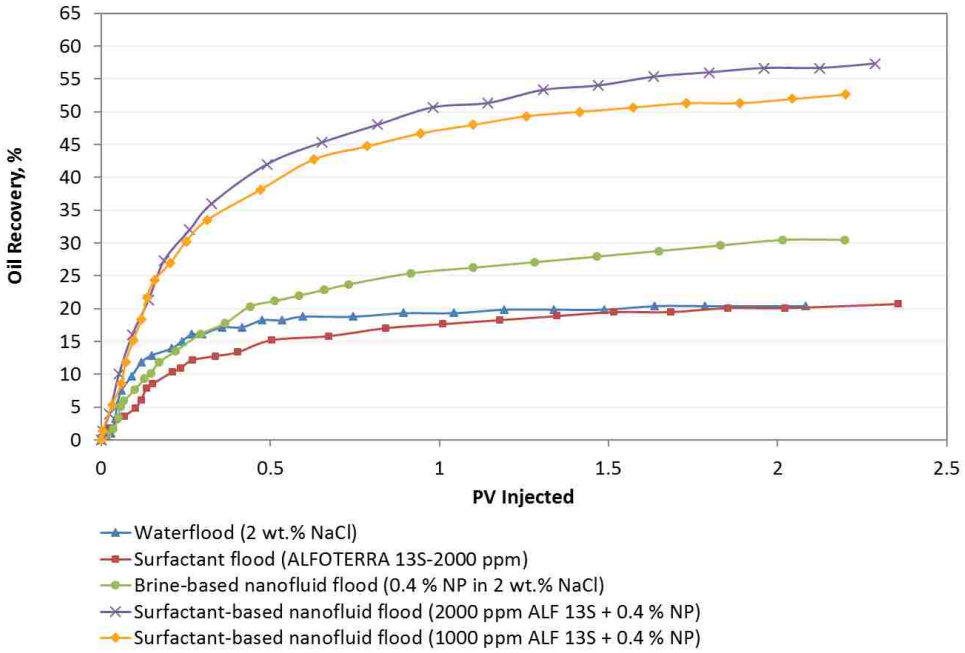

Figure 4.75. Experimental recovery of corefloods using nanofluids made by the least effective surfactant at 500 psi and 72 ˚F.

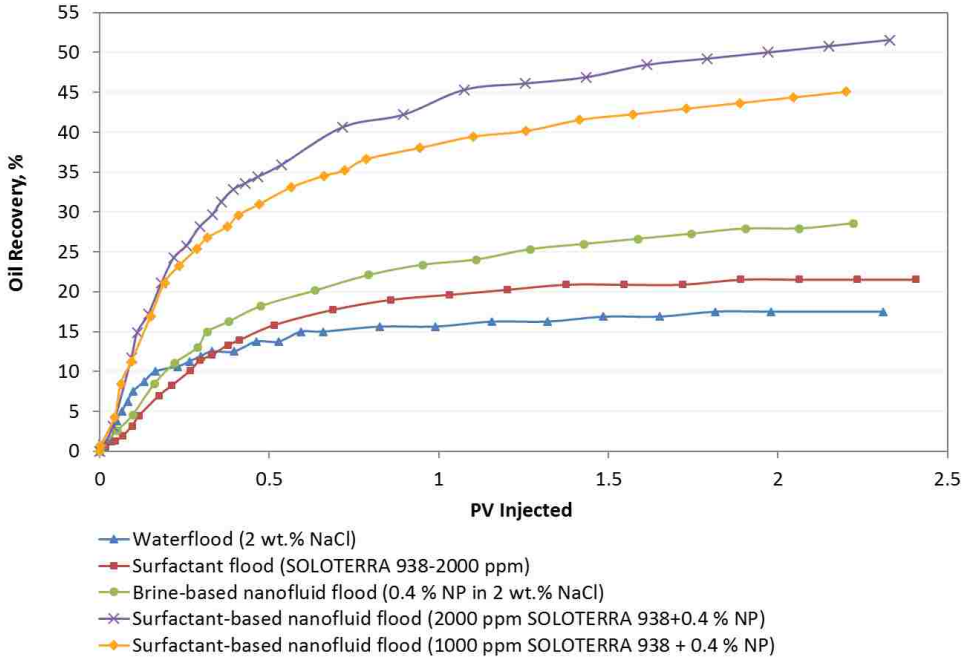

Figure 4.76. Experimental recovery of corefloods using nanofluids made by the least effective surfactant at reservoir conditions (700 psi & 150 ˚F).

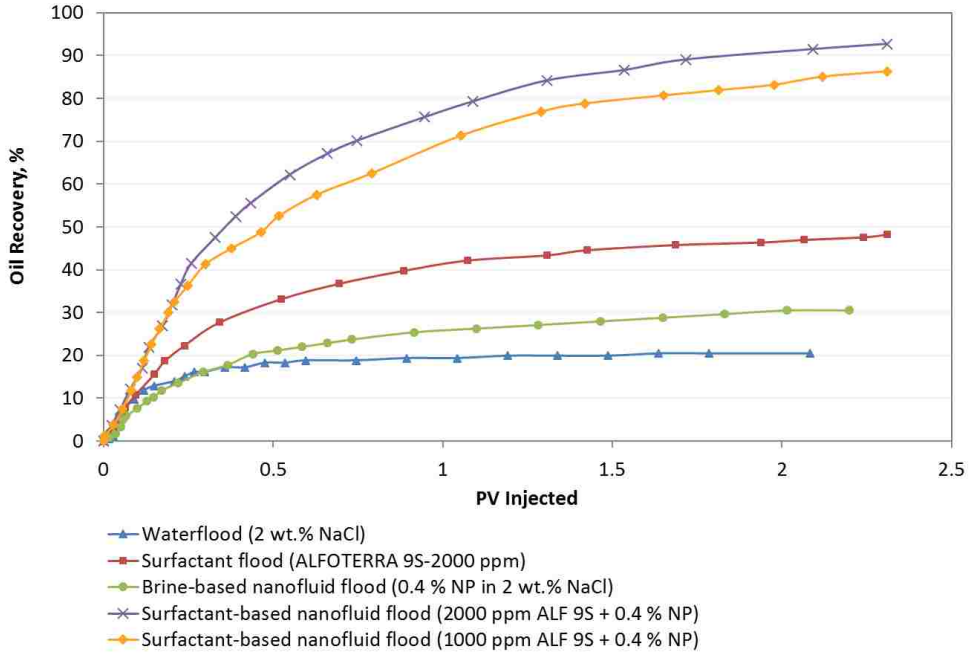

Figure 4.77. Experimental recovery of corefloods using nanofluids made by the most effective surfactant at 500 psi and 72 ˚F.

4.3.4. Overall relative permeability curves

To investigate the impact of nanofluids on the relative permeability curves, all the simulated curves are studied together in this part. Figure 4.78 shows that relative permeability curves of ALFOTERRA 13S (the least effective surfactant at 500 psi and 72 ˚F) stays in the strongly oil-wet zone as the waterflood curves, meaning no shift-to-right as the surfactant was not effective to change the wettability of the system toward less oil-wet. However, the combination of the same surfactant with nanoparticles resulted in a great shift-to-right and a significant reduction in the residual oil saturation, even better than brine-based nanoparticles (without surfactants). This type of improvement was still observed even after reducing the surfactant concentration in the combination, as it showed a great shift-to-right compared to using only surfactant. Therefore, nanoparticles showed a potential to compensate for a non-effective surfactant in order to enhance oil recovery at room temperature.

Figure 4.79 describes the same process at different experimental conditions (700 psi and 150 ˚F). SOLOTERRA 938, as the least effective surfactant at high temperatures, showed almost no improvement compared to the waterflood. The cross-over point of relative permeability curves stayed between water saturation of 0.2 and 0.3, representing a strongly oil-wet behavior. The brine-based nanofluid (without surfactant) slightly shifted the cross-over point to right. However, the shift was much larger using the combination of surfactant and nanoparticles, meaning a great wettability alteration of the system toward less oil-wet. This behavior was also observed when using a lower concentration of surfactants in the combination, as it led to a great shift compared to using only surfactant. Therefor, even at high temperature, nanoparticles showed a potential to compensate for a non-effective surfactant to eventually improve oil recovery.

A similar type of evaluation is performed by comparing the relative permeability curves generated using an effective surfactant (ALFOTERRA 9S at 500 psi and 72 ˚F). As shown in Figure 4.80, the most effective surfactant resulted in a great shift-to-right (even greater than that of the brine-based nanofluid with no surfactant) compared to the waterflood. This ability to change the wettability of the system toward less oil-wet was significantly enhanced after combining with nanoparticles. The cross-over point moved beyond the water saturation of 0.5, representing a system that is no longer oil-wet. The great shift led to a residual oil saturation of less than 0.1, meaning a highly significant improvement in the oil recovery. The reduction of surfactant concentration resulted in a slight shift back to left, but still showing a great potential for nanoparticles to compensate for an effective surfactant to enhance oil recovery.

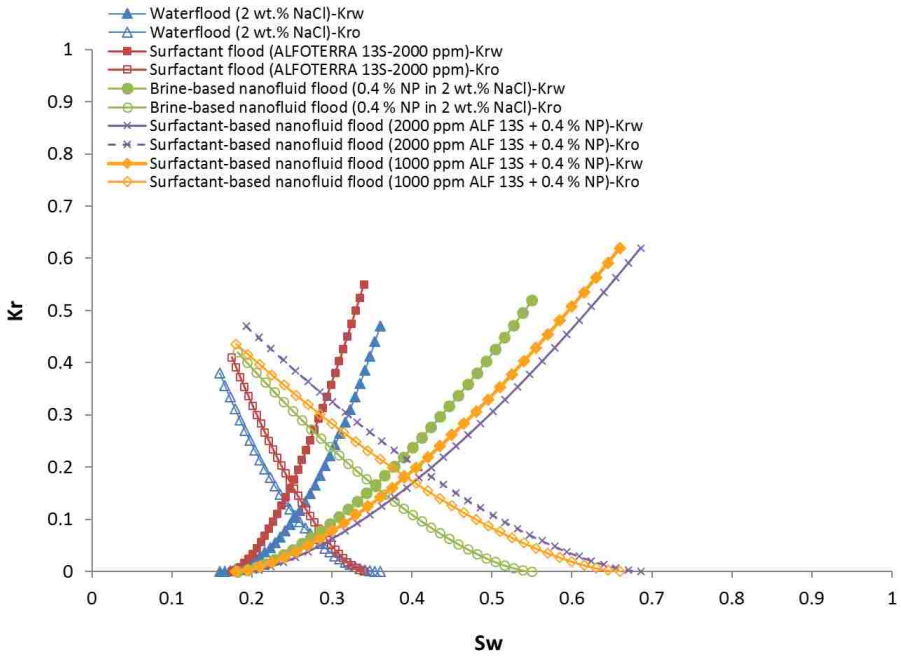

Figure 4.78. Relative permeability curves for nanofluids made by the least effective surfactant at 500 psi and 72 ˚F.

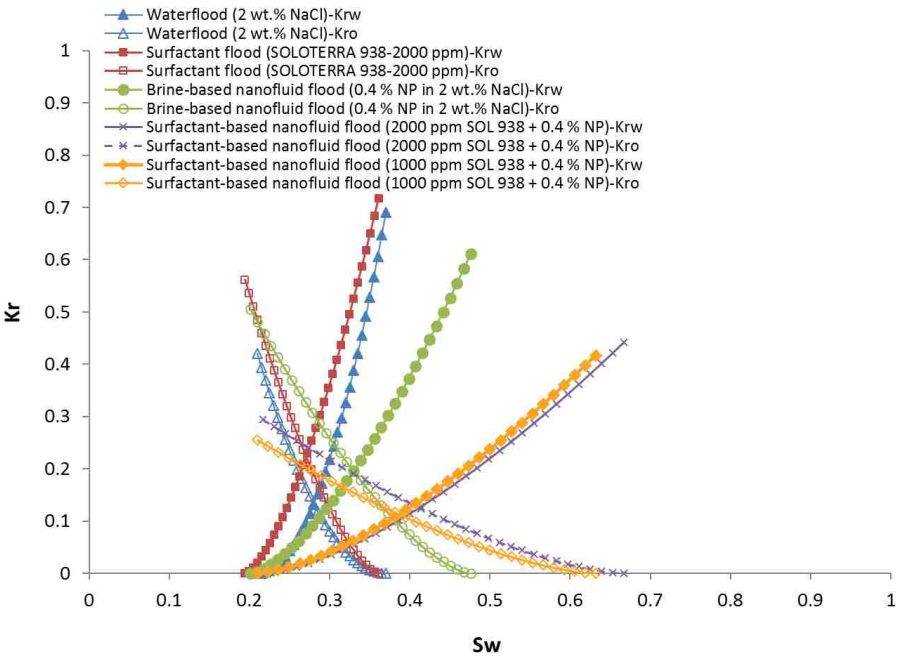

Figure 4.79. Relative permeability curves for nanofluids made by the least effective surfactant at 700 psi and 150 ˚F.

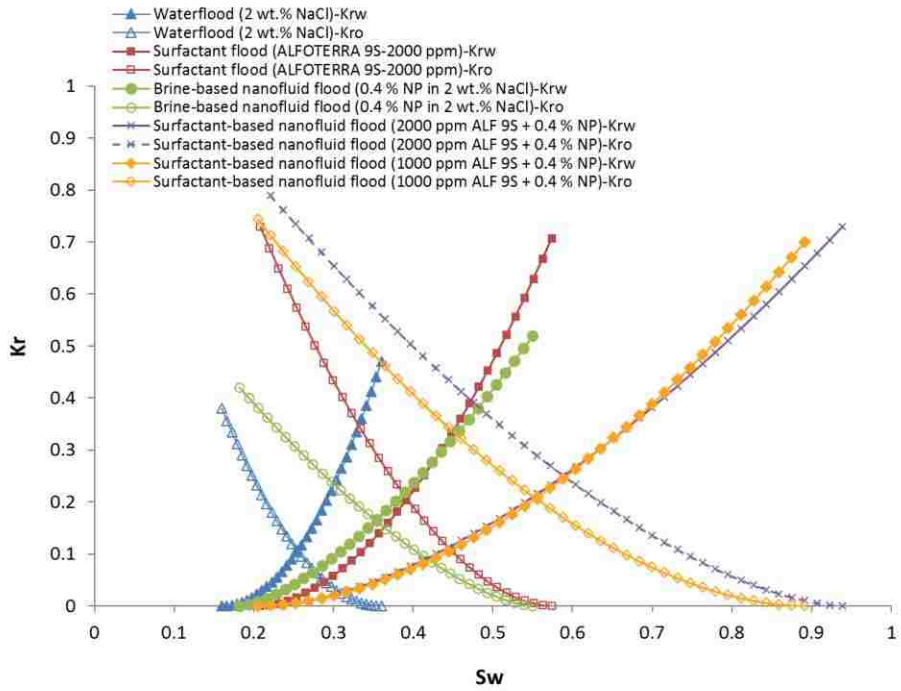

Figure 4.80. Relative permeability curves for nanofluids made by the most effective surfactant at 500 psi and 72 ˚F.

4.3.5. Overall fractional flow results

To evaluate the influence of nanofluids on the oil-water flow characteristic of the system, water fractional flow curves are studied for each coreflood. The fractional flow or water-cut equation is a model based on the Buckley-Leverett theory to determine the water fraction of the total fluid at a certain location and time along the flow line.

For a one-dimensional horizontal oil-water flow system with negligible capillary, the water fractional flow is defined as follow:

$$f_w = 1/\left(1 + \frac{k_{ro}}{\mu_o}\frac{\mu_w}{k_{rw}}\right) \quad \text{..... (4.1)}$$

, where f_w is water fractional flow, k_{ro} is oil relative permeability, k_{rw} is water relative permeability, μ_o is oil viscosity, and μ_w is water viscosity.

Figure 4.81 describes the water fractional flow curves versus water saturation for the nanofluids made by the least effective surfactant at 500 psi and 72 ˚F. Waterflood and surfactant flood seem to have a similar behavior in terms of flow characteristics, which means the surfactant has not been able to improve the oil recovery. The more inclined the curves are, the lower residual oil saturation and consequently the higher recovery they represent. In other words, as previously seen in the evaluation of relative permeability curves, the larger shift-to-right, the better performance in altering the wettability toward less oil-wet. The brine-based nanofluid generates a great shift-to-right. However, the shift becomes more pronounced when nanoparticles are added to the surfactant, which was non-effective by itself. The fractional flow curve slightly shifts back to the left when the concentration of surfactant is lowered to 1000 ppm, but still describes a great shift-to-right compared to the original position of surfactant curve.

This trend is repeated at reservoir conditions (Figure 4.82) except for the fact that the least effective surfactant used for the reservoir conditions shows a small shift-to-right compared to the waterflood. Then the shift becomes greater by introducing nanoparticles. In case of using nanofluids made by the most effective surfactant (Figure 4.83), the surfactant fractional flow curve shows a big shift-to-right compared to the waterflood, a shift that is even greater than that of brine-based nanofluid. This jump becomes even greater with nanoparticles and does not shrink even after lowering the surfactant concentration to 1000 ppm.

One other way to evaluate the fractional flow curves is to draw a vertical line at a certain water saturation, as seen in Figures 4.81 and 4.83, to evaluate the water-cut of each fluid. For instance, at water saturation of 0.25 in Figure 4.81, surfactant-based nanofluid (nanoparticles plus ALFOTERRA S23-13S 90 at 2000 ppm) produces the lowest water-cut (0.42) or highest amount of oil, while waterflood and surfactant flood led to a water-cut of 0.9 and 0.93 respectively, which means that the waterflood performed better than surfactant flood (the least effective surfactant at 500 psi and 72 ˚F) at water saturation of 0.25. Note that this surfactant showed no influence in changing wettability by resulting in a contact angle of 162° and no enhancement in the oil recovery by leading to an incremental coreflood recovery of 1% compared to the waterflood. However, the performance is improved using the brine-based nanofluid with water-cut of 0.62. The second surfactant-based nanofluid (nanoparticles plus ALFOTERRA S23-13S 90 at 1000 ppm) still performs well even after reducing the surfactant concentration, as it generates a water-cut of 0.55.

At reservoir conditions (Figure 4.82), surfactant-based nanofluid (nanoparticles plus SOLOTERRA 938 at 2000 ppm) provides the largest shift-to-right, meaning the lowest residual oil saturation or highest recovery with a water-cut of 0.22 at water saturation of 0.25. The surfactant flood (the least effective surfactant at reservoir conditions) with a water-cut of 0.6

demonstrates a small shift-to-right compared to the waterflood (water-cut of 0.86). However, it ends up with a similar residual oil saturation. This probably means that the surfactant has been able to improve the oil flow in the porous medium but not necessarily from the small pores to reduce the residual oil saturation. Note that this surfactant showed very small influence in changing wettability by resulting in a contact angle of 150° and just a little enhancement in the oil recovery leading to an incremental coreflood recovery of 4% compared to the waterflood. However, the performance is improved using the brine-based nanofluid with water-cut of 0.5. The second surfactant-based nanofluid (nanoparticles plus SOLOTERRA 938 at 1000 ppm) still performs well even after reducing the surfactant concentration, as it generates a water-cut of 0.31.

The coreflood using the most effective surfactant results in a water-cut of 0.23 at water saturation of 0.25 (Figure 4.83), which is significantly lower than that of the waterflood (water-cut of 0.92) and even lower than that of the brine-based nanofluid (water-cut of 0.63). Therefore, the surfactant seems to be working better than the brine-based nanofluid (also observed in the oil recovery plot). The lowest water-cut (0.07), however, is generated by the surfactant-based nanofluid made with 2000 ppm of the most effective surfactant, representing the highest amount of oil recovery. Lowering the surfactant concentration to 1000 ppm only changes the water-cut to 0.1, meaning that the performance of surfactant-based nanofluids does not change much even after saving on surfactant.

Therefore, nanoparticles seem to have a potential to compensate for surfactant in enhancing the flow characteristic of carbonate rock for this system by altering the wettability toward less oil-wet at both experimental conditions.

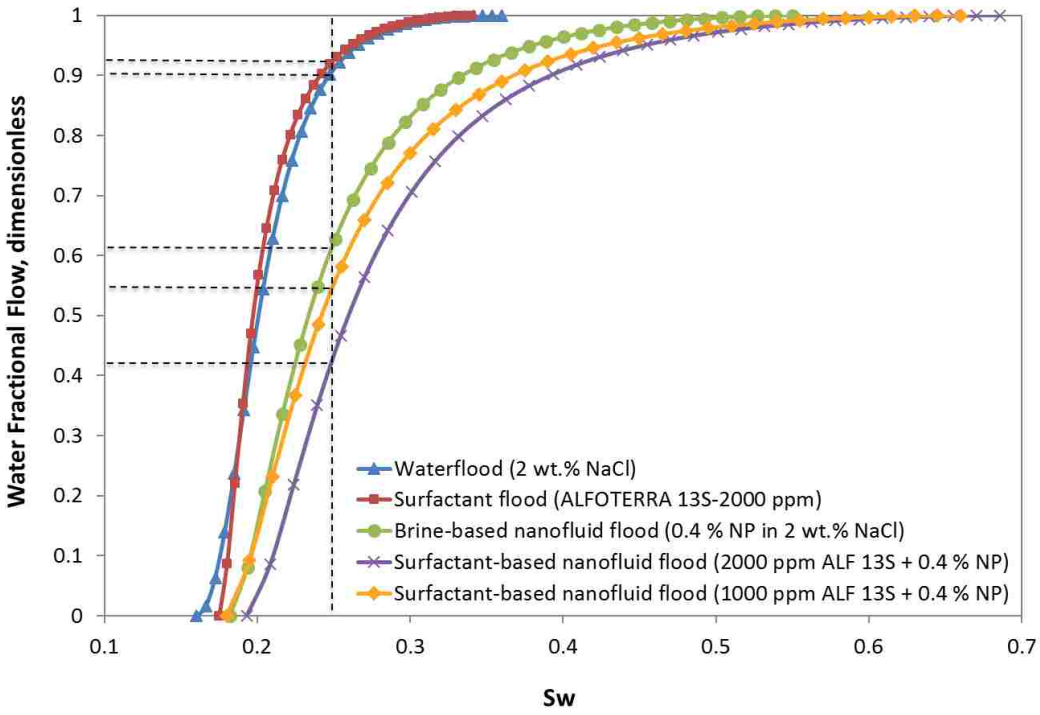

Figure 4.81. Water fractional flow curves for nanofluids made by the least effective surfactant at 500 psi and 72 ˚F.

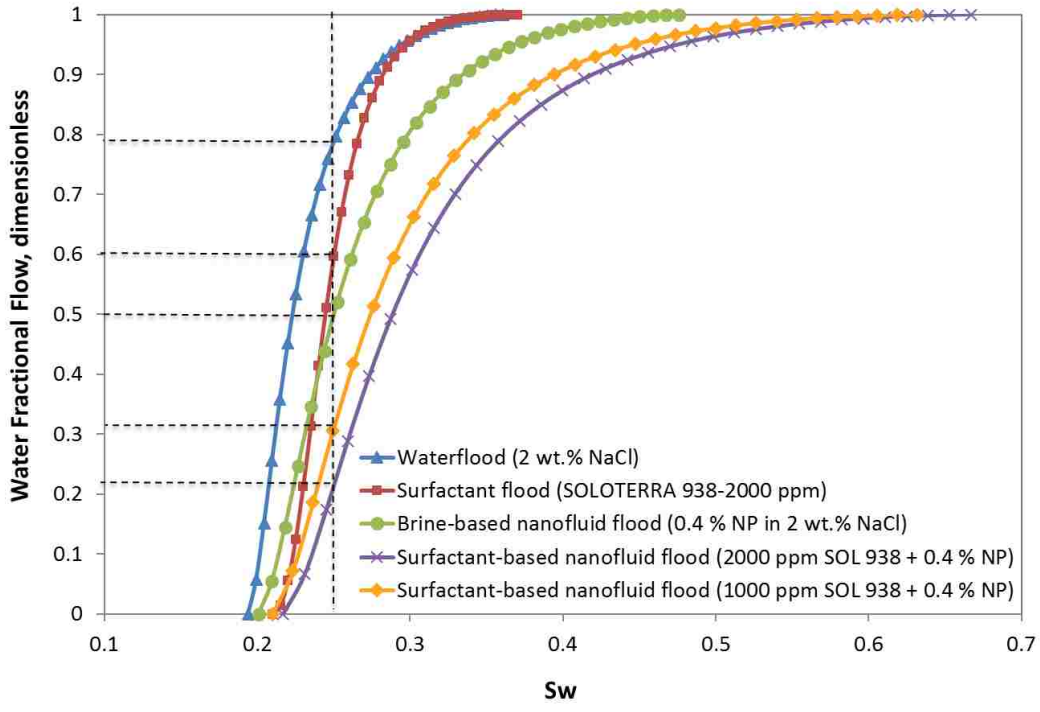

Figure 4.82. Water fractional flow curves for nanofluids made by the least effective surfactant at reservoir conditions (700 psi & 150 ˚F).

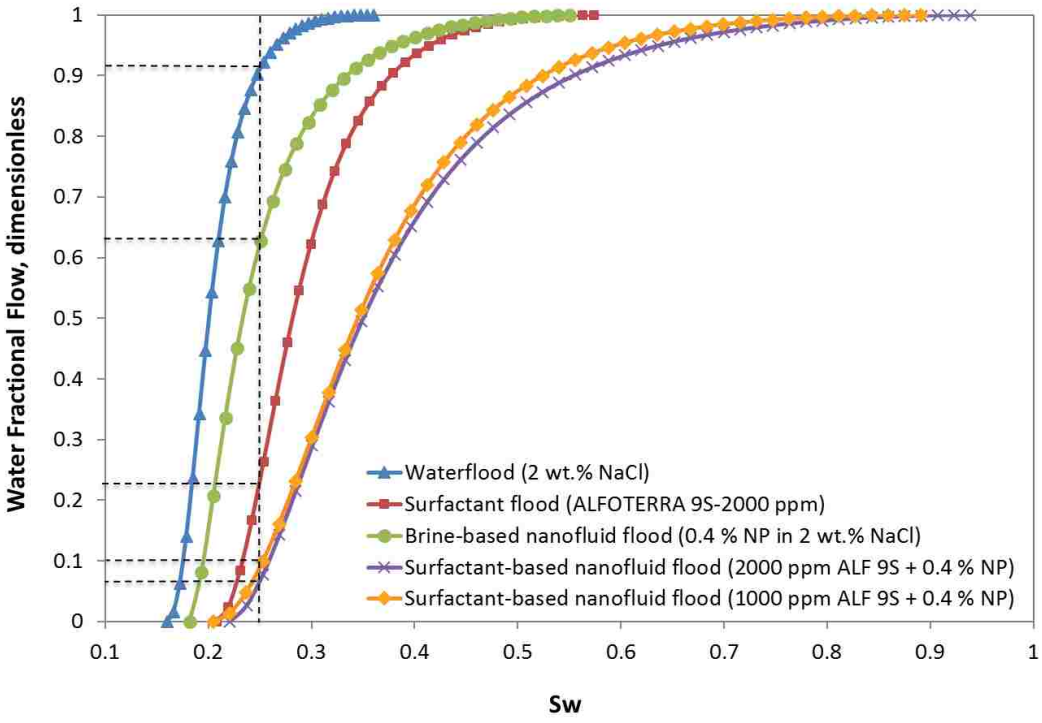

Figure 4.83. Water fractional flow curves for nanofluids made by the most effective surfactant at 500 psi and 72 ˚F.

4.3.6. Summary

Figures 4.84 to 4.86 show bar charts summarizing the coreflood results for each fluid along with their respective interfacial tension values and contact angle measurements. The waterfloods (brine) at both experimental conditions resulted in a low recovery and high contact angle representing the strongly oil-wet initial condition of the limestone cores. Using only nanoparticles in brine slightly lowered the contact angle and increased the recovery at both experimental conditions which led to an alteration in wettability from strongly oil-wet to weakly oil-wet. The least effective surfactants at both experimental conditions also failed in significantly improving the oil recovery and altering the wettability. However, the most effective surfactant resulted in a high recovery and change of wettability to intermediate-wet condition. The poor performance of the least-effective surfactants was enhanced by adding nanoparticles to result in a change of wettability to intermediate-wet zone

and an improvement in recovery of almost 30% incremental at both experimental conditions. Adding nanoparticles to the most effective surfactant also resulted in 44.5% incremental increase in recovery and wettability alteration to intermediate-wet condition. This enhancement was mostly due to the presence of nanoparticles, since the system stayed at the intermediate-wet zone (for both the least and most effective surfactants) leading to a high oil recovery even after reducing the surfactant concentration. Table 4.41 also lists the results at different experimental conditions along with their specific wettability alteration behavior. Rows 3 to 5 are showing the results from the least effective surfactant and rows 6 to 8 are related to the results from the most effective surfactant.

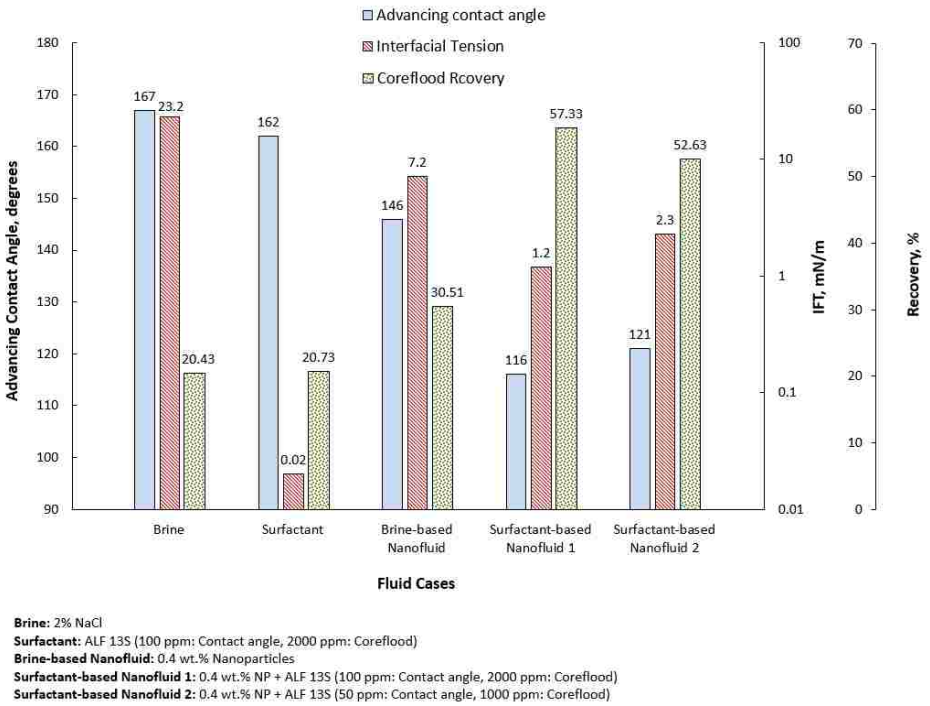

Figure 4.84. Comparison of IFT, contact angle measurements at ambient conditions and coreflood recovery values at 500 psi and 72 ˚F for surfactant-based nanofluids made by the least effective surfactant (ALF 13S).

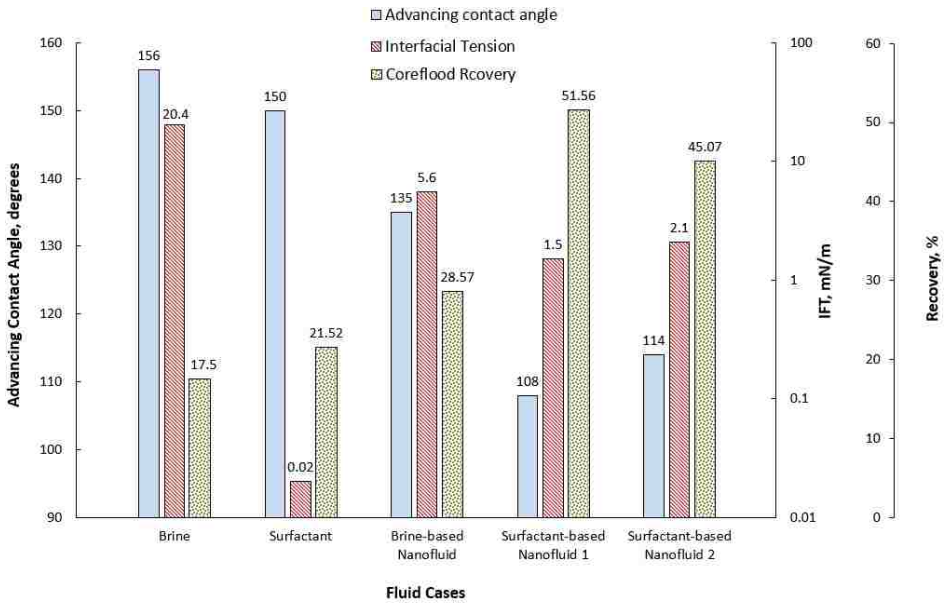

Figure 4.85. Comparison of IFT, contact angle measurements at reservoir conditions and coreflood recovery values at 700 psi and 150 ˚F for surfactant-based nanofluids made by the least effective surfactant (SOL 938).

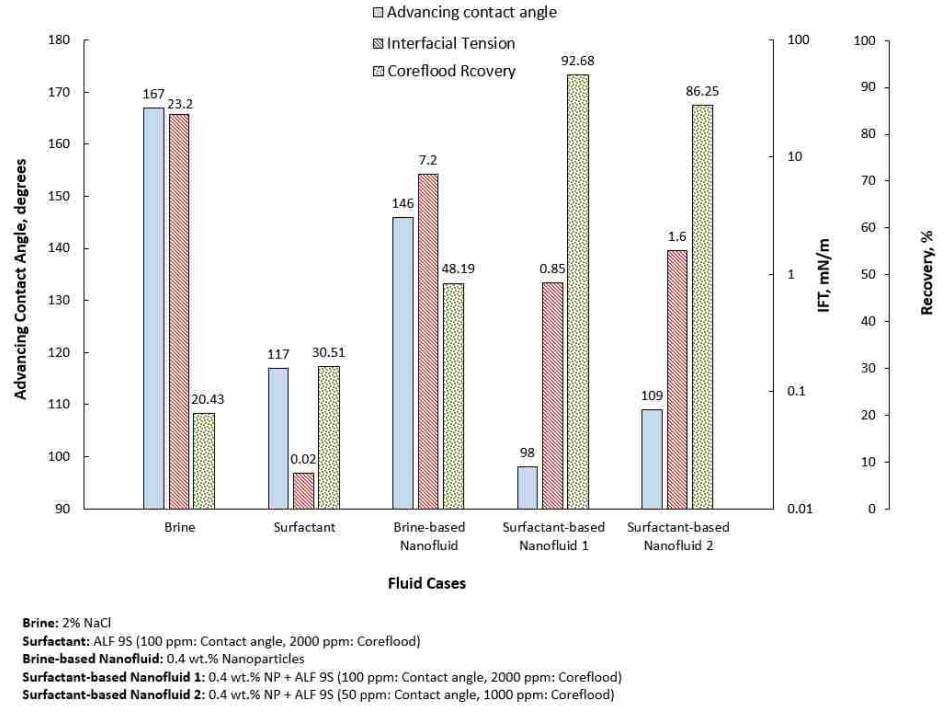

Figure 4.86. Comparison of IFT, contact angle measurements at ambient conditions and coreflood recovery values at 500 psi and 72 ˚F for surfactant-based nanofluids made by the most effective surfactant (ALF 9S).

Table 4.41. Summary of the coreflood results and contact angle measurements using nanofluids at both experimental conditions.

No.	Solution Type	Composition	Coreflood Experimental Conditions	Coreflood Recovery (%)	IFT (mN/m)	Contact Angle Measurements (degrees)	Wettability Alteration Behavior
1	Brine	2 wt.% NaCl	500 psi & 72 °F	20.43	23.2	167*	Strongly oil-wet
2	Brine-based nanofluid	0.4 wt.% Nanoparticles	500 psi & 72 °F	30.51	7.2	146*	Weakly oil-wet
3	Surfactant	ALFOTERRA S23-13S 90 (2000 ppm)	500 psi & 72 °F	20.73	0.02	162*	Strongly oil-wet
4	Surfactant-based nanofluid 1	0.4 wt.% Nanopartciles + ALFOTERRA S23-13S 90 (2000 ppm)	500 psi & 72 °F	57.33	1.2	116*	Intermediate-wet
5	Surfactant-based nanofluid 2	0.4 wt.% Nanopartciles + ALFOTERRA S23-13S 90 (1000 ppm)	500 psi & 72 °F	52.63	2.3	121*	Intermediate-wet
6	Surfactant	ALFOTERRA S23-9S 90 (2000 ppm)	500 psi & 72 °F	48.19	0.02	117*	Intermediate-wet
7	Surfactant-based nanofluid 1	0.4 wt.% Nanopartciles + ALFOTERRA S23-9S 90 (2000 ppm)	500 psi & 72 °F	92.68	0.85	98*	Intermediate-wet
8	Surfactant-based nanofluid 2	0.4 wt.% Nanopartciles + ALFOTERRA S23-9S 90 (1000 ppm)	500 psi & 72 °F	86.25	1.6	109*	Intermediate-wet
9	Brine	2 wt.% NaCl	700 psi & 150 °F	17.5	20.4	156**	Strongly oil-wet
10	Surfactant	SOLOTERRA 938 (2000 ppm)	700 psi & 150 °F	21.52	0.02	150**	Strongly oil-wet
11	Brine-based nanofluid	0.4 wt.% Nanopartciles	700 psi & 150 °F	28.57	5.6	135**	Weakly oil-wet
12	Surfactant-based nanofluid 1	0.4 wt.% Nanopartciles + SOLOTERRA 938 (2000 ppm)	700 psi & 150 °F	51.56	1.5	108**	Intermediate-wet
13	Surfactant-based nanofluid 2	0.4 wt.% Nanopartciles + SOLOTERRA 938 (1000 ppm)	700 psi & 150 °F	45.07	2.1	114**	Intermediate-wet

Least effective surfactant

Most effective surfactant

* Contact angle measurements at ambient conditions

** Contact angle measurements at reservoir conditions (700 psi & 150 °F)

Table 4.42 lists the experimental and simulated endpoints for all the corefloods at both experimental conditions. The residual oil saturation values for different cases can reveal the level of shift-to-right in relative permeability curves and comparatively show how efficient each fluid acts in terms of wettability alteration. In general, however, the comparison of experimental and simulated values can show how accurate the model is to estimate the relative permeability curves and determine the flow characteristics of the system.

Table 4.42. Summary of the experimental and simulation endpoints of the corefloods using nanofluids at both experimental conditions.

	Experimental				Simulation				
	Siw	Sor	Krw	Kro	Siw	Sor	Krw	Kro	
Corefloods at 500 psi and 72 °F	0.170	0.660	0.450	0.390	0.160	0.644	0.466	0.381	Waterflood (2% NaCl)
	0.168	0.682	0.532	0.386	0.175	0.656	0.549	0.410	Surfactant (ALF 13S, 2000 ppm)
	0.172	0.438	0.497	0.412	0.182	0.451	0.516	0.419	Brine-based nanofluid (0.4 wt.% NP in 2% NaCl)
	0.214	0.312	0.637	0.482	0.193	0.314	0.619	0.467	Surfactant-based nanofluid (0.4 wt.% NP+ALF 13S, 2000 ppm)
	0.201	0.342	0.645	0.447	0.182	0.339	0.621	0.436	Surfactant-based nanofluid (0.4 wt.% NP+ALF 13S, 1000 ppm)
	0.224	0.398	0.716	0.741	0.208	0.426	0.707	0.729	Surfactant (ALF 9S, 2000 ppm)
	0.235	0.088	0.684	0.733	0.221	0.061	0.730	0.790	Surfactant-based nanofluid (0.4 wt.% NP+ALF 9S, 2000 ppm)
	0.201	0.138	0.659	0.709	0.205	0.109	0.703	0.740	Surfactant-based nanofluid (0.4 wt.% NP+ALF 9S, 1000 ppm)
Corefloods at reservoir conditions (700 psi & 150 °F)	0.210	0.650	0.690	0.450	0.210	0.630	0.690	0.420	Waterflood (2% NaCl)
	0.207	0.645	0.701	0.543	0.218	0.639	0.717	0.562	Surfactant flood (SOL 938, 2000 ppm)
	0.212	0.508	0.597	0.489	0.223	0.524	0.611	0.505	Brine-based nanofluid flood (0.4 wt.% NP in 2% NaCl)
	0.225	0.335	0.420	0.321	0.217	0.333	0.442	0.294	Surfactant-based nanofluid (0.4 wt.% NP+SOL 938, 2000 ppm)
	0.201	0.378	0.437	0.238	0.210	0.368	0.417	0.255	Surfactant-based nanofluid (0.4 wt.% NP+SOL 938, 1000 ppm)

4.4. Discussion of potential mechanisms behind the observed wettability alteration and oil recovery enhancement

The application of nanoparticles dispersed in surfactants as wettability modifiers to enhance oil recovery especially in carbonate systems is still in its infancy. As mentioned in the literature review, previous researches showed that nanoparticles are mainly recognized by their high specific surface area. That means due to their nano-scale sizes, they have high ratio of surface area to volume. The great amount of surface area results in higher chances of interaction for nanoparticles in contact with rock and fluid surfaces in the medium. This makes nanoparticles active and energetic materials influenced by the Brownian motion and electrostatic repulsion. The Brownian motion is promoted by the random movement of numerous amount of extremely small particles in the fluid. The electrostatic repulsion of nanoparticles is related to their charges. The smaller the particles the higher the charge density and the larger electrostatic repulsion between the

nanoparticles (McElfresh et al., 2012). The combination of these two mechanisms helps the nanoparticles to raise the free energy of the system and significantly increase the surface activity, especially when they are dispersed in a solvent and in contact with a solid surface (Chengara et al., 2004). The surface activity of the nanoparticles is affected by their level of hydrophilicity. In the system of rock/oil/brine or rock/oil/surfactant, they could potentially be attached to the oil-water interface, absorbed on the rock surface, affiliated with surfactant molecules, or simply suspended inside the dispersion. Therefore, the type and concentration of nanoparticles, the type and concentration of surfactant, and the natural wettability of the rock play important roles in controlling the surface activity of the system. A better understanding of the surface activity could be achieved by comprehensively investigating the physio-chemical behavior of both nanoparticles and surfactant molecules and their interfacial interactions in contact with the rock surface.

On the other hand, nanoparticles have their own specific mechanism for spreading on solid surfaces (Wasan and Nikolov, 2003). Unlike the conventional theories for spreading behavior of a simple liquid on a solid surface, an increase in nanoparticles concentration or nanofluid viscosity results in an improvement in the spreading velocity of the nanofluid (Sefiane et al., 2008). When nanoparticles are confined in a space, they tend to order themselves in well-organized layers. This behavior increases the entropy of the whole suspension by allowing more freedom for the nanoparticles in the bulk volume (Wasan et al., 2011). This results in an extra pressure in the ordered layers compared to the bulk, which relates to the film thickness, diameter of the nanoparticles, and the distance from the wedge corner. This means that the magnitude of the extra pressure varies with the distance from the wedge corner, which generates a pressure gradient that drives the fluid motion into the wedge and makes the three-phase contact line at the wedge corner to move. This driving force that helps to separate the two surfaces (solid and oil), confining the

nanofluid, is called structural disjoining pressure gradient and known as the main mechanism for dynamic spreading of nanofluids over a solid surface. Chengara et al. (2008) suggested that the disjoining pressure is directly correlated with the spreading of nanofluid, which occurs due to the imbalance of interfacial forces at the oil/rock/nanofluid contact surface. With the forces focusing at the tip of the wedge area, the aqueous phase enters the highly confined space under the oil drop and dispersion of nanoparticles self-assemble as the wedge widens, which causes the oil phase to be displaced. However, in case of a strongly oil-wet system like Yates crude oil on limestone rocks of this research, the contact angles are so large that the wedge area is absent and the suggested mechanisms may not be sufficient to explain the observed changes in water-advancing contact angles. The following is believed to be the scenario behind the wettability alteration and oil recovery using the nanoparticles in a strongly oil-wet systems, such as Yates rock-fluid system.

A single nanoparticle applies an extremely weak force, but all the little particles together can create a great amount of force up to 7 psi as suggested by McElfresh et al. (2012). When the first few nanoparticles arrive at the three-phase contact point (Figure 4.87), there is no confined wedge area, under which they can form organized layers. But by increasing the concentration, more nanoparticles come to help to apply force on the contact point. Since nanoparticles tend to form ordered layers on the rock surface, the film of nanoparticles (ordered in lines at the three-phase contact line) is believed to act like a "sharp scraper" to remove a stain from a surface. At the same time, some nanoparticles are attached at the interface of oil/brine and reduce the interfacial tension. This reduction in oil-water interfacial tension, either by nanoparticles or by surfactant or both, could dislodge some of the oil from the solid surface at the three-phase contact line, which in turn could enable nanoparticles to get in-between the oil-water interface and solid-water interface. This could perhaps explain the change in contact angles observed. All these mechanisms

appear to be working together in changing the shape of the oil drop by lowering the contact angle (as shown in Figure 4.87), rather than needing a wedge region for nanoparticles to accumulate.

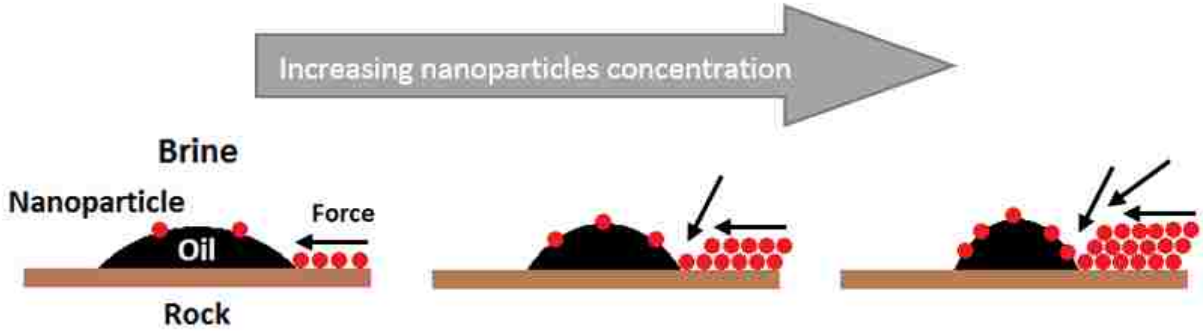

Figure 4.87. Schematic of wettability alteration using nanoparticles in a strongly oil-wet system.

This research showed that the increase of nanoparticles concentration resulted in lowering the contact angle and interfacial tension, when there were only nanoparticles (with no surfactant) in the system. It appears that, both natural tendency of nanoparticles to form organized layers and lowering the interfacial tension at the oil/nanofluid surface helps to gradually lift the oil drop and lower the contact angle. This scenario seems to be stimulated by higher concentration of nanoparticles, as it becomes easier to lift the oil and form organized layers with more nanoparticles under the disjoining pressure gradient mechanism.

Removing the oil by forming layers of the hydrophilic silica nanoparticles on the rock surface results in a wettability alteration toward less oil-wet. The higher the concentration of nanoparticles the higher the free energy in the system the more chances for particles to energetically act under the Brownian motion and electrostatic repulsion to apply force at the contact point to lift the oil drop. At the same time, the more nanoparticles the higher surface activity or the higher chances of attaching at the surface of oil/nanofluid to reduce the interfacial

tension to help lifting the oil drop. When surfactant molecules are also in the system, it seems like the increase of surface activity is more dominantly handled by surfactants, so more nanoparticles can join in applying force at the three-phase contact point to more easily lower than contact angle and eventually remove the oil. This is also confirmed by this research as the combination of surfactants and nanoparticles (surfactant-based nanofluids) performed better in lowering the contact angle and changing the wettability of the system toward less oil-wet to improve the oil recovery. It seems like the free energy of nanoparticles plus the surface activity of surfactants perfectly worked together in this research to enhance the oil recovery of carbonate rocks through wettability alteration.

The results from this research suggested that silica nanoparticles can improve the performance of certain surfactants in altering the wettability of the carbonate system toward less oil-wet and eventually reduce the residual oil saturation to enhance oil recovery. The nanoparticles, by themselves, changed the wettability of the system toward less oil-wet by partially lowering the interfacial tension (higher surface activity) and applying disjoining pressure at the three-phase contact point (higher free energy). This behavior was intensified by increasing the concentration of nanoparticles. The results showed that 0.1% of nanoparticles lowered the contact angle only from 167° to 165° and the interfacial tension from 23.2 mN/m to 13.1 mN/m, meaning that the free energy in the system was not enough to lower the contact angle by applying force at the contact point and the surface activity was not high enough to help with the lifting. However, a higher concentration of nanoparticles (0.4%) increased the free energy to apply more force at the contact point, which led to lowering the contact angle to 146°. It also raised the surface activity enough to lower the interfacial tension to 7.2 mN/m and help with lifting the oil drop more easily. Once nanoparticles were combined with the most effective surfactant, it is believed that the surface

activity of the system was mainly increased by the surfactant, while the nanoparticles had more freedom to increase the energy of the system and apply more force at the contact point. As a result, the contact angle was lowered to 98° and interfacial tension to 0.85 mN/m, representing an intermediate-wet condition.

Additionally, based on precise contact angle measurements and relative permeability curves resulting from coreflood experiments, it was shown that nanoparticles could compensate for surfactants. Therefore, in the combination of nanoparticles and surfactant (surfactant-based nanofluids), lowering the concentration of surfactant would not significantly change the wettability alteration behavior of the system. Using the analogy mentioned above, this means that performance of ordered nanoparticles films acting like a "sharp scraper" is more dominant in changing the wettability of the system and removing the oil than that of surfactant acting like a "detergent". Therefore, it seems like only a small rise in the surface activity of the system by surfactant is enough, since the major part of the wettability alteration job is being done by the increase in free energy and the disjoining pressure gradient using nanoparticles.

Based on the literature review and results of this research, it seems like the interfacial properties of the surfactant-based nanofluids are influenced by the combined impact of two main mechanisms, including the interfacial tension reduction ability of surfactants and specific spreading behavior of nanoparticles. The results of this research showed that the combination of surfactants and nanoparticles would not significantly reduce the interfacial tension in the system, unlike using only surfactant. The most effective surfactant lowered the interfacial tension from 23.2 mN/m to 0.02 mN/m, while the interfacial tension resulting from the combination of surfactant and nanoparticles was 0.85 mN/m. It is believed that there are some interactions between the surfactant molecules and nanoparticles, which stop some of the surfactant molecules from

attaching to the oil/nanofluid interface to drastically reduce the interfacial tension. Moreover, some of the nanoparticles might place themselves in between the surfactant molecules at the oil/nanofluid interface, which could cause the interfacial tension not to drop significantly. Further inter-molecular investigation is needed to microscopically study the interaction of nanoparticles with surfactant molecules at the three-phase contact line.

On the other hand, the combination of surfactant and nanoparticles lowered the contact angle and altered the wettability toward intermediate-wet, which consequently increased the ultimate oil recovery. In case of combining the most effective surfactant with nanoparticles, the contact angle was lowered to 98°, leading to a high recovery of about 93%. So the combination did not considerably lower the interfacial tension but it significantly lowered the contact angle and changed the wettability of the system to intermediate-wet condition. Therefore, working with the combination of surfactant and nanoparticles, it appears that the rock-fluid interactions (promoted by the structural disjoining pressure gradient applied by the ordered layers of nanoparticles) are more dominated by energetic nanoparticles, while only a slight reduction in interfacial tension (or increase in surface activity) is required by the diluted surfactant.

Another possible mechanism of wettability alteration using nanoparticles could be postulated by looking into the roughness of the rock surface. The rocks used in this research are limestone rocks, mainly composed of calcite. Vijapurapu & Rao (2003) characterized the surface roughness of different rock samples using optical profilometer and SEM images. They used the similar procedure for cutting and cleaning the samples and the same polishing techniques and materials as used in this research to smoothen the rock surfaces (240 grit size). Their results showed that calcite surface roughness varied between 1.17 μm for a smooth and 5.46 μm for a roughened surface. The silica nanoparticle used in this research are 30 nm, indicating that they are

three orders of magnitudes smaller than the average surface roughness. Therefore, there could be a possibility for nanoparticles to seep into the solid surface asperities, caused by the surface roughness, at the three-phase contact point and thereby dislodge the oil from the surface even in the strongly oil-wet systems like this research. As discussed in section 4 (Figure 4.23), contact angle of the strongly oil-wet system of limestone/Yate-oil/NaCl started to change, even by introducing 0.1 wt.% and 0.2 wt.% nanoparticles, from 167° to 165° and 156° respectively. The optimum concentration of nanoparticles (0.4 wt.%) lowered the contact angle to 146°. Therefore, it seems, even at low concentrations, the nanoparticles could potentially find their way to underneath the oil at the three-phase contact line through asperities of the rough surface and lower the contact angle and dislodge the oil. Further work is needed to confirm these proposed mechanisms of wettability alteration by surfactant-based nanofluids.

Based on the literature review and results of this research, the suggested mechanisms show how nanoparticles and surfactants could potentially work together for changing the wettability of a carbonate system toward less oil-wet or intermediate-wet and reduce the residual oil saturation, mainly due to the disjoining pressure gradient of nanoparticles and also the interfacial activity of surfactant molecules. Therefore, the combination of surfactant and nanoparticles would potentially lower the necessity of surfactant adsorption on the rock surface, which could eventually make the surfactant-based nanofluid an economically attractive agent for enhancing oil recovery in carbonate reservoirs.

4.5. Preliminary economic considerations

Silica nanoparticles are naturally abundant, environmentally friendly, and financially cost-effective compared to surfactants. This research was aimed at investigating the potential of nanoparticles to enhance surfactants performance for improving the oil recovery through

wettability alteration. For a detailed cost analysis in the field scale, major parameters such as production history, production rate, surfactant concentration, facilities and operation costs, saving on handling the produced water, and many other factors are required.

The following preliminary analysis is based on material balance calculations for waterflood, optimum brine-based nanofluid solution, optimum surfactant solution, and the optimum surfactant-based nanofluid made by the combination of most effective surfactant with optimum concentration of nanoparticles.

The typical limestone cores in this study had pore volume of about 100 cc and initial water saturation of about 20%. Let's assume that the reservoir to which we plan to apply chemical flooding has a pore volume of about 100,000 bbl. Using the same initial water saturation, the original oil in place (OOIP) of the reservoir will be as follow:

OOIP ($S_{wi} = 0.2, B_o = 1\ STB/bbl$):

$$OOIP = 100{,}000 \times (1 - 0.2) = 80{,}000\ STB$$

Based on the residual oil saturation values resulted from the corefloods of this research, the oil recovered from the reservoir after waterflood and each chemical flooding applied as a secondary recovery method will be estimated as follow:

Oil recovered after waterflood ($S_{or} = 0.6$):

$$WF\ Recovery = 100{,}000 \times (1 - 0.2 - 0.66) = 14{,}000\ STB$$

Oil recovered after using ALFOTERRA S23-9S (2000 ppm) for surfactant flood ($S_{or} = 0.26$):

$$SF\ Recovery = 100{,}000 \times (1 - 0.2 - 0.37) = 43{,}000\ STB$$

Oil recovered after using optimum (0.4 wt.%) brine-based nanofluid ($S_{or} = 0.45$):

$$NF\ Recovery = 100{,}000 \times (1 - 0.2 - 0.45) = 35{,}000\ STB$$

Oil recovered after using surfactant-based nanofluid made by the combination of 2000 ppm surfactant and 0.4 wt.% nanoparticles ($S_{or} = 0.05$):

$$SN\ Recovery = 100{,}000 \times (1 - 0.2 - 0.06) = 74{,}000\ STB$$

Oil recovered after using surfactant-based nanofluid made by the combination of 1000 ppm surfactant and 0.4 wt.% nanoparticles ($S_{or} = 0.11$):

$$SN\ Recovery = 100{,}000 \times (1 - 0.2 - 0.11) = 69{,}000\ STB$$

Let's assume 2 pore volume of surfactant solution at 2000 ppm is injected to reach the residual oil saturation of 0.25. Therefore, the surfactant consumption will be as follow:

$$SF\ consumption$$
$$= (2 \times 100{,}000\ bbl) \times (159\ litres/bbl) \times (2000\ mg/litres)$$
$$\times (2.2 \times 10^{-6}\ lbs/mg) = 139{,}920\ lbs$$

Cost of surfactants depends on a variety of factors such as chemical structure of the surfactant, oil price, manufacturer, operating facilities, etc. However, it is typically between \$0.5 to \$2.00 per lb (Thomas et al., 2001). If an average surfactant cost of \$1.25 per lb is used, the cost of consumed surfactant for the reservoir will be:

$$Cost\ of\ Consumed\ SF = 139{,}920\ lb \times 1.25\ \$/lb = \$174{,}900.00$$

Similarly, if 2 pore volume of brine-based nanofluid (prepared by adding 0.4 wt.% nanoparticles to brine) is injected to reach the residual oil saturation of 0.45, the brine-based nanofluid consumption will be as follow:

$$NF\ consumption$$

$$= (2 \times 100{,}000\ bbl) \times (159\ litres/bbl) \times (4000\ mg/litres)$$

$$\times (2.2 \times 10^{-6}\ kg/mg) = 279{,}840\ lb$$

Cost of nanoparticles also depends on many factors including the type of nanoparticles, the hydrophilicity nature of nanoparticles, the coating that controls the applicability of nanoparticles, the manufacturer, etc. Silica nanoparticles which were used in this research can be purchased on Internet for $700 per Metric Tons. Therefore, the cost of consumed surfactant-based nanofluid for the reservoir becomes:

$$Cost\ of\ Consumed\ NF = (279{,}840\ lb) \times (0.0004536\ \ Tons/lb \times \$700/Tons)$$

$$= \$88{,}853.43$$

Finally, if 2 pore volume of surfactant-based nanofluid (combination of 2000 ppm surfactant and 0.4 wt.% nanoparticles) is injected to reach the residual oil saturation of 0.1, the surfactant-based nanofluid consumption will be as follow:

$$SN\ consumption$$

$$= (2 \times 100{,}000\ bbl) \times (159\ litres/bbl) \times (6000\ mg/litres)$$

$$\times (2.2 \times 10^{-6}\ lb/mg) = 419{,}760\ lb$$

And in the case of using 1000 ppm surfactant to combine with 0.4 wt.% nanoparticles will be:

$$SN\ consumption$$

$$= (2 \times 100{,}000\ bbl) \times (159\ litres/bbl) \times (5000\ mg/litres)$$

$$\times (2.2 \times 10^{-6}\ kg/mg) = 349{,}800\ lb$$

Therefore, the cost of consumed surfactant-based nanofluid for the reservoir will be:

$$Cost\ of\ Consumed\ SN$$

$$= \left(419{,}760\ lb \times \frac{1}{3}\right) \times (\$1.25/lb)$$

$$+ \left(419{,}760\ lb \times \frac{2}{3}\right) \times (0.0004536\ Tons/lb \times \$700/Tons) = \$263{,}753.43$$

And in the case of using 1000 ppm surfactant to combine with 0.4 wt.% nanoparticles will be:

$$Cost\ of\ Consumed\ SN$$

$$= \left(349{,}800\ lb \times \frac{1}{5}\right) \times (\$1.25/lb)$$

$$+ \left(349{,}800\ lb \times \frac{4}{5}\right) \times (0.0004536\ Tons/lb \times \$700/Tons) = \$176{,}303.43$$

Assuming the conservative oil price of $65 per bbl, the income from the incremental oil recovery due to the surfactant flood will be:

$$SF\ Income = (SF\ Recovery - WF\ Recovery) \times Oil\ Price = (43{,}000 - 14{,}000) \times 65$$

$$= \$1{,}885{,}000.00$$

The income from the incremental oil recovery due to the brine-based nanofluid flood will be:

$$NF\ Income = (NF\ Recovery - WF\ Recovery) \times Oil\ Price = (35{,}000 - 14{,}000) \times 65$$

$$= \$1{,}365{,}000.00$$

The income from the incremental oil recovery due to the injection of surfactant-based nanofluid will be:

$$SN\ Income = (SN\ Recovery - WF\ Recovery) \times Oil\ Price = (74{,}000 - 14{,}000) \times 65 =$$

$3,900,000.00

And in the case of using 1000 ppm surfactant to combine with 0.4 wt.% nanoparticles will be:

$$SN\ Income = (SN\ Recovery - WF\ Recovery) \times Oil\ Price = (69{,}000 - 14{,}000) \times 65 =$$

$3,575,000.00

Finally, the net profit per bbl of incremental oil recovered due to the surfactant flood will be:

$$SF\ Profit = (SF\ Income - Cost\ of\ Consumed\ SF)/SF\ Recovery$$

$$= (\$1{,}885{,}000.00 - \$174{,}900.00)/29{,}000 = \$58.97\ per\ bbl$$

The net profit per bbl of incremental oil recovered due to the brine-based nanofluid flood will be:

$$NF\ Profit\ (NF\ Income - Cost\ of\ Consumed\ NF)/NF\ Recovery$$

$$= (\$1{,}365{,}000.00 - \$88{,}853.43)/21{,}000 = \$60.77\ per\ bbl$$

The net profit per bbl of incremental oil recovered due to the injection of surfactant-based nanofluid will be:

$$SN\ Profit = (SN\ Income - Cost\ of\ Consumed\ SN)/SN\ Recovery$$

$$= (\$3{,}900{,}000.00 - \$263{,}753.00)/55{,}000 = \$60.60\ per\ bbl$$

And in the case of using 1000 ppm surfactant to combine with 0.4 wt.% nanoparticles will be:

$$SN\ Profit = (SN\ Income - Cost\ of\ Consumed\ SN)/SN\ Recovery$$

$$= (\$3{,}575{,}000.00 - \$176{,}303.00)/50{,}000 = \$61.79\ per\ bbl$$

Therefore, the preliminary cost analysis, which is summarized in Table 4.43, indicates the positive economics of combining nanoparticles with surfactants to improve oil recovery. Note that, further comprehensive economic considerations are required for field implementation.

Table 4.43. Summary of preliminary economic considerations.

Pore Volume:	100,000	bbl	Surfactant Price:	1.25	$/lb
Bo:	1	STB/bbl	Nanoparticle Price:	700.00	$/Tons
Siw:	0.2		Oil Price:	65.00	$/bbl
OOIP:	80,000	bbl			

	Waterflood	Surfactant Flood (2000 ppm)	Brine-based Nanofluid (0.4 % NP)	Surfactant-based Nanofluid (0.4 % NP+2000 ppm Surf)	Surfactant-based Nanofluid (0.4 % NP+1000 ppm Surf)
Ultimate Residual Oil Saturation	0.66	0.43	0.45	0.06	0.11
Oil Recovered (bbl)	14,000	37,000	35,000	74,000	69,000
Incremental Oil Recoevry (bbl)	-	23,000	21,000	60,000	55,000
Income from Incremental Oil Recovery	-	$1,495,000.00	$1,365,000.00	$3,900,000.00	$3,575,000.00
Cunsumption (lb)	-	139,920	279,840	419,760	349,800
Cost of Consumption	-	$174,900.00	$88,853.43	$263,753.43	$176,303.43
Profit per bbl	-	$57.40	$60.77	$60.60	$61.79

4.6. Microscopic investigation

This section attempts to visualize the actual impacts of nanoparticles and their combination with surfactants on the wettability behavior of the carbonate rock at the microscopic level. The following is the extent of what has been done toward that goal at the Louisiana State University's Center for Advanced Microstructures and Devices (CAMD). To achieve a better understanding of the microscopic behavior of the system, however, further systematic investigation is required.

First set of tests were conducted using CAMD Tomography Beam Line with the following specifications:

- X-ray Energy: 38keV
- Interferometry Imaging: 3rd Talbot distance 524 mm used between Gratings
- Scattering length: 1.3µm
- Two rock samples: Clean rock and rock with oil
- Grating orientation: Vertical
- Spatial resolution: ~15µm with 4x4 binning on camera

Figure 4.88 compares the X-ray absorption in the rock (Indiana limestone) when it is clean on the left and after exposure to oil (Yates crude oil) and surfactant-based nanofluid (0.4 wt.% nanoparticles with 2000 ppm ALFOTERRA S23-13S) on the right. The images suggest that rock with oil shows more X-ray absorption than the clean rock representing more pores inside the rock.

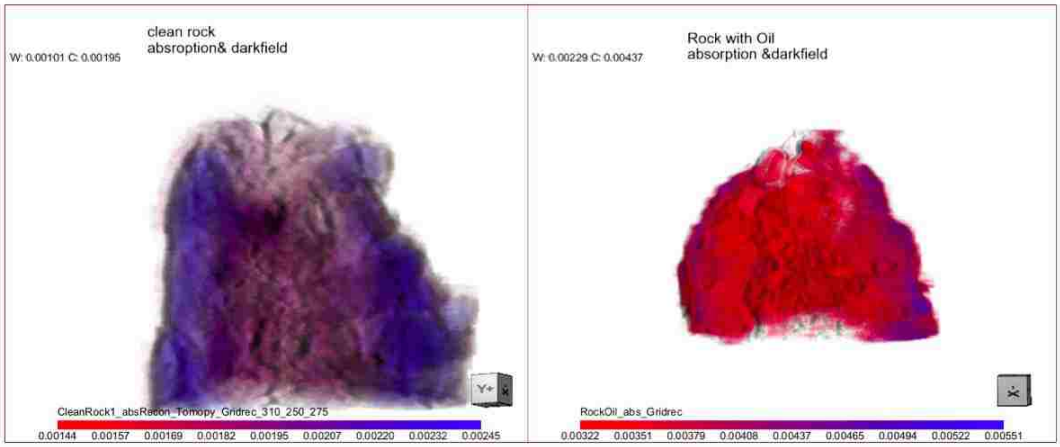

Figure 4.88. X-ray adsorption in the rock before (left) and after exposing to oil and surfactant-based nanofluid (right).

This phenomenon can also be observed in Figure 4.89, where absorption and dark-field images are shown in the same cross-section. In the dark-field images, the colorless regions show lower density while the darker color shows larger density changes, when compared to the absorption image. Dark-field images can visualize more details. The pores are more clearly seen when the oil is present due to the higher density oil in them. Unlike those expected in sandstones between grains, the pores appear to be cracks.

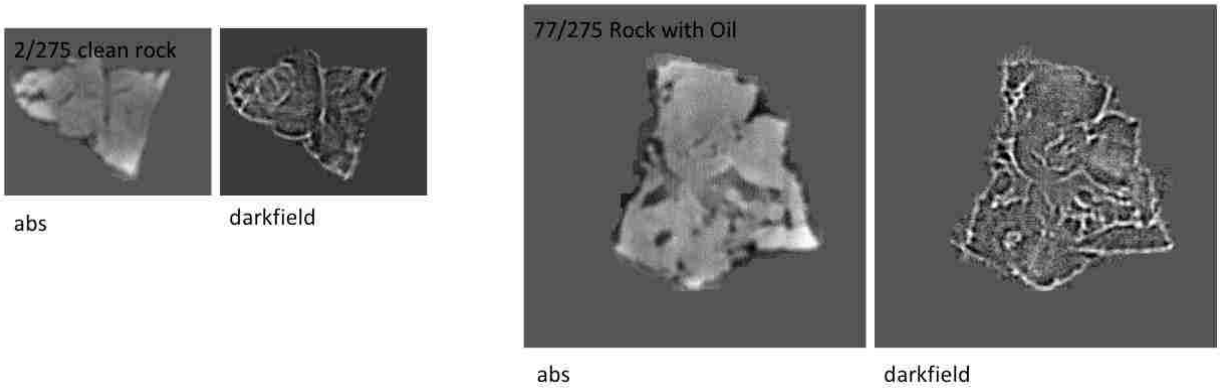

Figure 4.89. Absorption and dark-field images of the rock before (left) and after exposing to oil and surfactant-based nanofluid (right).

The second set of tests is on detecting the sulfur species in the system. Figure 4.90 describes the sulfur species in the Yates crude oil, clean Indiana limestone rock, the most effective surfactant (ALFOTERRA S23-9S), and the rock after exposure to oil and surfactant-based nanofluid. The results suggest that the special sulfur species in the crude oil is not observed in the rock after exposure to oil and surfactant-based nanofluid.

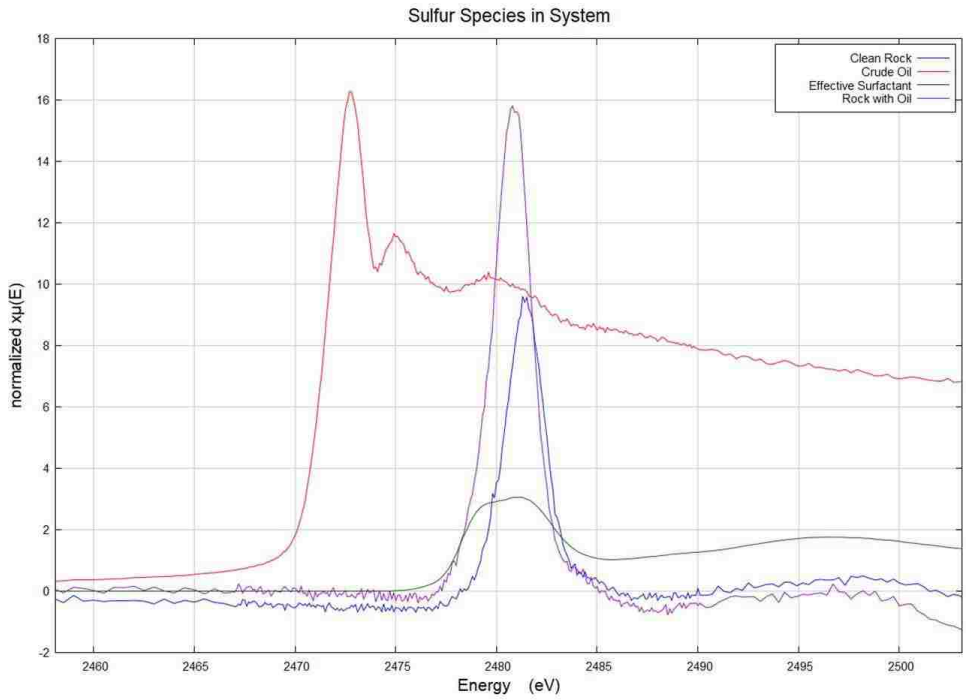

Figure 4.90. Detection of sulfur species in the system.

The sulfur species peak seen in crude oil is from dibenzothiophene. The amount of dibenzothiophene in crude oil ranges from a few tenths to a few percent. The sulfur species present in the clean rock is some form of sulfate and the surfactant has sulfonate. The sulfur peak location in the extracted rocks suggests that the sulfur species are both sulfonate and sulfate. There is no detectable dibenzothiophene in the rock, however, suggesting its removal during the extraction process.

5. CONCLUSIONS AND RECOMMENDATIONS

The goal of this research was to investigate the potential of nanoparticles and their combination with surfactants to enhance oil recovery through wettability alteration in carbonate rocks. Wettability was quantified by contact angle measurements at both ambient and reservoir conditions and coreflood experiments at different experimental conditions. The relative permeability curves, generated by the numerical simulation of corefloods, were studied to see how the ability of surfactants as wettability modifiers could be improved by adding nanoparticles. A potential that could lead to a significant reduction in the residual oil saturation in the carbonate reservoirs makes the surfactant-based nanofluid technology an economically appealing enhanced oil recovery method.

5.1. Conclusions

The following summarizes the most significant findings of this work:

- Surfactants can be chemically structured to serve any certain experimental or field purposes. In general, surfactants can enhance oil recovery by reducing the interfacial tension and altering the wettability of the system. The level of hydrophobicity/hydrophilicity of a surfactant, which can be managed through designing the number of PO and EO units (Propylene Oxide and Ethylene Oxide) in the structure, determines the performance of a surfactant as an interfacial tension and wettability modifier. Because reducing the interfacial tension, as the main role of surfactants, is typically costly due to the huge amount of required surfactant, this study focusses on the role of surfactant as a wettability modifier. Altering the wettability toward less oil-wet behavior results in lowering the residual oil saturation and consequently improves the oil recovery. Surfactants have different capabilities to change the wettability of a system.

Among the available surfactants in this research, only a few worked in favor of wettability alteration in the specific rock/oil/brine system. Finally, 4 surfactants (designed for low temperatures) at 500 psi and 72 ˚F and 2 surfactants (designed for high temperatures) for reservoir conditions (700 psi and 150 ºF) were evaluated using the system of Indiana limestone as the rock, Yates dead crude oil as the oil, and 2 wt.% NaCl as the brine.

- In order to change the wettability of the strongly oil-wet system toward less oil-wet, ALFOTERRA S23-9S 90 was selected as the best case to change the dynamic water advancing contact angle from 152° to 90° or from strongly oil-wet to intermediate-wet zone. The contact angle measurements (Gupta, 2016) agreed well with the coreflood experiment results of this research, as it generated the greatest shift-to-right in the relative permeability curves. On the other hand, ALFOTERRA S23-13S 90 was selected as the worst case to change the dynamic water advancing contact angle (no change at all). This surfactant did not also generate any shift-to-right in the relative permeability curves. Therefore, for the purpose of this research, the worst surfactant was selected as the candidate to discover whether its poor performance can be improved by nanoparticles.
- CMG STARS is used to model the flow in the core and generate relative permeability curves to evaluate the oil-water flow characteristics of the system. After history matching the experimental oil recovery and pressure drop data using CMG STARS, another software from CMG package, namely CMOST, was used for optimization to achieve the most possible accurate estimates for relative permeability endpoints and consequently the relative permeability curves. The accurate estimation of relative permeability curves provided the opportunity to profoundly study the level of shift-to-right and thus the ability of each composite solution to change the wettability of the system.

- Nanoparticles showed a great potential for enhancing oil recovery through wettability alteration in carbonate rocks. Through interfacial tension and contact angle measurements on brine-based nanofluids, this study verified that the higher concentration of nanoparticles generated lower water advancing contact angles without significantly lowering the interfacial tension, unlike surfactant solutions. This trend was only investigated within a certain range of nanoparticles concentrations (0.1 wt.% to 0.8 wt.%). In this work, silica nanoparticles dispersed in brine could change the wettability of the limestone/Yates-oil/NaCl system from strongly oil-wet to weakly oil-wet. The optimum concentration of brine-based nanofluid was found to be 0.4 wt.%, as it lowered the contact angle from 167° to 146° and the interfacial tension from 23.2 mN/m to 7.2 mN/m at ambient conditions. The advantage of using inexpensive environmentally friendly nanoparticles is revealed when compared to using huge amounts of costly chemically structured surfactants to reduce interfacial tension and change wettability.
- The optimum concentration of nanoparticles for changing the wettability of the system greatly improved the performance of the surfactant candidates at ambient conditions. While the least effective surfactant solution did not change the strongly oil-wet behavior of the system, its combination with nanoparticles lowered the water advancing contact angle from 162° to 116°, moving from strongly oil-wet to intermediate-wet. The surfactant-based nanofluid lowered the interfacial tension only to 1.2 mN/m. This reveals a potential to avoid using a huge amount of chemical solutions to lower the interfacial tension, while a surfactant/nanoparticles combination can serve the purpose without having to significantly reduce the interfacial tension by focusing on the wettability alteration capabilities of nanoparticles. To verify this finding, the concentration of surfactant in the surfactant-based

nanofluid was lowered and the new composite solution showed nearly the same behavior, as it generated an advancing contact angle of 121°, still representing a nearly intermediate-wet behavior, and an interfacial tension of 2.3 mN/m.

- The combination of nanoparticles with the most effective surfactant also resulted in a great wettability alteration. The surfactant, itself, changed the angle from 167 to 117, shifting from strongly oil-wet to weakly intermediate-wet zone. Adding nanoparticles further lowered the contact angle to 98° representing the intermediate zone and resulted in generating an interfacial tension of 0.85 mN/m. When the concentration of surfactant was decreased in the surfactant-based solution, the system still showed intermediate-wet behavior with a contact angle of 109° and interfacial tension of 1.6 mN/m. This reveals the potential of effective surfactants to generate excellent wettability alteration toward less oil-wet condition after combination with nanoparticles. A potential that can significantly reduce the residual oil saturation in the reservoir.
- The impressive behavior of nanoparticles in changing the wettability of the carbonate system and enhancing the performance of surfactant were similarly repeated in high pressure/high temperature or reservoir conditions (700 psi and 150 ºF). The optimum concentration of nanoparticles, 0.4 wt.%, lowered the water advancing contact angle from 156° to 135° and the interfacial tension from 20.4 mN/m to 5.6 mN/m. The combination of nanoparticles with the surfactant that had not been able to significantly change the wettability of the system, lowered the contact angle of 150° to 108°, a complete transfer from strongly oil-wet zone to intermediate-wet zone. Moreover, nanoparticles seemed to compensate for surfactant, as reducing the surfactant concentration in the surfactant-based nanofluid did not significantly change its wettability alteration behavior. In general, the

high pressure/high temperature conditions seemed to affect the same system of limestone/Yates-oil/NaCl by making it less oil-wet. For instance, at initial condition, where there was only brine in the cell, the contact angle was 167° at ambient and 156° at reservoir conditions. For all the other composite solutions also, the contact angles were higher at ambient conditions than their respective cases at reservoir conditions.

- The coreflood experiments results, in general, agreed well with the contact angle measurements. It was found that there is a direct relation between a lower contact angle and a higher oil recovery. Any fluid system, in which the contact angle was lowered due to the wettability alteration and a shift-to-right in the relative permeability curves or water fractional flow curves was observed, resulted in a higher oil recovery. The brine at 500 psi and 72 ˚F, which described a strongly oil-wet behavior of the system by generating a high contact angle (167°), produced only a limited amount of oil (20% of the original oil in place) through waterflood and the subsequent relative permeability curves stayed in the oil-wet zone. The surfactant with the poor performance in changing the wettability (the least effective surfactant at 500 psi and 72 ˚F) also demonstrated similar behavior, meaning a high contact angle and low recovery along with the relative permeability curves showing an oil-wet behavior. However, as nanoparticles significantly lowered the contact angle, they were also able to generate a shift in the relative permeability curves to the right and boost up the recovery by 10% incremental, resulting in a 30% reduction in the residual oil saturation compared to the waterflood at 500 psi and 72 ˚F.
- The ability of nanoparticles to increase the surface activity and alter the wettability of the system toward less oil-wet could also significantly enhance the performance of surfactants in reducing residual oil saturation and increasing the oil recovery. The combination of

nanoparticles and the least effective surfactant (surfactant-based nanofluid) that showed a change of contact angle from 162° to 116°, meaning from strongly oil-wet to intermediate-wet zone, also generated a great shift-to-right in the relative permeability curves following a 57% recovery (almost 37% increase compared to the surfactant flood). The high recovery and great shift-to-right was not much affected even after 50% reduction of the surfactant concentration, since 53% of the original oil in place was recovered leading to about 32% reduction in the residual oil saturation compared to the surfactant flood. Therefore, nanoparticles seemed to be able to compensate for surfactant in changing the wettability of the system and enhance oil recovery.

- The combination of nanoparticles with the most effective surfactant also led to an improvement in the recovery, going from about 48% for the surfactant to about 93% for the surfactant-based nanofluid at 500 psi and 72 ˚F. This improvement was also observed in the water fractional flow curves generated using the simulated relative permeabilities as a great shift-to-right representing a huge wettability alteration in the system toward less oil-wet behavior and an excellent reduction of about 86% in the residual oil saturation. The reduction of surfactant concentration did not significantly affect the great performance of the surfactant-based nanofluid, as the resulting fractional flow curve stayed fairly close to the that of the nanofluid made with the higher surfactant concentration.
- Nanoparticles could enhance the oil recovery for the system of this research through wettability alteration at different experimental conditions. The brine, which generated a high contact angle of 156° representing a strongly oil-wet behavior, produced only 17.5% of the original oil in place through waterflood and the relative permeability curves stayed in the oil-wet zone. However, this study showed that brine-based nanofluids (without

surfactants), could improve the recovery about 10% and shift the relative permeability curves to the right resulting in almost 17% reduction in the residual oil saturation compared to the waterflood at reservoir conditions. The surfactant-based nanofluid that showed a change of contact angle from 150° to 108°, meaning from strongly oil-wet to intermediate-wet zone, also generated a great shift-to-right in the relative permeability curves following about 52% recovery (almost 30% increase compared to the surfactant flood). This trend continued even after 50% reduction in the surfactant concentration, since 45% of the original oil in place was recovered leading to about 42% reduction in the residual oil saturation compared to the surfactant flood. Therefore, for the specific system of this research, nanoparticles seemed to be able to compensate for surfactant in enhancing oil recovery through wettability alteration at both experimental conditions.

- Although the recoveries at reservoir conditions were not as high and the shift-to-right in the relative permeability curves were not as large as those at 500 psi and 72 ˚F, the great influence of the nanoparticles on the recovery through wettability alteration, alone and in combination with surfactant, was clearly observed. The system of Indiana limestone/Yates-oil/NaCl seemed to be more oil-wet at high temperature, most likely due to the higher level of oil/rock interaction. This was verified by looking at the positions of relative permeability curves and the values of residual oil saturation. Therefore, the composite solutions generated lower recoveries and smaller shifts at reservoir conditions (700 psi and 150 ºF) compared to respective cases at 500 psi and 72 ˚F.
- The goal of this research was successfully achieved by using the most reliable contact angle measurement technique and corefloods to show the potential of nanoparticles to improve the ability of surfactants (including effective and non-effective) for enhancing oil recovery

through wettability alteration in carbonate rocks at ambient and reservoir conditions. In comparison to chemically structured costly surfactants, silica nanoparticles are naturally abundant, environmentally friendly, and cost-effective. Based on the experimental evaluation of this research and ongoing investigation of other researches on the mechanism of nanoparticles assisting in wettability alteration of a system, the following scenario is suggested by this research. It is known from literature that nanoparticles bring a high amount of free energy to the system due to their size, which leads to increasing the surface activity of the system specially when combined with surfactant molecules. Additionally, it is known from literature that nanoparticles have their own mechanism of spreading behavior prompted by forming ordered structures under the impact of disjoining pressure gradient. The experimental investigation of this study showed that nanoparticles could clearly compensate for surfactants, meaning that even lowering the concentration of surfactant in the surfactant-based nanofluid solution would not significantly change the overall wettability alteration behavior of the solution. Therefore, it seems like surfactant-based nanofluid utilizes both the interfacial tension reduction capability of surfactant (even slightly) and specific spreading behavior of the nanoparticles to change the wettability of the system. Hence, it appears that the rock-fluid interaction responsibility of the solution is more on the shoulders of nanoparticles than surfactant molecules, which may potentially bring down the necessity of surfactant adsorption on the rock to change its wettability and consequently lower the amount of financial concerns on using chemical flooding to enhance oil recovery.

- To understand how well nanoparticles can compensate for surfactants economically and how practical it is to apply them in the real field cases and how realistic will be to inject a

combination of nanoparticles and surfactants down into the reservoir, a thorough and comprehensive cost analysis considering important elements such as production history, production rate, surfactant concentration, facilities and operation costs, saving on handling the produced water, and etc. is required. However, the preliminary economic considerations of this research suggested that using only nanoparticles in brine could result in $3.37 extra profit per barrel of oil compared to using only surfactant. This analysis also indicated that combination of nanoparticles and surfactant could lead to $3.20 extra profit per barrel of oil compared to only surfactant. This extra profit grows to be $4.39 per barrel of oil even after lowering the concentration of surfactant in the surfactant-based nanofluid. Therefore, surfactant-based nanofluids seem to have the potential to be an economically appealing agent for enhancing oil recovery through wettability alteration of carbonate rocks at both experimental conditions.

5.2. Recommendations

In this research, the great potential of nanoparticles for enhancing the oil recovery by themselves and in combination with surfactants for the specific system of Indiana limestone/Yates-oil/NaCl was revealed. This enhancement in oil recovery seemed to be mostly due to the wettability alteration of the system, which was evaluated through the precise contact angle measurements and coreflood experiments along with optimized simulation of relative permeability curves at both experimental conditions.

Despite the broad range of experiments, profound analysis, and insightful observations, there are certain gaps and limitations which this study did not address and therefore define the stance for future work as follow:

- The concept of using nanotechnology for enhancing oil recovery is at the early stages of development. Although structural disjoining pressure gradient promoted by the Brownian motion and electrostatic repulsion between particles is believed by the literature to be the main driving force for spreading the nanoparticles, a complete understanding of the wettability alteration mechanisms particularly in confronting with surfactant molecules and different minerals is yet to be achieved.
- This work studied the influence of silica nanoparticles on enhancing oil recovery through wettability alteration using Dual-Drop-Dual-Crystal (DDDC) technique and coreflooding at two different experimental conditions only for a certain rock/oil/brine system. A more comprehensive investigation on the implications of nanoparticles can be attained by choosing a broader variety of core sizes (to provide larger pore volume), rock types (sandstone, shale, etc.), oil types (live-oil, condensate, etc.), and brine compositions (synthetic or reservoir brine depending on the formation under study). Furthermore, based on the hydrophilic/lipophilic nature of the system, different variations of nanoparticles type (other than silica) along with surfactant molecules (other than anionic surfactants) can be applied at a range of temperatures and pressures.
- Although the preliminary economic consideration provided in this research showed the positive economics of combining nanoparticles with surfactants to improve oil recovery, a further comprehensive cost analysis is required for field implementation considering important parameters such as production history, production rate, surfactant concentration, facilities and operation costs, saving on handling the produced water, and many other factors.

- Despite the attempt to perform a microscopic investigation on the impact of surfactant-based nanofluids on the characteristics of the system, further systematic study is required to get a better understanding of how nanoparticles influence wettability of the system at the pore-level. A microscopic visualization of nanoparticles and surfactant molecules interacting with oil at the rock surface can provide an opportunity to realistically observe the wettability alteration behavior leading to reduction in the residual oil saturation and enhancement in the oil recovery. Scanning Electron Microscopic (SEM) images or Computed Tomography (CT) Scans are the technologies that can facilitate a deep look inside the actual porous medium to visually determine the before and after effects in terms of wettability alteration. Moreover, X-ray Powder Diffraction (XRD) technique can offer a chance to study the role of crystal structure and mineral composition of the rock on the influence extent of nanoparticles along with the surfactant molecules in changing the wettability of the system.

REFERENCES

Abhishek, R., Kumar, G.S., and Sapru, K. 2015. Wettability Alteration in Carbonate Reservoirs Using Nanofluids. *J. Pet. Sci. Technol.* **33**(2015):794-801. http://dx.doi.org/10.1080/10916466.2015.1014967

Agbalaka, CC, Dandekar, A., Patil, S., Khataniar, S, and Hemsath, J. 2009. Coreflooding studies to Evaluate the Impact of Salinity and Wettability on Oil Recovery Efficiency. *Transport in Porous Media* **76**(1): 77–94.

Al-Anssari, S., Nwidee, L. N., Arif, M., Wang, S., Barifcani, A., Lebedev, M., & Iglauer, S. 2017. Wettability Alteration of Carbonate Rocks via Nanoparticle-Anionic Surfactant Flooding at Reservoirs Conditions. Society of Petroleum Engineers. doi:10.2118/189203-MS

Alagic E. and Skauge A. 2010. Combined Low Salinity Brine Injection and Surfactant Flooding in Mixed-Wet Sandstone Cores. *Energy & Fuels* **2010**(24): 3551–3559.

Alotaibi, M. B., Azmy, R. M., & Nasr-El-Din, H. A. 2010. Wettability Studies Using Low-Salinity Water in Sandstone Reservoirs. Offshore Technology Conference. doi:10.4043/20718-MS.

Anderson, W. G.1986. Wettability Literature Survey- Part 1: Rock/Oil/Brine Interactions and the Effects of Core Handling on Wettability. Society of Petroleum Engineers. doi:10.2118/13932-PA.

Anderson, W. G.1987. Wettability Literature Survey Part 5: The Effects of Wettability on Relative Permeability. Society of Petroleum Engineers. doi:10.2118/16323-PA.

Anderson, W. G.1987. Wettability Literature Survey- Part 4: Effects of Wettability on Capillary Pressure. Society of Petroleum Engineers. doi:10.2118/15271-PA.

Anderson, W. G.1987. Wettability Literature Survey-Part 6: The Effects of Wettability on Waterflooding. Society of Petroleum Engineers. doi:10.2118/16471-PA.

Arsalan, N., and Nguyen, Q. P. 2016. Characterization of Mixed Wettability using Surface Energy Distribution. Society of Petroleum Engineers. doi:10.2118/179706-MS.

Austad, T., Matre, B., Milter, J., Saelig Vareid, A., Oslashyno, L. 1998. Chemical Flooding of Oil Reservoirs 8: Spontaneous Oil Expulsion from Oil- and Water-Wet Low Permeable Chalk Material by Imbibition of Aqueous Surfactant Solutions. *Colloids & Surfaces A: Physicochemical & Engineering Aspects*, **137**(1998): 117–129.

Ayatollahi, Sh. and Zerafat, M.M. 2012. Nanotechnology-Assisted EOR Techniques: New Solutions to Old Challenges. Presented at the SPE International Oilfield Nanotechnology Conference, Noordwijk, The Netherland, 12-14 June. SPE 157094.

Ayirala, S.C., Vijapurapu, C.S., Rao D.N. 2006. Beneficial Effects of Wettability Altering Surfactants in Oil-wet Fractured Reservoirs. *J. Pet. Sci. Eng.* **52** (2006): 261-274. http://dx.doi.org/10.1016/j.petrol.2006.03.019

Babadagli, T. 2003. Analysis of Oil Recovery by Spontaneous Imbibition of Surfactant Solution. Society of Petroleum Engineers. doi:10.2118/84866-MS.

Bauer, R. G. and Klemmensen, D. F. 1982. A New Polymer for Enhanced Oil Recovery. Society of Petroleum Engineers. doi:10.2118/10711-MS.

Berg, S., Cense, A. W., Jansen, E., & Bakker, K. 2010. Direct Experimental Evidence of Wettability Modification by Low Salinity. *Petrophysics* **51**(5): 314–322.

Binks, B.P. 2002. Particles as Surfactants – Similarities and Differences. *Current Opinion in Colloid & Interface Science* **7**(2002): 21–41.

BP Statistical Review of World Energy. 2018. 67th Edition. www.bp.com/statisticalreview

Carpenter, C. 2015. A Study of Wettability-Alteration Methods with Nanomaterials Application. Society of Petroleum Engineers. doi:10.2118/1215-0074-JPT.

Castelijns, H. J., Pel, L., Huinink, H., & Zitha, P. L. J. 2006. Mass Transfer and Gelation in Sandstone Cores of a Novel Water Shutoff Chemical. Society of Petroleum Engineers. doi:10.2118/99684-MS.

Chen, P. and Mohanty, K. K. 2014. Wettability Alteration in High Temperature Carbonate Reservoirs. Society of Petroleum Engineers. doi:10.2118/169125-MS.

Chengara, A. Nikolov, A., Wasan D.T., Trokhymchuck, A., Henderson, D., 2004. Spreading of Nanofluids Driven by The Structural Disjoining Pressure Gradient. *Journal of Colloid & Interface Science.* **280** (1): 192-201. http://dx.doi.org/10.1016/j.jcis.2004.07.005

Chengara, A. Nikolov, A., Wasan D.T., 2008. New Paradigms for spreading of colloidal fluids on solid surfaces. *Journal of Advances in Polymer and Science.* **218** (2008): 117-141. http://dx.doi.org/10.1007/12_2008_164

Choi, S.U.S. 1998. Nanofluid Technology: Current Status and Future Research. Presented at the Korea-US Technical Conference on Strategic Technologies, Vienna, VA, 22-24 October.

Civan, F., Wei, W., & Gupta, A. 1999. Effect of Wettability and Matrix to Fracture Transfer on the Waterflooding in Fractured Reservoirs. Society of Petroleum Engineers. doi:10.2118/52197-MS.

Cuiec, L. 1984. Rock/Crude-Oil Interactions and Wettability: An Attempt to Understand Their Interrelation. Society of Petroleum Engineers. doi:10.2118/13211-MS

Das, S.K., Choi, S.U., Yu, W., and Pradeep, T. 2008. *Nanofluid: Science and Technology*. Hoboken, NJ: John Wiley & Sons Inc. ISBN-13: 9780470074732.

Delshad, M., Najafabadi, N. F., & Sepehrnoori, K. 2009. Scale Up Methodology for Wettability Modification in Fractured Carbonates. Society of Petroleum Engineers. doi:10.2118/118915-MS.

DOE official website. 2015. U.S. Department of Energy. http://energy.gov/fe/science-innovation/oil-gas-research

Eastoe, J., and Tabor, R.F. 2014. Surfactants and Nanoscience. In *Colloidal Foundations of Nanoscience,* ed. 1. Berti D. and Palazzo G, Chap. 6, 135–157. Amsterdam, The Netherlands: Elsevier B.V.

Edwards, S.A. 2006. *The Nanotech Pioneers: Where Are They Taking Us?* Germany: Wiley-Vch. ISBN-10: 3527312900.

Energy Information Administration. 2018. Annual Energy Outlook 2018 with Projections to 2050. Report: DOE/EIA-0035 (2015).

Froning, H. R., & Leach, R. O. 1967. Determination of Chemical Requirements and Applicability of Wettability Alteration Flooding. *JPT* **1967**(June): 839–843.

Ge, J., Wang, Y. 2015. Surfactant Enhanced Oil Recovery in a High Temperature and High Salinity Carbonate Reservoir. *Journal of Surfactant and Detergents*, **18**(2015): 1043–1050.

Giraldo, J., Benjumea, P., Lopera, S., Cortes, F.B., Ruiz, M.A. 2013. Wettability Alteration of Sandstone Cores by Alumina-Based Nanofluids. *Energy & Fuels* **27**(2013): 3659–3665. doi:10.1021/ef4002956.

Gupta, R., & Mohanty, K. K. 2008. Wettability Alteration of Fractured Carbonate Reservoirs. Society of Petroleum Engineers. doi:10.2118/113407-MS.

Gupta, S. 2016. *Effects of Chemical Structure of Anionic Surfactants on the Wettability of a Carbonate System*. MS Thesis. Louisiana State University, LA, USA.

Haroun, M., Al-Hassan, S., Ansari, A., Al-Kindy, N., Abou-Sayed, N., Ali, B., and Sarma, H. 2012. Smart Nano-EOR Process for Abu Dhabi Carbonate Reservoirs. Presented at the SPE International Petroleum Conference and Exhibition, Abu Dhabi, UAE, 11 – 14 November. SPE 162386.

Hatiboglu, C. U., & Babadagli, T. 2006. Primary and Secondary Oil Recovery from Different-Wettability Rocks by Countercurrent Diffusion and Spontaneous Imbibition. Society of Petroleum Engineers. doi:10.2118/94120-MS.

Hendraningrat, L., Li, Sh., and Torseter O. 2013. A Coreflood Investigation of Nanofluid Enhanced Oil Recovery. *J. Pet. Sci. Eng.* **111** (2013): 128-138. http://dx.doi.org/10.1016/j.petrol.2013.07.003

Hirasaki, G. J. 1991. Wettability: Fundamentals and Surface Forces. SPE Formation Evaluation. **1991**(June): 217–226.

Hirasaki, G., & Zhang, D. L. 2004. Surface Chemistry of Oil Recovery from Fractured, Oil-Wet, Carbonate Formations. *SPE Journal*, **2004**(June): 151–164.

Holcomb, D.L., Wasan, D.T., and Noklov, A.D. 2012. Method for Intervention Operations in Subsurface Hydrocarbon Formations. US Patent No. 2012/0168165 A1.

Jiang, R., Li, K., and Horne, R. 2017. A Mechansim Study of Wettability and Interfacial Tension for EOR using Silica Nanoparticles. Society of Petroleum Engineers. doi:10.2118/187096-MS.

Joonaki, E., Ghanaatian, S. 2014. The Application of nanofluids for Enhanced Oil Recovery: Effects on Interfacial Tension and Coreflooding Process. *J. Pet. Sci. Technol.* **32** (2014): 2599-2607. http://dx.doi.org/10.1080/10916466.2013.855228

Ju, B., Dai, S., Luan, Z., Zhu, T., Su, X., & Qiu, X. 2002. A Study of Wettability and Permeability Change Caused by Adsorption of Nanometer Structured Polysilicon on the Surface of Porous Media. Society of Petroleum Engineers. doi:10.2118/77938-MS.

Ju, B., Fan, T., and Ma, M. 2006. Enhanced Oil Recovery by Flooding with Hydrophilic Nanoparticles. *China Patricuology*. **4** (1): 41-46.

Kaasa, A.T. 2013. *Investigation of How Silica Nanoparticle Adsorption Affects Wettability in Water-wet Berea Sandstone*. MS Thesis. Norwegian University of Science and Technology, Norway.

Kalaei, M. H., Green, D., & Willhite, G. P. 2013. A New Dynamic Wettability-Alteration Model for Oil-Wet Cores during Surfactant-Solution Imbibition. Society of Petroleum Engineers. doi:10.2118/153329-PA.

Kapusta, S., Balzano, L., and Riele P.T. 2012. Nanotechnology Applications in Oil and gas Exploration and Production. Presented at the International Petroleum Technology Conference, Bangkok, Thailand, 7-9 February. IPTC 15152.

Karimi, A., Fakhroueian, Z., Bahramian, A., Pourkhiabani, N., Darabad, J.B., Azin, R., and Arya, Sh. 2012. Wettability Alteration in Carbonates Using Zirconium Oxide Nanofluids: EOR Implications. *J. Energy Fuels.* **26** (2012): 1028-1036. http://dx.doi.org/10.1021/ef201475u

Kathel, P., and Mohanty, K. K. 2013. Wettability Alteration in a Tight Oil Reservoir. *Energy & Fuels*, **27**(2013): 6460–6468.

Kerunwa, A., Onyekonwu, M. O., Anyadiegwu, C. I. C., & Olafuyi, A. O. 2016. Spontaneous Imbibition in Niger Delta Cores. Society of Petroleum Engineers. doi:10.2118/184353-MS.

Klins, M.A. 1984. Carbon Dioxide Flooding – Basic Mechanisms and Project Design, International Human Resources Development Corporation, Boston.

Kondiparty, K. 2011. *Spreading of Nanofluids on Solids Driven by Structural Disjoining Pressure*. PhD Dissertation. Illinois Institute of Technology, USA.

Kong, X., Ohadi, M.M. 2010. Applications of Micro and Nano Technologies in the Oil and Gas Industry-An Overview of the Recent Progress. Presented at the SPE International Petroleum Conference and Exhibition, Abu Dhabi, UAE, 1 – 4 November. SPE 138241.

Kumar, K., Dao, E. K., & Mohanty, K. K. 2005. Atomic Force Microscopy Study of Wettability Alteration. Society of Petroleum Engineers. doi:10.2118/93009-MS.

Kumar, K., Dao, E. K., Mohanty, K. K. 2008. Atomic Force Microscopy Study of Wettability Alteration by Surfactants. Society of Petroleum Engineers. doi:10.2118/93009-PA.

Kumar, M., Fogden, A., Senden, T., & Knackstedt, M. A. 2012. Investigation of Pore-Scale Mixed Wettability. Society of Petroleum Engineers. doi:10.2118/129974-PA.

Kumar, M., Senden, T., Sheppard, A. P., Latham, S., Knackstedt, M. A., Cinar, Y., & Pinczewski, W. V. 2008. Designing for Mixed Wettability. Society of Petroleum Engineers. doi:10.2118/113862-MS.

Le, N. Y. Th., Pham, D. Kh., Le, K. H., Nguyen Ph. T. 2011. Design and Screening of Synergistic Blends of SiO_2 Nanoparticles and Surfactants for Enhanced Oil Recovery in High-Temperature Reservoirs. *Adv. Nat. Sci.: Nanoscience Nanotechnology* **2**(2011): 1–6.

Li, G., Mu, J., Li, Y., Yuan, Sh. 2000. An Experimental Study on Alkaline/Surfactant/Polymer Flooding Systems using Nature Mixed Carboxylate. *Colloids & Surfaces A: Physicochemical & Engineering Aspects*, **173**(2000): 219–229.

Li, K., & Horne, R. N. 2001. Characterization of Spontaneous Water Imbibition Into Gas-Saturated Rocks. *SPE Journal* **2001**(Dec.): 375–384.

Li, Sh., Genys, M., Wang, K., & Torsæter, O. 2015. Experimental Study of Wettability Alteration during Nanofluid Enhanced Oil Recovery Process and Its Effect on Oil Recovery. Society of Petroleum Engineers. doi:10.2118/175610-MS.

Li, Sh., Hendraningrat, L., and Torseter O. 2013. Improved Oil Recovery by Hydrophilic Silica Nanoparticles Suspension: 2-Phase Flow Experimental Studies. Presented at the International Petroleum Technology Conference, Beijing, China, 26-28 March. IPTC 16707.

Li, Sh., Torsæter, O. 2014. An Experimental Investigation of EOR Mechanisms for Nanoparticles Fluid in Glass Micromodel. Presented at the Society of Core Analysts Annual Symposium, Avignon, France, September 2014.

Maestro, A., Guzman, E., Santini, E., Ravera, F., Liggieri, L., Ortega, F., Rubio, R.G. 2011. Wettability of Silica Nanoparticle-Surfactant Nanocomposite Interfacial Layers. *Soft Matter* **8**(2011): 837–843.

Maghzi, A., Mohammadi, S., Ghazanfari, M.H., Kharrat, R., Masihi, M. 2012. Monitoring Wettability Alteration by Silica Nanoparticles during Water Flooding to Heavy Oils in Five-spot Systems: A Pore-Level Investigation. *Experimental Thermal and Fluid Science* **40**(2012): 168–176.

Mandal, A. and Ojha, K. 2008. Optimum Formulation of Alkaline-Surfactant-Polymer Systems for Enhanced Oil Recovery. Society of Petroleum Engineers. doi:10.2118/114877-MS.

Mashat, A., Abdel-Fattah, A., and Gizzatov, A. 2018. NanoSurfactant: A Novel Nanopartciles-Based EOR Approach. Society of Petroleum Engineers. doi:10.2118/190861-MS.

Mcelfresh, P. M., Holcomb, D. L., & Ector, D. 2012. Application of Nanofluid Technology to Improve Recovery in Oil and Gas Wells. Presented at the SPE International Oilfield Nanotechnology Conference, Noordwijk, The Netherland, 12-14 June. SPE 154827-MS.

Melrose, J. C. 1982. Interpretation of Mixed Wettability States in Reservoir Rocks. Society of Petroleum Engineers. doi:10.2118/10971-MS.

Miranda, C.R., De-Lara, L.S., and Tonetto, B.C. 2012. Stability and Mobility of Functionalized Silica Nanoparticles for Enhanced Oil Recovery Applications. Presented at the SPE International Oilfield Nanotechnology Conference, Noordwijk, The Netherland, 12-14 June. SPE 157033.

Mohammadi, M.S., Moghadasi, J., and Naseri, S. 2014. An Experimental Investigation of Wettability Alteration in Carbonate Reservoir Using γ-Al_2O_3 Nanoparticles. *Iranian J. Oil Gas Sci. Technol.* **3** (2014): 18-26.

Mohanty, K.K., Wang, L. 2013. Improving Oil Recovery in Gas-flooded, Oil-Wet Carbonate Reservoirs by Wettability Altering Surfactants. Presented at SPE International Symposium on Oilfield Chemistry, Woodland, TX, 8-10 April. SPE 164126.

Morrow, N. (1990). Wettability and Its Effect on Oil Recovery. Journal of Petroleum Technology, **42**(12), 1476–1484. doi:10.2118/21621-PA 67.

Morrow, N.R., Ma, S., Zhou, X., & Zhang, X. 1994. Characterization of Wettability from Spontaneous Imbibition Measurements. Petroleum Society of Canada. doi:10.2118/94-47.

Morrow, N.R., Tang, G, Valat, M., Xie, X. 1998. Prospects of Improved Oil Recovery Related to wettability and brine composition. *Journal of Petroleum Science and Engineering* **20** (3): 267–276.

Mwangi, P., 2010, *An Experimental Study of Surfactant Enhanced Waterflooding*, MS Thesis, Craft & Hawkins Department of Petroleum Engineering, Louisiana State University.

Nasralla, R. A., Bataweel, M. A., & Nasr-El-Din, H. A. 2013. Investigation of Wettability Alteration and Oil-Recovery Improvement by Low-Salinity Water in Sandstone Rock. Society of Petroleum Engineers. doi:10.2118/146322-PA.

Nedjhioui, M., Moulai-Mostefa, N., Morsli, A., Bensmaili, A. 2005. Combined Effects of Polymer/Surfactant/Oil/Alkali on Physical Chemical Properties. *Desalination*, **185**(2005): 543–550.

Neog, A., & Schechter, D. S. 2016. Investigation of Surfactant Induced Wettability Alteration in Wolfcamp Shale for Hydraulic Fracturing and EOR Applications. Society of Petroleum Engineers. doi:10.2118/179600-MS.

Nguyen, D., Wang, D., Oladapo, A., Zhang, J., Sickorez, J., Butler, R., & Mueller, B. 2014. Evaluation of Surfactants for Oil Recovery Potential in Shale Reservoirs. Society of Petroleum Engineers. doi:10.2118/169085-MS.

OGJ Approach Screens Reservoir Candidates for EOR. 2016. *Oil & gas Journal*. **114** (4): 48-51.

OGJ Worldwide EOR Survey. 2006. Special Report. *Oil & gas Journal*. **104** (15): 40-53.

OGJ Worldwide EOR Survey. 2014. Special Report. *Oil & gas Journal*. **112** (4): 78-91.

Omurlu, C., Pham, H., and Nguyen, P. 2016. Interaction os surface-modified silica nanoparticles with clay minerals. *Applied Nanoscience.* **6**(8): 1167–1173.

Onyekonwu, M.O. and Ogolo, N.A. 2010. Investigating the Use of Nanoparticles in Enhancing Oil Recovery. Presented at the SPE International Conference and Exhibition, Tinapa-Calabar, Nigeria, 31 July – 7 August. SPE 140744.

Ranatunga, R.J.K.U., Nguyen, Ch.T., Wilson, B.A., Shinoda, W., and Nielsen, S.O. 2011. Molecular Dynamics Study of Nanoparticles and Non-ionic Surfactant at an Oil-Water Interface. *Soft Matter* **7**(2011): 6942–6952.

Rao, D. N., & Girard, M. G. (1996). A new technique for reservoir wettability characterization. Journal of Canadian Petroleum Technology, 35(1), 31–39.

Rao, D.N. 2002. Measurements of Dynamic Contact Angles in Solid-Liquid-Liquid Systems at Elevated Pressures and Temperatures. *Colloids and Surfaces A: Physicochemical and Engineering Aspects* **206** (1): 203-216. doi: 10.1016/S0927-7757(02)00077-8.

Rao, D.N. 2003. The Concept, Characterization, Concerns, and Consequences of Contact Angles in Solid-Liquid-Liquid Systems. *Contact Angle, Wettability and Adhesion* **3**(2003): 1-20.

Rao, D.N., Ayirala S.C., Abe, A.A., Xu, W. 2006. Impact of Low-Cost Dilute Surfactants on Wettability and Relative Permeability. Presented at the SPE/DOE Symposium on Improved Oil Recovery, Tulsa, Oklahoma, 22-26 April. SPE 99906, doi:10.2118/99609-MS.

Rao, D.N., Girard, M.G. 1996. A New Technique for Reservoir Wettability Characterization. *J Can Pet Technol* (January): 31-39.

Ravera, F., Santini, E., Loglio G., Ferrari M., Liggieri. 2006. Effect of nanoparticles on the interfacial properties of liquid/liquid and liquid/air surface layers. *J. Phys. Chem B* **110**(2006): 19543–19551.

Roustaei, A. 2014. An Evaluation of Spontaneous Imbibition of Water into Oil-Wet Carbonate Reservoir Cores Using Nanofluid. *J. Petrophysics* **55** (2014): 31-37.

Roustaei, A. and Bagherzadeh, H. 2015. Experimental Investigation of SiO_2 nanoparticles on Enhanced Oil Recovery of Carbonate Reservoirs. *J. Petrol Explor Prod Technol* **5**(2015): 27-33.

Roustaei, A., Moghadasi, J., Bagherzadeh, H., Shahrabadi, A. 2012. An Experimental Investigation of Polysilicon Nanoparticles' Recovery Efficiencies through Changes in Interfacial Tension and Wettability Alteration. Presented at the SPE International Oilfield Nanotechnology Conference, Noordwijk, The Netherland, 12-14 June. SPE 156976.

Ruschau, G. R. 1997. Considerations for Polymers in Enhanced Oil Recovery Operations. NACE International.

Salathiel, R. A. 1973. Oil Recovery by Surface Film Drainage in Mixed-Wettability Rocks. Society of Petroleum Engineers. doi:10.2118/4104-PA.

Seethepalli, A., Adibhatla, B., & Mohanty, K. K. 2004. Wettability Alteration during Surfactant Flooding of Carbonate Reservoirs. Society of Petroleum Engineers. doi:10.2118/89423-MS.

Sefiane, Kh., Skilling, J., MacGillivary, J. 2008. Contact Line Motion and Dynamic Wetting of Nanofluid Solutions. *Advances in Colloid and Interface Science* **138** (2008): 101–120.

Shabib-Asl, A., Ayoub, M. A., & Elraies, K. A. 2015. Laboratory Investigation into Wettability Alteration by different Low Salinity Water Compositions in Sandstone Rock. Society of Petroleum Engineers. doi:10.2118/176492-MS.

Shahrabadi, A., Bagherzadeh, H., Roustaei, A., and Golghanddashti, H. 2012. Experimental Investigation of HLP Nanofluid Potential to Enhance Oil Recovery: A Mechanistic Approach. Presented at the SPE International Oilfield Nanotechnology Conference, Noordwijk, The Netherland, 12-14 June. SPE 156642.

Shaker Shiran, B., & Skauge, A. 2012. Wettability and Oil Recovery by Low Salinity Injection. Society of Petroleum Engineers. doi:10.2118/155651-MS.

Sharma, G., & Mohanty, K. K. 2011. Wettability Alteration in High Temperature and High Salinity Carbonate Reservoirs. Society of Petroleum Engineers. doi:10.2118/147306-MS.

Smith, F. W. 1978. Ion-Exchange Conditioning of Sandstones for Chemical Flooding. *JPT* **1978**(June): 959–968.

Standnes, D.C., Nogaret, L., Chen, H., Austad, T. 2002. An Evaluation of Spontaneous Imbibition of Water into Oil-Wet to Water-Wet Carbonate Reservoir Cores using a Nonionic and a Cationic Surfactant. *Energy & Fuels*, **16**(2002): 1557–1564.

Strand, S., Høgnesen, E.J., and Austad, T. 2005. Wettability alteration of carbonates—Effects of potential determining ions (Ca^{2+} and SO_4^{2-}) and temperature. *Colloids and Surfaces A: Physicochemical and Engineering Aspects*, **275**(2006): 1–10.

Suleimanov, B.A., Ismailov, F.S., and Veliyev, E.F. 2011. Nanofluid for Enhanced Oil Recovery. *J. Pet. Sci. Eng.* **78** (2011): 431-437. http://dx.doi.org/10.1016/j.petrol.2011.06.0014

Suresh, R., Kuznetsov, O., Agrawal, D., Darugar, Q., & Khabashesku, V. 2018. Reduction of Surfactant Adsorption in Porous Media Using Silica Nanoparticles. Offshore Technology Conference. doi:10.4043/28879-MS

Thomas, S., Ali, S. M. F., Scoular, J. R., & Verkoczy, B. 2001. Chemical Methods for Heavy Oil Recovery. Petroleum Society of Canada. doi:10.2118/01-03-05

Tola, S., Sasaki, K., & Sugai, Y. 2017. Wettability Alteration of Sandstone with Zinc Oxide Nano-Particles. Society of Petrophysicists and Well-Log Analysts.

Tong, Zh., Xie, X., and Morrow N. R. 2003. Crude Oil Composition and the Stability of Mixed Wettability in Sandstones. *Petrophysics* **44**(4): 233–242.

Vijapurapu, C. S., Rao, D. N. 2003. The Effect of Rock Surface Characteristics on Reservoir Wettability. *Contact Angle, Wettability and Adhesion*, **3**(2003): 1–20.

Vijapurapu, C.S., & Rao, D. N. 2003. Effect of Brine Dilution and Surfactant Concentration on Spreading and Wettability. Presented at International Symposium on Oilfield Chemistry, Houston, TX, 5-7 February. SPE 80273.

Wasan, D. T., Nikolov, A.D. 2003. Spreading of Nanofluids on Solids. *Nature*, **423**(2003): 156–159. doi:10.1038/nature01591.

Wasan, D., Nikolov, A., and Kondiparty, K. 2011. The Wetting and Spreading of nanofluids on Solids: Role of the Structural Disjoining Pressure. *J. Current Opinion in Colloid & Interface Science.* **16** (2011): 344-349. http://dx.doi.org/10.1016/j.cocis.2011.02.001

Webb, K.J., Black, C.J.J., and Al-Ajeel, H. 2004. Low Salinity Oil Recovery—Log-Inject-Log. Paper SPE 89379 presented at the SPE/DOE Symposium on Improved Oil Recovery, Tulsa, 17–21 April. doi: 10.2118/89379-MS.

Wood, A. R., Wilcox, T. C., MacDonald, D. G., Flynn, J. J., & Angert, P. F. 1991. Determining Effective Residual Oil Saturation for Mixed Wettability Reservoirs: Endicott Field, Alaska. Society of Petroleum Engineers. doi:10.2118/22903-MS.

Wu, W., Vaskas, A., Delshad, M., Pope, G. A., & Sepehrnoori, K. 1996. Design and Optimization of Low-Cost Chemical Flooding. Society of Petroleum Engineers. doi:10.2118/35355-MS.

Xiaoqin, Z., Wenting, G., & Feng, P. 2013. Polymer Flooding for Middle and Low Permeability Sandstone Reservoirs. International Petroleum Technology Conference. doi:10.2523/IPTC-16536-MS.

Xu, W. 2005. *Experimental Investigation of Dynamic Interfacial Interactions at Reservoir Conditions*. MS Thesis. Louisiana State University, LA, USA.

Xu, W., Ayirala, S. C., & Rao, D. N. 2008. Measurement of Surfactant-Induced Interfacial Interactions at Reservoir Conditions. *SPE Reservoir Evaluation & Engineering*. **11** (1): 83-94, doi:10.2118/96021-P.

Zhang, Y., Xie, X., & Morrow, N. R. 2007. Waterflood Performance by Injection of Brine with Different Salinity for Reservoir Cores. Society of Petroleum Engineers. doi:10.2118/109849-MS.

Zheng, Y. 2012. *Effect of Surfactants and Brine Salinity and Composition on Spreading, Wettability, and Flow Behavior in Gas-Condensate Reservoirs*. PhD Dissertation. Louisiana State University, LA, USA.

Zheng, Y. and Rao, D. N. 2010. Surfactant-Induced Spreading and Wettability Effects in Condensate Reservoirs. Presented at SPE Improved Oil Recovery Symposium, Tulsa, Oklahoma,24-28 April. SPE 129668.

VITA

Mohammad Foad Haeri was born on June 21, 1980 in Tehran, Iran, and raised in an educated family. His enthusiasm for learning and discovering the world made him travel to the Unites States after receiving a bachelor's degree from Petroleum University of Technology. He began to work as a petroleum engineering consultant after receiving a master's degree from University of Louisiana at Lafayette. But his passion for deepening the knowledge convinced him to return to school to purse a doctoral degree at Louisiana State University. Upon completion, he wants to be a research scientist and a contributor to academia.